NOTTINGHAM TRENT UNIVERSITY

Regulation of microRNA activity and intestinal stem cell properties by IWS1

NIKI CHRISTODOULOU

N0892576

A thesis submitted in partial fulfilment of the requirements of Nottingham Trent University for the degree of Doctor of Philosophy

September 2023

THE OHIO STATE UNIVERSITY

This research programme was carried out in collaboration with the Cancer Biology and Genetics department at The Ohio State University, Comprehensive Cancer-Centre- Arthur G. James Cancer Hospital and Richard J. Solove Research Institute.

ABSTRACT

MicroRNAs are small single-stranded non-coding RNAs that regulate gene expression post-transcriptionally, by targeting the 3‘-untranslated region (3’-UTR) of mRNAs. The regulation of microRNAs at the transcriptional level is well-studied, however, how their activity is regulated remains largely elusive. The family of Akt serine/threonine protein kinases, comprised of Akt1, Akt2 and Akt3, regulates essential cell functions including metabolism, survival, proliferation, and migration. We have previously shown that IWS1 (Interacts with Spt6), a factor involved in mRNA splicing and nuclear export, is phosphorylated specifically by Akt1 and Akt3 at Ser720/Thr721.

Here, RNA extracts from NCI-H522 lung cancer cells, transduced with shIWS1 and reconstituted with wild type (Ser720/Thr721-IWS1) or phosphorylation-deficient IWS1 (Ala720/Ala721-IWS1) were subjected to RNA and microRNA sequencing. Bioinformatic analysis suggested that microRNAs expressed at similar levels in the two cell types have a different impact on their mRNA targets. microRNA activity reporter assays and western blot analysis for microRNA targets in these cells revealed increased microRNA activity in Ala720/Ala721-IWS1-expressing cells. Our findings were verified in a second cell line, the non-transformed immortalized colonic epithelial cells NCM460. microRNA activity reporter assays, western blot analyses and cell growth assays showed that microRNA effects are enhanced in cells expressing Ala720/Ala721-IWS1. Immunoprecipitation and proximity ligation assays showed that IWS1 interacts with proteins known to be associated with RNA-induced silencing complex (RISC), and this interaction is enhanced by Akt-mediated IWS1 phosphorylation. To evaluate the dependence of IWS1/RISC interaction on IWS1 phosphorylation, we employed Akt1-/-Akt2-/-Akt3-/- immortalized mouse lung fibroblasts, transduced with myc-Akt1 or myc-Akt2 or the empty retroviral vector. Immunoprecipitation experiments in these cells, before and after treatment with

IGF1, revealed that IWS1 interacts with the RISC components specifically in Akt1-expressing cells upon Akt1 activation by IGF1. Using intestinal epithelial cells from *Iws1* intestinal stem cell (ISC)-specific KO mice and human colonocytes, we found that *Iws1* and IWS1 phosphorylation regulates the maintenance and differentiation of ISCs.

Overall, our data demonstrate that IWS1 interacts with RISC in a conserved Akt1-dependent manner and regulates the activity of microRNAs with significant implications in effects on cellular properties.

ACKNOWLEDGEMENTS

Firstly, I would like to acknowledge and express my gratitude to my director of studies, Dr Christos Polytarchou for giving me the opportunity to work on this exciting project and for providing me with balanced supervision to become an independent scientist. I am really inspired by his critical and scientific acumen and really grateful for his continuous guidance. I would also like to thank my co-supervisors Dr Maria Hatziapostolou, Dr Cristina Montiel-Duarte and Prof Elisabetta Verderio Edward, who supported me patiently, motivated and inspired me during these four years. A great thank you to my external supervisor Prof. Philip N. Tsichlis for his supervision and support at Ohio State University.

The experimental work of this thesis would not have been completed without the contribution of the members of the John Van Geest Cancer Centre at NTU and the Cancer Biology and Genetics department at OSU, for always being there for me when needed. I am very grateful to Carles Puig Saenz (NTU), Dr Evangelia Chavdoula (OSU), Dr Burak Soysal (OSU) and Dr Eri Anastas (OSU) for their support during difficult times and for sharing experimentally ideas.

Special thanks to Dr Jayakumar (Jay) Vadakekolathu (NTU) for his help in the Nanostring work and GeoMX experiments and Dr Maria Mihaylova (OSU) for her guidance with the isolation of ISCs. Also, I would like to thank Dr Gemma Foulds (NTU) and Mr Stephen Reeder (NTU), who helped me with FACS and cell sorting, respectively.

I would not be able to finish my phD without the support of Dr Eleni Birli, a phD graduate member of my research lab, who supported me experimentally during her time at NTU and by supporting me during the writing of my thesis. I am delighted for the time and the experimental ideas we shared together.

Finally, this journey would not be the same without the support of my wonderful parents, Spyros and Evi and my sisters Stephanie, Chrystalla and Elena for their loving support and for making me feel strong even during the hardest days. A great thank you to my little nephew Christianos and my nieces Evelina, Joanna and Galatia for making me laugh hard, even when I was feeling miserable. During the hardest days, all my strength was coming from my little nephew, Demetris. I would like to thank my grandparents Adamos and Eleni, who visited me and stayed with me during the difficult times. Last but not least, a special thanks to my beloved partner Michalis and his parents Stephanos and Kyriaki, because of their unconditional and loving support.

PUBLICATIONS

1. Polytarchou C, Hatziapostolou M, Yau T, **Christodoulou N**, Hinds P, Kottakis F, Sanidas I, Tsichlis P. “Akt3 induces oxidative stress and DNA damage by activating the NAPDH oxidase via phosphorylation of p47^{phox}”. *Proc Natl Acad Sci USA*, 2020. ***(Impact factor: 9.412).***

2. Monaghan TM, Hatziapostolou M, Yau TO, Seekatz AM, Markham NO, Jilani T, Pomenya O, Roach B, **Christodoulou N**, Birli E, Louie T, Borden L, Kim P, Lee C, Kao D, Polytarchou C. Fecal microbiota transplantation for recurrent Clostridioides difficile infection associates with functional alterations in circulating microRNAs. Gastroenterology, *2021*. **(Impact factor: 20.877).**

3. Monaghan TM, Biswas RN, Nashine RR, Joshi SS, Mullish BH, Seekatz AM, Blanco JM, McDonald JAK, Marchesi JR, Yau TO, **Christodoulou N**, Hatziapostolou M, Pucic-Bakovic M, Vuckovic F, Klicek F, Lauc G, Xue N, Dottorini T, Ambalkar S, Satav A, Polytarchou C, Acharjee A, Kashyap RS. Multiomics Profiling Reveals Signatures of Dysmetabolism in Urban Populations in Central India. Microorganisms, 2021. **(Impact Factor: 4.926).**

4. Tanya M Monaghan; Niharika A. Duggal; Elisa Rosati; Ruth Griffin; Jaime Hughes; Brandi Roach; David Y. Yang; Christopher Wang; Karen Wong; Lynora Saxinger; Maja Pučić-Baković; Frano Vučković; Filip Klicek; Gordan Lauc; Paddy Tighe; Benjamin H. Mullish; Jesus Miguens Blanco; Julie A.K. McDonald; Julian R. Marchesi; Ning Xue; Tania Dottorini; Animesh Acharjee; Andre Franke; Yingrui Li; Gane Ka-Shu Wong; Christos Polytarchou; Tung On Yau; **Niki Christodoulou**; Maria Hatziapostolou; Minkun Wang; Lindsey Russell; Dina H. Kao “A Multi-Factorial Observational Study on Sequential Fecal Microbiota Transplant in Patients with Medically Refractory Clostridioides difficile Infection” *Cells, 2021. (***Impact Factor 7.666*).***

5. Polytarchou C, Hatziapostolou M, Koutsioumpa M, Kottakis F, Mahurkar-Joshi S, Pomenya O, Birli E, **Christodoulou N**, Verspaget HW, Hommes DW, Struhl K, Iliopoulos D. HOTAIR lncRNA-PCAF histone acetyltransferase complex induces colorectal oncogenesis through regulation of a metabolic kinase network. Cancer Cell, *under second revision*. **(Impact factor: 26.602).**

CONFERENCES

1. Monaghan T, Pomenya O, Yau T, **Christodoulou N**, Hatziapostolou M, Jilani T, Kao D, Polytarchou C. "Faecal microbiota transplantation regulates circulating microRNA levels in patients with recurrent Clostridioides infection". DDW session: "*Clostridiodes Difficile* Colitis Pathogenesis, Diagnosis, Management and Therapy", at the San Diego Convention Center, San Diego, CA, May 18-21, 2019. Lecture Presentation.

2. Monaghan T, Jilani T, Frankowski M, Pomenya O, Yau T, **Christodoulou N**, Hatziapostolou M, Wojcik I, Pucic-Bakovic M, Vuckovic F, Louie T, Lauc G, Kao D, Polytarchou C. "Circulating microRNAs linked to immunometabolic traits associate with faecal microbiota transplantation for *Clostridioides difficile* infection". BSG Annual Meeting, Glasgow, June 17-20, 2019.

3. Polytarchou C, Hatziapostolou M, Koutsioumpa M, Kottakis F, Mahurkar-Joshi S, Pomenya O, Birli E, **Christodoulou N**, Verspaget HW, Hommes DW, Struhl K, Iliopoulos D. "A lncRNA-histone acetyltransferase complex induces colorectal oncogenesis through regulation of a metabolic kinase network" at the American Association for Cancer Research (AACR), Virtual Annual Meeting, June 22-24, 2020.

4. **Niki Christodoulou**, Maria Hatziapostolou, Cristina Montiel-Duarte, Elisabetta Verderio Edwards, Philip N. Tsichlis, Christos Polytarchou. "Regulation of microRNA activity by the Akt-IWS1 signalling axis" The PGR STAR conference, NTU, Virtual Meeting June 8-9, 2021. 10-minutes Presentation.

5. **Niki Christodoulou**, Maria Hatziapostolou, Cristina Montiel-Duarte, Elisabetta Verderio Edwards, Philip N. Tsichlis, Christos Polytarchou. "Regulation of microRNAs by Akt-IWS1 signalling axis" at the organising committee of the Gene Regulation and Epigenetics Conference for Early Career Scientists (GREECS), virtual meeting, January 18-19, 2022. Poster Presentation.

6. **Niki Christodoulou**, Maria Hatziapostolou, Cristina Montiel-Duarte, Elisabetta Verderio Edwards, Philip N. Tsichlis, Christos Polytarchou. "The Akt-IWS1 signalling axis regulates microRNA activity" at the American Association for Cancer Research (AACR), Orange County Convention Center Orlando, Florida, April 14-19,2023. Poster Presentation.

Table of Contents

LIST OF TABLES

LIST OF FIGURES

LIST OF ABBREVIATIONS

β-TrCP	β- transducing repeat-containing protein
4E-BP1	4E-binding protein 1
4EHP	cap-binding protein eIF4E-homologous protein
AGO	Argonaute
AKT	AKR mouse T-cell lymphoma
Aly/Ref	Aly-THO complex subunit 4/ Export factor binding protein 1
APC	Adenomatous Polyposis Coli
ARM	Armadillo
AS160	AKT substrate of 160 kDa
ATOH1	Atonal Homolog 1
BAD	BCL2 Associated Agonist of Cell Death
BCAM	Basal cell adhesion molecule
BCL9	B-cell CLL/Lymphoma 9
bHLH	Basic helix-loop-helix
BRCA1	Breast Cancer gene 1
CAC	Colitis-associated colon cancer
CAF1	Chromatin Assembly Factor 1
camKII	Calcium/calmodulin-dependent kinase II
CASP9	Caspase 9
CBC	Crypt Base Columnar
CCR4	C-motif chemokine receptor 4
CCR4-NOT	Carbon catabolite repression 4-negative on TATA-less
CD	Crohn's Disease
CDK2	Cyclin Dependent Kinase 2
Cdx	Caudal type homeobox
CH_3	Methyl group
ChgA	Chromogranin A
CHIP	Chaperone-associated ubiquitin ligase
CIMP	CpG island methylator phenotype
CIN	Chromosomal instability pathway
CK1a	Casein kinase 1a
CLDN4	Claudin 4
CRC	Colorectal cancer
CREB1	cAMP response element binding protein 1

CSF1	Colony Stimulating Factor 1
CTD	C-Terminal Domain
CTHRC1	Collagen triple helix repeat-containing protein 1
CYLD	Cylindromatosis
Dclk1	Double cotrin-like kinase 1
DCP1/2	Decapping mRNA 1/2
DCUN1D1	Defective in Cullin Neddylation 1 Domain Containing 1
DDX6	Dead Box Helicase 6
DEPTOR	DEP-domain containing mTOR-interacting protein
DGCR8	DiGeorge syndrome critical region 8
DLBCL	Diffuse Large B Cell Lymphomas
DNA	Deoxyribonucleic acid
DNMTs	DNA methyltransferases
Dsh	Dishevelled
DSIF	DRB Sensitivity Inducing Factor Spt4/Spt5
DSS	Dextran Sodium Sulphate
DUB	Deubiquitinating enzyme
DUB	Deubiquitinating enzyme
EGFR	Epidermal Growth Factor Receptor
ELF3	E47 like EST Transcription factor 3
Elf4E	Eukaryotic translation initiation factor 4E
Elf4G	Eukaryotic translation initiation factor 4G
EMT	Epithelial-mesenchymal transition
eNOS	Endothelial Nitric Oxide Synthase
EPCAM+	Epithelial cell adhesion molecule positive
ER	Estrogen Receptor
ErbB2	Erb-B2 Receptor Tyrosine kinase 2
ERKs	Extracellular-signal-regulated kinases
ESE1	Enterocyte-specific Ets Transcription Factor
Exp5	Exportin 5
FACS	Flow cytometry
FACT	Facilitates Chromatin Transcription
FANCD2	Fanconi anemia group D2
FGFR2	Fibroblast Growth Factor Receptor 2
fl	Floxed
FMRP	Fragile X mental retardation protein

FOXO1	Forkhead Box O1
Fz	Frizzled
GATA6	GATA binding protein 6
GBM	Glioblastoma
gDNA	Genomic DNA
GFI1	Growth Factor Independent 1
GLI1	Glioma-associated oncogene homolog 1
GLUT1	Glucose Transporter 1
GPCR	G protein coupled receptors
GSK3	Glycogen synthase kinase-3
HCC	Hepatocellular carcinomas
HEAT	Huntingtin, Elongation factor 3, protein phosphatase 2A, TOR1
HES1	Enhancer of split 1
HGSC	High-grade serous ovarian carcinomas
HNF1A	Hepatocyte nuclear factor-1A
HNF1B	Hepatocyte nuclear factor-1B
HNF4A	Hepatocyte nuclear factor 4 alpha
hPMS2	Human post meiotic segregation increased 2
HXK2	Hexokinase 2
IBD	Inflammatory Bowel Disease
IGF-1	Insulin Growth Factor 1
IKKa	Inhibitor of nuclear factor-κB kinase a
INPP5	Inositol polyphosphate-5-phosphatase
IRF5	Interferon regulatory factor 5
ISCs	Intestinal Stem Cells
ISL1	Islet 1
IWS1	Interacts with SUPT6H, CTD assembly factor 1
JAK	c-Jun N-terminal kinases
KDM4B	Lysine Demethylase 4B
KLF4	Kruppel-like factor 4
KO	Knockout
KRAS	Kirsten RAS
LEDGF	Lens Epithelium-derived growth factor
LEDGF	SPT6 and Lens Epithelium-derived growth factor
Let	Lethal
Lgr5	Leucine-rich repeat containing G protein-coupled receptor

lncRNAs	Long ncRNAs
LPS	Liposarcomas
LRIG1	Leucine Rich Repeats And Immunoglobulin Like Domains 1
LRP5/6	Low-density-lipoprotein-related protein 5/6
LYZ	Lysozyme
MAPK	Mitogen-activated protein kinases
MCL1	Myeloid cell leukaemia
MCP1	Motif Chemokine Ligand 2
MDM2	Mouse double minute 2
MED26	Mediator Complex subunit 26
miRNAs/miRs	microRNAs
MLK1	Megakaryoblastic leukaemia 1
mLST8	mammalian lethal with SEC13 protein 8
MMR	Mismatch Repair
MOV10	The Moloney leukaemia Virus 10
MRG15	MORF-related gene on chromosome 15
mRNAs	messenger RNAs
MSI	Microsatellite instability
Msi1	Musashi-1
mTOR	Mammalian target of rapamycin
mTORC2	mTOR Complex 2
MTSS1	Metastasis suppressor 1
MULAN	Mitochondrial E3 Ubiquitin Protein Ligase 1
MYCN	MYCN Proto-oncogene, bHLH transcription factor
NADPH	Nicotinamide adenine dinucleotide phosphate
NBF	Neutral Buffered Formalin
ncRNAs	Noncoding RNAs
NEDD4-1	Neural precursor cell-expressed developmentally downregulated gene 4
NER	Nucleotide excision repair
Neurod1	Neuronal Differentiation 1
Neurog3,Ngn3	Neurogenin 3
NF-κB	Nuclear Factor kappa B
NHEJ	Non homologous end-joining
nt	Nucleotides
NTR	N-terminal region

OCT4	Octamer-binding transcription factor 4
OGT	O-GlcNAc transferase
ORF	Open Reading Frame
PABP	Poly(A)-binding protein 1
PABP	Poly(A)-binding protein
PACT	Protein kinase RNA activator
PAF	Platelet-activating factor
PAZ	PIWI-AGO-Zwille
PCAF	p300/CBP-associated factor
PCAF	p300/CBP-associated factor
PCP	Planar cell polarity pathway
PDCD4	Programmed Cell Death 4
PDK1	PI3K-dependent kinase 1
PDX1	Pancreatic and Duodenal Homeobox 1
PDX1	Pancreatic and duodenal homeobox 1
PFKB2	6-phosphofructo-2kinase/fructose-2,6-Biphosphatase 2
PH	Pleckstrin Homology
PHLPP1/2	PH domain and leucine rich repeat protein phosphatase 1/2
PI (3,4,5) P3	Phosphatidylinositol 3,4,5-trisphosphate
PI (4,5) P2	Phosphatidylinositol 4,5- bisphosphate
PI3K	Phosphatidylinositol 3 Kinase
PIAS1	Protein inhibitor of activated STAT1
PIK3CA	Phosphatidylinositol-4,5-Bisphosphate 3-kinase catalytic subunit Alpha
PIPs	Proinflammatory polyps
piRNAs	P-element induced wimpy testis (PIWI)-interacting RNA
PIWI	P-element induced wimpy testis
PKB	Protein Kinase B
PML	Promyelocytic leukaemia
PP2A	Protein phosphatase 2A
PRAS40	Proline-rich AKT1 Substrate of 40 kDa
Pre-miRNAs	Precursor microRNAs
Pri-miRNAs	Primary microRNAs
PROX1	Prospero Homeobox 1
PRR5/Protor	Proline-rich 5
PRRL5L	Proline-rich 5 like

PTB	Polypyrimidine track binding protein
PTEFb	Positive transcription elongation factor b
PTEN	Phosphatase and Tensin homolog
PTPN1	Protein tyrosine phosphatase nonreceptor type 1
pVHL	Von Hippel-Lindau protein
Pygo	Pygopus
PyMT	Polyoma middle T
RAS	Rat sarcoma virus
Rictor	Rapamycin-insensitive companion of mTOR
RISC	RNA induced Silencing Complex
RNA	Ribonucleic Acid
RNAi	RNA interference
ROS	Reactive oxygen species
RTK	Receptor tyrosine kinases
SAE1	SUMO-activating enzyme subunit 1
SAPKs	Stress-activated protein kinases
SCF	Skp, Cullin, F-box containing complex
SENP1	Sentrin-specific protease 1
Ser	Serine
SETD2	SET domain containing 2
SIN1	Stress-activated protein kinase interacting protein 1
siRNAs	Small interfering RNAs
SIRT1	Sirtuin (silent mating type information regulation 2 homolog) 1
SKP2	S-phase kinase associated protein 2
SMAD4	Smad-related protein 4
snoRNAs	Small nucleolar RNAs
SOCS1	Suppressors of cytokine signalling
SOS1	SOS Ras/Rac Guanine Nucleotide Exchange Factor 1
SOX9	SRY-Box transcription factor 9
Spn1	Suppressor or Post-recruitment gene Number 1
SSC	Saline-sodium citrate
STAT3	Signal transducer and activator of transcription 3
SUPT6H	SPT6 Homolog, Histone Chaperone and Transcription Elongation Factor
TA	Transit Amplifying
TCF/LEF	T-cell specific factor/lymphoid enhancer–binding factor

TCF4	T-Cell Factor 4
TCGA	The Cancer Genome Atlas
TCL1A	T-cell leukaemia/lymphoma protein 1A
TCM	T-central memory
TERT	Telomerase Reverse Transcriptase
TFIIs	Transcription elongation Factor
Thr	Threonine
TLR4	Toll like receptor
TMA	Tissue Microarray
TNBC	Triple negative breast cells
TNRC6	Trinucleotide repeat containing 6
TRAF6	TNF Receptor- Associated Factor 6
TRBP	Transactivation response RNA binding protein
TSC2	Tuberous sclerosis Complex 2
TTC3	Tetracopeptide Repeat Domain 3
UBA2	Ubiquitin-like activating subunit 2
UC	Ulcerative Colitis
UTR	Untranslated regions
Wnt	Wingless-related integration site
XPC	Xeroderma pigmentosum complementation group C
XRN1	Exoribonuclease 1

CHAPTER 1: Introduction

1.1 The AKT Signalling Pathway

AKT (PKB) is a family of three related serine-threonine protein kinases AKT1/PKBα, AKT2/PKBβ and AKT3/PKBγ, which play key signalling roles in all cell types. The AKT kinases contain an N-terminal Pleckstrin Homology (PH) domain, a linker region, a kinase domain, and a C-terminal tail. The three AKT isoforms are encoded by three different but closely related genes. Given their relatedness, the three AKT isoforms exhibit significant overlaps in their regulation and function. However, they also exhibit significant differences. In the absence of activation signals, all three isoforms are enzymatically inactive. Their activation depends on signals that are transduced by phosphatidylinositol 3 Kinase (PI3K), although alternative mechanisms of activation that may be PI3K-independent have also been described. The PI3K/AKT signals regulate membrane, cytoplasmic, nuclear and cytoskeletal processes, including membrane and cytoskeletal dynamics, molecular trafficking, gene expression, DNA replication and repair and other processes involved in the regulation of the cell cycle, intermediary metabolism and the response to stress. By regulating these processes, AKT controls a diverse array of cellular functions, including cell survival, cell migration, proliferation, and differentiation.

AKT activation in all cells depends on PI3K-transduced signals, including receptor tyrosine kinases (RTK), integrins, B and T cell receptors, cytokine receptors and G-protein-coupled receptors (GPCRs) (Hugen *et al.*, 2015). Type I PI3Ks phosphorylate the D3 position of the inositol ring of PI (4,5) P2, to generate PI (3,4,5) P3, which can be dephosphorylated at the D5 position of the inositol ring by Inositol polyphosphate 5 phosphatases (INPP5), to generate PI (4,5) P2. AKT binds via its PH domain these D3 phosphorylated phosphoinositides, and translocates to cell membranes, where it undergoes phosphorylation at two sites, one in the activation loop (Thr308 in AKT1) and one in the carboxy-terminal hydrophobic domain (Ser473 in AKT1). Thr308 phosphorylation is mediated by the PI3K-dependent kinase 1

(PDK1) and Ser473 phosphorylation is mediated primarily by mTOR Complex 2 (mTORC2) (Altomare and Testa, 2005). However, depending on the signal and the cell type, other kinases can also phosphorylate these sites. Activated AKT eventually undergoes dephosphorylation by phosphatases, such as PTEN (Phosphatase and Tensin homologue deleted chromosome ten) and returns to the inactive state. This is a simplified version of the AKT activation cycle. In real life AKT regulation is fine-tuned via additional posttranslational modifications, including phosphorylation at additional sites. The functional role of these additional post-translational modifications, however, is incompletely understood **(Figure 1.1).**

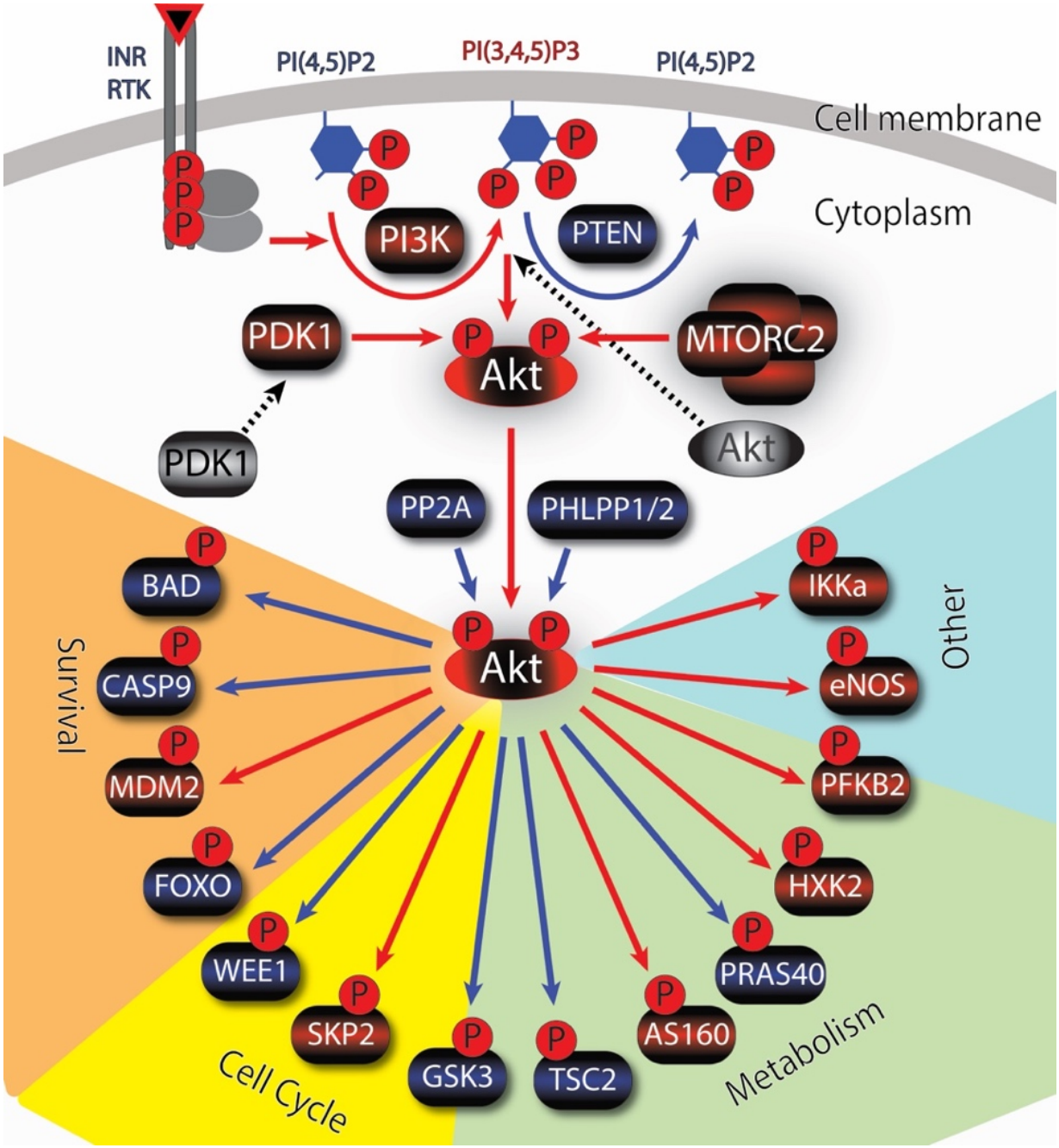

Figure 1. 1: The AKT regulation and function. Schematic representation of the AKT activation mechanisms, and the downstream substrates associated with AKT functions. PI3K activates AKT by converting PI (4,5) P2 to PI (3,4,5) P3. Activation of AKT leads to the phosphorylation of substrate proteins to regulate cell cycle, metabolism and survival. Designed using Adobe Illustrator.

These observations opened up the field of PI3K/AKT signalling because they linked AKT to PI3K, which was known to play an important role in cell physiology but had no other known targets at the time of this discovery. In addition, they revealed the function of the PH domain, and they provided the framework for new studies on the regulation of phosphoinositide metabolism and its role in the regulation of other PI3K-dependent kinases (Chan, Rittenhouse and Tsichlis, 1999). With more than 80,000 publications linking the PI3K/AKT pathway to cell biology, this pathway is important to our basic understanding of the regulation of cell function. Importantly, molecules involved in this pathway represent some of the most promising therapeutic targets for cancer and other human diseases.

The three AKT isoforms mentioned above, are encoded by three different but closely related genes **(Figure 1.2** and **Table *i*)**. Given their relatedness, the three AKT isoforms exhibit significant overlaps in their regulation and function. However, they also exhibit significant differences. These differences became apparent for the first time during the characterization of *AKT1, AKT2* and *AKT3* knockout mice (Iliopoulos *et al.*, 2009).

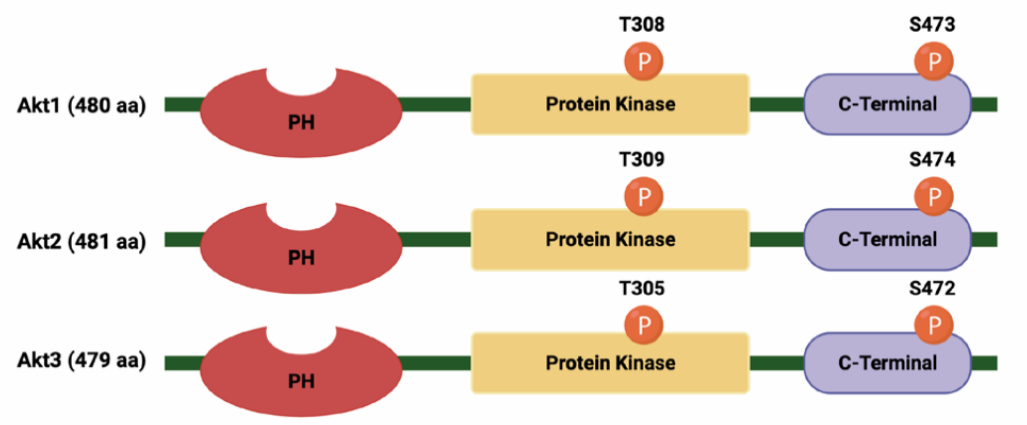

Figure 1. 2: The three AKT proteins. Schematic representation of the AKT isoforms including the Pleckstrin homology domain (PH), the catalytic domain (protein kinase) and the C-Terminal domain and major phosphorylated sites [Threonine (T) and Serine (S)]. Figure designed using BioRender (www.biorender.com).

Table i: AKT genes and proteins

AKT Isoforms	Genomic Locus (Human)	Genomic Locus (Mouse)	Protein Sequence	Protein Homology
AKT1	Chr.14q32	Chr.12qC1	480 aa	AKT1/AKT2 80%
AKT2	Chr.19q13	Chr.12qC1	481 aa	AKT2/AKT3 76%
AKT3	Chr.1q44	Chr.12qC1	479 aa	AKT3/AKT1 84%

1.2 The three AKT isoforms in development

The ablation of AKT1 resulted in significant perinatal lethality that was due to a combination of muscle and adipose tissue defects in the newborn and paucity of milk production by the mother. *Akt1* knockout mice surviving perinatal lethality were characterized by reduced body mass, but they were otherwise phenotypically normal. These mice also displayed increased rates of apoptosis in several tissues and cells from them were more susceptible to DNA damage-induced cell death (Chen *et al.*, 2001). Akt2 knockout mice developed insulin-resistant diabetes, but their body size was normal (Cho *et al.*, 2001) and Akt3 knockout mice had reduced brain mass but no growth defects in other organs (Tschopp *et al.*, 2005). $Akt2^{-/-}/Akt3^{-/-}$ mice were viable and fertile, while $AKT1^{-/-}/AKT2^{-/-}$ mice exhibited perinatal lethality that was due to major defects in muscle and adipose tissue development. Finally, the combination of Akt1 and Akt3 deletion resulted in embryonic lethality at E12.5, which was due to cardiovascular and neural defects. These data combined, suggest that AKT1 is the primary isoform required for development, and that AKT2 and AKT3 can complement its developmental role (Dummler *et al.*, 2006). Whereas the ablation of AKT1 inhibits mammary gland development, both during adolescence and during pregnancy, the ablation of AKT2 promotes it (Maroulakou *et al.*, 2007). However, the differential effects of AKT isoforms in organ development and

oncogenesis are context specific. Thus, whereas AKT1 and AKT2 compete in the mammary gland, they synergize in the hematopoietic system during T cell development (Juntilla *et al.*, 2007).

1.3 The three AKT isoforms in human diseases

AKT was originally identified as the gene transduced by the acute transforming retrovirus AKT8, which was isolated from an AKR mouse T-cell lymphoma. Its isolation from a transforming virus cultured from a murine hematopoietic neoplasm was evidence that *AKT* contributes to oncogenesis, and this has been amply confirmed by a very long list of studies, published over the last 30 years. These studies show that the enzymatic activity of AKT is increased in most tumours, relative to the normal tissues from which the tumours were derived, because of genetic changes, which upregulate the levels of PI3K-generated PtIIns-3-4-5-P3 and PtIIns-3-4-P2. Activated mutations in PI3K and in many receptor and adaptor molecules lead to mutations in other lipid kinases and phosphatases. In a small percentage of human tumours, AKT itself is mutated. The most common mutation is the E17K mutation in the PH domain of AKT, observed in breast cancer, colorectal cancer, ovarian and lung cancer (Wu *et al.*, 2020). In the AKT8 virus from which *AKT* was originally cloned, AKT was activated because it was fused in frame with the retroviral gag gene, which introduced a membrane-targeting myristoylation signal to the N-terminus of the protein. The activation of AKT via fusion with membrane-targeting molecules was also observed recently in human high-grade serous ovarian carcinomas (HGSC). Specifically, in approximately 7% of these tumours, AKT2 is fused in frame with the membrane adhesion molecule BCAM (Basal cell adhesion molecule), giving rise to an AKT2/BCAM hybrid protein, which is membrane-bound, constitutively active and oncogenic (Kannan *et al.*, 2015).

Despite that the three AKT isoforms share mechanisms of activation via PI3K-transduced signals and their biological activities overlap, they have differences, and opposing functional roles. This was first demonstrated in studies addressing the role of AKT in animal models of breast cancer, which showed that AKT1 and AKT2 have opposing roles in both Polyoma middle T (PyMT) and ErbB2-induced mammary oncogenesis, while deletion of AKT3 was phenotypically closer to the wild type (Maroulakou *et al.*, 2008). In a different study, the opposing roles of AKT isoforms were confirmed as AKT1 inhibits cell migration in breast cancer whereas, the AKT2 promotes it (Hinz and Jücker, 2019). Downregulated AKT3 reduces cell motility in PyMT cells (Chung *et al.*, 2013). Other studies have shown that disruption of AKT1 leads to growth retardation leading to a decrease in the sizes of all organs and increased apoptosis and neonatal mortality (Chen *et al.*, 2001; Yang *et al.*, 2003). Moreover, AKT1 deficiency delays tumour progression and suppresses thyroid cancer however, in endothelial cells, it promotes prostate cancer metastasis due to β-catenin activation (Saji *et al.*, 2011; Gao *et al.*, 2018). AKT3 also promote metastasis of prostate cancer however, it inhibits growth and migration of tumour in endothelial cells (Galbraith *et al.*, 2021). Moreover, AKT1 promotes melanoma brain cancer metastasis and regulates negatively the Epithelial-mesenchymal transition (EMT) (Kircher *et al.*, 2019). On the other hand, AKT2 promotes cancer metastasis by inducing EMT (Dong *et al.*, 2019).

1.4 Regulation of AKTs

AKT1 is ubiquitously expressed and is implicated in cell growth and survival, whereas AKT2 is highly expressed in adipocytes and muscles, and it contributes to insulin-mediated regulation of glucose homeostasis (Chen *et al.*, 2001; Cho *et al.*, 2001). AKT3 distribution is expressed mainly in the testes and brain (Yang *et al.*, 2003). The expression of the three AKT isoforms translated into biological

differences between tumours could be due to transcriptional regulation, DNA methylation, RNA stability and translation and protein stability.

The regulation of transcription is under the control of multiple transcription factors whose recruitment to DNA and functional activity depend on epigenetic marks, including DNA methylation, ATP-dependent chromatin remodelling and histone modification that are controlled by epigenetic regulators (Jin *et al.*, 2015). There is a number of studies addressing the transcriptional regulation of AKT, showing that the three isoforms are differentially regulated. One of the factors linked to the differential regulation of AKT1 is Signal Transducer and activator of transcription 3 (STAT3), which is activated by growth factor-initiated signals (Xu *et al.*, 2005), or reactive oxygen species (ROS) (Zhang *et al.*, 2013). STAT3 is the integration point for different tumourigenic signalling pathways, and it regulates the immune response against cancer (Gargalionis, Papavassiliou and Papavassiliou, 2021). STAT3 is activated and promotes cell proliferation, tumour growth, invasion, and migration (Xiong *et al.*, 2008). The binding of RTK, cytokine receptors and GPCRs lead to JAK recruitment, which activates STAT3. Activated STAT3 enters the nucleus and enhances gene transcriptions, which induces specific properties such as cell proliferation, resistance to apoptosis, survival, and angiogenesis. Activated STAT3 binds the AKT1 promoter, and induces AKT1 expression (Park *et al.*, 2005). Another factor which selectively regulates AKT1 transcription is Glioma-associated oncogene homolog 1 (GLI1), a zinc finger protein activated by Hedgehog signalling. The Hedgehog/GLI1 pathway plays a key role in embryonic development and stem cell maintenance by controlling cell- cell interaction and tissue patterning (Pietrobono, Gagliardi and Stecca, 2019). The regulation of AKT1 by GLI1 is relevant to the biology of human cancer as evidenced by the fact that GLI1 expression correlates positively with the expression of AKT1 in Diffuse Large B Cell Lymphomas (DLBCL) (Agarwal *et al.*, 2013). Another direct transcriptional regulator

of AKT1 is Octamer-binding transcription factor 4 (Oct4), a transcription factor involved in stem cell self-renewal and the maintenance of pluripotency. Oct4 is a repressor of AKT1 in embryonal carcinoma cell lines and its phosphorylation relieves the AKT1 repression and promotes stem cell survival and self-renewal (Lin *et al.*, 2012).

AKT2 expression appears to be under the control of TWIST, a basic helix-loop-helix (bHLH) transcription factor, an important inducer of Epithelial to Mesenchymal Transition (EMT). TWIST binds the AKT2 promoter to drive its expression. As a result, the expression of TWIST correlates positively with the expression of AKT2 in late stage of breast cancer and their expression is associated with cancer cell invasion and chemoresistance (Cheng *et al.*, 2007). Early studies shows that AKT3 is expressed at high levels in hormone unresponsive breast and prostate cancer and that its expression in mammary adenocarcinomas may contribute to their clinical aggressiveness and metastatic potential (Nakatani *et al.*, 1999). The overexpression of AKT3, correlates inversely with the expression of the Estrogen Receptor (ER), suggesting that the ER may inhibit AKT3 expression (Nakatani *et al.*, 1999). Despite that these factors may have the potential to regulate the expression of AKT1, AKT2 and AKT3, their contribution to AKT isoform regulation in human cancer is limited.

DNA methylation is a chemical modification by a methyl group ($-CH_3$), which is added on Carbon 5 atom of Cytosine by DNA methyltransferases (DNMTs), resulting in 5-methylcytosine. It can exclusively occur when a cytosine nucleotide is next to a guanine nucleotide and this is known as CpG dinucleotides (Bird, 2002; Jones and Liang, 2009). DNA methylation occurs at CpG dinucleotides and contributes to transcriptional silencing. Histone modifications, such as acetylation, methylation, phosphorylation, ubiquitination, sumoylation and ADP ribosylation are

involved in transcriptional regulation by dictating DNA accessibility, often in association with DNA methylation (Feinberg and Tycko, 2004). Chromatin modifications occur either prior to or after the initiation of transcription. The former regulates the initiation of transcription, while the latter occurs co-transcriptionally and they regulate RNA elongation and RNA processing.

MicroRNAs, small non-coding RNAs, 18 to 25 nucleotides in length, have emerged as major players in the complex network of the regulation of gene expression and they have been implicated in the pathogenesis of human diseases. MicroRNAs target mRNAs and long non-coding RNAs through imperfect base-pairing and regulate gene expression either by mRNA degradation or inhibition of translation (Bartel, 2009; Guo *et al.*, 2010). They commonly target the 3' UTRs of mRNAs, although other mRNA regions may also be targeted. The 3'-UTRs of AKT1, AKT2 and AKT3 harbour microRNA target sequences that are highly conserved among vertebrates, including mammals **(Figure 1.3)**. The conservation of these sequences suggests an evolutionarily ancient regulatory mechanism of AKT isoform expression. The spectrum of expressed microRNAs differs among tissues and among cell types within a given tissue or organ (Hatziapostolou, Polytarchou and Iliopoulos, 2013). Pathologic conditions, including cancer, are also associated with shifts in microRNA profiles, relative to the microRNA profiles of the corresponding normal cells (Calin *et al.*, 2005). Given that each AKT isoform has a unique 3' UTR, their regulation by microRNAs has the potential to induce selective shifts in their expression.

Figure 1. 3: AKT regulation by microRNAs. Highlighted in yellow are the experimentally validated microRNAs found in the literature, whereas the others are based on TargetScan prediction software. Red indicates microRNAs broadly conserved among vertebrates and green poorly conserved among vertebrates and mammals. Figure designed using Abode Illustrator.

The microRNAs targeting AKT1 include miR-495-3p, which targets the AKT1 mRNA at three separate sites, the microRNA cluster miR-302/miR-372/miR-373/miR-520, miR-409-3p, miR-542-3p (Cai *et al.*, 2015), miR-637-3p (Que *et al.*, 2015), miR-153 (Yuan *et al.*, 2015) and miR-9500 (Yoo *et al.*, 2014) (The last three do not appear in Figure 1.3). miR-495-3p targets several regulators of tumour growth, invasion and metastasis and functions as a tumour suppressor in gastric cancer (Eun *et al.*, 2018; Zhang *et al.*, 2022). One of its targets is AKT1, which is downregulated when miR-495-3p is induced. The miR-302/miR-372/miR-373/miR-520 cluster is known to convert human somatic cells into induced pluripotent stem cells (Lin *et al.*, 2008).

Its expression in cervical carcinomas is generally low and exhibits a negative correlation with clinical stage and metastasis. Its targets in cervical carcinoma and GBM cell lines include, in addition to AKT1, PIK3CA, cyclin D1, Defective in Cullin Neddylation 1 domain containing 1 (DCUN1D1) and SOS Ras/Rac Guanine Nucleotide Exchange Factor 1 (SOS1) (Cai, Wang and Zheng, 2013; Cunha *et al.*, 2017). miR-409-3p functions as a tumour suppressor in several types of cancer including gastric cancer, lung adenocarcinoma, bladder and breast cancer. Since one of its targets is AKT1, its downregulation results in AKT1 upregulation. Finally, miR-542-3p, miR-637-3p, miR-153 (Yuan *et al.*, 2015) and miR-9500 (Yoo *et al.*, 2014) also target AKT1. Importantly, the downregulation of miR-542-3p and miR-637-3p correlates with poor prognosis in patients with astrocytoma and glioma. Moreover, miR-153 (Yuan *et al.*, 2015) and miR-9500 (Yoo *et al.*, 2014) are repressed in lung cancer and restoration of their expression downregulates AKT1 and elicits anti-tumour effects.

Examples of microRNAs that target AKT2 include miR-302b (Wang *et al.*, 2014) and miR-612 (Tao *et al.*, 2013). Both are downregulated in primary and metastatic hepatocellular carcinomas (HCC), and their downregulation promotes HCC growth and invasiveness. Other microRNAs specifically targeting AKT2, include members of the miR-29 family (Zhang *et al.*, 2014), miR-194 (Zhao *et al.*, 2014) and miR-184 (Foley *et al.*, 2010). miR-29 family members are repressed in gastric cancer, miR-194 in colorectal cancer and miR-184 in *MYCN*-amplified neuroblastomas, leading to the upregulation of AKT2 in these tumours. MiR-29b is also downregulated in ovarian carcinomas and restoration of its expression results in the downregulation of its targets AKT2 and AKT3 and in inhibition of tumour progression (Teng *et al.*, 2015).

Examples of microRNAs that target AKT3 include miR-15a and miR-16. Both of these microRNAs are downregulated in bone marrow-derived $CD138^{+}$ cells in multiple myeloma, and this results in AKT3 upregulation and cell proliferation (Roccaro *et al.*, 2009). miR-144, which is downregulated in HCC (Ma et al., 2015) and miR-145, which is downregulated in thyroid cancer (Boufraqech *et al.*, 2014), also target AKT3. More importantly, restoring the expression of miR-144 in HCC (Roccaro *et al.*, 2009) and the expression of miR-145 in thyroid carcinomas (Boufraqech *et al.*, 2014), results in the downregulation of AKT3 and inhibition of tumorigenesis.

Ubiquitination is a regulatory protein that plays an important role in protein homeostasis and degradation and regulates the stability and activity of proteins (Suresh *et al.*, 2016). The addition of ubiquitin to the protein is mediated by three enzyme ligases (E1, E2 and E3) (Paccosi, Balzerano and Proietti-De-Santis, 2023). AKT proteolysis is mediated by K48 ubiquitination, which targets AKT to the 26S proteasome, and by autophagy. Ubiquitination is under the control of four E3 ubiquitin ligases of which two, Chaperone-associated ubiquitin ligase (CHIP) (Dickey *et al.*, 2008; Su *et al.*, 2011), and Mitochondrial ubiquitin ligase activator of Nuclear Factor kappa B (NF-κB- MULAN) (Bae *et al.*, 2012) are localized in the cytosol, whereas Breast Cancer gene 1 (BRCA1) (Suizu *et al.*, 2009) and Tetracopeptide Repeat Domain 3 (TTC3) (Xiang *et al.*, 2008) are localized in the nucleus. Among these ubiquitin ligases, MULAN is the only one exhibiting AKT isoform specificity, in that it interacts with and ubiquitinates only at K284 of AKT1 and AKT2 (Bae *et al.*, 2012). In all cases, the ubiquitin ligases target catalytically active AKT, phosphorylated at Thr308 and/or Ser473. There are seven lysine residues (K6, K11, K27, K29, K33, K48 and K63) in the amino acid chain of ubiquitin, where K48 and K63 are the two most common mechanisms of linkage to proteins (Paccosi, Balzerano and Proietti-De-Santis, 2023). K48 ubiquitination is one of the

mechanisms responsible for the termination of AKT activation signals. Briefly, BRCA1 binds phosphorylated AKT and triggers K48-linked ubiquitination and degradation, leading to the oncogenic activation of AKT (Xiang *et al.*, 2008). MULAN also binds to AKT in phosphorylated site, K284, and induces degradation. This regulate negatively the AKT signalling by inducing cell proliferation and migration (Bae *et al.*, 2012). Finally, the two ubiquitin ligases, CHIP and TTC3, after the binding on phosphorylated AKT, they promote proteasomal degradation of AKT leading to the turning off its activity and the downstream responses (Suizu *et al.*, 2009; Su *et al.*, 2011). Inhibition of this activity in several cancers, results in prolonged AKT activation and increased cancer aggressiveness. In 2009, it was discovered that AKT undergoes a K63-linked ubiquitination at K8 and K14 in PH domain through the TNF Receptor- Associated Factor 6 (TRAF6), which orchestrates AKT activation (Yang *et al.*, 2009). Interaction of Lysine Demethylase 4B (KDM4B) with AKT accelerates glucose metabolism and colorectal cancer growth, through the stimulation of TRAF6-mediated K63-linked ubiquitination and AKT activation (Li *et al.*, 2020).

An important regulator of the ubiquitination-dependent degradation of AKT is mTORC2, an mTOR complex containing rapamycin-insensitive companion of mTOR (Rictor), stress-activated protein kinase interacting protein 1 (SIN1), mammalian lethal with SEC13 protein 8 (mLST8, GbetaL), proline-rich 5 (PRR5/Protor), proline-rich 5 like (PRRL5L) and DEP-domain containing mTOR-interacting protein (DEPTOR). mTORC2 has dual opposing roles in the regulation of AKT stability. First, mTORC2 is present in actively translating ribosomes by binding the large ribosomal subunit protein rpL23a, leading to the phosphorylation of AKT co-translationally in the turn motif (Thr450). Phosphorylation of this site inhibits the K48 ubiquitination of AKT and stabilizes the protein. Once released from the ribosome in cells responding to AKT activation signals, AKT is phosphorylated

also by mTORC2, on Ser473 in the C-terminal tail hydrophobic motif. In addition to promoting AKT activation, phosphorylation of AKT on Ser473 also promotes AKT ubiquitination and degradation, unless the AKT kinase is protected by phosphorylation at Thr450, or by binding to HSP90, and/or to the peptidyl/prolyl cis/trans isomerase Pin1 (Facchinetti *et al.*, 2008; Liao *et al.*, 2009).

There is no direct evidence that any of the processes regulating the AKT stability, with the exemption of MULAN-mediated ubiquitination, are AKT isoform-specific. However, since the expression of the three AKT isoforms varies widely between different cell types and between individual tumours, the activity of these pathways may indirectly exhibit AKT isoform specificity.

1.5 Mechanisms of AKT activation and inactivation

The enzymatic activity of AKT isoforms is regulated by growth factors, cytokines, hormones and other extracellular signals, as well as by genotoxic stress and environmental factors, such as hypoxia. These signals increase the abundance of membrane-associated D3 phosphorylated phosphoinositides, by regulating the activity of the PI3K and other lipid kinases and phosphatases. AKT recognizes the D3 phosphorylated phosphoinositides and translocate to membranes where it is phosphorylated on Thr308 and Ser473, in AKT1, and on the corresponding sites in AKT2 and AKT3. Other posttranslational modifications occurring either before or after the membrane translocation, include phosphorylation at additional sites, glycosylation, oxidation, proline hydroxylation, acetylation, ubiquitination and SUMOylation. Some of these modifications contribute to the membrane translocation of AKT, others influence its enzymatic activity and finally other modifications target and inactivate the activated AKT **(Figure 1.1).** By regulating AKT activity, these modifications may contribute to the pathogenesis of various diseases, including obesity, diabetes mellitus, neurodegenerative diseases, and cancer.

The Thr308 phosphorylation site of AKT is dephosphorylated by Protein Phosphatase 2A (PP2A). Structurally, PP2A targets equally all AKT isoforms. However, AKT isoforms may be differentially dephosphorylated because of parallel events that may alter their sensitivity to PP2A. Specifically, mutations at critical residues of one isoform, or small molecules that bind differentially its ATP binding pocket, may differentially affect the ability of PP2A to access the phosphorylated Thr308. In addition, the targeting of AKT by PP2A is modulated by posttranslational modifications, other than phosphorylation, whose abundance on different isoforms may vary significantly. For example, AKT1 and AKT2, undergo proline hydroxylation more efficiently than AKT3. Proline hydroxylated AKT isoforms bind pVHL, which interacts with PP2A. As a result, proline hydroxylated AKT1 and AKT2 should be more sensitive to dephosphorylation by PP2A than AKT3. Ser473 in the C-terminal hydrophobic motif of AKT is selectively dephosphorylated by the PHLPP phosphatases (Gao, Furnari and Newton, 2005) . Interestingly, whereas PHLPP1 selectively dephosphorylates AKT2, PHLPP2 dephosphorylates AKT1, and both dephosphorylate AKT3 (Brognard *et al.*, 2007). As a result, the phosphorylation of protein targets of AKT2 and AKT3 (GSK3α and HDM2), was downregulated by PHLPP1 and the phosphorylation of AKT1 and AKT2 targets (TSC2) and AKT1, AKT2 and AKT3 targets (GSK3β and FOXO1-phosphorylated at Thr24) was downregulated by both PHLPP1 and PHLPP2. Unexpectedly, the phosphorylation of the AKT3 target p27KIP1 was downregulated only by PHLPP2.

1.6 AKT isoform-specific posttranslational modifications

1.6.1 Phosphorylation:

Differences between AKT isoforms at the animal level may be caused by a multitude of mechanisms. Despite that there are phosphorylation sites that are common to all three isoforms of AKT, there are some unique ones for the individual isoform. This was clearly demonstrated in a study, which employed a

nanofluidic proteomics immunoassay to monitor the phosphorylation of AKT1 and AKT2 in insulin-treated isogenic AKT1-/- and AKT2-/- HCT116 cells. Based on this assay, 12 insulin-induced phosphorylation peaks were detected in AKT1 and only 5 in AKT2 (Guo *et al.*, 2014). These data were confirmed with additional studies, which employed a similar assay to detect phosphorylation differences among all three AKT isoforms in breast cancer (Iacovides *et al.*, 2013). The reason for the isoform specificity of some of these phosphorylation events is that the residues that are phosphorylated may be present in only some of the isoforms or the target residues may be present, but they may be selectively phosphorylated in some of the isoforms. Perhaps because sequence differences between isoforms may render the sites in some of the isoforms suboptimal targets of the kinase(s) targeting them.

The isoform specificity of the phosphorylation of some AKT sites is supported by studies focusing on the phosphorylation of these sites and its consequences. One such site is Thr92, whose phosphorylation is AKT1-specific. The phosphorylation of this site, along with the phosphorylation of Thr450 promotes the interaction of AKT1 with the peptidyl-prolyl cis/trans isomerase Pin1 which regulates AKT1 folding, maturation and stability (Facchinetti *et al.*, 2008; Ikenoue *et al.*, 2008; Liao *et al.*, 2009; Oh *et al.*, 2010). Whereas the kinase phosphorylating AKT1 at Thr92 remains elusive, phosphorylation at Thr450 in the Turn motif (TM), is mediated by the mTORC2 kinase complex, which also phosphorylates all AKT isoforms in the hydrophobic motif (HM) (Ser473 in AKT1 and the corresponding sites in AKT2 and AKT3). Another kinase, which may phosphorylate AKT1 at Thr450 in cells exposed to ischemia/hypoxia, is c-Jun N-terminal kinases (JNK). Phosphorylation of this site during hypoxia facilitates the phosphorylation of Thr308 by PDK1 (Shao *et al.*, 2006; Wei *et al.*, 2011).

Ser129, another residue undergoing phosphorylation, is present only in AKT1 and AKT2, but not in AKT3. This site is phosphorylated by casein kinase II (CK2) and its phosphorylation has been linked to AKT activation (Di Maira *et al.*, 2005; Girardi *et al.*, 2014). Although this site is present in both AKT1 and AKT2 however, it appears to be phosphorylated only in AKT1. More important, its phosphorylation appears to determine the selective targeting of paladin by AKT1 (Di Maira *et al.*, 2005). Phosphorylation of Tyr474, promotes the phosphorylation of Thr308, a critical event in AKT activation (Conus *et al.*, 2002). However, since this site is phosphorylated in all AKT isoforms, this form of AKT regulation does not appear to be isoform specific. The phosphorylation of the AKT1 extreme C-terminal residues Ser477 (Ser478 in AKT2 and Ser476 in AKT3) and Thr479 (unique to AKT1), by cyclin-dependent kinase 2 (Cdk2)/cyclin A or mTORC2, activates AKT by either facilitating or compensating for Ser473 phosphorylation (Liu *et al.*, 2014). However, whereas the phosphorylation of AKT at Ser473 (in AKT1), or the corresponding sites in AKT2 and AKT3, promotes AKT activation by driving an interaction between the C-terminal tail and the linker region, the phosphorylation of Ser477 and Thr479 activates AKT1 by promoting an interaction between its C-terminal tail and the activation loop (Chu *et al.*, 2018). Phosphorylation of AKT1 at Ser477/Thr479 fluctuates with the activity of CDK2 during cell cycle progression and promotes cell proliferation.

1.6.2 Proline hydroxylation: Prolyl hydroxylases EglN1, EglN2, and EglN3 are oxygen-sensing enzymes which regulate the levels of hypoxia-inducible factor HIF1α. Upon hydroxylation HIF1a is recognized and ubiquitinated by the Von Hippel Lindau (pVHL) E3 ubiquitin ligase complex. Ubiquitination of HIF1α is followed by proteasomal degradation. Surprisingly, AKT was shown to be constitutively active in pVHL-null tumours and its activation was HIF1α-independent, but Egln1-dependent. EglN1 binds catalytically active phosphorylated AKT1 and AKT2, but

not AKT3 and hydroxylates it at four proline sites. Hydroxylation of Pro125 and Pro313, creates a docking site for the binding of pVHL. The latter interacts with PP2A, whose recruitment results in the dephosphorylation of the phosphorylated Thr308 site, resulting in AKT1 and AKT2 inactivation. Thus, inactivating type 1 mutations in *pVHL*, interfere with AKT1 and AKT2 dephosphorylation, promoting activation (Guo *et al.*, 2016).

1.6.3 Oxidation: Oxidation is a covalent protein modification that is induced either directly by reactive oxygen species (ROS) or indirectly by secondary by-products of oxidative stress. AKT residues targeted for oxidation include several cysteines (Cys60, Cys77, Cys124. Cys297, Cys311), one of which (Cys124) appears to play a major regulatory role in AKT activation. The fact that Cys124 is present only in AKT2, renders AKT2 particularly sensitive to oxidative conditions (Wani, Bharathi, *et al.*, 2011). Growth factor-induced AKT2 oxidation occurs in NADPH oxidase containing endosomes (Wani, Bharathi, *et al.*, 2011) and in the plasma membrane and results in the formation of Cys-Cys disulphide bonds (Wani, Qian, *et al.*, 2011; Klomsiri *et al.*, 2014), which inhibit AKT2 activity. AKT3 also upregulate ROS by promoting mitochondrial biogenesis. Few years ago, we have shown that among AKT isoforms, AKT3 phosphorylates $p47^{phox}$ and activates NAPDH oxidase, leading to ROS induction. AKT3 induces ROS, activates the DNA damage response and upregulates the expression of p53 which is a direct transcriptional target of miR-34 (Polytarchou *et al.*, 2020).

1.6.4 Glycosylation: O-GlcNAcylation is an abundant reversible posttranslational modification that consists in the addition of β-linked *N*-acetylglucosamine to the hydroxyl groups of serine and threonine residues and is catalysed by O-GlcNAc transferase (OGT). The attached moiety is removed by O-GlcNAcase-catalyzed hydrolysis. AKT1 undergoes O-GlcNAcylation at four residues, Ser126, Ser129,

Thr305 and Thr312. O-GlcNAcylation of the latter two residues, disrupts the interaction between AKT1 and PDK1, and suppresses Thr308 phosphorylation (Wang *et al.*, 2012). It has been demonstrated that O-GlcNAcylation of AKT inhibits Thr308 phosphorylation in various cell types (Shi *et al.*, 2012). Other studies suggested that glycosylation also inhibits the nuclear translocation of AKT1 (Gandy, Rountree and Bijur, 2006). While O-GlcNAcylation of AKT1 on Ser473 in murine pancreatic β-cells mitigated phosphorylation, in a mouse model of diabetes (Kang *et al.*, 2008), O-GlcNAcylation of Thr430 and Thr479, a residue unique for AKT1, enhanced Ser473 phosphorylation (Heath *et al.*, 2014). How the interplay between glycosylation and phosphorylation affects the activation of the three AKT isoforms and their functional output in human cancer remains to be determined.

1.6.5 Ubiquitination: Ubiquitination, the covalent attachment of a 70 amino acid peptide via peptide or isopeptide bonds to target proteins, is catalysed by an enzyme system that includes ubiquitin-activating enzymes (E1), ubiquitin-conjugating enzymes (E2) and ubiquitin ligases (E3). With the exemption of linear ubiquitination in which ubiquitin is attached to lysine in the target protein via its N-terminal methionine, ubiquitination involves the attachment of ubiquitin via one of its seven lysines to a lysine in the target. This may consist of the addition of a single ubiquitin molecule (monoubiquitination) or a chain of molecules (polyubiquitination). K48-linked polyubiquitination is a signal for protein degradation via the proteasome, while K63 mono and polyubiquitination regulate target-protein localization, interaction with other molecules and activity. The role of K48 polyubiquitination in AKT stability was discussed in the preceding paragraphs.

IGF-1 (insulin-like growth factor 1) and several cytokines promote AKT polyubiquitination by TRAF6 (tumour-necrosis-factor-receptor-associated factor 6), an E3 ubiquitin ligase. TRAF6 ligates K63-linked polyubiquitin chains to the AKT PH

domain residues K8 and K14 and promotes AKT recruitment to the plasma membrane. Interestingly, TRAF6 catalyses the ubiquitination of AKT1 and AKT2, but not AKT3 (Yang *et al.*, 2009). Epidermal growth factor (EGF) also promotes the K63-linked polyubiquitination of AKT1 and AKT2, but not AKT3. AKT polyubiquitination is also catalysed by the S-Phase Kinase-Associated Protein 2 - Skp, Cullin, F-box containing complex (Skp2-SCF), whose overexpression in HER2-positive human mammary adenocarcinomas promotes the activation of AKT1 and AKT2 and correlates with metastasis, resistance to Herceptin treatment, and poor prognosis (Chan *et al.*, 2012a). The E3 ubiquitin ligase NEDD4-1 also catalyses K63-linked polyubiquitination of AKT at the plasma membrane, in response to IGF-1 or insulin but not EGF or serum. Ubiquitinated phospho-AKT translocates to perinuclear regions and from there, it is released into the cytoplasm, or transported into the nucleus (Fan *et al.*, 2013). K63-linked polyubiquitin chains ligated to AKT K14 are cleaved and removed by cylindromatosis (CYLD), a deubiquitinating enzyme (DUB) which downregulates AKT activity (Lim *et al.*, 2012).

1.6.6 SUMOylation: SUMOylation, the covalent attachment of the SUMO peptide to target proteins, is catalysed by an enzyme system which is primed by ubiquitin-like and sentrin-specific proteases (Ulps and SENPs) that process SUMO to its mature form. The latter is adenylated by the SUMO-activating enzyme subunit 1 (SAE1)-ubiquitin-like activating subunit 2 (UBA2) E1 complex and is transferred to the catalytic cysteine of UBA2. Subsequently, SUMO is transferred to the catalytic cysteine of the E2 conjugating enzyme Ubc9. The Ubc9-mediated transfer of SUMO to target proteins containing the ψKXE motif, can be E3 ligase-independent. Alternatively, it may be facilitated by E3 ligases, which bind Ubc9 and SUMO and may or may not bind the substrate, allowing the SUMOylation of lysine residues in non-consensus sites. De-SUMOylation is catalyzed by Ulp and SENP proteases, which also process SUMO for a new cycle (Yang and Sharrocks, 2010).

SUMO conjugation targets AKT residues K276 (Li *et al.*, 2013; Risso *et al.*, 2013), K301 (Risso et al., 2013), K64, K189 and K182 (De La Cruz-Herrera *et al.*, 2015). Of these sites, K301 is present only in AKT1, and K64, K189 and k182 are present only in AKT1 and AKT3, providing the basis for isoform specificity of the SUMO-dependent AKT regulation. AKT SUMOylation is modulated by the E3 SUMO ligase protein inhibitor of activated STAT1 (PIAS1), which interacts with and promotes the sumoylation of AKT, and by Sentrin-specific protease 1 (SENP1), a key enzyme for SUMO deconjugation. SUMOylation of the K276 site is required for AKT regulation, as mutation of this site completely abolishes AKT activity (Li *et al.*, 2013). The efficiency of AKT SUMOylation can be modulated by cancer-associated mutations of non-SUMOylated residues. Thus, the cancer-associated mutant AKT1 E17K exhibited increased levels of SUMOylation, along with enhanced functional activity.

SUMOylation also regulates AKT trafficking by modulating the AKT interaction with regulatory proteins and downstream targets (Risso *et al.*, 2015). In addition, it regulates other AKT-dependent activities, such as alternative RNA splicing, as evidenced by experiments showing that inhibition of AKT SUMOylation interferes with the alternative RNA splicing of fibronectin and BCL-x (Risso *et al.*, 2013). AKT1 SUMOylation was suppressed by promyelocytic leukaemia (PML). Interestingly, AKT activation resulted in the silencing of *PML,* suggesting that activated AKT may trigger a signalling pathway which results in the repression of PML, thus preventing the suppression of AKT SUMOylation (De La Cruz-Herrera *et al.*, 2015).

1.6.7 Acetylation: Acetylation, the addition of acetyl group on the ε-amino group of lysine, is catalysed by lysine acetyltransferases and is reversed by deacetylases. AKT undergoes acetylation on two PH domain lysines, Lys14 and Lys20, catalysed by two acetyltransferases, p300/CBP-associated factor (PCAF) and p300. Deacetylation is catalysed by Sirtuin-silent mating type information regulation 2

homolog 1 (SIRT1). Lys20 acetylation interferes with the interaction of AKT with PIP3, its translocation to the plasma membrane and its activation by phosphorylation. As a result, it promotes cell death and inhibits tumour formation in xenograft models in nude mice (Sundaresan *et al.*, 2011).

The preceding posttranslational modifications, with the exemption of acetylation, exhibit various degrees of isoform specificity, suggesting potential mechanisms of differential regulation of AKT isoforms. However, even in the absence of specificity, pathways regulating the posttranslational modification of AKT, may give rise to isoform-specific phenotypes, because every tumour exhibits a unique signature of AKT isoform expression.

1.7 AKT isoform-specific regulation of biological processes.

Differences between AKT isoforms in their ability to phosphorylate AKT target proteins and in their ability to regulate the transcriptome will result in differences in the regulation of AKT-dependent basic biological processes.

1.7.1 Gene Expression. Transcription, RNA Processing and mRNA translation

AKTs mediate long-lasting effects on cellular phenotype through the phosphorylation of several transcription factors. AKT phosphorylates members of the forkhead family of transcription factors on Thr24, Ser256, and Ser319 for FOXO1, or the equivalent sites FOXO3a and FOXO4, to facilitate the binding of 14-3-3 and their cytoplasmic sequestration. AKT regulates nuclear factor NFκB and cAMP response element binding protein 1 (CREB1). The binding of accessory proteins upon CREB1 phosphorylation induces the expression of *bcl-2* and *mcl-1* antiapoptotic genes. The opposing effects of AKT1 and AKT2 activity on cancer cell metastatic properties have been associated with the differential phosphorylation of Twist which in turn may interact with a large set of transcription factors and modulate

their activity (King *et al.*, 2004; Puc *et al.*, 2005). AKT2 phosphorylates Twist on Ser42 to promote metastasis, while AKT1 phosphorylates Twist on Thr121 and Ser123, induces its ubiquitination and degradation, and promotes cell proliferation (Jia *et al.*, 2013).

1.7.2 DNA replication and repair

Constitutive or stress-induced AKT activation mediates therapy resistance through induction of DNA double-strand breaks (DNA-DSB) repair. DNA damage sensors (including ATM, ATR, DNA-PK,) are involved in AKT activation. NAD+ depletion downstream of PARP inactivates SIRT1 and derepresses AKT. In parallel, AMP accumulation causes AMPK and AKT activation. AKT phosphorylates p300 at Ser 1834 to induce nucleotide excision repair (NER). Phosphorylated p300 initially acetylates histones to relax heterochromatin and then is degraded to allow damage recognition factors and repair protein recruitment to damaged DNA. AKT phosphorylates the DNA damage checkpoint kinase Chk1 on S280 (Plo *et al.*, 2008; Plo and Lopez, 2009) resulting in its cytoplasmic sequestration and loss of the checkpoint function (Plo and Lopez, 2009) and may contribute to genomic instability. Active AKT downregulates Xeroderma pigmentosum complementation group C (XPC) expression and contributes to oncogenic transformation through the accumulation of mutations. AKT through transcriptional activation of Fanconi Anaemia group D2 (FANCD2), induces the repair of interstrand DNA crosslinks and promotes chemoresistance. AKT1 activity has been associated with human post-meiotic segregation increased 2 (hPMS2), stability and localization. hPMS2 is a MutL-related protein involved in DNA Mismatch Repair (MMR) which corrects errors occurring during DNA replication. Defects of MMR genes result in genomic instability and carcinogenesis. Activated Akt1 binds and induces the degradation of hPMS2. Inversely, its inhibition results in nuclear accumulation of hPMS2 in cancer cells (Xiang *et al.*, 2008).

AKT1 has been linked with the DNA damage response through the sequestration of BRCA1 and RAD51 from the nucleus to the cytoplasm. BRCA1 is involved in homologous recombination an essential process for maintaining genome integrity. AKT1 inhibits BRCA1 recruitment to sites of DNA damage after exposure to ionizing radiation and the control of homologous recombination (Sun *et al.*, 2001). In agreement, cells overexpressing AKT1 have a higher frequency of supernumerary centrosomes (Yang *et al.*, 2006; Chan *et al.*, 2012b). Furthermore, AKT1 suppresses BRCA1 expression (Chan *et al.*, 2012b). AKT1 has been associated with DNA DSB repair in tumour cells. The DNA-dependent protein kinase (DNA-PK) is the key enzyme of nonhomologous end-joining (NHEJ) repair, the predominant process of DNA-Double stranded breaks (DSB) repair (Lal *et al.*, 2009). AKT1, activated downstream of DNA-PK, regulates transcriptionally p21, to inhibit DNA damage-induced apoptosis (Dunham *et al.*, 2012). In agreement, in normal cells, AKT1 activation has been found sufficient to bypass the genotoxic stress G (1)/S checkpoint. Thus, AKT1-mediated G (1)/S transition under genotoxic damage may increase genomic instability (Turner *et al.*, 2015). AKT3 in gliomas has been associated with the expression of a set of DNA repair genes. AKT3 overexpression in human GBM cells, compared to AKT1 and AKT2, enhances the activation of DNA repair proteins, and results in increased DNA repair and resistance to radiation and temozolomide (Liberali, Snijder and Pelkmans, 2014).

1.7.3 Membrane microdomains, vesicular trafficking and cytoskeletal dynamics

Endocytosis and cellular signalling have been previously viewed as separate processes. A map of endocytic membrane trafficking revealed links between AKT2 and endocytic pathways. In cancer cells, AKT2 activity promotes the recruitment of Dynamin 2 during maturation of clathrin-coated pits regulating internalization events

and the lifetime of clathrin-coated pits. Thus, knockdown of Akt2 severely reduces endocytosis (Yoshizaki *et al.*, 2007).

AKT2 regulates the anterograde movement of GLUT4 vesicles along actin to the cell surface. AKT2 upon insulin stimulation phosphorylates myosin 5a and enhances its ability to interact with the actin cytoskeleton and mediate glucose transport (Yamada *et al.*, 2005). Synip, a Syntaxin4 interacting protein, is involved in the docking and fusion of GLUT4 vesicles. Phosphorylation of Synip on Ser99, specifically by AKT2, results in the dissociation of Synip from Syntaxin4 and allows vesicle-membrane fusion (Garofalo *et al.*, 2003; Chin and Toker, 2010).

Palladin localizes in areas of actin stress fiber-dense regions and focal adhesions and controls the organization of actin networks. AKT1 phosphorylates palladin at Ser507 and maintains the organization of actin cytoskeleton thus inhibiting breast cancer cell migration (Garofalo *et al.*, 2003).

1.7.4 Metabolism

AKT plays a major role in metabolic regulation. Specifically, it has been shown to regulate carbohydrate, amino acid, lipid, purine and pyrimidine, redox and energy metabolism. By regulating these metabolic pathways AKT exerts global effects on cell function. For some of the regulatory effects of AKT on metabolism it has been shown that they are isoform-specific, while for others, their specificity if any, has not been adequately addressed. As discussed for other cell functions, AKT regulates metabolism by regulating the expression of metabolic enzymes and their functional partners, and/or the activity of the enzymes. The latter may be the result of direct phosphorylation by AKT. The role of AKT in glycolysis has been associated with GLUT1 trafficking to the cell surface, and activation of phosphofructokinase and hexokinase. AKT promotes glucose uptake and storage through the phosphorylation of GSK-3A at Ser21 and GSK-3B at Ser9 and inhibition of its

activity, resulting in the activation of glycogen synthase. Inactivation of GSK3 promotes cell cycle progression in cancer cells. AKT phosphorylates tuberous sclerosis 2 (TSC2) at Ser939 and activates mTORC1 signalling. mTORC1 activation leads to insulin-stimulated protein synthesis and ribosomal protein synthesis through the phosphorylation of 4E-binding protein 1 (4E-BP1) and P70-S6 kinase 1, promoting cell growth.

AKT isoform specificity is well-established in the regulation of glucose homeostasis. AKT signals, downstream of insulin, induce glucose uptake in muscle and fat tissue and inhibit glucose output in liver to regulate glucose homeostasis. Knockout AKT2 mice, develop glucose intolerance, hyperglycaemia and impaired glucose uptake (Cho *et al.*, 2001; Garofalo *et al.*, 2003). In the same line, a mutation in the catalytic domain of AKT2 results in severe insulin resistance and diabetes in humans (George *et al.*, 2004). Knockdown of AKT2 impairs glucose transport through inhibition of GLUT4 trafficking to the plasma membrane (Jiang *et al.*, 2003; Gonzalez and McGraw, 2009a). The specificity of AKT2 in the control of GLUT4 trafficking has been attributed to differential subcellular localization with increased accumulation of AKT2 at the plasma membrane in response to insulin (Gonzalez and McGraw, 2009a). Membrane recruited AKT2 colocalizes with, phosphorylates (Bruss *et al.*, 2005) and inhibits RabGAP AS160 (TBCD1D4) resulting in the activation of Rab proteins and translocation of GLUT4. AKT1 contributes to the regulation of metabolic signals. AKT1 inhibits the phosphatase activity of protein tyrosine phosphatase nonreceptor type 1 (PTPN1), through its phosphorylation at Ser50, and prolongs the phosphorylation and activity of insulin receptor (Gonzalez and McGraw, 2009a, 2009b; Ji *et al.*, 2014).

1.7.5 Tumour microenvironment and anti-tumour immunity

Tumour growth depends on its vascularization for nutrients and oxygen, while blood vessels consist of the primary route through which cancer cells move to establish distant secondary tumours. Therefore, angiogenesis has occurred as an alternative target for cancer treatment. It has been shown that AKT1 accounts for approximately 75% of the total AKT activity in endothelial cells (ECs) (Chen *et al.*, 2005). AKT1 deficiency impairs the ability of ECs to migrate *in vitro* in response to VEGF (Ackah *et al.*, 2005) and ECM proteins and ex vivo (Ackah *et al.*, 2005; Chen *et al.*, 2005), attributed to defective integrin signalling. *In vivo*, loss of AKT1 has been associated with altered composition of extracellular matrix in tissues and vessel walls and increased vascular permeability (Chen *et al.*, 2005). AKT phosphorylates (S1177) and activates endothelial Nitric Oxide Synthase (eNOS) to regulate vasodilation and blood vessel maturation (Dimmeler *et al.*, 1999). In tumors grown in Akt1 KO mice, blood vessels appear smaller and immature, attributed to the deficiency in active (eNOS) (Chen *et al.*, 2005). Loss of AKT1, but not AKT2, *in vivo* suppresses edema formation under acute inflammation due to a reduced influx of neutrophils and monocytes at the site of injury. This phenomenon has been attributed to the reduction in vascular permeability rather than an effect on inflammatory cells (Di Lorenzo *et al.*, 2009).

AKT1 and AKT2 have been assigned complementary roles in the regulation of CD8+ T-central memory (TCM) cells, important mediators of antitumor immunity. AKT1 and AKT2, but not AKT3, drive the terminal differentiation of CD8+ T cells. The inhibition of AKT1 and AKT2, enhances their proliferative ability and survival, delays exhaustion and preserves naïve TCM cells. Thus, AKT1 and AKT2 inhibition may enhance the therapeutic properties of CD8+ TCM and improve tumour immune response (Eid *et al.*, 2015).

Macrophages are major effectors of the immune response and play an important role in tumorigenesis and metastasis. AKT1 KO macrophages are highly responsive to LPS and AKT1 KO mice do not develop endotoxin tolerance *in vivo*. This has been attributed to the deregulation of two microRNAs, let-7e and miR-155. These two microRNAs target TLR4 and SOCS1, respectively, two genes involved in the regulation of endotoxin sensitivity and tolerance. In AKT1 KO macrophages restoration of microRNA levels is sufficient to induce sensitivity and tolerance to LPS *in vitro* and *in vivo* (Androulidaki *et al.*, 2010). AKT1 KO mice are more sensitive while AKT2 KO mice are more resistant to LPS-induced endotoxin shock and chemically induced colitis. This effect associates with the M1 and M2 polarization of macrophages, respectively. miR-155 and its target C/EBPβ mediate the M2 polarization in AKT2 KO macrophages (Arranz *et al.*, 2012). Interferon regulatory factor 5 (IRF5) regulates inflammatory M1 macrophage polarization in human macrophages. IRF5-dependent activation of AKT2 signalling is required for M1 macrophage polarization, expression of glycolytic genes and HIF1A (Hedl, Yan and Abraham, 2016). On the other hand, disruption of AKT2 expression inhibits colony-stimulating factor 1 (CSF1) and Monocyte Chemoattractant Protein-1 (MCP1) induced macrophage chemotaxis. AKT2 suppression reduces Lim domain kinase 1 (LIMK/Cofilin) phosphorylation, contributing to defects in actin polymerization and chemotaxis (Zhang, Ma, *et al.*, 2009).

AKT2, but not AKT1 or AKT3, plays an important role in regulating neutrophil recruitment and neutrophil-platelet interactions during vascular inflammation. The effects of Akt2 are attributed to the regulation of β2-integrin interaction and intracellular Ca2+ mobilization during neutrophil activation (Li *et al.*, 2014).

Interferons through the stimulation of NK cells tumour infiltration and the induction of MHCs and antigen presentation by dendritic cells play a significant role in cancer

biology. AKT1 regulates the response to interferon or viral infection. Phosphorylation of EMSY (Ser209) by AKT1 is required for full activation of a subset of interferon-stimulated genes while AKT2 has minimal or no effect (Arboleda *et al.*, 2003).

1.7.6 Integration of AKT-dependent functional changes in cancer cells

1.7.6.1 Cell growth: Akt has been characterized as proto-oncogene due to its pro-survival and cell growth properties. The first stems from the phosphorylation and inactivation of pro-apoptotic effectors such as the BCL-2 antagonist of cell death (BAD), caspase 9, and forkhead box class O (FOXO) transcription factors. The second relates to the phosphorylation of TSC2, an inhibitory component of mTORC2, and the activation of mTOR. However, other than the differential phosphorylation of some of these targets assessed by phosphoproteomic analyses, isoform-specific information does not exist.

Genetic mouse models have provided the first solid evidence of the AKT isoforms unequal contribution to tumour initiation and growth. AKT1 deletion inhibits, whereas Akt2 deletion accelerates, PyMT and ErbB2-driven mammary mouse adenocarcinomas (Juntilla *et al.*, 2007). In the same line, AKT1 deletion, or even single allele deletion, inhibits the development of tumours in Pten+/− mice in the prostate, endometrium, and small intestine (Chen *et al.*, 2006) whereas AKT2 deletion has minor or no effects on prostate, endometrial, intestinal cancer in the same mouse model (Xu *et al.*, 2012). AKT1, but not AKT2 or AKT3, deletion prevents lung tumorigenesis in carcinogen-induced and K-Ras genetic mouse models of lung carcinogenesis. Interestingly, Akt3 deletion increases tumour incidence and tumour size in the same models (Hollander *et al.*, 2011). Similarly, in a viral oncogene-induced mouse model of lung cancer, AKT1 deletion significantly delays, whereas AKT2 deficiency dramatically accelerates the initiation of tumour

growth and AKT3 has minor effects (Linnerth-Petrik *et al.*, 2014). In the IGF-IR-driven lung cancer mouse model, loss of AKT1 inhibits while loss of AKT2 enhances lung tumour development. Akt2 enhanced tumours phenocopy the expression of several genes (Actc1, Bpifa1, Mmp2, Ntrk2, Scgb3a2) involved in human lung cancer. The differential role of AKT1 and 2 is further supported by the demonstration that a pan-Akt inhibitor (MK-2206) is less efficient than an AKT1-specifc inhibitor (A-674563) in suppressing human lung cancer cell survival (Elizabeth Franks *et al.*, 2016).

IWS1 phosphorylation by AKT3 and AKT1, but not AKT2, has been shown to regulate RNA splicing. In human lung cancer, IWS1 phosphorylation regulates the alternative splicing of FGFR-2 and contributes to oncogenesis at least through the amplification of FGF-2 signalling. Interruption of IWS1 phosphorylation suppresses the proliferation, migration and invasiveness of tumour cells both in culture and animals (Sanidas *et al.*, 2014).

The combinational deletion of AKT1 and AKT2 has been shown to inhibit carcinogen (DEN)-induced liver cancer but resulted in the early onset of spontaneous hepatocarcinogenesis. This effect was attributed to hepatocyte cell death-induced inflammation and STAT3 activation by cytokines in the double-knockout surviving cells (Wang *et al.*, 2016). This finding challenges the prospects of pan-Akt inhibitors in systemic cancer therapy.

1.7.6.2 Cell cycle: The role of AKT family in cell cycle regulation has been attributed to the inhibition of cyclin dependent kinase inhibitors p27 Kip1 and p21 Waf1/Cip1 and protection of cyclin D1 from GSK-3β mediated degradation.

The distinct roles of AKT1 and AKT2 have been demonstrated in both non-transformed and transformed mammalian cells. Inhibition of AKT1 suppresses

cyclin A and cycle entry to the S-phase. In contrast, AKT2 overexpression inhibits M/G1 transition through binding to the cyclin-dependent kinase inhibitor p21, a modulator of cell cycle transition. Interestingly, p21 phosphorylation (T145) by AKT1 prevents AKT2 binding, whereas AKT2 binding prevents AKT1-mediated p21 phosphorylation (Héron-Milhavet *et al.*, 2006). In the same line, during mouse PyMT-induced mammary oncogenesis knockout of AKT1 associates with lower cyclin D1 expression, while AKT2 knockout with increased cyclin D1 levels, compared to wild type mice (Juntilla *et al.*, 2007). In agreement, in a panel of NSCLC cell lines, it was shown that an AKT1-specific inhibitor, A-674563, is more efficient in suppressing NSCLC cell survival and cell cycle progression compared to a pan-AKT inhibitor (MK-2206) (Chorner and Moorehead, 2018).

In TNBC cell lines, AKT3 regulates the growth *in vitro* and the ability to form tumors *in vivo* through the regulation of p27 cell-cycle inhibitor (Chin *et al.*, 2014). AKT3, highly expressed in a subset of ovarian cancers, modulates G2/M transition in ovarian cancer cell lines, concomitant with reduced phosphorylation on the inhibitory site (Tyr15) of Cdc2 (Cristiano *et al.*, 2006).

1.7.6.3 Invasion/metastasis: AKT1 and AKT2 have been attributed opposing roles in cancer cell migration, invasion and metastasis. AKT2 enhances cell motility and invasiveness whereas Akt1 opposes them (Arboleda *et al.*, 2003; Hutchinson *et al.*, 2004; Irie *et al.*, 2005; Liu *et al.*, 2006; Iliopoulos *et al.*, 2009; Chin and Toker, 2010). AKT2 induces the expression of β1 integrins and promotes breast and ovarian cancer cell invasion and metastasis (Arboleda *et al.*, 2003). While AKT2 accelerates, AKT1 suppresses ErbB2-induced breast tumour invasion (Hutchinson *et al.*, 2004; Iliopoulos *et al.*, 2009). AKT2 is required for chemotaxis and invasion of breast cancer (Hutchinson *et al.*, 2004; Irie *et al.*, 2005; Yoeli-Lerner *et al.*, 2005; Liu *et al.*, 2006; J. Wang *et al.*, 2008; Iliopoulos *et al.*, 2009) and glioma cells (Zhang,

Gu, *et al.*, 2009). Mechanistically, the inhibitory effects of AKT1 have been attributed to the degradation of the transcription factor Nuclear Factor of Activated T cells (NFAT) (Yoeli-Lerner *et al.*, 2005), the regulation Tuberous Sclerosis Complex 2 (TSC2) (Liu *et al.*, 2006) and extracellular signal-regulated kinase/mitogen-activated protein kinase (ERK/MAPK) pathways (Irie *et al.*, 2005). AKT1/AKT2 balance has been shown to regulate the epithelial-mesenchymal transition (EMT), a characteristic of tumour-initiating cells and an important premetastatic step in cancer cells (Irie *et al.*, 2005; Iliopoulos *et al.*, 2009). AKT2, but not AKT1, suppresses the expression of miR-200 family resulting in the activation of transcription factors ZEB1/2 and suppression of E-cadherin. The Akt2/miR-200/ZEB/E-cadherin axis is active in human breast cancer, regulates EMT and stem-cell properties *in vitro* and invasiveness of mammary adenocarcinomas *in vivo* (Iliopoulos *et al.*, 2009). In agreement, AKT2 silencing in CRC cells inhibited the development of liver lesions/metastases in an orthotopic CRC mouse model, whereas AKT1 deficiency had no effect. Expression analysis of human metastatic genes identified the scaffolding protein metastasis suppressor 1 (MTSS1) as a novel gene involved in the pro-metastatic effects of AKT2 (Agarwal *et al.*, 2013).

1.8 Target specificity of the three AKT isoforms

In 2014, Sanidas and colleagues performed a phosphoproteomics screen to determine whether the functional differences between AKT1, AKT2 and AKT3 are due to signalling differences. Specifically, they used isogenic cell lines expressing one AKT isoform at a time and a phosphoproteomic analysis was performed where 606 AKT targets were identified to be phosphorylated by at least one AKT isoform **(Figure 1.4).** Also, the results revealed significant differences between the phosphoproteomes of cells expressing AKT1, AKT2 or AKT3, supporting the hypothesis that signalling differences contribute to the functional differences between isoforms (Sanidas *et al.*, 2014). One of the differentially regulated functions

was the post-transcriptional processing of mRNA (Moore and Proudfoot, 2009). IWS1 (interacts with SUPT6H, CTD assembly factor 1) was one of the targets found to be phosphorylated by AKT3 and AKT1. The isoform specificity of IWS1 was confirmed by *in vitro* kinase assays. AKT promotes tumour growth by activating IWS1. The preferential phosphorylation of IWS1 by two AKT isoforms in *in vitro* kinase assays may be caused by subtle structural differences, or by differences in posttranslational modification and/or binding partners between isoforms (Moore and Proudfoot, 2009).

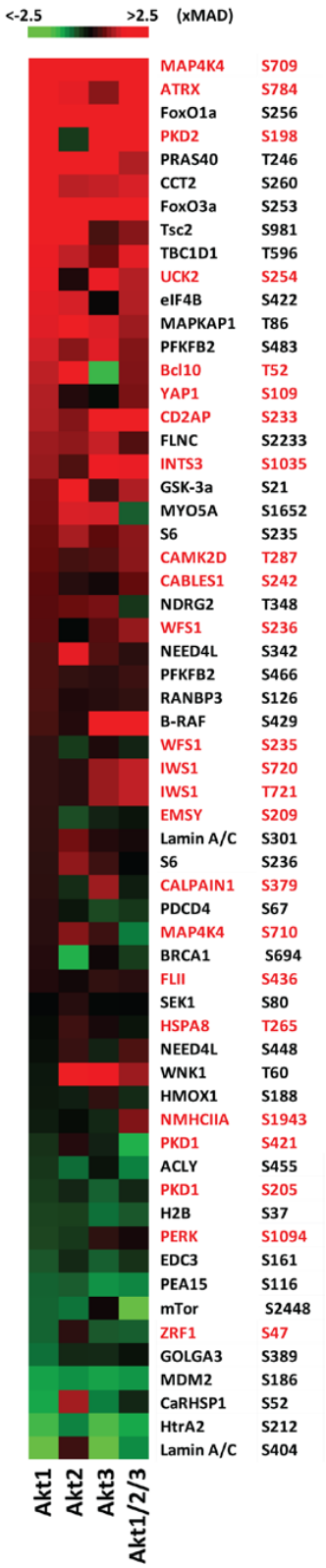

Figure 1. 4: Phosphoproteomic screen analysis of AKT isoform-expressing cells. Heatmap of the abundance of phosphorylation of known AKT phosphorylation substrates (Black) and new substrates identified in the screen (Red) and the respective phosphorylated residue, in cells expressing in AKT1, AKT2 or AKT3-expressing cells and their combination *(Sanidas* et al.*, 2014)*.

1.9 IWS1 is phosphorylated by AKT

IWS1 is a protein involved in the regulation of RNA metabolism, specifically in mRNA splicing and export. It was originally identified in the yeast *Saccharomyces Cerevisiae* through its interaction with Spt6 (Krogan *et al.*, 2003). The function of IWS1 requires the association with Spt6. Spt6 is a histone H3/H4 chaperone which binds the C terminal domain (CTD) of RNA polymerase II (RNAP II) (Yoh *et al.*, 2007; Duina, 2011). SPT6/IWS1 complex interacts with two proteins Aly-THO complex subunit 4, and export factor binding protein 1 (Aly/REF) and SET domain containing 2, histone lysine methyltransferase (SETD2). Aly/REF is an adaptor involved in nucleocytoplasmic RNA transport and SETD2 is a histone trimethyl transferase. Also, SPT6/IWS1 complex contribute to alternative RNA splicing and RNA transport (Yoh *et al.*, 2007; Yoh, Lucas and Jones, 2008). IWS1 is phosphorylated at Ser720/Thr721 by AKT3 and AKT1 but not AKT2. Phosphorylation by AKT3 and AKT1 at these sites, regulates transcriptional elongation and catalyse multiple processes in RNA processing (Sanidas *et al.*, 2014; Oqani *et al.*, 2019), transcriptional elongation or both (Sanidas *et al.*, 2014).

IWS1-mediated transcription elongation is an important regulator in the pathobiology of retroperitoneal liposarcomas (LPS) in an AKT-dependent manner, which implicates IWS1 as an important molecular target to treat LPS. It has been shown that phosphorylation of IWS1 by AKT promotes the maintenance of cancer stem cells in LPS and contributes to a metastable cell phenotype. Moreover, the expression of phosphorylated IWS1 promotes growth, migration, invasion and tumour metastasis (Wang *et al.*, 2023).

1.10 Non-Coding RNAs

The central dogma of molecular biology states that genetic information encoded in DNA is transcribed by RNA polymerase, to messenger RNA (mRNA), which is then translated to protein by ribosomes (Li and Xie, 2011). Some years ago, unique non-coding RNAs (ncRNAs) were discovered as “junk” transcriptional products (Saw *et al.*, 2021). A large part of the genome, is transcribed into RNA but, lacks protein-coding information and thus, is never translated. These are known as non-coding RNAs (ncRNAs) and their main function is to regulate gene expression at transcriptional and post-transcriptional levels (Bertrand-Lehouillier, Legault and McGraw, 2018). ncRNAs are divided into two groups, according to their size. Short/small ncRNAs, that are less than 200 nucleotides (nt) in length, (<30nt) include microRNAs (miRNAs, miRs), small interfering RNAs (siRNAs), P-element induced wimpy testis (PIWI)-interacting RNA (piRNAs) and small nucleolar RNAs (snoRNAs). ncRNAs longer than 200nt in length, are known as long ncRNAs (lncRNAs) (Bartel, 2004; Siomi *et al.*, 2011; Derrien *et al.*, 2012). In the last years, various studies have shown that ncRNAs play an important role in epigenetic processes (Amaral *et al.*, 2008; Costa, 2008).

1.11 microRNAs

microRNAs (miRNAs) are endogenous, small single-stranded non-coding RNAs (18-25 nucleotides) that regulate gene expression at the post-transcriptional level, either through degradation or inhibition of translation of mRNAs. microRNAs are master regulators of gene expression which control many physiological and pathological processes, by binding in the 3’ Untranslated region (3’UTR) of target mRNAs (Guo *et al.*, 2010; Polytarchou *et al.*, 2015). In 1993, Ambros and Ruvkun groups discovered the first microRNA, lin-4 in *Caenorhabditis elegans (C.elegans)* (Wightman, Ha and Ruvkun, 1993; Feinbaum, Ambros and Lee, 2004). They found that lin-4, a non-protein coding gene, produces a single-stranded RNA molecule,

about 22 nt long. They validated that lin-4 binds to complementary regions in the 3'-UTR of lin-14 mRNA, which is involved in early larval development stages. Inhibition of lin-14 translation and protein levels were suppressed by lin-4 (Wightman, Ha and Ruvkun, 1993; Feinbaum, Ambros and Lee, 2004). In 2000, seven years later, another microRNA was identified in C. elegans (Reinhart *et al.*, 2000). lethal-7 (Let-7) was identified as a regulatory RNA that is involved in gene expression. Since then, various microRNAs have been identified in other species and this led scientists to study microRNAs in more depth. Nowadays, numerous microRNAs from different species are validated and registered in the miRbase online website (https://www.mirbase.org/), along with their targets (Griffiths-Jones *et al.*, 2008). It is believed that microRNAs regulate 1/3 of the genes in the genome and are clustered within the introns of protein-coding and non-coding genes as well as within the exons of the non-coding genes (Wang, 2008).

1.12 microRNA processing-biogenesis

The microRNA pathway is a critical mechanism to control gene expression. Since the first microRNAs discovery, researchers focused on the biogenesis and maturation of microRNAs (Graves and Zeng, 2012). There are two pathways involved in the biogenesis of microRNAs, the canonical and non-canonical pathway. Most microRNAs are generated by RNA polymerase II transcripts, which are cleaved in two steps. One is mediated in the nucleus by the endoribonucleases Drosha together with DiGeorge syndrome critical region 8 Gene (DGCR8) proteins and the second by the endoribonuclease Dicer in the cytoplasm (La Rocca *et al.*, 2015; Michlewski and Cáceres, 2019). Drosha is responsible for the initiation of the microRNA's maturation process. Specifically, the long hairpin primary microRNAs (pri-miRNAs) after cleavage by Drosha, produce ~85 nt stem-loop structures, known as the precursor microRNAs (pre-miRNAs) (Lee *et al.*, 2003; Peng and Croce, 2016). Pre-miRNAs are subsequently transported from the nucleus to the cytoplasm

by an Exportin-5 (Exp-5) -dependent mechanism, where Dicer together with TAR RNA-binding protein/ Protein Activator of Protein kinase R (TRBP/PACT) proteins, cleave pre-miRNAs into a ~20-22 nt double-stranded mature microRNAs (Peng and Croce, 2016). The small RNA duplex guide strands loaded onto Argonaute (AGO) proteins to form the RNA-induced silencing complex (RISC), to regulate the translation of complementary mRNAs. RISC is responsible for gene silencing, known as RNA interference (RNAi). Mature microRNAs recognise the 3'-UTR complementary sequence of mRNAs and induce gene silencing either via mRNA degradation, mRNA cleavage or by inhibition of translation (Joshua-Tor and Hannon, 2011; Reddy, 2015). In the non-canonical pathway, the same protein complexes with different combinations are involved. **Figure 1.5** shows the microRNA biogenesis pathway.

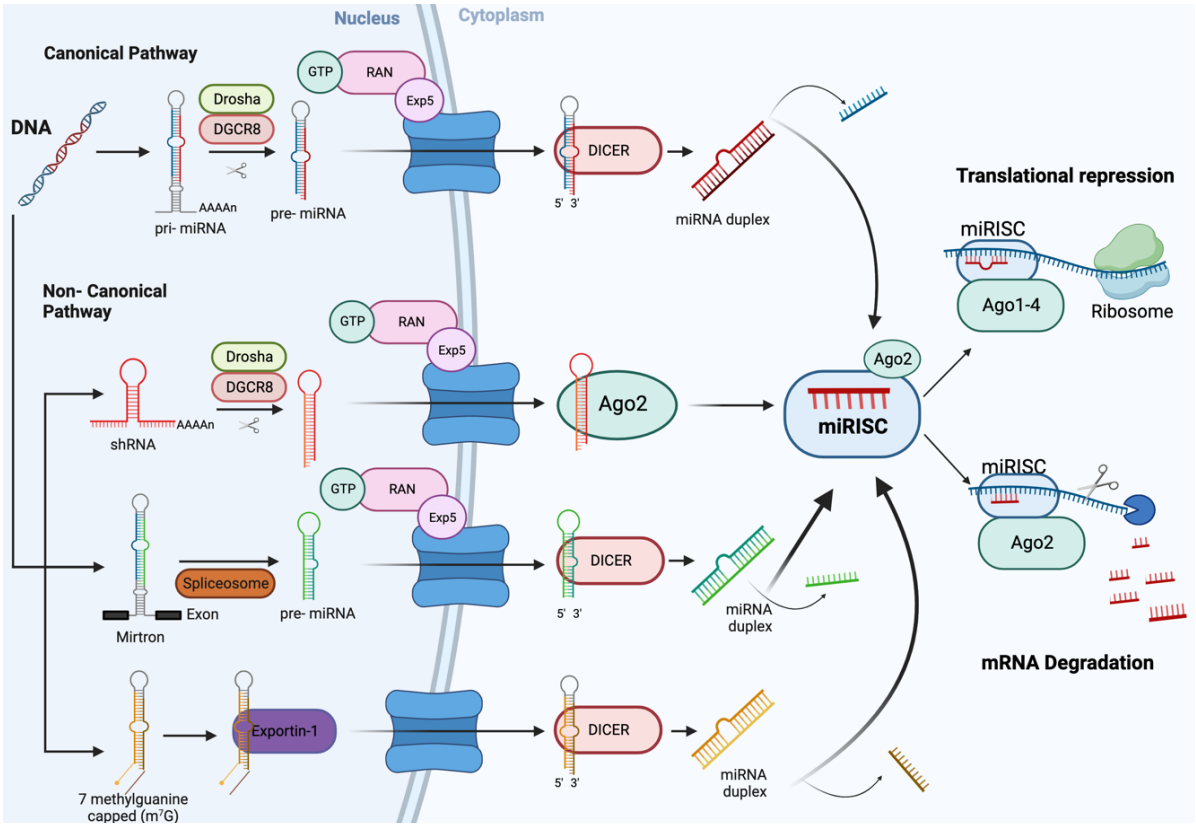

Figure 1. 5: microRNAs biogenesis and mechanisms of action. In the canonical pathway, transcription of microRNAs genes by RNA polymerase II produces pri-miRNAs transcripts which are cleaved by the Drosha-DGCR8 complex to form pre-miRNAs. The pre-miRNAs are transported from the nucleus to the cytoplasm by Exportin 5, where cleavage by the Dicer-TRBP complex produces microRNAs duplexes. One strand (5p or 3p) is loaded into AGO family of proteins to form the RISC, which suppresses target mRNAs by translational repression or degradation. In the non-canonical pathways, small hairpin RNA (shRNA) is initially cleaved by Drosha-DGCR8 complex and exported to the cytoplasm. They are processed via AGO2-dependent but Dicer-independent cleavage. On the other hand, mirtrons after spliceosome are exported to the cytoplasm via Exportin5 and m^7G via Exportin1. All pathways lead to RISC complex which suppresses target mRNAs by translational repression or degradation. Designed using BioRender (www.biorender.com).

1.13 Functions of microRNAs

The general function of microRNAs is to regulate gene expression, in many physiological and pathological processes, by the complementary binding to the 3'UTR of targeted mRNAs. microRNA target regulation occurs post-transcriptionally by miRNA: mRNA formation. This leads to inhibition of translation, mRNA degradation, or mRNA cleavage (Joshua-Tor and Hannon, 2011; Reddy, 2015). microRNAs play an important role in the development process, including metabolism, apoptosis, and cell proliferation. microRNA dysregulation has been associated with human diseases, including cancer and inflammation (Calin and Croce, 2006; Orellana and Kasinski, 2015).

1.14 The RNA-induced silencing complex (RISC)

A small RNA together with a member of AGO protein family forms the RISC, a family of molecular complexes that target genes for silencing by RNA cleavage, by prevention of protein synthesis, transcriptional repression, or by triggering chromatin remodelling (MacRae *et al.*, 2008; Pratt and MacRae, 2009). Briefly, a small RNA duplex is integrated into an AGO protein, during the loading step, where the pre-RISC complex is formed. Following that, in the maturation step, one strand of the duplex is ejected from AGO whereas, the other one remains bound to AGO, to form mature RISC (Iwakawa and Tomari, 2022). The mature RISC binds target mRNAs, complementary to the guide strand to regulate gene expression. Human RISC is composed of three proteins, AGO2, Dicer, and the transactivation response RNA binding protein (TRBP) (Chendrimada *et al.*, 2005). AGO2 is an RNA-binding protein and the main effector of RNA-silencing pathways, with a central role in microRNA maturation and activity. It can modulate chromatin remodelling, gene transcription regulation, and RNA splicing (Tarallo *et al.*, 2017). Dicer is a riboendonuclease with a critical role in the regulation of microRNA biogenesis and

other small RNAs (Song and Rossi, 2017). It cleaves double-stranded RNAs into small interfering RNAs (siRNAs) and miRNA precursors (pre-miRNAs) into microRNAs (Koscianska, Starega-Roslan and Krzyzosiak, 2011). TRBP contains three double-stranded, RNA binding domains and it is an essential component of Dicer-containing complex (Chendrimada *et al.*, 2005). TRBP is essential for the recruitment of AGO2 to the small RNAs bound by Dicer. Knockdown of TRBP in human cells, results in lower levels of microRNAs, suggesting that the absence of TRBP reduces the stability of Dicer (Chendrimada *et al.*, 2005).

In human RISC, protein kinase RNA activator (PACT) can also modify and enhance RISC function in gene silencing. PACT is associated with Dicer-AGO2-TRBP complex and is important in RNA silencing (Lee *et al.*, 2006). TRBP and PACT interact together and associate with Dicer to enable the cleavage of double-stranded RNAs (Kok *et al.*, 2007). During the last years, RISC has been characterised in more detail and its important role in the microRNA regulation in gene expression was evaluated. However, little is known about its role in regulating the activity of microRNAs.

1.15 The AGO family

AGO protein family was discovered in 1998 in a plant mutagenesis screen, performed to identify new genes in Arabidopsis thaliana (Bohmert *et al.*, 1998). Later it was found that AGOs are conserved throughout evolution (Swarts *et al.*, 2014). They are ~100kDa proteins and composed of four different functional core domains, the N- Terminal domain, the PIWI-AGO-Zwille (PAZ) domain, the middle (MID) domain, the PIWI domain two linkers (L1 and L2) (Iwakawa and Tomari, 2022). L1 connects the N-Terminal and PAZ domains whereas, the L2 reinforces the N-terminal-L1-PAZ structure and connects it with MID-PIWI domains (Wang, 2008; Nakanishi, 2016; Iwakawa and Tomari, 2022). PIWI and PAZ contribute to the

recognition of the Dicer bound microRNA duplex, where PAZ domain recognises the RNase III digested end of the microRNA duplex (Song *et al.*, 2003; Lingel and Izaurralde, 2004; Ma *et al.*, 2005) and the PIWI domain interacts with Dicer (Tahabaz *et al.*, 2004). PIWI domain has a similar structure to RNAse H and is critical for the endonuclease cleavage activity of RISC (Ma *et al.*, 2005). Finally, the MID domain binds the 5' phosphate of the microRNA and attaches it to the RISC (Parker, Roe and Barford, 2005). Four AGO family proteins have been identified in humans, but only AGO2 is catalytically active with the PIWI domain as the catalytic centre (Hauptmann *et al.*, 2015).

1.16 Regulation of RISC

Once the small RNA duplex is bound to AGO, the passenger strand is ejected, and the guide strand forms the mature RISC **(Figure 1.5)**. The mature RISC binds target mRNAs complementary to its guide leading to gene silencing either by translational repression and/ or degradation and cleavage. This depends on the complementarity of guide-targets and the set of other effectors recruited by the AGO family member (Iwakawa and Tomari, 2022).

In RISC the small RNAs are divided into 4 domains, the seed (nt 2-8), the central (nt 9-12), the 3' supplementary (nt 13-17) and the tail (nt 18-3'end) region **(Figure 1.6).** The seed region is important for the recognition of target RNAs, the central region is critical for the cleavage of the passenger strand and the target RNAs. The supplementary region stabilizes target binding and the tail region regulates the recruitment of other factors and determines the fate of RISC (Chandradoss *et al.*, 2015; Iwakawa and Tomari, 2022). RISC pre-organizes the first segment of seed region (nt 2-5) into alpha helix to find targets and increase the rate of binding (Chandradoss *et al.*, 2015; Salomon *et al.*, 2015). In humans, helix-7 blocks the

access to nt 6-8 suggesting that it repositions the 3' supplementary region for further target recognition (Schirle, Sheu-Gruttadauria and MacRae, 2014).

The position and the number of target sites also affects the RISC binding and the silencing efficiency. Generally, microRNAs binding the 3' UTR sites are more effective than those binding the 5' UTR or the open reading frame (ORF) (Moretti, Thermann and Hentze, 2010). This is due to the balance between the time needed for RISC to perform its function and the time for translocating ribosomes, to remove RISC from the mRNA (Iwakawa and Tomari, 2022). As mentioned earlier, the number of target sites also affects the RISC binding and the silencing of efficiency, with each binding site acting individually, and the additive silencing effects. If there are two binding sites in proximity, the efficiency exceeds the expected repression (Grimson *et al.*, 2007). Translational repression is the most predominant type of gene silencing by RISC. Recently, it was suggested that translational repression is not only a step in mRNA degradation, but it also has an important physiological role (Mayya *et al.*, 2021). microRNA-mediated translational repression is a complicated process not fully understood. There are several mechanisms by which RISC represses translation including the inhibition of translation initiation.

RISC blocks protein-protein interactions between the initiation factors eukaryotic translation initiation factor 4E and 4G (eIF4E and eIF4G). These factors are required to form a competent pre-initiation complex on the target mRNA (Duchaine and Fabian, 2019). After translation arrest, the RISC promotes mRNA deadenylation, decapping and 5'-3' degradation. Carbon catabolite repression 4- negative on TATA-less (CCR4-NOT) deadenylase complex initiates the microRNA-mediated deadenylation. CCR4-NOT is associated with RISC through the interaction of GW182 with CNOT1. CNOT1 is the largest subunit in the CCR4-NOT complex (Braun *et al.*, 2011; Fabian *et al.*, 2011). After their interaction, Decapping mRNA 2

(DCP2), a decapping enzyme and its associated stimulatory factors including DEAD-Box Helicase 6 (DDX6), removed the 5' cap. The decapped microRNA targets are then degraded (Rouya *et al.*, 2014). DDX6 has a key role in translational repression and the mRNA decapping activation (Carroll, Munchel and Weis, 2011). Recently, it has been found that 4E-T, an eIF4E binding protein that interact with DDX6, and the cap-binding protein eIF4E-homologous protein (4EHP) are also involved in microRNA-mediated translational repression (Mayya *et al.*, 2021; Iwakawa and Tomari, 2022).

Another mechanism involves the poly(A)-binding protein (PABP) displacement from the poly(A) tail of the mRNA (Fabian *et al.*, 2009). Briefly, PABP bound to the 3' poly(A) tail, increases translation initiation by stabilizing the association of the translation initiation complex eIF4F to the 5' cap structure through its interaction with eIF4G (Kahvejian *et al.*, 2005; Iwakawa and Tomari, 2022). The PABP-eIF4G interaction induces a closed-loop structure that promotes ribosome recycling and the initiation of translation (Kahvejian *et al.*, 2005; Sonenberg and Hinnebusch, 2009). Finally, RISC promotes PABP dissociation from poly (A) tail targeted mRNAs to inhibit initiation of translation (Moretti *et al.*, 2012).

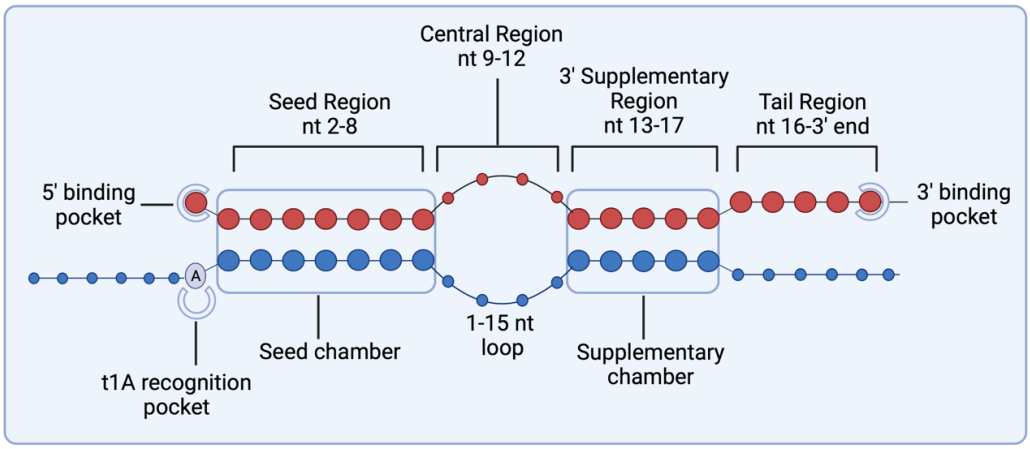

Figure 1. 6: Target recognition by RISC. A schematic representation of the base pairing between the guide and target strands. The diagram shows the 4 functional domains formed by the guide strand after the RISC assembly with their corresponding nucleotides (nt) nucleotides included in each region from 5' end of the guided strand. The figure was adapted/modified from Iwakawa and Tomari, 2022.

1.17 AGO2 protein interactions

AGO2 is important in the small RNA-guided gene silencing process. As described above, one strand of microRNA is loaded into AGO2 and enables microRNAs to downregulate partially complementary target mRNAs (Müller, Fazi and Ciaudo, 2020). AGO proteins and microRNAs are localized in processing bodies (P-bodies) (Liu *et al.*, 2005; Sen and Blau, 2005). P-bodies are cytoplasmic foci which contain untranslated mRNAs that provide sites of microRNA-induced degradation (Liu *et al.*, 2005; Teixeira *et al.*, 2005; Ma *et al.*, 2015) and play an important role in the cytoplasmic regulation of mRNAs (Teixeira *et al.*, 2005). Trinucleotide repeat containing 6 (TNRC6) proteins TNRC6A/GW182, TNRC6B and TNRC6C act as docking factors to bind AGO proteins for the initiation of translational repression and target degradation (Liu *et al.*, 2005; Rehwinkel *et al.*, 2005). AGO2 colocalize with TNRC6B in cytoplasmic P-bodies. TNRC6B is a protein homologous to GW182, which regulates microRNA function at the level of RISC (Meister *et al.*, 2005; La Rocca *et al.*, 2015). GW182 is characterized by multiple repeats of glycine (G) and

tryptophan (W) (Yao *et al.*, 2011). Furthermore, AGO2 interacts with GW182 through GW182 contains multiple binding sites for AGO2 (Takimoto, Wakiyama and Yokoyama, 2009). This interaction of AGO2/GW182 is important for the colocalization of AGO2 into GW bodies which are cytoplasmic structures linked to mRNA decay (Eystathioy *et al.*, 2003; Yang *et al.*, 2004). The Moloney leukaemia Virus 10 (MOV10) and Fragile X mental retardation protein (FMRP) regulate AGO2 association with microRNA recognition elements (Kenny *et al.*, 2014). FMRP, an RNA binding protein, controls the translation of bound mRNAs through a microRNA-mediated suppression mechanism (Muddashetty *et al.*, 2011; Kenny *et al.*, 2014). Like FMRP, MOV10 an RNA helicase, is implicated in microRNA-mediated translational suppression (Banerjee, Neveu and Kosik, 2009; Sievers *et al.*, 2012). By blocking AGO2 binding, MOV10 increases the expression of bound RNAs (Kenny *et al.*, 2014).

1.18 IWS1

(Interactor With SUPT6H, CTD Assembly Factor 1 (IWS1) is an essential transcription elongation factor, involved in mRNA splicing and nuclear export (Yoh *et al.*, 2007; Yoh, Lucas and Jones, 2008), with conserved sequence from yeast to humans. IWS1 in yeast is known as Suppressor or Post-recruitment gene Number 1 (Spn1) (Fischbeck, Kraemer and Stargell, 2002). It was originally discovered in the yeast *Saccharomyces cerevisiae* through its direct interaction with Spt6 (Krogan *et al.*, 2003). The Human IWS1 interacts with SUPT6H (Yoh *et al.*, 2007). Spt6 is associated with transcription elongation of many genes, mediated by RNA Polymerase II (RNAP II) (Yoh *et al.*, 2007; Ardehali *et al.*, 2009) and functions as a histone H3:H4 chaperone to alter chromatin structure during transcription by depositing nucleosomes (Bortvin and Winston, 1996; Kaplan, Laprade and Winston, 2003; Adkins and Tyler, 2006; Duina, 2011; Dronamraju *et al.*, 2018).

1.19 Structure and Function of IWS1

Human IWS1 homolog is encoded in chromosome 2q14.3 and the protein is composed of 819 amino acids, whereas, the Mouse *Iws1* homolog is located in chromosome 18 and protein is composed of 766 amino acids. The N-terminal region (NTR) of IWS1 is highly acidic (residues 1-495) and the 262 amino-acid domains (amino acids 523-819) at the C-terminus are highly conserved (Ling, Smith and Morgan, 2006; Liu *et al.*, 2007). Part of the conserved region of the C-Terminal Domain (CTD) of IWS1 is homologous with the NTR (Domain I) of the transcription elongation Factor II (TFIIs) are related domains in Elongin A and Mediator Complex subunit 26 (MED26) (Ling, Smith and Morgan, 2006; Orlacchio *et al.*, 2018). This conserved TFIIs sequence is known as LW motif due to the invariant Leucine and Tryptophan residues and is required for transcriptional regulation and RNA processing (Ling, Smith and Morgan, 2006; Orlacchio *et al.*, 2018). Crystallographic analysis of Iws1 in *Saccharomyces cerevisiae* and *Encephalitozoon cuniculi* identified two binding subdomains, Huntingtin, Elongation factor 3, protein phosphatase 2A, TOR1 (HEAT) and Armadillo (ARM). The HEAT subdomain recognises large negatively charged ions and phosphoproteins, in addition to the Spt6-independent function of IWS1, whereas the ARM subdomain recognises the NTR of Spt6 (Diebold *et al.*, 2010; Pujari *et al.*, 2010). IWS1 is a multifunctional transcription elongation factor, whose activities depend on its interaction with several proteins involved in the regulation of transcription and RNA processing. Spt6-IWS1 complex contributes to alternative RNA splicing and nuclear export (Yoh *et al.*, 2007; Yoh, Lucas and Jones, 2008). Moreover, IWS1 is essential for mammalian cell proliferation (Liu *et al.*, 2007) and in the embryonic development (Orlacchio *et al.*, 2018), through its involvment in genome activation, lineage specification and histone modification (Oqani *et al.*, 2019).

1.19.1 Transcription Elongation

Transcription produces the mRNAs, which are subsequently used as a template for gene expression. In Transcription elongation, RNAP II moves along the template DNA strand and codes for the mRNA (Clancy and Brown, 2008). Transcription Elongation is a complex process where various factors are involved in the regulation of the catalytic activity of RNAP II (Liu *et al.*, 2007). RNAP II is regulated by different factors including TFIIS, DRB Sensitivity Inducing Factor Spt4/Spt5 (DSIF), Facilitates Chromatin Transcription (FACT) and Platelet-activating factor (PAF) (Sims, Belotserkovskaya and Reinberg, 2004). Elongation factors control the rate of elongation or the processivity of RNAP II enabling transcription through nucleosomes or by reactivating RNAP II whose activity had been blocked by various defects (Wind and Reines, 2000; Sims, Belotserkovskaya and Reinberg, 2004). For the transcription, histone chaperones including FACT, SPT6 and Lens Epithelium-derived growth factor (LEDGF) control the structure of nucleosomal DNA during elongation and for efficient transcription elongation, super elongation complex, positive transcription elongation factor b (P-TEFb) and Mediator are required (Peterlin and Price, 2006; Takahashi *et al.*, 2011; Liu *et al.*, 2020; Cermakova *et al.*, 2021). Disruption of transcription elongation is implicated in cancer, in the deregulation of immune response and in developmental defects (Adelman *et al.*, 2009; Bai *et al.*, 2010; Miller *et al.*, 2017). IWS1 has been implicated in transcriptional elongation, by interacting with RNAP II and its activity depends on the interaction with other proteins involved in the regulation of transcription and RNA processing.

IWS1 interacts with Spt6 which acts as a histone H3 chaperone and binds histones, assembles nucleosomes and remodels chromatin, and has an important role in elongation (Bortvin and Winston, 1996; Andrulis *et al.*, 2000). Spt6 binds the CTD of RNAP II and phosphorylates Ser2, the primary target for phosphorylation, by p-

TEFb, which recruits a methyltransferase that mediates trimethylation of histone H3 at Lysate 36 (H3K36me3) in genes (Yoh *et al.*, 2007). Following the recruitment of p-TEFb, other components of the elongation complex are loaded onto the CTD. Phosphorylated Ser2 in CTD serves as a scaffold for pre-mRNA splicing, mRNA export and chromatin modification factors, which are essential for chromatin during transcription elongation.

1.19.2 Nuclear Export and RNA splicing

Spt6-IWS1 complex is associated with two proteins, Aly-THO complex subunit 4 and export factor binding protein (Aly/REF) and SET domain containing 2 (SETD2). Aly/REF is an RNA export factor that contributes to nucleocytoplasmic RNA transport and RNA splicing, whereas SETD2 acts as a histone H3 trimethyltransferase (Yoh *et al.*, 2007; Yoh, Lucas and Jones, 2008). IWS1 interacts directly with Aly/REF, and both, IWS1 and Aly/REF, recognise the same region of Spt6, implying that Spt6 recognise Aly/REF through its interaction with IWS1 (Yoh et al., 2007). IWS1 binds RNAP II, through Spt6. Spt6-IWS1 complex functions as an adaptor for the assembly of the transcriptional elongation complex. IWS1 interacts directly with Spt6 and REF1/Aly, after binding with the RNAP II elongation complex. IWS1 interacts with Spt6 and SETD2, to recruit RNAP II to the coding region of active genes for elongation, dependent on H3K36me3. This interaction regulates mRNA export and histone modification (Yoh, Lucas and Jones, 2008).

IWS1 regulates alternative splicing on specific genes by modifying the recruitment and activity of splicing factors (Sanidas *et al.*, 2014; Oqani *et al.*, 2019). Splicing is a key mechanism that promotes the maturation of mRNAs within pre-mRNA (Lee and Blenis, 2014). It is estimated that 90% of metazoan genes are alternatively spliced (E. T. Wang *et al.*, 2008). Alternative splicing regulation depends on the interplay of cis-acting RNA elements such as intronic and exonic splicing enhancers, with trans-acting splicing factors and epigenetic modifications (Chen and Manley,

2009; Luco *et al.*, 2011; Tang *et al.*, 2020). Regulation of RNA splicing plays an important role in differentiation and the development of various diseases (Kalsotra and Cooper, 2011). Disruptions of RNA splicing generally attributed to mutations in cos and trans-splicing elements or altered expression of splicing factors can lead to neurodegenerative diseases and cancers (Cooper, Wan and Dreyfuss, 2009; Coltri, dos Santos and da Silva, 2019).

In 2014, Sanidas and colleagues has found that phosphorylation of IWS1 at Ser720/Thr721 by AKT3 and AKT1 is required for the recruitment of SETD2 to Spt6-IWS1-ALY/REF complex. During transcription, H3K36 is trimethylated by SETD2 and alternative RNA splicing is initiated. After trimethylation of H3K36, a docking site for MORF-related gene on chromosome 15 (MRG15) and polypyrimidine track binding protein (PTB) is formed, which regulates the alternative splicing of FGF receptor-2 (FGFR-2). FGFR-2 is a gene that undergoes alternative splicing during development and cancer. Alternative splicing of FGFR2 generates the IIIb and IIIc isoforms. The IIIc isoform has been linked to FGF2-mediated cell migration, invasion and Epithelial-Mesenchymal Transition (EMT). IWS1 knockdown reduces the binding of MRG15 and PTB and their binding is restored by wild-type IWS1 (Ser720/Thr721) but not the phosphorylation-deficient mutant (Ala720/Ala721). SETD2 regulates the alternative splicing of FGFR-2 in an IWS1 phosphorylation-dependent manner **(Figure 1.7).** Thus, Akt isoform-dependent phosphorylation of IWS1 is essential for RNA processing and promotes cancer cell proliferation, through the regulation of RNA splicing (Sanidas *et al.*, 2014). Importantly, the role of IWS1 in microRNA regulation has not been identified or studied before.

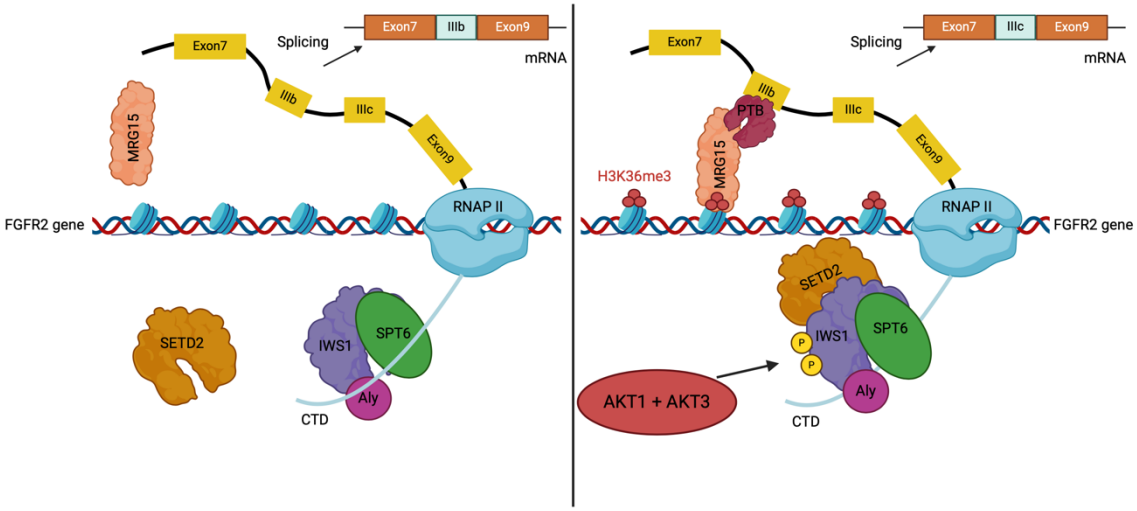

Figure 1. 7: Regulation of FGFR-2 alternative splicing by IWS1 phosphorylation at Ser720/Thr721 by AKT1/AKT3. Phosphorylation of IWS1 attracts SETD2, which trimethylates H3K36 and the PTB-IIIb exon binding promotes exclusion of this exon from the spliced transcript. The figure was adapted from Sanidas et al., 2014 and modified using BioRender (www.biorender.com).

1.20 General aims

Our working hypothesis is that IWS1 interacts with RISC and regulates the activity of microRNAs, upon phosphorylation by AKT. This interaction mediates the effect of IWS1 on intestinal cell properties and its role in intestinal inflammation and cancer.

The aims of this study are to:

i. To investigate the role of IWS1 in microRNA regulation.
ii. To characterise the mechanism of microRNA activity regulation by the AKT/IWS1 axis.
iii. To investigate the role of IWS1 in intestinal stem cell maintenance and differentiation in health and disease.

CHAPTER 2: Materials and Methods

2.1 Materials

2.1.1 Chemicals and Reagents

Table ii: List of Chemicals and reagents used in this study

Reagents	Product Code	Supplier
0.4% Trypan Blue Stain	T10282	Life Technologies
0.5M, EDTA	15575-038	Invitrogen
0.5M, EDTA-DEPC Treated	BP2483-100	Thermo Fisher Scientific
1% Triton X-100	T9284	Sigma Aldrich
1.5M, TRIS-Base Buffer pH 8.8	J831	VWR
10% Sodium dodecyl sulphate (SDS)	BP2436	Fisher Bioreagent
10x RIPA Buffer	9806S	Cell Signalling Technology
10x Running Buffer (Tris-Glycine-SDS, TGS)	BP1341-4	Fisher Bioreagents
10x TBE Buffer	15581044	Invitrogen
10x TBS (Tris Buffered Saline, pH 7.4)	BP2471-1	Fisher Bioreagents
1M, Dithiothreitol (DTT)	327190	Acros Organics
1M, HEPES	BP299	Thermo Fisher Scientific
1M, TRIS-Base Buffer pH 6.8	A4987	AppliChem
1M, Tris-HCl pH 6.8	T1819	Sigma Aldrich
1M, Tris-HCl pH 7.4	T2194	Sigma Aldrich
30% Acrylamide/Bisacrylamide 37.5:1	J61505.K2	Thermo Fisher Scientific
50x TAE (Tris -Acetate-EDTA)	BP1332-1	Fisher Bioreagents
Agarose	R0491	Thermo Fisher Scientific
Ammonium Persulphate (APS)	A3678	Sigma Aldrich
Ampicillin Sodium Salt	BP1760-5	Thermo Fisher Scientific
Bovine Serum Albumin (BSA)	BP9702-100	Thermo Fisher Scientific
Bromophenol Blue	B0126	Sigma Aldrich
Chloroform	0219400290	Thermo Fisher Scientific

Complete, Mini, EDTA-free Protease Inhibitor Cocktail	11836170001	EMD-Millipore
DEPC (Dienthylpyrocarbonate)	A0881	PanReac AppliChem
DNA ladder (100bp)	N3232S	New England Biolab (NEB)
DNA ladder (1kb)	N3132S	New England Biolab (NEB)
dNTPs	N0446S	New England Biolab (NEB)
ECL Plus Western Blotting substrate	32132	Thermo Scientific
EDTA (Ethylenediaminetetraacetic acid)	E6758	Sigma Aldrich
Ethanol 200 proof	BP2818-4	Fisher BioReagents
Ethanol Absolut	BP2818500	Fisher BioReagents
Eukitt Mounting medium	03989	Sigma Aldrich
Gel Red Nucleic acid	41003	Biotium
Glycerol	G5516	Sigma Aldrich
Glycine	G7126	Sigma Aldrich
HyClone Water, Molecular Biology Grade	SH3053802	Ge Healthcare Bio-Science
Hydrochloric Acid (HCL)	320331	Sigma Aldrich
Isopropanol	BP2618-4	Thermo Fisher Scientific
Kanamycin Sulfate	11815-024	Thermo Fisher Scientific
LB Agar	BP1425	Thermo Fisher Scientific
LB Broth	BP1426	Thermo Fisher Scientific
Magnesium Chloride (MgCl)	M8266	Sigma Aldrich
Methanol	M/4000/17	Fisher Chemical
NP-40	CA-630	Sigma Aldrich
Nuclear Fast Red	H-3403	Vector Laboratories
Phosphatase Inhibitor Mini tablets	A32957	Thermo Scientific
Pierce BCA Protein Assay Kit	23225	Thermo Scientific
Potassium Chloride (KCl)	P9333	Sigma Aldrich

Protease inhibitor Mini Tablets	A32955	Thermo Scientific
Protein Ladder	1610374	Bio-Rad
PVDF Transfer membrane	IPVH00010	Merck
RNAase Inhibitor	R1158-10KU	Sigma Aldrich
S.O.C Medium	15544034	Invitrogen
SFCA Syringe Filters	431220	Corning
Sodium Chloride (NaCl)	S5150	Sigma Aldrich
Sodium Hydroxide	221465	Sigma Aldrich
Sterile Syringe Filter, PVDF 0,1 µm	SLVV033RS	Merck
Sucrose	S0389	Sigma Aldrich
TEMED (N,N,N,N-Tetramethylenediamine)	17919	Thermo Fisher Scientific
Trizma Base	T6066	Sigma Aldrich
Trizol Reagent	15596026	Invitrogen
Tween-20	P1379	Thermo Fisher Scientific
WhatMan	3030-335	Cytiva
Xylene	158770025	Acros Organics

Table iii: Tissue Culture consumables.

Reagents	Product Code	Supplier
0.25% Trypsin-EDTA, phenol Red	25200056	Gibco
Blasticidin	ant-bl-05	InvivoGen
DEAE-Dextran Hydrochloride	30461	Sigma Aldrich
Dimethyl Sulfoxide (DMSO)	D4540	Sigma Aldrich
Dulbecco's Modified Eagle's Medium (DMEM) High Glucose	11995073	Gibco
Dulbecco's phosphate-buffered saline (DPBS)	14040091	Gibco
Fetal Bovine Serum (FBS)	10270106	Gibco
FuGene6	E2691	Promega
G418 disulfate Salt Solution	G8168	Sigma Aldrich
Hygromycin B solution (50mg/ml in PBS)	Sc-29067	ChemCruz
L-Glutamine	25030024	Gibco
Lipofectamine 3000	L3000008	Invitrogen
Lipofectamine RNAimax	13778150	Invitrogen
MEM Non-Essential Amino Acid solution (NEAA)	11140050	Gibco
Opti-MEM Reduce Serum Medium	51985026	Gibco
Penicillin-Streptomycin (5,000 U/mL)	15070063	Gibco
Plasmocin- Mycoplasma Elimination Reagent	Ant-mpp	InvivoGen
Puromycin Dihydrochloride	A11138-03	Invitrogen

2.1.2 Plasticware

All plastics used were sterilized and all glassware was washed out and sterilized using an autoclave before use.

Table iv: List of plasticware used in this study.

Consumables	Product code	Supplier
Sterile Syringes (2ml)	BD 300928	BD
Sterile Syringes (5ml)	BD 309050	BD
Sterile Syringes (10ml)	14955459	Fisher Scientific
Needles and 1ml Sterile syringes	BD303176	BD
Screw cap tube (15ml)	62.554.502	Sarstedt
Falcon Tubes (15ml)	352096	Corning
Falcon Tubes (50ml)	352098	Corning
Sterile Polysterene Serological pipets (1ml)	86.1251.001	Sarstedt
Sterile Polysterene Serological pipets (5ml)	86.1253.001	Sarstedt
Sterile Polysterene Serological pipets (10ml)	86.1254.001	Sarstedt
Sterile Polysterene Serological pipets (25ml)	86.1685.001	Sarstedt
RNase-free Microfuge Tubes	AM12450	Invitrogen
Microcentrifuge tubes (1.5ml)	11532293	Fisherbrand
Microcentrifuge tubes (2ml)	11558252	Fisherbrand
96-well white plates	136101	Thermo Scientific
96-well transparent plates	353070	Corning
6-well plates	3533224	Corning
12-well plates	353043	Falcon
Cell Culture plates (60mm)	430166	Corning
Cell culture plates (100mm)	430167	Corning
Cell Culture plates (150mm)	430599	Corning
PCR tubes	N8010580	Applied Biosystems
PCR caps	N8010535	Applied Biosystems
Cryovials	5000-0020	Thermo Scientific
Cell lifters	11577692	Fisherbrand
Cell Spreaders	15625467	Fisherbrand
Cell Counting Chamber Slides	C10228	Invitrogen

Pipette Tips (1000µl)	9032	Corning
Filter Pipette Tips (0.1-2µl)	70.1130.212	Sarstedt
Filter Pipette Tips (1-30µl)	70.1116.210	Sarstedt
Filter Pipette Tips (200µl)	70.760.211	Sarstedt
Filter Pipette Tips (1000µl)	70.3050.255	Sarstedt
Towerpack refill (0.1-10µl)	F167201	Gilson
Gel loading tips	11927734	Fisherbrand
Tip Stations (0.1-10µl)	4143	Corning
Tip Stations (1-200µl)	4144	Corning
PCR 384-well plates	HSP3801	BioRad
PCR plate sealing	MSB1001	BioRad

2.1.3 Laboratory Equipment

Table v: List of laboratory equipment.

Instrument	Company
Digital Vortex mixer	VWR
Laboratory Centrifuge LMC-3000 – for plates	Grant-bio
Heraeus Megafuge 16R Centrifuge	Thermo Scientific
Eppendorf Refrigerated Centrifuge	Eppendorf
EVOS microscopy	Life Technologies
Leica	Biosystems
Cell Counter- Countess II FL	Invitrogen
Water bath Isotemp GPD05	Fisher Scientific
HeatBlock	Fisher Scientific
BB 15 CO_2 Incubator	Thermo Scientific
S220 Focused-ultrasonicator	Covaris
NanoDrop 8-sample spectrophotometer	Labtech
Thermal cycler Applied Biosystems ProFlex PCR System	Thermo Fisher Scientific
CFX384 real-time PCR detection system	BioRad
IncuCyte S3 Live Cell Analysis System	Essen Bioscience
BioPlex 200 System	BioRad
NanoString	NanoString Technologies
CLARIOstar plate reader	BMG Labtech
GeoMX DSP Spatial Genomics	NanoString Technologies

2.1.4 Software

Table vi: List of software used.

Program/Software	*URL*
Venny 2.1.0	*https://bioinfogp.cnb.csic.es/tools/venny/*
DIANA Tools	*http://diana.imis.athena-innovation.gr/DianaTools/index.php*
TargetScan	*https://www.targetscan.org/vert_80/*
Primer3 (v.0.4.0)	*https://bioinfo.ut.ee/primer3-0.4.0/*
UCSC In-Silico PCR	*https://genome.ucsc.edu/cgi-bin/hgPcr*
NCBI	*https://www.ncbi.nlm.nih.gov/gene/*
OriginLab software	
BioRad CFX Manager	
IncuCyte 2021A	
Adobe photoshop	
Adobe Illustrator	
Metacore	

2.1.5 Parental Cell lines

Table vii: Parental cell lines used, including their description/ morphology and the culture conditions.

Cell Line	Description	Gender/Age	Media	Morphology
HEK293T	Kidney cells isolated from a human embryo	Fetus	EMEM supplemented with 10% FBS, 1% Pen/Strep and 1% Glutamine	Epithelial
NCI-H1299	Lung cells derived from a metastatic lymph node	White male/ 43 years old	RPMI 1640 supplemented with 10% FBS, 1% Pen/Strep and 1% Glutamine	Epithelial
NCI-H522	Lung cancer cells obtained from a patient before therapy	White male/ 58 years old	RPMI 1640 supplemented with 10% FBS, 1% Pen/Strep and 1% Glutamine	Epithelial
NCM356	Mucosal epithelium cells derived from normal human colon	Black male/ 65 years old	DMEM with Glutamine supplemented with 10% FBS, 1% NEAA, and 1% Pen/Strep	Epithelial
NCM460	Epithelial cells derived from normal human colon cells	Hispanic male/ 68 years old	DMEM with Glutamine supplemented with 10% FBS, 1% NEAA, and 1% Pen/Strep	Monolayer/ suspension

2.1.6 Utilised Cell lines

Table viii: Manipulated cells developed.

Cell line Infected	Target Vector	Empty Vector (as control)	Antibiotic used for selection	Concentration of Antibiotic used	Utilised cells
NCM460	pLKO.1 puro+GFP	pLKO.1 puro+GFP	Sorting with GFP	N/A	NCM460 + shIWS1
NCM460+ shIWS1	pLentri puro Ser720/Ser721-IWS1	pLenti puro	Puromycin	5 µg/ml	NCM460 + shIWS1 + Ser720/Ser721 IWS1
NCM460+ shIWS1	pLentri puro Ala720/Ala721-IWS1	pLenti puro	Puromycin	5 µg/ml	NCM460 + shIWS1 + Ala720/Ala721 IWS1
NCM460	pLV 4xSTAR-sTomato-NLS-blast	N/A	Blasticidin	4 µg/ml	NCM460 + pLV 4xSTAR-sTomato-NLS-blast
NCM356	pLV 4xSTAR-sTomato-NLS-blast	N/A	Blasticidin	4 µg/ml	NCM356 + pLV 4xSTAR-sTomato-NLS-blast
NCM356+ shIWS1	pLentri puro Ser720/Ser721-IWS1	pLenti puro	Puromycin	5 µg/ml	NCM356 + shIWS1 + Ser720/Ser721 IWS1
NCM356+ shIWS1	pLentri puro Ala720/Ala721-IWS1	pLenti puro	Puromycin	5 µg/ml	NCM356 + shIWS1 + Ala720/Ala721 IWS1
NCI-H1299	pLKO.1 blast	pLKO.1 blast	Blasticidin	N/A	NCI-H1299 + shIWS1
NCI-H1299 + shIWS1	pLentri puro Ser720/Ser721-IWS1	pLenti puro	Puromycin	5 µg/ml	NCI-H1299 + shIWS1 + Ser720/Ser721 IWS1
NCI-H1299 + shIWS1	pLentri puro Ala720/Ala721-IWS1	pLenti puro	Puromycin	5 µg/ml	NCI-H1299 + shIWS1 + Ala720/Ala721 IWS1
NCI-H522	pLKO.1 blast	pLKO.1 blast	Blasticidin	N/A	NCI-H522 + shIWS1
NCI-H522 + shIWS1	pLentri puro Ser720/Ser721-IWS1	pLenti puro	Puromycin	5 µg/ml	NCI-H522 + shIWS1 + Ser720/Ser721 IWS1

NCI-H522 + shIWS1	pLentri puro Ala720/Ala721-IWS1	pLenti puro	Puromycin	5 µg/ml	NCI-H522 + shIWS1 + Ala720/Ala721 IWS1
NCM460	pLKO-1 shAgo2-Neo	pLKO.1 neo	G-418	800 µg/ml	NCM460 + shAgo2
Murine lung fibroblasts	pBabe puro Myc-Akt1	pBabe puro	Puromycin	4 µg/ml	Murine lung fibroblasts + myc-Akt1
Murine lung fibroblasts	pBabe puro Myc-Akt2	pBabe puro	Puromycin	4 µg/ml	Murine lung fibroblasts + myc-Akt2
Murine lung fibroblasts + myc-Akt1	Wzl neo Cre	N/A	G-418	800 µg/ml	Murine lung fibroblasts + myc-Akt1 + Cre
Murine lung fibroblasts + myc-Akt2	Wzl neo Cre	N/A	G-418	800 µg/ml	Murine lung fibroblasts + myc-Akt2 + Cre

2.1.7 Vectors

Table ix: List of Vectors

NAME	CAT. NUMBER	COMPANY
WZLneo Cre	34568	Addgene
pLenti CMV Neo DEST	17392	Addgene
pLenti CMV Hygro DEST	17454	Addgene
pLKO.1 puro	8453	Addgene
pLenti CMV puro DEST	17452	Addgene
pLKO.1 blast	26655	Addgene
pLKO.1 neo	13452	Addgene
pBABE puro	1764	Addgene
shRNA against human IWS1	RSH4430-101101545 Clone ID: V3LHS_389019	Open Biosystems
pLV 4xSTAR-sTomato-NLS-blast	136259	Addgene

2.1.8 Primary and Secondary Antibodies

Table x: Primary antibodies used in this project.

The concentration of each antibody for WB and IP are summarised. All antibodies were stored according to the manufacturer's guidelines.

Antigen	Antibody	Product Code	Supplier	WB concentration	IP concentration	Storage
AGO2	Rabbit Polyclonal	2847	Cell Signalling	1:1000	1:50	-20°C
AKT3	Rabbit Monoclonal	14982	Cell Signalling	1:1000	1:50	-20°C
a-Tubulin	Mouse Monoclonal	T5168-100UL	Sigma	1:8000	1:500	-20°C
B-ACTIN	Rabbit Monoclonal	8457	Cell Signalling	1:1000	n/a	-20°C
CDK2	Mouse Monoclonal	Sc-6248	SantaCruz	1:100-1:1000	1-2 µg /100-500 µg lysate	4°C
CDK6	Mouse Monoclonal	Sc-7961	SantaCruz	1:100-1:1000	1-2 µg /100-500 µg lysate	4°C
CREB	Rabbit Monoclonal	9197S	Cell Signalling	1:1000	1:250	-20°C
DNMT3a	Mouse Monoclonal	Sc-365769	SantaCruz	1:100-1:1000	1-2 µg /100-500 µg lysate	4°C
DNMT3A	Rabbit Polyclonal	2160	Cell Signalling	1:1000	1:25	-20°C
DNMT3b	Mouse Monoclonal	Sc-376043	SantaCruz	1:100-1:1000	1-2 µg /100-500 µg lysate	4°C
DYKDDDDK Tag (FLAG)	Rabbit Polyclonal	2368	Cell Signalling	1:1000	1:50	-20°C
DYKDDDDK Tag (FLAG)	Mouse Monoclonal	8146	Cell Signalling	1:1000	1:50	-20°C
FMRP	Rabbit Polyclonal	4317	Cell Signalling	1:1000	1:50	-20°C
GW182	Rabbit Polyclonal	A302-330A	Thermo Fisher Scientific	1 µg /ml	2-5 µg /mg lysate	4°C
GW182	Mouse Monoclonal	Sc-374458	Insight Bio-technology	1:250	1-2 µg /100-500 µg lysate	4°C
HNF4A	Rabbit Monoclonal	3113	Cell Signalling	1:1000	n/a	-20°C
IWS1	Rabbit Polyclonal	5681	Cell Signalling	1:1000	1:50	-20°C
MCL1	Mouse Monoclonal	Sc-12756	SantaCruz	1:100-1:1000	1-2 µg /100-500 µg lysate	4°C
MDM2	Rabbit Monoclonal	86934	Cell Signalling	1:1000	1:100	-20°C
MLK1	Rabbit Monoclonal	5029	Cell Signalling	1:1000	1:50	-20°C

MOV10	Mouse Monoclonal	Sc-515722	Insight Biotechnology	1:250	1-2 µg /100-500 µg lysate	4°C
PDCD4	Rabbit Monoclonal	9535	Cell Signalling	1:1000	1:50	-20°C
Phosphor-EGFR Receptor (Tyr1086)	Rabbit Polyclonal	2220	Cell Signalling	1:1000	n/a	-20°C
TCL1A	Rabbit Polyclonal	4042	Cell Signalling	1:1000	1:100	-20°C

Table xi: Secondary antibodies

Antigen	Antibody	Product Code	Supplier	Dilution	Storage
Anti-Mouse IgG	Mouse polyclonal	A4416	Sigma Aldrich	1:2000	-20°C
Anti-Rabbit IgG	Rabbit polyclonal	A6154	Sigma Aldrich	1:2000	-20°C

2.1.9 Primers

Table xii: Primers and sequences for qPCR analysis.

Forward and Reverse sequences and their melting temperatures (TM) are shown.

Primers	Forward (5'-3')	Tm (°C)	Reverse (5'-3')	Tm (°C)
AKT1	ATCACCATCACACCACCTGA	59.80	TAGGAGAACTGGGGGAAGTG	59.10
AKT2	ACGTGGTCCAGAAGAAGCTC	59.50	TGGGCGGTAAATTCATCAT	58.80
AKT3	GATCCAAATAAACGCCTTGG	59.40	CATCTTGCCAGTTTACTCAGA	55.60
ASCL2	CGCCTACTCGTCGGACGACAG	67.60	GCCGCTCGCTCGGCTTCCG	74.80
B-Actin	CCCAGCACAATGAAGATC	57.60	ACATCTGCTGGAAGGTGGAC	61.50
BMI1	TTTATACCTGGAGAAGGAATGGTC	59.75	TGGTGACTGATCTTCATTCTTTT	57.85
CD44	CAACACAAATGGCTGGTACG	60.03	TCATCAATGCCTGATCCAGA	60.16
CDK4	GCTGCTGGAAATGCTGACTT	60.55	TGCTCACTCCGGATTACCTT	59.69
DLL1	GGATGAGTGCGTCATAGCAA	59.83	TGGGGCATATATCCTTGGAA	60.11
DOCK7	CCTGCCACAGAGATTCCTTC	59.80	CATGGCTCTTTGCAGATGAA	59.95
GAPDH	ATGTTCGTCATGGGTGTGAA	59.20	GGTGCTAAGCAGTTGGTGGT	62.30
GATA6	GCAAAAATACTTCCCCCACA	59.80	CTCGGGATTGGTGCTCTCT	60.36
IFNB1	CTTGGATTCCTACAAAGAAGCAGC	62.60	TCCTCCTTCTGGAACTGCTGCA	62.60
LRIG1	GATGGGAAAGGGGATTCTTC	59.70	GCTCTGGACTGCCTGAAGTT	59.60
LYZ	TCGCTGATGCTGTAGCTTGT	59.77	TGACAACGATTTCTCCATGC	59.65
mBcl2	AGTACCTGAACCGGCATCTG	60.13	CATGCTGGGGCCATATAGTT	59.81
mIl-12b	GCAAGCTCAGGATCGCTATT	59.58	CTTTCCAACGTTGCATCCTA	58.77
mIl-18	GCTGTGACCCTCTCTGTGAA	58.97	TCAGGTGGATCCATTTCCTC	59.86
MMP9	GCACGACGTCTTCCAGTACC	60.72	TCAACTCACTCCGGGAACTC	60.24
mTnfrsf9	TGTGCTCAAATGGATCAGGA	60.20	ATCGGCAGCTACAAGCATCT	60.01
PDCD4	GGCTGGAATAATTTCCAAACA	58.93	CCTCCATCTCCTTCGCTTAC	58.89
PDX1	CCTTTCCCATGGATGAAGTC	59.34	CGTCCGCTTGTTCTCCTC	59.50

Pri-let-7i	CTGTTGGTCGGGTTGTGAC	59.99	GCTGAGCATCACCAGCACTA	60.17
Pri-miR-17	GCAGTGAAGGCACTTGTAGC	58.68	AAAAAGCACTCAACATCAGCA	58.57
Pri-miR-21	CCAGTTTTCTTGCCGTTCTG	60.80	TTCCTCCCAAGCAAAACAAA	60.59
PROX1	GCAAATGACTTTGAGGTTCCA	60.10	TGCGATAATGGCATTGAAAA	60.04
PTEN	TGAGTCATATTTGTGGGTTTTCA	59.37	GCTAGCCTCTGGATTTGACG	59.98
SMOC2	CCCAGAGGTCATGCTGAAAG	60.79	TGCTCTTTGGTGAGGGAAAT	59.67
TERT	GTCACCTACGTGCCACTCCT	60.18	AGGGCAGTCAGCGTCGTC	62.65
VIM	CCCTCTGGTTGATACCCACT	58.87	GGTCATCGTGATGCTGAGAA	59.79
HNF4G	ATCACGTGGCAAATGATTGA	59.93	GATGACTGCCATCATTGGAA	59.46
FZD1	ATCGTCATCGCCTGCTACTT	59.87	AGCGTAGCTCTTGCAGCTCT	59.69

Table xiii: microRNA primers.

Primers - QIAGEN	Catalog Number	GeneGlobe ID
hsa-let-7i-5p miRCURY LNA miRNA PCR Assay	339306	YP00204394
hsa-let-7a-3p miRCURY LNA miRNA PCR Assay	339306	YP00206084
hsa-miR-103a-3p miRCURY LNA miRNA PCR Assay	339306	YP00204063
hsa-miR-200c-3p miRCURY LNA miRNA PCR Assay	339306	YP00204482
hsa-miR-182-3p miRCURY LNA miRNA PCR Assay	339306	YP00204098
hsa-miR-182-5p miRCURY LNA miRNA PCR Assay	339306	YP00206070
hsa-let-7b-5p miRCURY LNA miRNA PCR Assay	339306	YP00204750
hsa-miR-124-3p miRCURY LNA miRNA PCR Assay	339306	YP00206026
hsa-miR-1285-5p miRCURY LNA miRNA PCR Assay	339306	YP02118966
hsa-miR-1290 miRCURY LNA miRNA PCR Assay	339306	YP02118634
hsa-miR-137-3p miRCURY LNA miRNA PCR Assay	339306	YP00206062
hsa-miR-138-5p miRCURY LNA miRNA PCR Assay	339306	YP00206078
hsa-miR-142-3p miRCURY LNA miRNA PCR Assay	339306	YP00204291
hsa-miR-146a-5p miRCURY LNA miRNA PCR Assay	339306	YP00204688
hsa-miR-147b-3p miRCURY LNA miRNA PCR Assay	339306	YP00204368
hsa-miR-150-5p miRCURY LNA miRNA PCR Assay	339306	YP00204660
hsa-miR-155-5p miRCURY LNA miRNA PCR Assay	339306	YP02119311
hsa-miR-15b-5p miRCURY LNA miRNA PCR Assay	339306	YP00204243
hsa-miR-16-2-3p miRCURY LNA miRNA PCR Assay	339306	YP00204309
hsa-miR-16-5p miRCURY LNA miRNA PCR Assay	339306	YP00205702
hsa-miR-17-5p miRCURY LNA miRNA PCR Assay	339306	YP02119304
hsa-miR-185-5p miRCURY LNA miRNA PCR Assay	339306	YP00206037
hsa-miR-200b-3p miRCURY LNA miRNA PCR Assay	339306	YP00206071
hsa-miR-214-3p miRCURY LNA miRNA PCR Assay	339306	YP00204510
hsa-miR-21-5p miRCURY LNA miRNA PCR Assay	339306	YP00204230
hsa-miR-22-3p miRCURY LNA miRNA PCR Assay	339306	YP00204606
hsa-miR-23a-3p miRCURY LNA miRNA PCR Assay	339306	YP00204772
hsa-miR-24-3p miRCURY LNA miRNA PCR Assay	339306	YP00204260
hsa-miR-26a-5p miRCURY LNA miRNA PCR Assay	339306	YP00206023
hsa-miR-29a-3p miRCURY LNA miRNA PCR Assay	339306	YP00204698
hsa-miR-29b-3p miRCURY LNA miRNA PCR Assay	339306	YP00204679
hsa-miR-34b-3p miRCURY LNA miRNA PCR Assay	339306	YP00204005

hsa-miR-34c-5p miRCURY LNA miRNA PCR Assay	339306	YP00205659
hsa-miR-4454 miRCURY LNA miRNA PCR Assay	339306	YP02114119
hsa-miR-451a miRCURY LNA miRNA PCR Assay	339306	YP02119305
hsa-miR-486-3p miRCURY LNA miRNA PCR Assay	339306	YP00204107
hsa-miR-486-5p miRCURY LNA miRNA PCR Assay	339306	YP00204001
hsa-miR-548ac miRCURY LNA miRNA PCR Assay	339306	YP02118887
hsa-miR-548as-3p miRCURY LNA miRNA PCR Assay	339306	YP02108615
hsa-miR-548c-3p miRCURY LNA miRNA PCR Assay	339306	YP00204697
hsa-miR-548d-3p miRCURY LNA miRNA PCR Assay	339306	YP00205608
hsa-miR-607 miRCURY LNA miRNA PCR Assay	339306	YP00204649
cel-miR-39-3p miRCURY LNA miRNA PCR Assay	339306	YP00203952
RNU1A1 miRCURY LNA miRNA PCR Assay	339306	YP00203909
RNU5G miRCURY LNA miRNA PCR Assay	339306	YP00203908
5S rRNA miRCURY LNA miRNA PCR Assay	339306	YP00203906
hsa-miR-130a-3p miRCURY LNA miRNA PCR Assay	339306	YP00204658
hsa-miR-34a-5p miRCURY LNA miRNA PCR Assay	339306	YP00204486
hsa-miR-548a-3p miRCURY LNA miRNA PCR Assay	339306	YP00205650
hsa-miR-548b-3p miRCURY LNA miRNA PCR Assay	339306	YP00204485

Table xiv: Primers designed for pri-miRNA cloning into pGIPz Vector.

Primer	Forward (5'-3')	Tm (°C)	Reverse (5'-3')	Tm (°C)
Pri-miR-29a-3p	CTCTCGAGAAGGATACCAAGGGATGAATG	**57.86**	ACACGCGTAAAACCCCCACCAAGTCTATG	**60.10**
Pri-miR-16-5p	CTCTCGAGCTTTTTATTCATAGCTCTTATGATAGC	**55.90**	ACACGCGTTCAATAAAACTGAAAACACATTAGTAACA	**58.70**
Pri-miR-21-5p	CTCTCGAGGAATTGGGGTTCGATCTTAACAG	**57.51**	ACACGCGTAAATCCTCCCTCCATACTGCT	**58.22**
Pri-miR-200c-3p	CTCTCGAGGTGATCAGCGACCCAGGG	**66.67**	ACACGCGTCAGCCAACAAGAACCACCC	**57.89**
Pri-miR-519d-3p	CTCTCGAGCTAACCTGCAGAGCCTTTGAA	**58.22**	ACACGCGTAAAACAGACTCCCAACATCATCC	**58.92**
Pri-miR-218-5p	CTCTCGAGACTCTTACTGTGGTCATAAACATTCTG	**59.15**	ACACGCGTATACTCAGGCTTTTAAATTTTCTATGG	**58.79**
Pri- Let-7i-5p	CTCTCGAGCGAGGAAGGACGGAGGAG	**60.90**	ACACGCGTATTCCCAGCCATTGTCCT	**57.85**
Pri-miR-103a-3p	CTCTCGAGATATATTCTCTTCCAAACAAAGAATCC	**58.59**	ACACGCGTGAAAGTTCTAAGCATAAGACATTTTGA	**58.63**
Pri-miR-17-5p	CTCTCGAGTTTTTCTTCCCCATTAGGGATT	**60.02**	ACACGCGTTTCTTATGCCAGAAGGAGCA	**58.60**

Table xv: Forward and reverse primers designed for shRNAs

Primer	Forward (5'-3')	Reverse (5'-3')
shAgo2	5'-CCGGCCAGATTTCAAACTTGGATTTCTGCAGAAATCCAAGTTTGAAATCTGGTTTTTG-3'	5'-AATTCAAAAACCAGATTTCAAACTTGGATTTCTGCAGAAATCCAAGTTTGAAATCTGG-3'

Table xvi: Mutagenesis Primers

Primer	Forward (5'-3')	Reverse (5'-3')
IWS1 (S720A)	CAACGACGAAGAATGAACGCCACTG GTGGTCAGACACC	GGTGTCTGACCACCAGTG GCGTTCATTCTTCGTCGTT G
IWS1 (T720A)	ACGAAGAATGAACAGCGCTGGTGGT CAGACACC	GGTGTCTGACCACCAGCG CTGTTCATTCTTCGT
TIM3 F213A	GAATCTGGTGATGAAGAGGAA GAAGAA GCTACAGGTGCTAACCAAGAAGATCTGG AAGAAGAAAA	
TIM3 F210A	TTTTCTTCTTCCAGATCTTCTTGGTTA GCACCTGTAGCTTCTTCTTCCTCTTC ATCACCAGATTC	
TIM2 F199	GCAATGAAGAAGAAAATCTTATTG C AGACGCAGCTG GAG AATCTGGTGA TGAAGAGGAAGAAG	
TIM2 I198A	CTTCTTCCTCTT CATCACCAGATT CT C CAGCTGCGTCTGCAATAAGATTTT CTTCTTCATTGC	
TIM1 F181A	GAATTGTCTGATAAGAAAAATGAAGA GAAGGATGCGGCTGGGAGTGACAGT GAGTC	
TIM1 L180A	GACTCACTGTCACTCCCAGCCGCAT CCTTCTCTTCATTTTTCTTATCAGACA ATTC	

Table xvii: MicroRNA reporter assay vectors.

microRNA reporter Assays- AddGene	Catalog Number
LSB-hsa-miR-21-5p	103272
LSB-hsa-miR-16-5p	103272
LSB-hsa-let-7f-5p	103156
LSB-hsa-let-7c-5p	103149
LSB-hsa-let-7i-5p	103159
LSB-hsa-miR-103a-3p	103168
LSB-hsa-miR-182-5p	103283
LSB-hsa-miR-25-3p	103375
LSB-hsa-miR-29a-3p	103391
LSB-hsa-miR-218-5p	103357
LSB-hsa-miR-17-5p	103274
LSB-hsa-miR-200c-3p	103332

2.2 Methods

2.2.1 Tissue Culture

2.2.1.1 Cell Cultures and Growth Conditions

Human Lung cancer cell lines NCI-H522, NCI-H1299 and HEK-293T were purchased from ATCC, while colon epithelial cell lines NCM356 and NCM460 were purchased from INCELL **(Table vii)**. Cell culture experiments were performed in a flow hood using sterile handling techniques. Cells were grown in DMEM, high glucose, pyruvate (11995-065, Gibco), supplemented with 10% Foetal Bovine Serum (FBS) (10270-106, Gibco), 50 U/mL penicillin and 50 µg/ml streptomycin (15070-063, Gibco), MEM non-essential amino acids solution (NEAA) (11140-050, Gibco) and Plasmocin (ant-mpp, InvivoGen). All cell lines were cultured at 37 °C in 5% CO_2. Mouse immortalised Lung Fibroblast from $Akt1^{lf/fl}$/ $Akt2^{-/-}$/ $Akt3^{-/-}$ mice were transduced with myc-tagged wild type Akt1, Akt2 and Akt3. Ablation of endogenous Akt1 by Cre rises Akt-null cells (Triple Knockout, TKO) or cells expressing a single Akt isoform at a time. Passage of these cells every 3-4 days led to immortalized cell lines which, were cultured in the same medium as human cells, under standard culture conditions.

2.2.1.2 Maintenance and passaging of human cell lines

Confluent cells (80-90%) were washed with pre-warmed Dulbecco's phosphate-buffered saline (DPBS) (14040091, Gibco) and incubated with 0.25% Trypsin-EDTA, phenol red (25200056, Gibco) for 5 minutes at 37 °C. To deactivate trypsin, two volumes of complete growth medium were added. Cells were centrifuged at 91-161 x g for 4 minutes; the pellet was resuspended with fresh culture medium and 1/3 of the cells were seeded in a new 100 mm cell culture plate.

2.2.1.3 Cryopreservation and Thawing

After trypsinization and centrifugation, cells were resuspended in 1 ml FBS. In a cryovial containing 100 µl of dimethyl sulfoxide (DMSO), 900 µl of cell suspension was transferred. Cryovials were stored at -80 °C in an isopropanol box (Cryobox) for 24 hours and then were transferred into liquid nitrogen N_2, for long-term storage. To revive the cells from the frozen stock, cryovial was transferred in dry ice until resuscitation. Cells were rapidly thawed by transferring the cryovial in a pre-warmed, sterile water bath at 37°C for a few seconds. Cells were resuspended in a pre-warmed growth medium and transferred in a Falcon tube containing 10 ml Full medium. Cells were centrifuged at 91 x g for 4 minutes, resuspended in 1 ml fresh medium, and cultured overnight. The next day, the medium was replaced with a fresh medium to remove every trace of DMSO.

2.2.1.4 Cell counting

After trypsinization and centrifugation, cells were re-suspended in full medium and 20 µl were mixed with 20 µl of 0.4% Trypan Blue stain solution. In a cell counting chamber slide, 10 µl of the mixture was added to each side. Following that, the slide was placed into the Countess II FL automated cell counter (AMQAF1000; Invitrogen) where the number of viable cells was considered for both sides and the mean was calculated.

2.2.1.5 Mycoplasma testing

All cell lines used in this study were treated with plasmocin to prevent mycoplasma. Although, all the cell lines were regularly checked for mycoplasma contamination using the EZ-PCR mycoplasma test kit (20-700-20, Biological industries), following the manufacturer's protocol. Briefly, 1ml of supernatant collected from an ~80% confluent plate, was centrifuged at 250 x g for 1 minute to pellet cell debris, followed by higher speed centrifugation, 16,000 x g for 10 minutes, to sediment mycoplasma.

The pellet was resuspended in the supplied buffer and heated for 3 minutes at 95°C. PCR was followed using the provided primers, detecting the 16S mycoplasma-specific rRNA region. Every time, positive and negative control was included. The amplified PCR product was analyzed on a 2% agarose gel (w/v in TAE) containing 1x Gel-Red Nucleic acid (41003, Biotium) by Agarose gel electrophoresis. The gel was running for 30-40 minutes at a constant voltage (80V) and then, it was visualized using a UV transilluminator (Syngene). Cells contaminated by mycoplasma presented a band at 270 bp.

2.2.2 microRNA target prediction analysis

Target genes of equally expressed miRNAs in Ser720/Thr721-IWS1 and Ala720/Ala721-IWS1 expressing cells, as evaluated by miRNA sequencing, were collected from Targetscan (TargetScanHuman 7.2) and Diana Tools (DIANA TOOLS (athena-innovation.gr) websites. For each micrRNA, predicted and experimentally validated targets were identified. Data were compared with RNA sequencing data in the same cell types for common genes. The number of predicted micrRNA targets was divided by the total number of TargetScan Genes (n=28353) and the observed suppressed miRNA targets in Ala720/Ala721-IWS1 expressing cells, with the total number (n=474) of downregulated genes in the RNA sequencing data.

2.2.3 Protein extraction

Protein samples were collected with 300 μl 1X RIPA lysis Buffer (1x RIPA Buffer + 1mM PMSF in DMSO + Thermo Scientific Pierce Phosphatase + Protease Inhibitor Mini Tablets, vF=10ml). Samples were sonicated for nuclei lysis (3x Duty Factor 20, 20 Sec; Delay for 30 seconds), using the S220 Focused-ultrasonicator (Covaris), incubated on ice for 15 minutes, gently vortex, and centrifugation at 14,000 x g for

10 minutes at 4 °C. Supernatant was transferred to new Eppendorf tube and protein concentration was quantified with BCA protein assay.

2.2.4 Protein quantification

Pierce BCA Protein Assay Kit (23227; Thermo Fisher Scientific) was used for the quantification of proteins. A standard curve was produced prior the quantification assay by a series of diluted albumin (BSA) standards (15mg/ml, 1mg/ml, 0.75mg/ml, 0.25mg/ml, 0.125mg/ml, and blank). BCA reagent was prepared prior to use, by mixing Reagent A and Reagent B 50:1 (v/v). 200 µl of BCA working reagent was added in triplicates to a transparent 96-well plate with 5 µl of each unknown protein or blank sample and incubated for 30 minutes at 37°C in the dark. Absorbance was measured at 562 nm.

2.2.5 Subcellular fractionation

2.2.5.1 Protein

NE-PER Nuclear and cytoplasmic extraction kit (78833, Thermo Scientific), was used to lyse cells and separate cytoplasmic and nuclear protein fractions. Before starting, protease and phosphatase inhibitors were added to Cytoplasmic Extraction Reagent I (CER I) and Nuclear Extraction Reagent (NER). Cells were harvested with 500 µl Trypsin-EDTA and when detached, 900 µl cold PBS was added. Cells were centrifuged at 500 x g for 5 minutes at 4 °C. Supernatant was discarded and 200 µl of ice-cold CER I was added and mixed vigorously by vortexing for 15 seconds. Samples were incubated for 10 minutes on ice and then, 11 µl of ice-cold CER II was added. Samples were vortexed for 5 seconds, incubated on ice for 1 minute and vortexed again for 5 seconds, prior to 5-minute centrifugation at 16,000 x g at 4°C. Immediately after centrifugation, the supernatant containing the cytoplasmic extract was transferred to a clean pre-chilled tube and the pellet was resuspended in 100 µl ice-cold NER. Every 7 minutes, the sample was vortexing for

15 seconds for a total of 40 minutes following centrifugation at 16,000 x g for 10 minutes at 4 °C. Immediately after centrifugation, the supernatant containing the nuclear extract was transferred to a new pre-chilled tube. Both extracts, nuclear and cytoplasmic were transferred at -80 °C.

2.2.5.2 RNA

SurePrep Nuclear or Cytoplasmic RNA purification (BP2805-50, Fisher BioReagents) was used for the isolation and purification of nuclear and cytoplasmic RNA. Cells were lysed with 200 µl Lysis solution and centrifuged for 3 minutes at 18928 x g. 100 µl binding solution was added in supernatant and pellet and mixed by vortexing for 10 seconds. Following that, 100 µl of 100% ethanol was added, mixed by vortexing for 10 seconds, and then transferred into a spin column provided for 1-minute centrifugation at 18928 x g. Wash solution was used to wash the column three times, 400 µl/ wash. For RNA elution, 30 µl pf RNase- Free water was added and after 1 minute of centrifugation, RNA samples were analysed with the NanoDrop 8-sample spectrophotometer (ND-8000; Labtech) and then stored at -80 °C until further use.

2.2.6 Sucrose gradient fractionation

NCI-H522 cells were grown in 150 mm plates, either with Serum (S) or without Serum (w/o Serum) at 37°C. 100 µg/ml Cycloheximide (C7698-1G; Sigma-Aldrich) was added to the cells and after 5 minutes of incubation, cells were washed with cold PBS. Cells were lysed using 500 µl of Hypotonic Buffer (5mM Tris-HCL pH 7.5, 2.5mM $MgCl_2$, 1.5mM DTT, and 100 µg/ml Cycloheximide, protease and RNase inhibitors, 0.5% Deoxycholate, 0.5% Triton X-100 and 50 µg/ml Digitonin), incubated on ice for 10-15 minutes and centrifuged t 1,000 x g for 5 minutes at 4 °C. Supernatants were collected and centrifugation was repeated at 14,000 x g for 5 minutes at 4 °C. A sucrose gradient Lysis Buffer (100mM Tris pH 7.5, 100mM NaCl,

and 2.3mM $MgCl_2$) was used to prepare 5% and 60% Sucrose solutions and 5-60% gradients were produced in ultracentrifuge tubed using the Gradient Master 108 BioComp. 500 µl of lysates were transferred on the surface of the gradient and centrifugation at 46,000 rpm for 90 minutes at 4 °C was followed. Then, fractions were collected from the bottom of the tubes and transferred to 14 new Eppendorf tubes. Proteins were subjected to Methanol/Chloroform (MeOH/$CHCl_3$) precipitation. Volumes of MeOH and $CHCl_3$ equal to 1/5 and 4/5 of fraction volumes s, respectively, were added to fractions, followed by a vortex for 30 seconds, 20 minutes incubation on ice, and centrifugation at 16,100 x g for 30 minutes at 4 °C. Upper phase was removed and 9-fold volume of MeOH was added to the lower phase. The mixture was centrifuged at 16,000 x g for 30 minutes at 4 °C. Supernatant was removed, and the protein pellet was dried and dissolved in sample buffer. Samples were boiled for 5 minutes and analysed by western blot.

2.2.7 Immunoprecipitation of proteins (IP)

Confluent cells in a 100 mm plate were washed once with PBS on ice and protein samples were extracted and sonicated as in protein extraction. After quantifying protein concentration, 1mg of Protein was diluted with 1x RIPA Buffer in a final volume of 500 µl. Antibodies (according to the company's instructions) or 1 µg of normal IgG antibody, were combined with protein samples and incubated overnight under rotation at 4 °C. The following day, 50 µl/reaction of protein A Magnetic Beads (73778S, Cell Signalling Technologies) or protein G Magnetic Beads (70024S, Cell Signalling Technologies) were resuspended with 500 µl RIPA lysis Buffer. Using a magnetic separator, the supernatant was removed and 500 µl of new RIPA lysis Buffer was added. The magnetic beads were resuspended in 50 µl of lysis buffer/500 µl reaction and combined with the antibody, followed by incubation, under rotation for 1 hour at 4 °C and 30 minutes at RT. After incubation, the magnetic beads – antibody complexes were resuspended with 500 µl of 1x RIPA buffer. Using

the magnetic separator, the supernatant was removed, and samples were washed 5 times in total. The pellet was resuspended with 40 µl of 3x SDS sample Buffer containing 39mM Tris-HCl pH 6.8; 12% Glycerol; 0.06% Bromophenol blue and 100mM DTT. Samples were boiled for 5 minutes and centrifuged for 5 minutes at 11,200 x g Samples may be stored at -20 °C until further use.

2.2.8 Immunoblotting assay-Western Blot (WB)

Acrylamide/bis-acrylamide separating gels (8-15%) were prepared as shown in ***Table xviii***. The percentage of the gel depends on the size of the protein of interest. For each gel, 10 ml solution was prepared, poured into the apparatus, and let to solidify. Once the gel was solidified, 5 ml of 5% acrylamide/bis-acrylamide stacking gel was prepared **(**

***Table xix*)** and poured on top of the separating gel. Immediately 10-well combs were placed to form the wells. When the gel was solidified, it was placed in the electrophoresis tank containing 1x Running Buffer (Tris-Glycine-SDS) (BP13414; Fisher Bioreagents). Protein samples and 7 µl of molecular weight maker (1610374; Bio-Rad) were loaded and separated, by electrophoresis, at constant voltage (80V) through the stacking gel, increased to 120V through the separating gel. Once the run was completed, a polyvinylidene difluoride (PVDF) membrane (IPVH00010, Merck) was used to transfer the proteins overnight at 0.05 Ambers at 4 °C using the 1x Transfer Buffer (25mM Tris-base; 192 mM Glycine; 20% methanol). Before using the PVDF membrane, incubation with methanol was performed for 5 minutes with shaking and then, rinsed with transfer buffer. The next day, the membrane was blocked for 1 hour at RT in 5% milk in 1x TBS-T (10mM Trizma base; 150mM NaCl; 0.1% Tween-20) in shaking. Primary Antibodies were diluted according to instructions **(*Table x*)** in 5% Bovine Serum Albumin (BSA) in 1x TBS-T and incubated with the membrane overnight at 4 °C with shaking. The next day, the membrane was washed 3 times with TBS-T, 5 minutes each, at RT with shaking,

following incubation with the recommended dilution of conjugated secondary Antibody (***Table xi***) in 5% milk (in TBS-T) at RT for 1 hour, shaking. Before development, the membrane was washed again with TBS-T (3 times, 5 minutes each) at RT. The bands were developed using ECL Plus Western Blotting chemiluminescent substrate (32132; Thermo Fisher Scientific), following the manufacturer's instructions. The signal was captured using the GBOX-Chemi-XX6 gel documentation system.

Table xviii: Acrylamide/bis-acrylamide separating gels (8-15%).

Mixture for 10ml separating Gel				
Components	**8% Gel**	**10% Gel**	**12% gel**	**15% Gel**
Distilled H_2O	4.6 ml	4.0 ml	3.3 ml	2.3 ml
30% Acrylamide/Bisacrylamide 37.5:1	2.7 ml	3.3 ml	4.0 ml	5.0 ml
1.5M tris (pH8.8)	2.5 ml	2.5 ml	2.5 ml	2.5 ml
10% SDS	0.1 ml	0.1 ml	0.1 ml	0.1 ml
10% APS	0.1 ml	0.1 ml	0.1 ml	0.1 ml
TEMED	6 µl	4 µl	4 µl	4 µl

Table xix: Mixture for 5% stacking gel for Tris-Glycine SDS-polyacrylamide gel electrophoresis.

Mixture for 5ml stacking Gel	
Components	**5% Gel**
Distilled H_2O	3.4 ml
30% Acrylamide/Bisacrylamide 37.5:1	830 µl
1M tris (pH6.8)	630 µl
10% SDS	50 µl
10% APS	50 µl
TEMED	5 µl

2.2.9 Stripping

To detect a different protein with a different molecular weight, the previously immunoprobed membrane was treated with the Restore PLUS western Blot stripping buffer (46430, Thermo Scientific). Briefly, the membrane was washed with 1x TBST to remove the chemiluminescent substrate and incubated with the stripping buffer for 15 minutes in shaking, at RT. Then another wash with 1x TBST for 5 minutes was followed, before re-blocking with 5% milk and re-probing with a new antibody.

2.2.10 gDNA Isolation

DNA was isolated with QIAamp DNA Mini Kit (51304; Qiagen). Briefly, cell pellet was resuspended in 200 µl of DBPS, plus 20 µl Proteinase K and 100 mg/ml (4 µl) RNase A. Then, 200 µl of Buffer AL was added to the sample and mixed by vortexing for 15 seconds. Sample was incubated at 56 °C for 10 minutes and spin down. 200 µl of 100% Ethanol was added to the sample following by 15 seconds of vortexing and quick spin down. The mixture was transferred to the QIAmp Mini spin column in a 2ml collection tube and centrifuged for 1 minute at 7168 x g. The QIAmp Mini spin column was transferred in a new 2ml collection tube and 500 µl of Buffer AW1 was added, following by centrifugation for 1 minute at 7168 x g. The QIAmp Mini spin column was placed in a clean 2ml collection tube and 500 µl of Buffer AW2. Centrifugation at full speed for 4 minutes was followed. The QIAmp Mini spin column was placed in a new collection tube and centrifuged for 1 minute to dry the filter. Finally, the QIAmp Mini spin column was placed in a clean 1.5ml Eppendorf tube, where 200 µl of distilled water was added and incubated for 1 minute at room temperature before a centrifugation at 7168 x g for 5 minutes. DNA was analysed with an 8-sample NanoDrop spectrophotometer (ND-8000; Labtech) and samples were stored at –20 °C until needed.

2.2.11 Total RNA Isolation

2.2.11.1 Trizol

For RNA isolation with Trizol, the medium was removed from the well, and cells were rinsed with ice-cold PBS once. 1 ml of Trizol reagent was added per well and using a cell scraper, cells were lysed. Cell lysates were transferred to an Eppendorf tube, mixed by pipetting and vortexed thoroughly. For 1 ml Trizol reagent, 200 µl of Chloroform was added. Samples were mixed vigorously for 15 seconds, followed by 15 minutes of incubation at room temperature. Then, centrifugation at 16,128 x g was performed for 15 minutes at 4 °C, to get 3 phases. The RNA remains in the aqueous phase, and immediately aqueous phase (~500 µl) was transferred to a new Eppendorf tube containing 500 µl of 100% Isopropanol. Samples were stored at -20 °C overnight for RNA to precipitate. The following day, samples were centrifuged at 16,128 x g for 10 minutes at 4 °C. Supernatant was removed and the pellet was washed twice with 1 ml of 75% Ethanol. The RNA pellet was dried for 5-10 minutes in a hot block at 60 °C. RNA was dissolved in 50 µl of RNase Free water and incubated at 65 °C for 5 minutes. RNA was analysed with an 8-sample NanoDrop spectrophotometer (ND-8000; Labtech) and samples were stored at –80 °C.

2.2.11.2 RNeasy Plus Mini Kit

Total RNA was extracted with RNeasy Plus Mini Kit (74134; Qiagen). Briefly, cells were lysed with 350 µl Buffer RLT Plus (with 0.04M DTT) and vortexed for 30 seconds to homogenise. The homogenized lysate was transferred into a QIAshredder column (79654; Qiagen) and centrifuged for 2 minutes at 18,928 x g. The flow-through was transferred into a gDNA Eliminator Spin Column placed in a 2ml collection tube and centrifuged for 30 seconds at 13,552 x g. The column was discarded and the flow-through was mixed with 350 µl of 70% Ethanol. The sample was transferred to an RNeasy spin column placed in a 2ml collection tube and centrifuged for 15 seconds at 13,552 x g. The flow-through was discarded and 700

µl of Buffer RW1 was added to the RNeasy Mini Spin column and centrifuged for 15 seconds at 13,552 x g. Then, the RNeasy Spin column was washed twice with 500 µl of Buffer RPE. Then, after centrifugation the RNeasy Spin column was transferred to a new 2 ml collection tube and centrifuged for 1 minute at 18,928 x g, to dry the membrane. RNA was eluted with 35 µl of RNase-free water and analysed with an 8-sample NanoDrop spectrophotometer (ND-8000; Labtech). RNA samples were stored at –80 °C.

2.2.11.3 miRNeasy Tissue/ cells advanced mini kit

Cells were lysed with 260 µl RLT (with 0.004M DTT) and vortexed for 30 seconds. The homogenized lysate passed through a QIAshredder column and was centrifuged for 2 minutes at full speed. 80 µl of AL Buffer was added and mixed thoroughly, followed by an incubation of 3 minutes at room temperature. The lysate was transferred to a gDNA Eliminator Spin Column and centrifuged for 30 seconds at 8,000 x g. 1 volume of isopropanol was added to the flow-through and mixed. The sample was transferred to an RNeasy Mini spin column and centrifuged for 15 seconds at 8,000 x g. The flow-through was discarded and 700 µl of RWT Buffer was added to the RNeasy Mini column. After 15 seconds of centrifugation, flow-through was discarded, and 500 µl of RPE Buffer was added, followed by a 15 second centrifugation. The flow-through was discarded and the column was washed with 500 µl of 80% Ethanol. Followed by 2 minutes of centrifugation at 8,000 x g. The RNeasy Mini spin column was transferred in a new 2ml collection tube and centrifuged at full speed for 1 minute to dry the membrane. The RNeasy Mini spin column was placed in a new 1.5ml collection tube and RNA was eluted with 35 µl of RNase- Free water. RNA samples were stored at -80 °C until needed.

2.2.12 RNA Purification

Isolated RNA was passed through the Merck Amicon Ultra centrifugal Filter units (UFC500396; Merck) to regenerate cellulose membranes for RNA purification. Briefly, the Amicon Ultra centrifugal Filter was inserted into the provided microcentrifuge tubes, where sample (vF=500 µl) was added. The capped filter device was placed into centrifugation and spined at 14,000 x g for 30 minutes at 4°C. After centrifugation, the Amicon Ultra centrifugal Filter was placed upside down in a clean microcentrifuge tube and centrifuged with open cap for 2 minutes at 1,000 x g. Samples were stored at -80 °C until needed.

2.2.13 RT-qPCR for genes

2.2.13.1 Reverse Transcription (RT)

500 ng of RNA were reverse transcribed with iScript Reverse Transcription Supermix (1708841; BioRad) in a final volume of 10 µl with nuclease-free water. Reactions were mixed and spin quickly prior to incubation in a thermal cycler Applied Biosystems ProFlex PCR System (4484073; Thermo Fisher Scientific). Cycling conditions **(*Table xx*).** cDNA samples were used for quantitative polymerase chain reaction (qPCR).

Table xx: Cycling conditions for RT-Genes.

Steps	Temperature	Time
Priming	25°C	5 minutes
Reverse Transcription	46°C	20 minutes
RT Inactivation	95°C	1 minute

2.2.13.2 Quantitative PCR (qPCR)

cDNA samples were subjected to qPCR using iTaq Universal SYBR Green Supermix (1725124; Bio-Rad). cDNA was diluted 1:10 with nuclease-free water and 2.3 µl of the diluted cDNA was added per well in a 384-well plate. In an Eppendorf tube, 0.4 µM of primer mix/ well was mixed with 2.5 µl of iTaq Universal SYBR Green Supermix/ well. 2.7 µl of the reaction was added in each well, containing the diluted cDNA. For each sample, the analysis was performed in quadruplicates with the CFX384 real-time PCR detection system (185-5484; Bio-Rad). **Figure 2. 1: Thermal cycles employed for gene amplification using RT-qPCR on a BioRad CFX qPCR instrument.** The first step in the Denaturation, where the thermocycler heats up to 95 °C, to open the double-stranded DNA helix into two single-stranded DNA templates. Then is the annealing step where the temperature cools between 60°C and finally during the extension, the temperature increases to 72°C. The cycles are repeated for 39 cycles. **Figure 2. 1** illustrates the cycling conditions used for the analysis. The PCR data were gained as graphs of SYBR Green Signal. CFX Manager Software calculated the cycle threshold (Ct values), as the intersection points of the fluorescence curves with the selected threshold. Gene expression analysis performed by normalized expression (ΔΔCq) with the levels of B-actin and Glyceraldehyde-3-phosphate dehydrogenase (GAPDH) and quantified to the corresponding control.

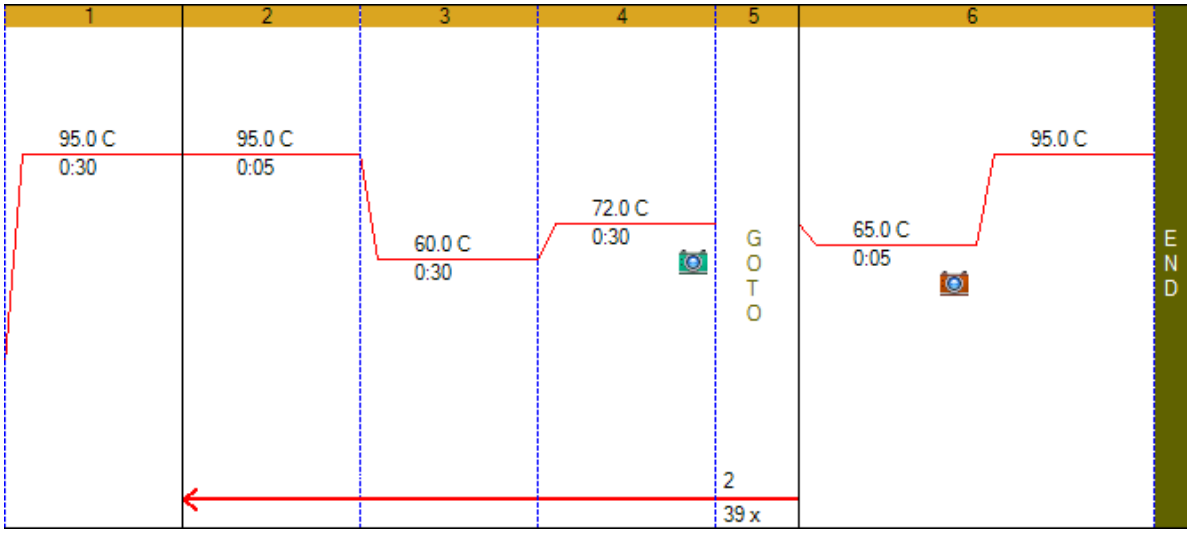

Figure 2. 1: Thermal cycles employed for gene amplification using RT-qPCR on a BioRad CFX qPCR instrument. The first step in the Denaturation, where the thermocycler heats up to 95 °C, to open the double-stranded DNA helix into two single-stranded DNA templates. Then is the annealing step where the temperature cools between 60°C and finally during the extension, the temperature increases to 72°C. The cycles are repeated for 39 cycles.

Primers used for qPCR were designed using Primer 3 (v.0.4.0), validated with UCSC, *In silico* PCR Browser, and ordered to be synthesized by Eurofins Genomics. Undiluted primers were resuspended in nuclease-free water at 100 µM stock and diluted further to 20 µM working concentration. ***Table xii*** shows the primers used for qPCR analysis.

2.2.14 RT-qPCR for micrRNAs

2.2.14.1 Reverse Transcription (RT)

200 ng of RNA were reverse transcribed with 2 µl of Reaction Buffer and 1 µl of Enzyme from miRCURY LNA RT Kit (Qiagen, 339340), in a total volume of 10 µl with nuclease-free water. Reactions were mixed and spin quickly prior to incubation in a thermal cycler Applied Biosystems ProFlex PCR System (4484073; Thermo Fisher Scientific). Cycling conditions were as shown in ***Table xxi***. cDNA samples were used for qPCR for miRNAs.

Table xxi: Cycling conditions for RT-microRNAs.

Step	Temperature	Time
Reverse Transcription	42°C	60 minutes
Inactivation of Reaction	95°C	5 minutes
Hold	4°C	∞

2.2.14.2 Quantitative PCR (qPCR)

cDNA samples were subjected to qPCR using miRCURY LNA SYBR PCR Kit (1725124, BioRad). cDNA was diluted 1:10 with nuclease-free water and 2 µl of the diluted cDNA was added per well in a 384-well plate. In an Eppendorf tube, 0.5 µl of primer/ well was mixed with 2.5 µl of miRCURY LNA SYBR / well. 3µl of the reaction was added in each well, containing the diluted cDNA. For each sample, the analysis was performed in quadruplicates with the CFX384 real-time PCR detection system (185-5484; Bio-Rad). **Figure 2. *2*** illustrates the cycling conditions used for the analysis. The PCR data were gained as graphs of SYBR Green Signal over cycle. The software calculated the cycle threshold (Ct values), as the intersection points of the fluorescence curves with the selected threshold. Gene expression levels were normalized (ΔΔCq) to the levels of RNUA1, RNU5S, and RNU5G and quantified to the corresponding control. ***Table xiii***, shows the miRNAs used for the RT-qPCR.

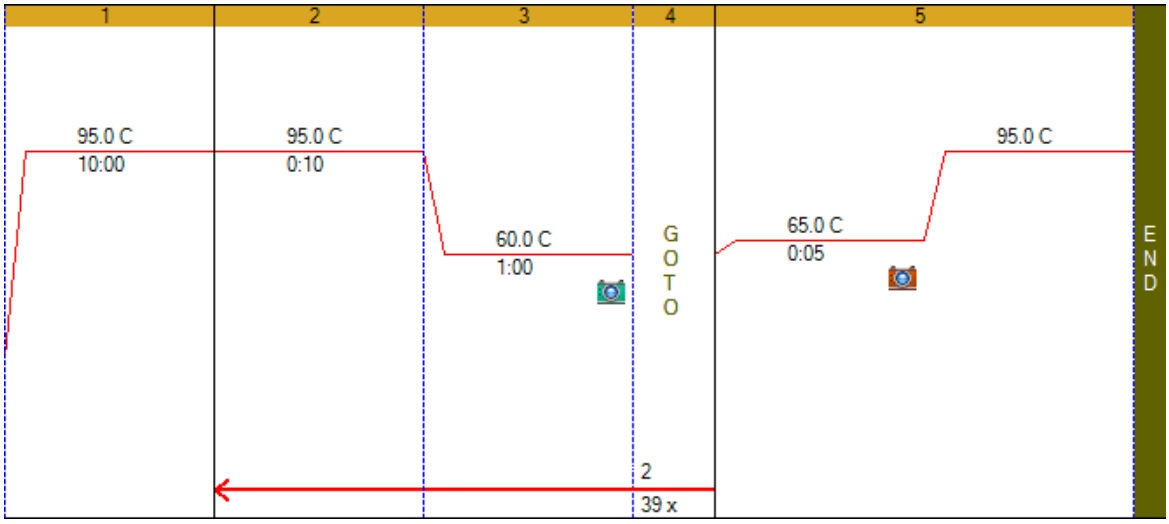

Figure 2. 2: Thermal cycles employed for gene amplification using RT-qPCR on a BioRad CFX qPCR instrument. The first step in the Denaturation, where the thermocycler heats up to 95 °C. Then temperature cools between 60°C and finally during the extension, the temperature increases to 65°C and heats up to 95 °C. The cycles are repeated for 39 cycles.

2.2.15 Cells growth assays

2.2.15.1 Cell Titre-Glo Luminescence cell viability assay

Cells were transfected with the respective miRNAs and plated in quadruplicates in a 96-well plate (25,000 cells/well). 48 hours following transfection, growth was assessed using the CellTitre Glo Luminescence Cell Viability Assay (G7573; Promega), according to the manufacturer's instructions. Briefly, cells were incubated at RT for 30 minutes before adding 100 µl of CellTitre-Glo reagent per well. Then, the contents were mixed gently by tapping the plate for 2 minutes and incubated at RT for 10 minutes before measurement. Luminescence readings were recorded with CLARIOstar plate reader (BMG Labtech). Data were expressed as mean luminescence (± S.E.M), where the control cells were set as 100%.

2.2.15.2 IncuCyte- Live cell growth assay

Cells were transfected with the respective miRNAs and plated in quadruplicates in a 96-well plate (25,000 cells/well). The plate was transferred to the IncuCyte live-cell analysis system and images (10x magnification) were captured every 2 hours for a total of 72 hours. Data were analysed using the IncuCyte software. Data were expressed as mean % confluency (± S.E.M).

2.2.16 Molecular Cloning

Primers for pri-miRNAs were designed for cloning in pGIPz vector by adding 300 bp of genomic DNA surrounding the miRNA coding sequence and the XhoI restriction site in the forward primer and the MluI site in the reverse primer. Primers shown in ***Table xvi*** were used for the amplification by PCR using the Phusion High-Fidelity DNA polymerase (M0530S; NEB). PCR products were digested with XhoI (R0146S; NEB) and MluI-HF (R3198S; NEB) and ligated with T4 DNA polymerase (M0203S; NEB) in the pGIPz vector digested with the same enzymes. Ligation was performed at 16°C overnight followed by heat-inactivation at 65°C for 10 minutes. 2µl of ligation

mix was transformed in 30µl of DH5a competent cells (EC0112; Thermo Scientific) with 250µl of Super Optimal Broth with Catabolite repression (SOC) media (15544034; Invitrogen). The bacterial suspension was plated on Luria broth (LB) agar plates containing ampicillin and incubated overnight at 37°C. Colonies from the plates were transferred in sterile 5ml of LB broth with ampicillin. Plasmid isolation was performed using QIAprep Spin Miniprep Kit (27104, QIAGEN). Cloning success was evaluated by digestion with the same enzymes.

2.2.17 Cloning into PLKO.1

Forward and Reverse shAgo2 oligos were designed through www.broadinstitute.org/rnai/public. When received, were dissolved in nuclease-free water at 50µM final concentration. Diluted oligos were resuspended in annealing buffer (10 mM Tris-HCL pH 7.5; 50 mM NaCl; 1 mM EDTA) at a final concentration of 2.5µM. The reaction was incubated for 5 minutes at 95 °C and then, overnight at RT. The next day, 1µl of annealed shAgo2 oligos was mixed with 1mM ATP (P0756S; NEB), PNK Reaction Buffer (B0201S; NEB) and 1000U/ml T4 polynucleotide kinase (M0201S; NEB) in a final volume of 10µl. The mixture was incubated for 30 minutes at 37 °C and then for 10 minutes at 70°C. At the same time, reactions for restriction enzyme digestion were prepared by incubating 1µg PLKO.1-puro Vector (8454; Addgene) with 1µl Cutsmart Buffer (B72045; NEB), 1000U/ml AgeI Restriction enzyme (R3552L; NEB) and 1000U/ml EcoRI Restriction enzyme (R3101S; NEB) and nuclease-free water at 50ul final volume, at 37 °C for 3 hours. The digested vector was extracted with QIAquick Gel Extraction kit (28704, Qiagen). The extracted vector was used for ligation reaction, where it was mixed with shAgo2 oligos, T4 Ligation buffer (B0202A; NEB) and 20,000 U/ml T4 DNA Ligase (M0202S; NEB). The mixture was incubated at RT for 1 hour and then, for 10 minutes at 65 °C. The reaction was incubated on ice followed by transformation

with one Shot Stbl3 Chemically Competent *E.coli* Cells (C737303; Invitrogen) according to manufacturer's instructions. ***Table xv*** shows the primers designed for shAgo2.

2.2.18 TOPO Cloning -LR Clonase

IWS1 sequence obtained by gene synthesis (Eurofin Genomics) was cloned into the pLenti CMV Neo DEST Vector (17392; Addgene), using the pENTR directional TOPO cloning Kit (K2435; Invitrogen) and Gateway LR Clonase II Enzyme mix (11791; Life Technologies). IWS1 primers were designed manually through Primer3, validated with UCSC *In-Silico* PCR browser and synthesised by Eurofins Genomics, to get the complete sequence of IWS1. The gene was amplified by PCR using the Q5 High- Fidelity DNA Polymerase (M0491G; NEB) according to the protocol. Briefly, 200 µM dNTPs (N0447S, NEB), 0.5 µM of each primer (Forward and Reverse), 1 ng of DNA and 0.02 U/µl Q5 High-fidelity DNA polymerase were mixed together in a PCR tube. The thermocycling conditions for the PCR are shown on **Table xxii**.

Table xxii: Thermocycling conditions for Q5 High-Fidelity PCR

Step	Temperature (°C)	Time
Initial Denaturation	98	30 seconds
25-35 cycles	98	5-10 seconds
	60	10-30 seconds
	72	20-30 seconds/Kb (of plasmid length)
Final Extension	72	2 minutes
Hold	4	∞

Agarose gel electrophoresis was used to determine the yield of PCR products. Bands were cut and DNA sample was extracted by QIAquick Gel Extraction kit (28704; Qiagen). 4µl of PCR product was mixed with 0.2 M Salt solution and 1 µl of TOPO vector (vF=6 µl). The reaction was mixes gently and incubated at RT for 15 minutes and then on ice. Transformation was followed by mixing 2 µl of TOPO cloning reaction into One Shot Stbl3 Chemically competent *E.coli* cells and the positive clones was used for plasmid isolation. Sanger sequencing was used to confirm the presence of insert and LR Clonase Reaction was followed. Briefly, 100 ng of the entry clone was mixed with 150 ng of pLenti CMV Neo DEST Vector and TE buffer pH 8.0 (10 mM Tris-HCl pH 8; 0.1 mM EDTA, pH 8) up to 8 µl. Then, 2 µl of LR Clonase II enzyme mix was added to the reaction, mixed briefly and incubated at 25 °C for 1 hour. To terminate the reaction, Proteinase K solution (0.2 µg/µl) was added and incubated at 37 °C for 10 minutes. Transformation was performed using one shot Stbl3 Chemically competent *E.coli* cells and positive clones were isolated. Sanger sequencing analysis was followed to verify the LR recombination reaction.

2.2.19 QuickChange II Site-Directed mutagenesis kit

IWS1 primers **(*Table xvi*)** containing the desired mutations were designed manually through Primer3, validated with UCSC *In-Silico* PCR browser, and synthesised by Eurofins Genomics. QuickChange II site directed mutagenesis kit (200523; Agilent) was used to prepare the samples. Briefly, 5 µl of 10x reaction buffer, 50 ng of DNA template, 125 ng of each primer (Forward and Reverse), 1 µl of dNTP mix and water up to 50 µl were mixed in a PCR tube. Then 1 µl (2.5U/µl) of *PfuUltra* HF DNA polymerase was added and PCR was performed with the following cycling conditions **(*Table xxiii*)**. Following PCR, 1 µl (10U/µl) of the *Dpn I* restriction enzyme was added to the reaction and incubated for 1 hour at 37 °C. Transformation was performed with XL1-Blue super competent cells according to the manufacturer's

instructions. After plasmid isolation, samples were sequenced by Sanger sequencing.

Table xxiii: Cycling parameters for the QuickChange II Site-Directed mutagenesis.

Cycles	Temperature (°C)	Time
1	95	30 seconds
12-18	95	30 seconds
	55	1 minute
	68	1 minute/ Kb (of plasmid length)

The number of cycles depends on the type of mutation desired. For point mutations, 12 cycles, for single amino acid changes, 18 cycles and for multiple amino acid deletions/insertions, 18 cycles.

2.2.20 Agarose Gel Electrophoresis

DNA samples were separated according to their size on an agarose gel, by Gel Electrophoresis. 1-2% Agarose was diluted in 40ml TBE buffer (15581044; Invitrogen) and by warming up the mixture in a microwave, the agarose was dissolved. Immediately, 0.01% Gel Red Nucleic acid (41003; Biotium) was added. The gel was poured into the electrophoresis apparatus, containing an 8-well comb. Once the gel solidified, the comb was removed and the gel was placed in the electrophoresis tank, containing TBE buffer. Molecular weight marker and DNA samples diluted in DNA gel loading dye (B7024S; NEB) were loaded into the wells. Gel electrophoresis was performed at 70-80V for about 40-60 minutes. Once the run finished, DNA fragments were visualized under a UV transilluminator (Syngene).

2.2.21 Gel Extraction

QIAquick Gel Extraction kit (28704; Qiagen) was used to extract the DNA from an agarose gel. DNA fragment was excised, and the gel slice was weighted in an

Eppendorf tube. 3 volumes of QG Buffer were added to 1 volume gel (100mg gel= ~100 µl) and incubated for 10 minutes at 50 °C. Once the gel dissolved, 1 gel volume of isopropanol was mixed with the sample. The sample was transferred to a QIAquick column and centrifuged for 1 minute at 18,928 x g. Flow-through was discarded and 500 µl of Buffer QG was added to the column, where centrifugation was performed for 1 minute at 18,928 x g. Flow-through was discarded and then, 750 µl Buffer PE was added into the column following centrifugation as previously. Finally, DNA was eluted with 30 µl of nuclease-free water and centrifuged for 1 minute at 13,552 x g. DNA samples were stored at -20 °C.

2.2.22 Bacterial Transformation

In an Eppendorf tube, 50-100 ng of plasmid was combined with 30 µl of competent bacterial cells (One Shot Stbl3 Chemically Competent *E. coli (*C737303; Invitrogen) or Max Efficiency DH5a Competent Cells (EC0112; Thermo Scientific)) incubated on ice for 30 minutes, followed by a heat shock for 45 seconds at 42°C and 2 minutes on ice. 250 µl of S.O.C medium (15544034; Invitrogen) was added and the mixture was incubated at 37°C for 1 hour shaking at 225 rpm. The mixture was spread on a pre-warmed selective agar plate, following an overnight incubation at 37°C. Colonies were transferred to Liquid culture followed by plasmid isolation.

2.2.23 Preparation of LB Agar plates

Distilled water was mixed with LB-Agar powder (40g/L) and autoclaved. 50 µg/ml of antibiotic (depending on the resistance of the plasmid) was added to the autoclaved LB-agar before getting solidified. The solution was poured into Petri-Dishes and let solidify at RT. Then, plates were stored at 4 °C upside-down. Before use, plates were pre-warmed at 37 °C for ~30 minutes.

2.2.24 Bacterial liquid cultures

LB Broth Powder was diluted in distilled water (25g/L) and then autoclaved. Following Bacterial transformation, each colony was transferred into 10ml liquid culture containing 50 µg/ml of the appropriate antibiotic and incubated overnight at 37 °C, 225 rpm shaking. In an Eppendorf tube, a Glycerol stock was prepared, containing 500 µl of bacteria culture with 500 µl of 50% Glycerol. The Glycerol stock was stored at -80°C until needed.

2.2.25 Plasmid Isolation

2.2.25.1 MiniPrep

A single colony from an LB Agar plate or from glycerol stock was used with 10 ml LB Broth containing 50 µg/ml antibiotic, depending on the resistance carried by the plasmid. Bacteria were incubated overnight at 37 °C, 225 rpm shaking. The next day, bacteria were pellet by centrifugation at 2,800 x g for 7 minutes at Room Temperature. For plasmid isolation, QIAprep Spin Miniprep Kit (27104; Qiagen) was used, according to the manufacturer's protocol. In the end, DNA was eluted at 30 µl of nuclease-free water and quantified with the NanoDrop 8-Sample Spectrophotometer. Constructs were stored at -20°C until needed.

2.2.25.2 MidiPrep

A single colony from an LB Agar plate or from glycerol stock was used to inoculate 100 ml of LB Broth containing 50 µg/ml antibiotic, and incubated overnight at 37 °C, at constant shaking (225 rpm). Bacteria were pelleted by 20 minutes of centrifugation at 2,800 x g at 4 °C. For the plasmid isolation, HiSpeed MidiPrep Kit (12643; Qiagen) was used based on the protocol. Finally, DNA was eluted with 500 µl Tris-EDTA (TE) Buffer and DNA concentration and quantification were analyzed with the NanoDrop 8-Sample Spectrophotometer. Constructs were stored at -20°C until needed.

2.2.26 Diagnostic Digestion

Diagnostic digestion was used to confirm that the plasmid contains the expected insert. For diagnostic digestion, 1 µg of Plasmid was mixed with 1µl of CutSmart Buffer and 1000 U/ml of the corresponding restriction enzymes. The mixture was incubated for 1 hour at 37 °C followed by an agarose gel electrophoresis for the fragments to be purified.

2.2.27 Sanger Sequencing

Sequencing analysis was performed to specify if the plasmid contains the expected insert. For each reaction, 5 µl of 100 ng/ µl DNA plasmid and 5 µl of 3.2 pmol/ µl of sequencing primer were diluted in nuclease free water. Results as a chromatograph sequencing file, were inspected with Chromas version 2.22 (Technelysium Ltd.) and the sequencing results were analysed by nucleotide Blast Program (Nucleotide BLAST: Search nucleotide databases using a nucleotide query (nih.gov)).

2.2.28 Transient Transfection

Cells were seeded in a 6-well plate (500,000 cells/well) and transfected with 20 nM miRNA mimics or 2-10 nM miRNA control, using Lipofectamine RNAiMAx transfection reagent (13778-150; Life Technologies). miRNAs were resuspended in nuclease-free water at 20nM stock concentration. For each transfection, 12 µl of Lipofectamine RNAiMAx was added to 100 µl Opti-MEM. Diluted miRNAs were added and incubated for 15 minutes at RT. The mixture was added to the cells dropwise and incubated at 37 °C in a humidified 5% CO_2 incubator. Cells were lysed for 24 or 48 hours, depending on the experiment.

2.2.29 Lentiviral/Retroviral Transduction

2.2.29.1 Propagation and passaging of HEK293T cells

HEK293T cells were cultured in DMEM medium containing 10% FBS, 50U/mL penicillin and 50 µg/mL Streptomycin at 37 °C in a humidified 5% CO_2 incubator. At 80% confluency, cells were incubated at 37 °C for 3-5 minutes, with 0.25% Trypsin-EDTA. Trypsin was deactivated by adding two volumes of DMEM followed by centrifugation at 91 x g for 4 min. In a new cell culture plate, containing fresh medium, HEK293T cells were sub-cultured at 30% confluency in a 60mm plate.

2.2.29.2 Lentiviral-Virus production

Table xxiv shows the transfection mixture used for virus production in a 60mm plate. Briefly, the target vector was mixed with the viral packaging plasmids, FuGene 6 and Opti-MEM, and incubated for 45 minutes at RT. HEK293T cells plated at 30% confluency at a 60mm plate, were transfected dropwise with the mixture. Cells were incubated overnight at 37 °C. The following day, transfected cells were re-transfected as previously. 24 h and 48 h after the second transfection, 1st and 2nd batches of viruses were collected respectively and filtered through a 0.45 µm filter. Viruses were stored at -80 °C until use.

Table xxiv. Lentiviral transfection mixture used for 60mm plates

Reagents	Concentration/ Volume
OptiMEM	450 µl
Fugene 6	9 µl
Target Vector	1.5 µg
psPAX2	1 µg
pCMV-VSV-G	0.5 µg

2.2.29.3 Retroviral-Virus production

Table xxv shows the transfection mixture used for virus production in a 60mm plate for retroviruses. Briefly, the target vector was mixed with Ecopack, FuGene, 6 and Opti-MEM, and incubated for 45 minutes at RT. HEK293T cells plated at 30% confluency at a 60mm plate, were transfected dropwise with the mixture. Cells were incubated overnight at 37 °C. The following day, transfected cells were re-transfected as previously. 24 h and 48 h after the second transfection, 1st and 2nd batches of viruses were collected respectively and filtered through a 0.45 μm filter. Viruses can be stored at -80 °C until needed.

Table xxv: Transfection mixture used for 60mm plates for Retroviruses.

Reagents	Concentration/ Volume
OptiMEM	200 μl
Fugene 6	25 μl
Target Vector	7.5 μg
Ecopack	2.5 μg

2.2.29.4 Cell Transduction

Cells were plated at ~30% confluency in a 6-well plate and incubated overnight at 37°C. The next day, cells were washed once with DMEM without serum and then, incubated with DMEM without serum, containing 0.4mg/ml DEAE-Dextran Hydrochloride for 45 minutes at 37°C. Then, cells were incubated in DMEM full medium for 1 hour at 37°C. Following that, cells were infected with the 1st batch of the virus (collected 24 hours after 2nd transfection), and incubated overnight at 37°C. The following day, the steps above, were repeated and cells were infected with the 2nd batch of virus (collected 48 hours after 2nd transfection). To verify the transduction efficiency non-infected cells were used as control and the appropriate

antibiotic was used for selection, 24 hours after the second infection. ***Table viii*** shows the manipulated cells developed.

2.2.30 Statistical Analysis

All experiments were performed three times unless otherwise stated. Data were expressed as means ± standard error of the mean (SEM). OriginLab was used to perform statistical analysis of the differences between data sets, by two sample T-test. A p-value lower than 0.05 was regarded as significant (*= $p<0.05$, **= $p<0.01$, ***= $p<0.001$).

CHAPTER 3. Regulation of microRNAs by IWS1/AKT signals in lung cancer cells

3.1 Introduction and Aims

3.1.1 Activation of AKT

The Akt family is a group of serine/threonine protein kinases, which regulate important cell functions by promoting survival, cell growth, proliferation, migration, tissue invasion, and angiogenesis. Briefly, AKT mediates cellular signalling downstream of PI3K, which phosphorylates PI (4,5) P2 to generate PI (3,4,5) P3. The PH domain of AKT binds PI (3,4,5) P3 to induce the translocation of the kinase to the plasma membrane, to co-localize with PDK1. PDK1 phosphorylates AKT at Thr308 and mTORC2 phosphorylates Ser473, to activate AKT. Whereas dephosphorylation of PI (3,4,5) P3 by PTEN, inhibits AKT activation. For a maximal activation of AKT both, Thr308 and Ser473 are required.

AKT membrane translocation and activation depend on the interaction of the AKT PH domain with PI (4,5) P2 and PI (3,4,5) P3. This interaction was originally suggested by the observation that point mutants in the AKT PH domain, could not be activated by PI3K-transduced signals. Ultimately, these mutants were critical in confirming the specificity of the phosphoinositide-PH domain interaction and in showing that the PH domain was functionally crucial for AKT activation **(Figure 3.1)**.

There are three Akt isoforms, Akt1, Akt2 and Akt3. Although the three AKT isoforms share similar mechanisms of activation and are structurally homologous, they also exhibit distinct characteristics. Specifically, AKT1 and AKT2 are ubiquitously expressed, whereas AKT3 has been reported to have less tissue distribution (Yang *et al.*, 2003).

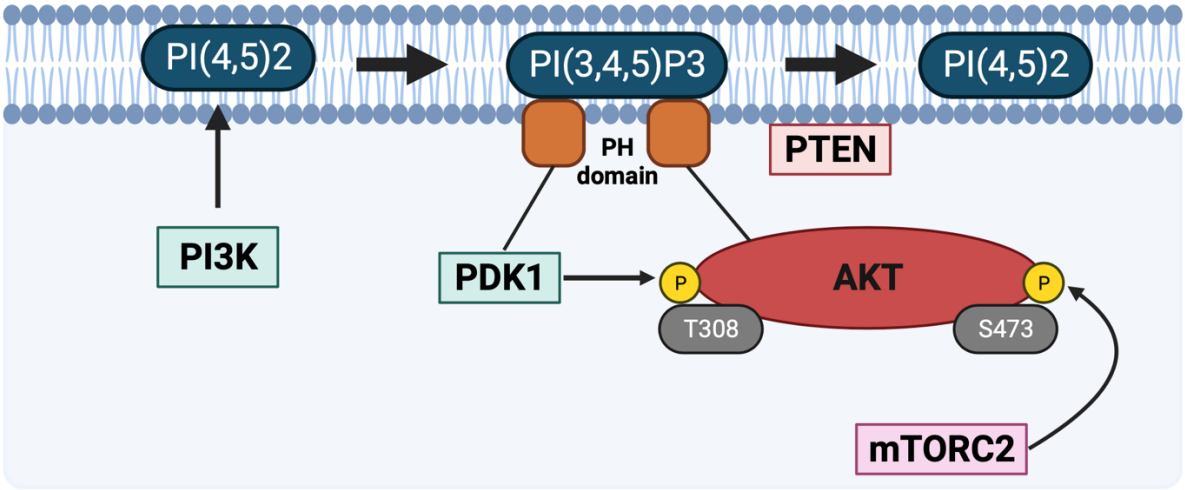

Figure 3. 1: AKT activation. PI3K phosphorylation converts PI (4,5) P2 to PI (3,4,5) P3. The PH domain of AKT and PDK1 recruits them to the plasma membrane, where PDK1 phosphorylates AKT on Thr308. mTORC2 phosphorylates AKT at Ser473 to fully activate AKT, which phosphorylates targets in the cytoplasm and nucleus. Designed using BioRender (www.biorender.com).

3.1.2 IWS1 is phosphorylated by AKT

It is already known that IWS1 and SUPT6 are involved in the pre-mRNA splicing as their deletion exhibited Pol II-dependent transcripts with increased splicing defects (Yoh *et al.*, 2007). IWS1 plays an essential role in pre-mRNA splicing by recruiting SETD2 to chromatin (Sanidas *et al.*, 2014). IWS1 is phosphorylated primarily by AKT3 and AKT1 but not AKT2 at Ser720/Thr721 and this phosphorylation is required for the recruitment of SETD2 to the SPT6-IWS1-Aly/REF complex. Also, SETD2 trimethylates H3K36 during transcriptional elongation and creates a docking site for MRG15 and PTB to regulate alternative splicing of FGFR2 (Sanidas *et al.*, 2014).

It is known that H3K36me3 is regulated by IWS1 (Yoh, Lucas and Jones, 2008). In a recent study focusing on mouse early embryos, it has been shown that H3K36me3 is modulated by PI3K/AKT pathway. Inhibition of the PI3K/AKT pathway reduces

the H3K36me3 levels while its activation increases the modification levels. Also, it was indicated that AKT regulates H3K36me3 through interaction with Iws1. They have also shown that Iws1 and Supt6 are important factors in the early stages of development, and they confirmed that IWS1 is crucial for H3K36me3 regulation and that AKT signalling regulates the pre-mRNA splicing through IWS1 phosphorylation (Oqani *et al.*, 2019).

IWS1 is also important for cell viability and interacts with the arginine methyltransferase PRMT5, which regulates the methylation of SUPT5H and its interaction with pol II (Liu *et al.*, 2007). Recently, it has been also found that IWS1 regulates the pathobiology of retroperitoneal LPS in an AKT-dependent manner.

3.1.3 microRNAs and RISC

microRNAs, are small single-stranded noncoding RNAs that regulate various physiological and pathological processes by binding in the 3'UTR of target mRNAs (Polytarchou *et al.*, 2015). microRNAs function in post-transcriptional regulation of gene expression and regulate growth, differentiation, development and apoptosis. Regulation of microRNA expression is well-studied however, the knowledge about their activity is limited. RISC is a family of molecular complexes that target genes for silencing (Pratt and MacRae, 2009). In RISC, an Ago family protein binds a small RNA to guide RISC to RNA transcripts (MacRae *et al.*, 2008). Briefly, a member of the Ago family binds the guided RNAs to mediate the repression of genes. Ago binds the microRNA duplexes, where the passenger strand is discarded and the guide strand is loaded into Agos, where mature RISC is guided to target 3'UTR of mRNA transcripts. RISC can silence its targets by RNA cleavage, by prevention of protein synthesis, transcriptional repression or by triggering chromatin remodelling. Human RISC is composed of a variety of proteins including, Ago2, Dicer, TRBP, TNRC6, MOV10 and FMRP (Chendrimada *et al.*, 2005; Liu *et al.*, 2005; Rehwinkel *et al.*, 2005; Kenny *et al.*, 2014). TNRC6 proteins TNRC6A/GW182, TNRC6B and

TNRC6C act as docking factors to bind Ago proteins for the induction of enzymes involved in translational repression and target degradation (Liu *et al.*, 2005; Rehwinkel *et al.*, 2005) whereas MOV10 and FMRP proteins, regulate the association of Ago2 with microRNA recognition elements (Kenny *et al.*, 2014).

3.2 Aims of Chapter 3

After assessing the global gene expression by RNA sequencing in wild-type and phosphorylation-deficient IWS1-expressing cells, bioinformatic analysis for common gene regulators, we found that in phosphorylation-deficient IWS1-expressing cells, gene expression is largely regulated by microRNAs. Our hypothesis is that IWS1 interacts with components of the RISC and regulates the activity of microRNAs upon phosphorylation by AKT.

In this chapter, we aimed:

1. To validate the hypothesis that IWS1 regulates the activity of microRNAs.
2. To characterise the mechanism of RISC regulation by AKT with a focus on the interaction of Ago2 with IWS1.

3.3 Methods

3.3.1 Transcriptomic Analysis

Lung cancer cells (NCI-H522 and NCI-H1299) were transduced with shIWS1 and reconstituted with wild-type IWS1 (Ser720/Thr721-IWS1) or phosphorylation deficient IWS1 (Ala720/Ala721-IWS1). In these cells, global gene expression was assessed by RNA sequencing and bioinformatic analysis.

3.3.2 Library preparation and RNA sequencing

Total RNA was isolated from shControl, shIWS1, shIWS1/Ser720/Thr721-IWS1 and shIWS1/Ala720/Ala721-IWS1 NCI-H522 cells, using PureLink RNA Kit (12183018A, Invitrogen). Advanced Analytical Fragment Analyzer was used to analyse RNA samples, using an RNA kit for integrity check and quantification. 100-500 ng of Total RNA was used for library preparation with the Illumina TruSeq stranded mRNA Library preparation kit (RS-122-2101, Illumina) and they were indexed individually. Next-generation sequencing was used to quantify the libraries on Fragment Analyzer. The libraries of all samples were pooled in equal molar concentration and sequenced on an Illumina HiSeq 2500 platform with Rapid V2 chemistry and 100 bp paired-end reads. Results were demultiplexed with bcl2fastq, compressed and analysed. The procedure was performed in the Tufts University Core Genomic Facility (TUCF, http://tucf-genomics.tufts.edu/). All RNA-sequencing experiments were performed in duplicates with an average depth of sequenced samples of 37.5M (±5M Fragments). Data pre-processing and alignment were conducted as previously described (Vlachos *et al.*, 2016).

RNA-seq libraries were quality-checked using FastQC (https://www.bioinformatics.babraham.ac.uk/projects/fastqc/). Adapters and sequence contaminants were detected and removed using an in-house developed algorithm and additional software including Kraken suite and Cutadapt. Paired-end

reads were aligned against the human reference genome (GRCh38/hg38) with GSNAP spliced aligners. For annotation of genes and transcript, Ensembl v85 reference database was utilized.

3.3.3 Bioinformatic analysis

Regulatory RNA (RegRNA) is an integrated web server that was used to identify elements against an input mRNA sequence and homologs of the regulatory RNA motifs. Through the server, both, sequence and structural homologs of regulatory RNA motifs were recognized. RegRNA surveying literature to extract known regulatory RNA motifs with several regulatory RNA motif databases including UTRSite (Mignone *et al.*, 2005), TRANSFAC (Matys *et al.*, 2006), alternative splicing database (Stamm *et al.*, 2006) and miRbase (Griffiths-Jones *et al.*, 2006). Moreover, RegRNA collects known regulatory RNA motifs including motifs in the 3'UTR / 5'UTR, microRNA target sites, motifs involved in transcriptional regulation, exonic/intronic splicing, splicing donor/acceptor sites and inverted repeats (Huang *et al.*, 2006).

3.3.4 microRNA target prediction analysis

Target transcripts of equally expressed microRNAs in Ser720/Thr721-IWS1 and Ala720/Ala721-IWS1-expressing cells, quantified by miRNA sequencing, were identified using Targetscan (TargetScanHuman 7.2) and Diana Tools [DIANA TOOLS (athena-innovation.gr)] databases. For each microRNA, predicted and experimentally validated targets were identified. Data were compared with RNA sequencing data in the same cell types for common genes. The number of predicted microRNA targets was divided by and expressed as % of the total number of TargetScan Genes (n=28,353). The number of observed suppressed microRNA targets in Ala720/Ala721-IWS1-expressing cells was divided by and expressed as

a % of the total number of downregulated genes (n=474) in the RNA sequencing data.

3.3.5 microRNA activity assays

Cells were plated in a 6-well plate (500,000 cells/well). The following day, cells were transfected with 2.5 µg of microRNA reporter constructs **(Table xvii)**, expressing mkate2 (Red Fluorescent Protein, RFP) and EBFP2 (Blue Fluorescent Protein, BFP), using Lipofectamine 3000 (L3000001, Invitrogen) transfection reagent according to manufacturer's instructions. Briefly, in one Eppendorf tube, 125 µl of Opti-MEM (51985026, Gibco) were combined with 6 µl of L3000. In a second tube, 125 µl of Opti-MEM were combined with 8 µl of P3000 and 2.5 µg of microRNA reporter constructs. Contents were combined, incubated for 15 minutes at room temperature, and added dropwise to the cells. Transfected cells were plated in quintuplicates 24 hours later, in a 96-well plate (30,000 cells/ well). Fluorescence measurements were performed 48 hours later to calculate RFP/BFP ratio. The plate read at 561 nm excitation and 610 nm emission for RFP and for BFP at 405 nm excitation and 450 nm emission.

3.4 Results and Discussion

3.4.1 Bioinformatics analysis of the transcriptome of IWS1-expressing cells.

Since their discovery, multiple studies assessed the regulation of microRNA expression, but studies on the regulation of their activity remain limited. microRNA target evaluation is a fundamental step in the understanding of microRNA activity. In this project, miRNA sequencing data and gene expression data from lung cancer cells were used to evaluate microRNA activity.

Lung cancer cells (NCI-H522), transduced with shIWS1 and reconstituted with Ser720/Thr721-IWS1 or Ala720/Ala721-IWS1, were utilized. Using RNA seq, we found that 545 genes are downregulated in Ser720/Thr721-IWS1-expressing cells and 474 genes are downregulated in Ala720/Ala721-IWS1-expressing cells. Bioinformatic analysis for common regulators of the genes whose expression is suppressed in either cell line revealed that in Ala720/Ala721-IWS1-expressing cells, gene expression is largely regulated by microRNAs **(Figure 3.2)**.

microRNA sequencing analysis in the same cells revealed that 255 microRNAs are upregulated in Ser720/Thr721-IWS1 and 291 microRNAs in Ala720/Ala721-IWS1-expressing cells, suggesting that the effects on gene expression (mRNA) are less likely to be due to differences in microRNA expression levels. This analysis suggested that microRNAs have different effects upon IWS1 phosphorylation by AKT, potentially due to different levels of microRNA activity.

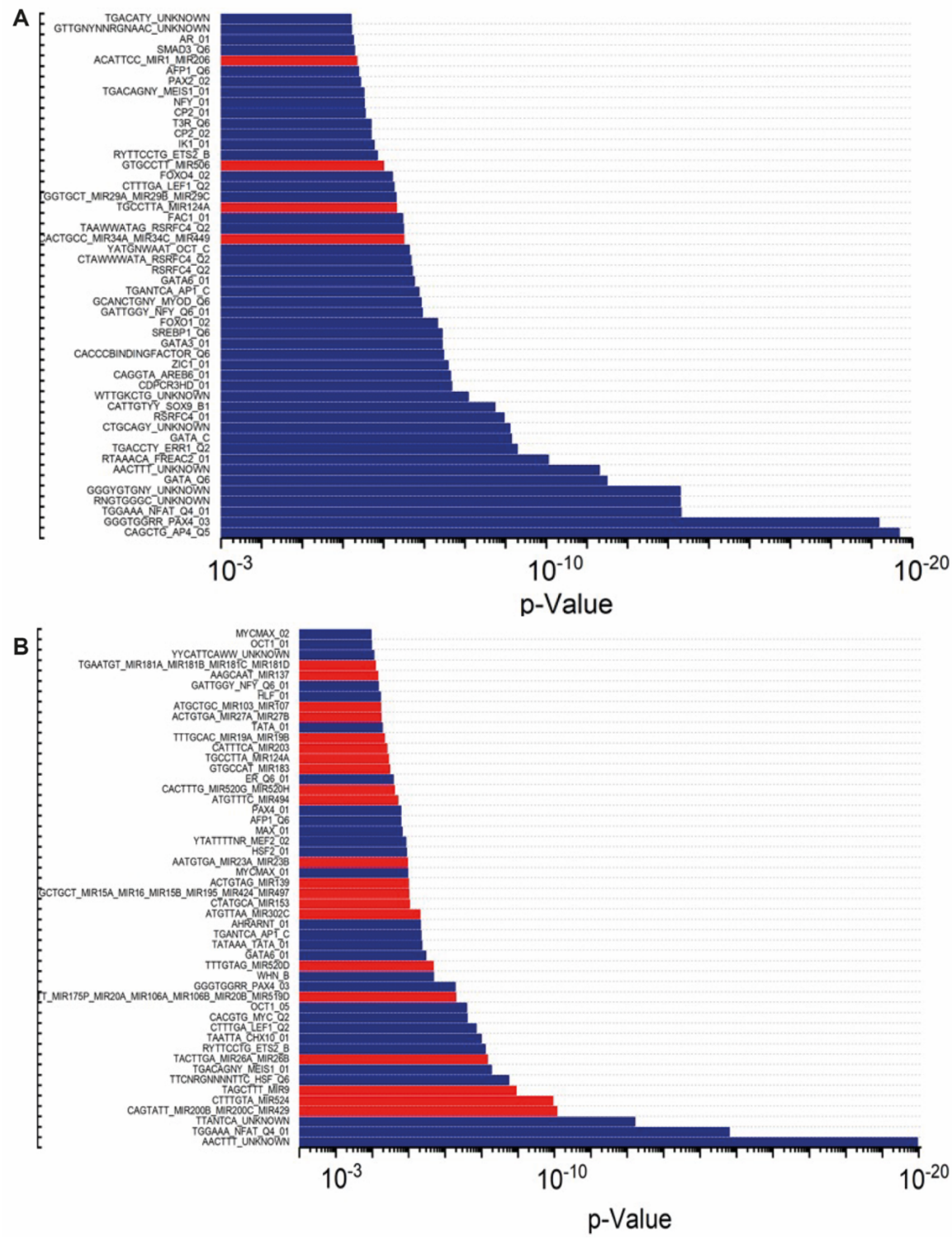

Figure 3. 2: Bioinformatic comparison between the transcriptomes of cells expressing wild type and phosphorylation deficient IWS1. Common regulators of genes downregulated in Ser720/Thr721-IWS1 and Ala720/Ala721-IWS1-expressing cells. (A) Regulators of genes downregulated in Ser720/Thr721-IWS1, and (B) Regulators of genes downregulated in Ala720/Ala721-IWS1-expressing cells. Blue indicates transcriptional regulation and red indicates posttranscriptional regulation by microRNAs. Bioinformatic analysis was performed using miRNAome analysis (RegRNA web server).

To investigate this hypothesis, we evaluated microRNAs with similar expression levels in both cell lines. Specifically, we focused on microRNAs expressed at high levels in both cell lines, we found their predicted and experimentally validated targets and compared them with the RNA sequencing data. Venn diagrams show the number of microRNA target genes in predicted, validated and RNA sequencing datasets **(Figure 3.3)**.

Although the microRNA expression levels were similar, we found differences in the expression of predicted microRNA targets in Ala720/Ala721-IWS1-expressing cells. We calculated the numbers and percentages (%) of predicted and validated microRNA targets and suppressed in Ala720/Ala721-IWS1-expressing cells compared to Ser720/Thr721-IWS1-expressing cells. We found that the % of targets that may be suppressed by these microRNAs in Ala720/Ala721-IWS1-expressing cells is higher than expected (predicted and validated) **(*Table xxvi*)**. Thus, we propose that microRNA activity is increased in Ala720/Ala721-IWS1-expressing cells.

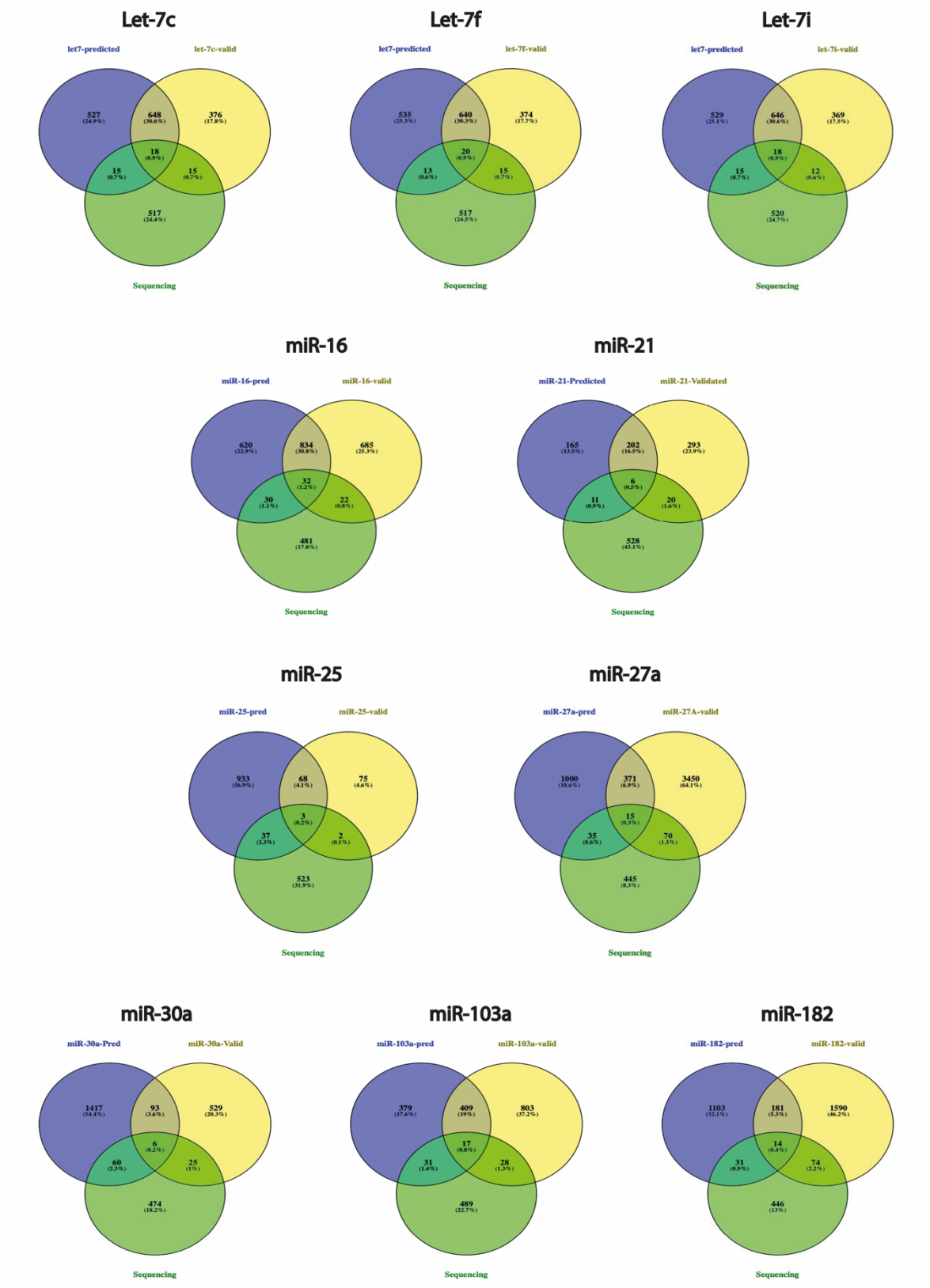

Figure 3. 3: microRNA target transcripts. Venn diagrams of the number of predicted and validated target transcripts for different microRNAs in, compared to transcripts downregulated in Ala720/Ala721-IWS1-expressing cells. Predicted and validated targets were identified using the DIANA software and downregulated transcripts were obtained from the RNA sequencing data.

Table xxvi: Predicted and validated microRNA targets downregulated in Ala720/Ala721- IWS1-expressing cells

miRNAs	Predicted	%	Validated	%	Predicted + Validated	%	Observed	%	Fold change
miR-21	384	1.3	521	1.8	697	**2.5**	37	**7.8**	**0.79**
miR-103a	836	2.9	1257	4.4	1667	**5.9**	76	**16**	**0.95**
miR-16	1516	5.3	1573	5.5	2223	**7.8**	84	**18**	**0.81**
let-7c	1208	4.3	1057	3.7	1599	**5.6**	48	**10**	**0.86**
let-7f	1208	4.3	1046	3.7	1597	**5.6**	48	**10**	**0.77**
let-7i	1208	4.3	1045	3.7	1596	**5.6**	45	**9.5**	**0.97**
miR-30a	1576	5.6	653	2.3	2130	**7.5**	91	**19.2**	**1.35**
miR-25a	1041	3.7	148	0.5	1118	**3.9**	42	**8.9**	**0.97**
miR-182	1329	4.7	1859	6.6	2993	**10.6**	119	**25.1**	**0.82**
miR-27a	1421	5.0	3906	13.8	4941	**17.4**	120	**25.3**	**0.81**

[1] Percentages calculated against the whole transcriptome (TargetScan).
[2] Percentages calculated against the differentially regulated transcripts (RNA seq).
[3]The relative expression of miRNA in Ala720/Ala721-IWS1 compared to Ser720/Thr721-IWS1-expressing cells (miRNA seq).

3.4.2 Enhanced microRNA activity in Ala720/Ala721-IWS1- expressing cells.

The expression levels of microRNAs can be determined upon RNA extraction through next-generation sequencing or by qPCR. To assess and quantify microRNA activity in live cells, a defined set of targets or microRNA reporter activity assays are required. Quantification of microRNA levels without cell lysis can be acquired by microRNA activity reporters. In the reporters used here, four repeats of microRNA target sites are inserted into the 3'UTR of a reporter gene (Gam, Babb and Weiss, 2018). These vectors encode the expression of two fluorescent proteins, the red fluorescent protein (RFP) mKate2, which is regulated by microRNA target sites in its 3'UTR, and the blue fluorescent protein (BFP) EBFP2, which serves as a reference for data normalization **(Figure 3.4)**. The corresponding microRNAs, target the 3'UTR of mKate2 and induce a decrease in red fluorescence without affecting the blue fluorescence (Gam, Babb and Weiss, 2018).

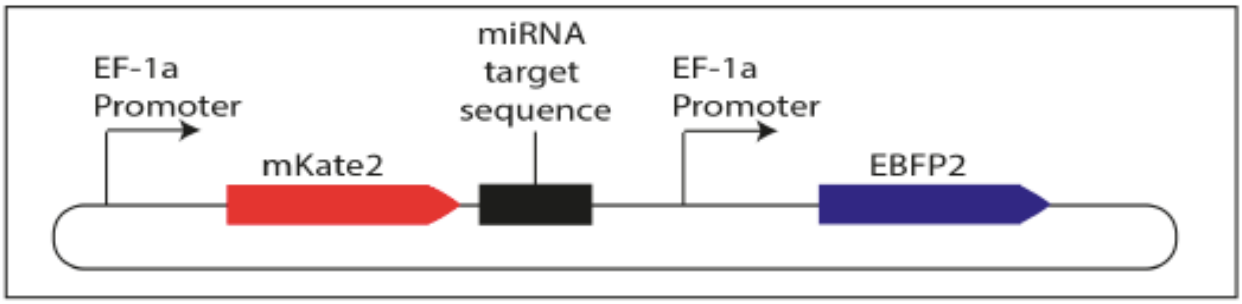

Figure 3. 4: Schematic representation of microRNA reporter constructs. Repeats of the microRNA target sequence are inserted in the 3'UTR of mKate2, therefore RFP fluorescence is under the control of the microRNA whereas BFP fluorescence is not affected.

To test our hypothesis of enhanced microRNA activity in Ala720/Ala72-IWS1-expressing cells, we performed a series of microRNA activity reporter assays. We transduced the lung cancer cell line NCI-H1299, with shIWS1 and reconstituted with Ser720/Thr721-IWS1 or Ala720/Ala72-IWS1, to perform microRNA activity assays and directly measure the post-transcriptional effects of microRNAs. We focused on equally expressed microRNAs in Ser720/Thr721-IWS1 and Ala720/Ala721-IWS1-expressing cells: Let-7a, Let-7c, miR-16, miR-21, miR-30a and miR-103a. These assays revealed the enhanced activity of all microRNAs tested in Ala720/Ala721-IWS1-expressing cells **(Figure 3.5)**. These findings support our hypothesis that microRNAs exhibit increased activity in cells expressing phosphorylation deficient IWS1. Furthermore, the use of a second cell line indicated that this is not a cell line-specific effect. The regulation of microRNA activity and not microRNA expression proposes that IWS1 may interact with Ago proteins, affecting either Ago-RISC interactions or Ago-IWS1-RISC interactions (Gam, Babb and Weiss, 2018).

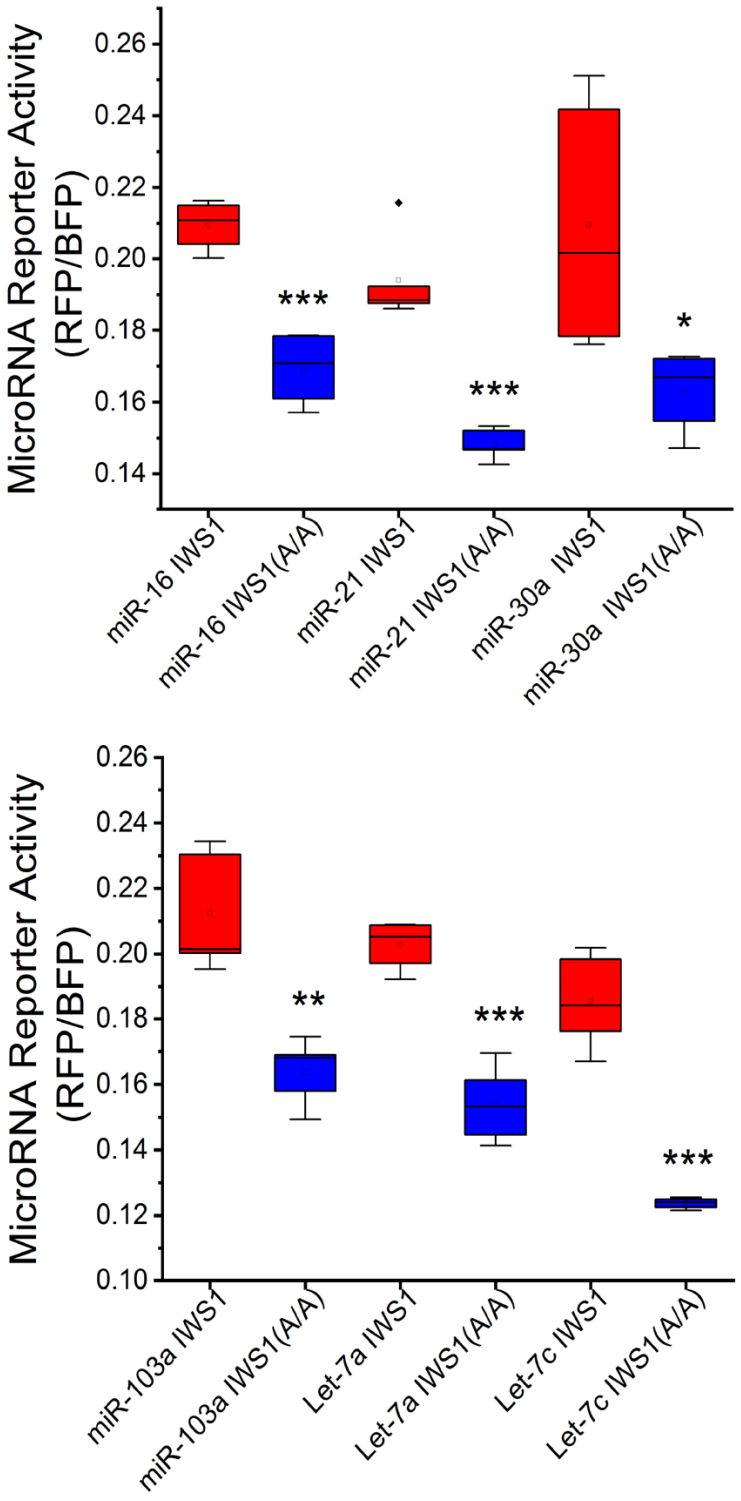

Figure 3. 5: Effects of Ala720/Ala721-IWS1 on microRNA activity. microRNA reporter activity measurements in NCI-H1299 cells expressing Ser720/Thr721-IWS1 or Ala720/Ala721-IWS1 cells. The expression of mKate2 (RFP), is regulated by microRNA target sites in its 3'UTR, and the EBFP2 (BFP), serves as a reference for data normalization. Data are presented as box plots of assays performed in quintuplicates. Statistically significant differences were determined by Student's t-test, *P<0.05, **P<0.01, ***P<0.001.

3.4.3 Expression of microRNA-validated targets is suppressed in Ala720/Ala721-IWS1- expressing cells.

To further verify the increased activity in cells expressing phosphorylation deficient IWS1, we examined the expression of known microRNA targets in Ser720/Thr721-IWS1 or Ala720/Ala721-IWS1-expressing cells at the protein level. Lysates derived from NCI-H1299 cells transduced with shIWS1 and reconstituted with Ser720/Thr721-IWS1 or Ala720/Ala72-IWS1 were used to assess protein levels by western blot. ***Table xxvii*** shows the experimentally validated microRNA targets analysed. Western blot analysis confirmed that the expression of targets of microRNAs equally expressed in both cell types, is lower in Ala720/Ala72-IWS1-expressing cells **(Figure 3.6)**.

Table xxvii: Experimentally validated microRNA targets

microRNAs					
miR-16	**miR-17**	**miR-21**	**miR-29a**	**miR-30a**	**miR-218**
AKT3	CDK2	EFGR	DNMT3a	CDK6	CDK6
		PDCD4	DNMT3b		
			CDK6		
			MCL1		
			TCL1A		

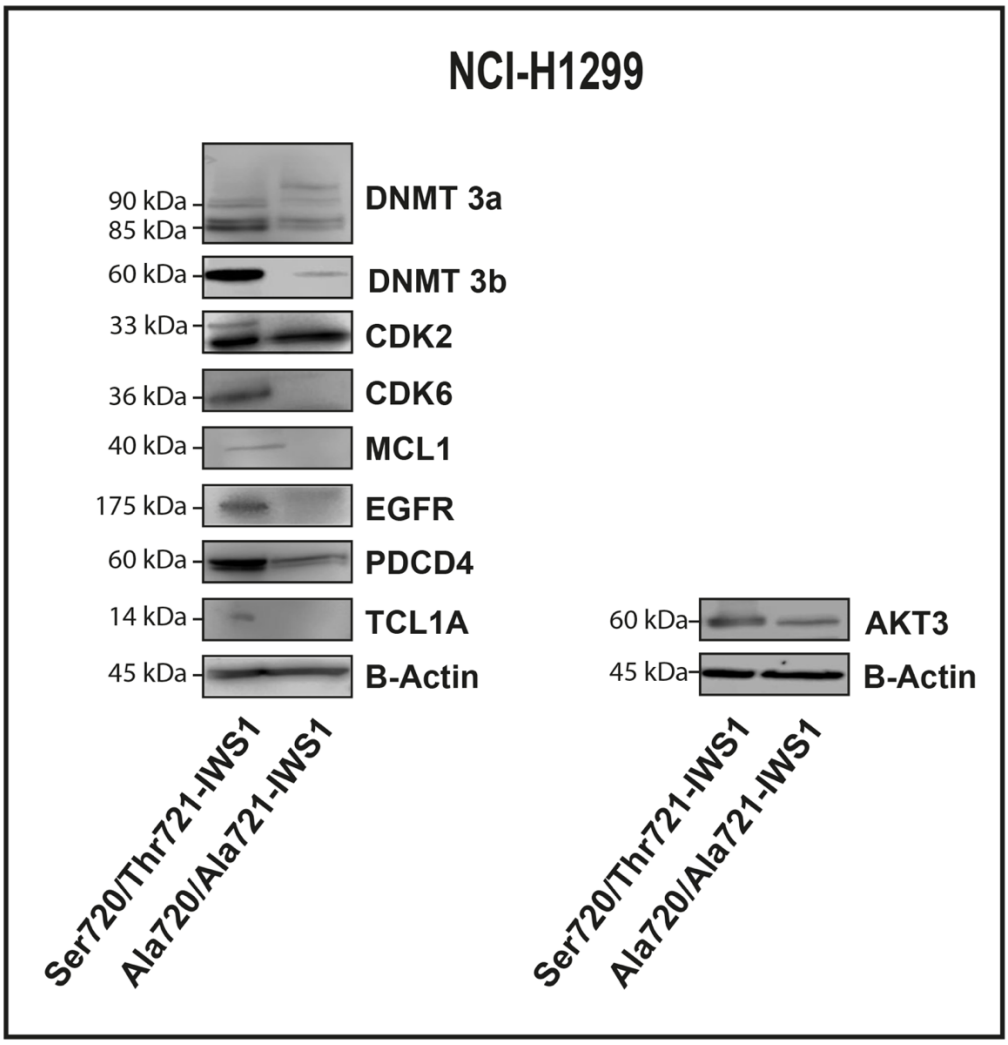

Figure 3. 6: Western blot analysis of microRNA targets. Lysates derived from NCI-H1299 cells transduced with shIWS1 and reconstituted with Ser720/Thr721-IWS1 or Ala720/Ala72-IWS1 were analysed by Western blot using the respective antibodies. B-Actin was used as a loading control (Western blot representative n=3).

3.4.4 IWS1 interacts with Ago2.

We questioned whether microRNA activity is affected by the interaction of IWS1 with Ago2, the catalytic core of RISC which recognizes and cleaves mRNAs with complementary sequences. It has been shown that Ago2 is post-transcriptionally regulated by microRNAs and it is unstable and degraded in the absence of microRNAs (Martinez and Gregory, 2013). Sucrose Gradient Fractionation followed by western blot analysis was used to detect potential protein complexes. We found that IWS1 and Ago2 are detected in the same fraction, and both are shifting to larger

protein complexes upon serum activation **(Figure 3.7)**. These data indicate that there is a possible interaction between IWS1 and Ago2, mediated by signalling pathways activated by growth factors, such as AKT.

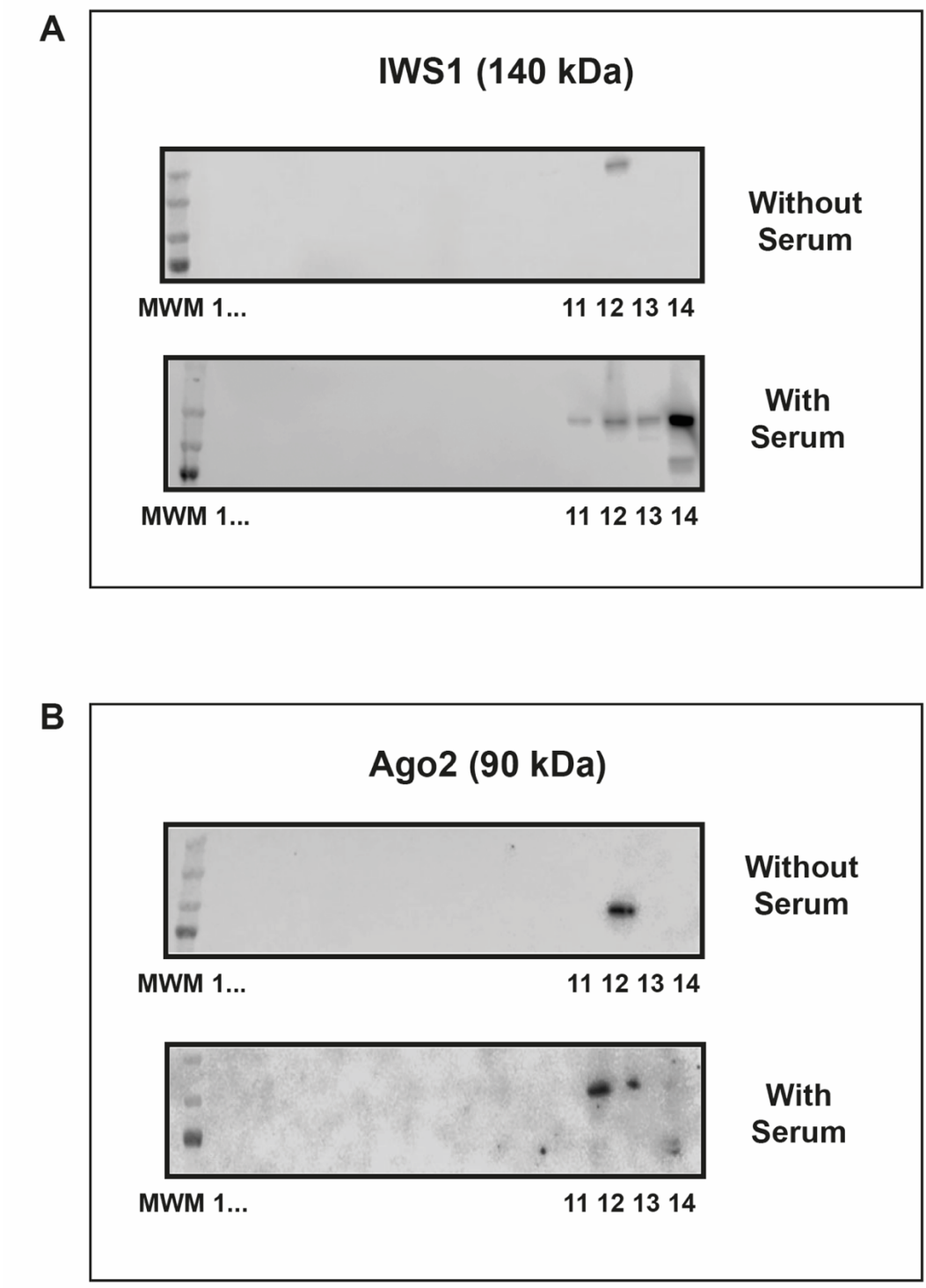

Figure 3. 7: Sucrose gradient fractionation for the detection of Ago2 and IWS1. NCI-H522 cells were cultured with or without serum and lysates were fractionated on a 5-60% sucrose gradient. Western blot analysis for **(A)** IWS1 and **(B)** Ago2 after sucrose gradient fractionation (Highest molecular weight fraction (14) to Lowest molecular weight (1).

Sucrose Gradient Fractionation suggested that IWS1 and Ago2 are found in the same fraction and that there is a possible interaction. To validate this hypothesis NCI-H522 cells were cultured with or without serum and lysates were subjected to immunoprecipitation for Ago2. AKT is activated by growth factors and serum. Briefly, PI3K pathway is activated and then activates AKT via phosphorylation at Thr308, while phosphorylation of Ser473 leads to the maximum activation (Fruman *et al.*, 2017). Thus, in cells deprived of serum, AKT is inactive. Immunoblot analysis of Ago2 immunoprecipitates for IWS1 revealed that serum induces the interaction of Ago2 and IWS1 **[Figure 3.8 (A)]**. This confirms that IWS1 interacts with Ago2 in a serum and potentially AKT-dependent manner.

To confirm the role of AKT in regulating this interaction, we used lysates from the same cell line, transduced with shIWS1 and reconstituted with Ser720/Thr721-IWS1 or Ala720/Ala721-IWS1. Lysates were subjected to immunoprecipitation for Ago2. Immunoblot analysis for IWS1 showed that Ago2 interacts stronger with IWS1 phosphorylated by AKT **[Figure 3.8 (B)]**. In the same lysates, immunoprecipitation for FLAG-tagged (IWS1), followed by immunoblot analysis for Ago2, verified the enhanced interaction of Ago2 with the phosphorylated IWS1 **[Figure 3.8 (C)]**.

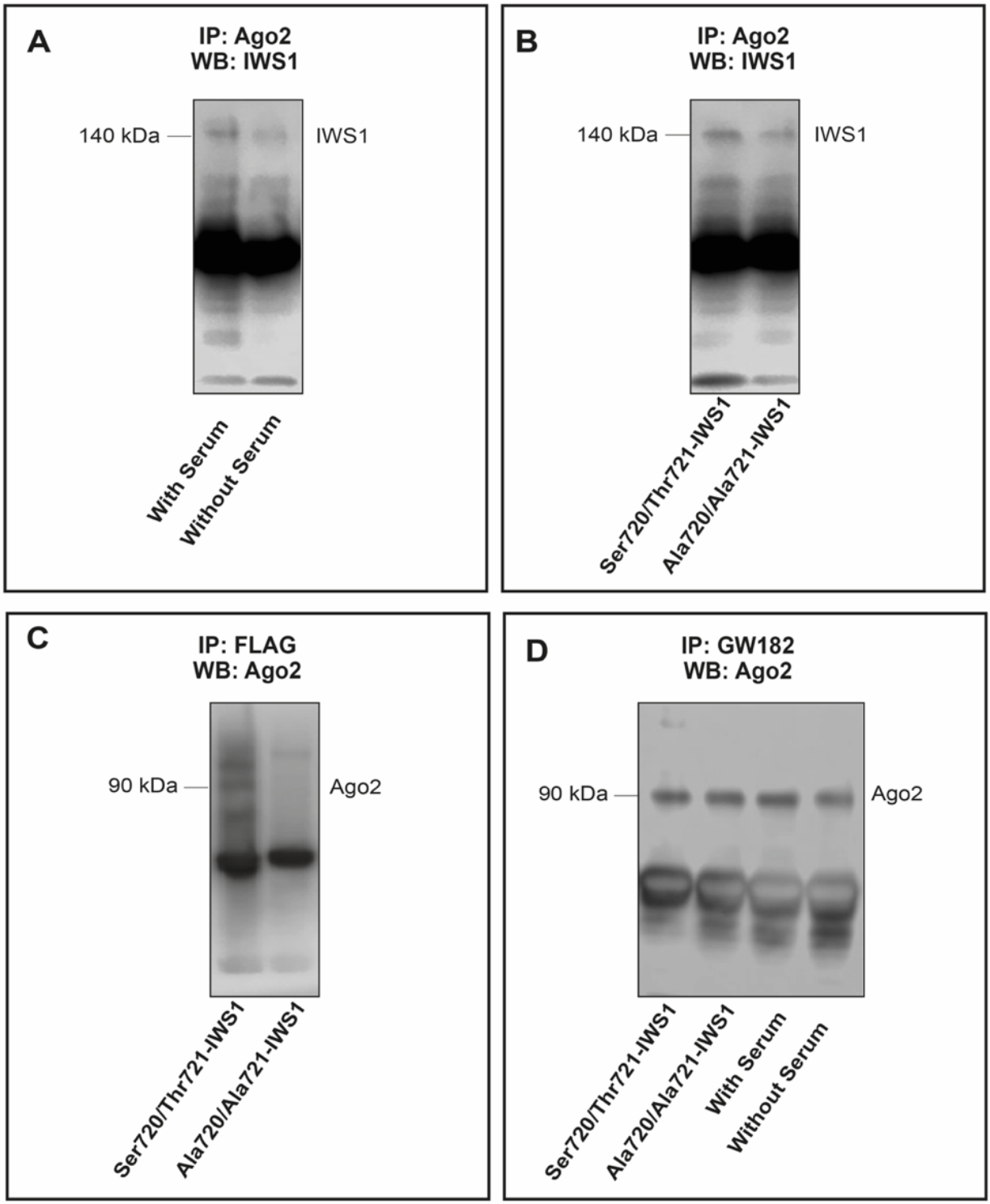

Figure 3. 8: Immunoprecipitation assays for the detection of protein interactions. (A) Immunoblot analysis for IWS1 in lysates of NCI-H522 cells cultured with or without serum, immunoprecipitated for Ago2. Immunoblot analysis for **(B)** IWS1 and **(C)** Ago2 in lysates from Ser720/Thr721-IWS1 and Ala720/Ala721-IWS1-expressing cells subjected to immunoprecipitation for Ago2 and FLAG-tagged IWS1, respectively. **(D)** Immunoprecipitation for GW182 followed by immunoblot analysis for Ago2.

It has been shown that GW182 is recruited to microRNA targets through direct interaction with Ago proteins and it has a key role in miRISC (Eulalio, Huntzinger and Izaurralde, 2008). GW182 contains multiple Ago-binding sites and functions in microRNA-mediated translational repression. Each of the Ago-binding sites can bind to Ago2, and GW182 acts as a scaffold protein to target mRNAs (Takimoto, Wakiyama and Yokoyama, 2009). GW182 is localized in processing bodies (P bodies) which are cytoplasmic foci related to translational repression and mRNA degradation (Eystathioy *et al.*, 2003; Ding and Han, 2007; Takimoto, Wakiyama and Yokoyama, 2009). Loss of its function reduces microRNA-mediated gene silencing (Jakymiw *et al.*, 2005). **Figure 3.9** shows the role of GW182 in microRNA-mediated gene silencing.

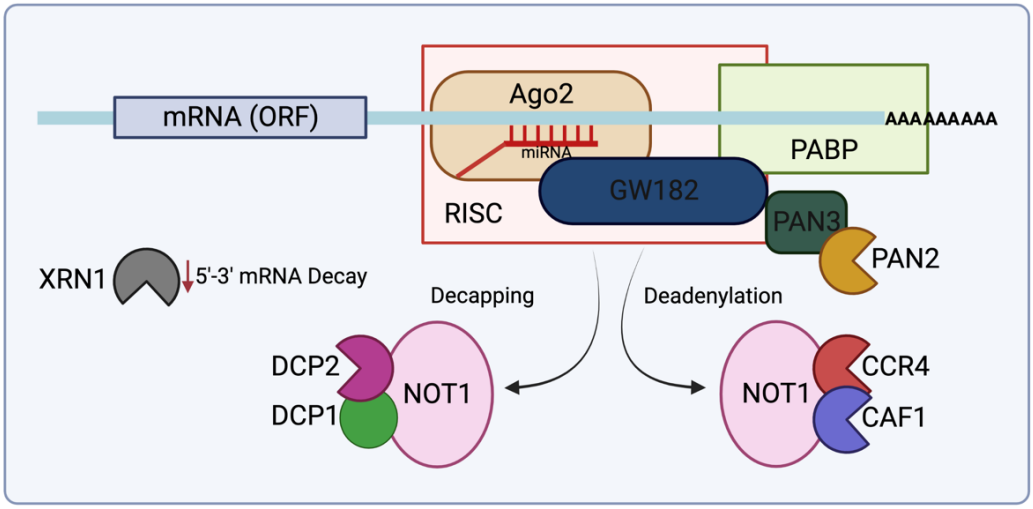

Figure 3. 9: Role of GW182 in microRNA-mediated gene silencing. GW182 destabilizes target mRNAs through the recruitment of deadenylating complexes CCR4-NOT1 and PAN2-PAN3. Decapping factors DCP1-DCP2 are involved in decapping and decapped mRNAs are degraded by XRN1. Figured prepared by Niaz and Hussain, 2018 and modified using BioRender (www.biorender.com).

We were interested to check if the interaction of GW182 and Ago2 is dependent on IWS1. Immunoprecipitation for GW182 followed by western blot analysis for Ago2, revealed that GW182-Ago2 interaction is IWS1-independent **[Figure 3.8 (D)]**. We concluded that Ago2 interacts with IWS1 in an AKT-dependent manner and whereas the GW182-Ago2 interaction does not depend on IWS1 phosphorylation.

3.5 Conclusion of Chapter 3

RNA and miRNA sequencing using RNAs isolated from shControl, shIWS1, shIWS1-Ser720/Thr721 and shIWS1-Ala720/Ala721-IWS1 NCI-H522 cells, and bioinformatic analysis for common regulators revealed that transcripts downregulated in Ala720/Ala721-IWS1-expressing cells are primarily regulated by microRNAs. Whole microRNAome analysis revealed that there are similar numbers of upregulated microRNAs in the two cell types in contrast to their effects on gene expression. Focusing on a set of microRNAs with similar expression levels in the two cell types, microRNA activity reporter assays were performed showing that the microRNA activity in Ala720/Ala721-IWS1-expressing cells is enhanced compared to Ser720/Thr721-IWS1-expressing cells. Sucrose gradient fractionation revealed that Ago2 and IWS1 are found in the same fragment and immunoprecipitation and western blot analyses revealed the interaction between IWS1 and Ago2. Furthermore, we have shown that IWS1 interacts with Ago2, and this interaction is mediated by the phosphorylation of IWS1 by AKT, whereas, Ago2-GW182 interaction is independent of IWS1 phosphorylation.

CHAPTER 4: Molecular characterisation of intestinal epithelial cell lines

4.1 Introduction and Aims

Pathway analysis of the differentially regulated genes in Ser720/Thr721 VS Ala720/Ala721-IWS1 expressing lung cancer cells revealed that the deregulated genes are involved in colorectal cancer and intestinal diseases. Through this analysis, we went on to identify these pathways using the appropriate bonding, which are intestinal stem cells, colon and mucosal epithelial cells.

4.1.1 Structure and Function of Intestinal epithelium

The primary function of the gut is the reabsorption of water, minerals and nutrients and forms a protective barrier against pathogens in the intestinal lumen. The intestinal epithelium is the most vigorous self-renewing tissue of adult mammals to maintain the integrity of the epithelium (Crosnier, Stamataki and Lewis, 2006). The intestinal epithelium consists of villi and crypts of Lieberkühn. Small and large intestines have similar crypt structures, where the Intestinal Stem cells (ISCs) reside at the bottom of the crypts and give rise to daughter or progenitor cells that are differentiated into mature cells needed for normal gut function (Umar, 2010) **(Figure 4.1)**.

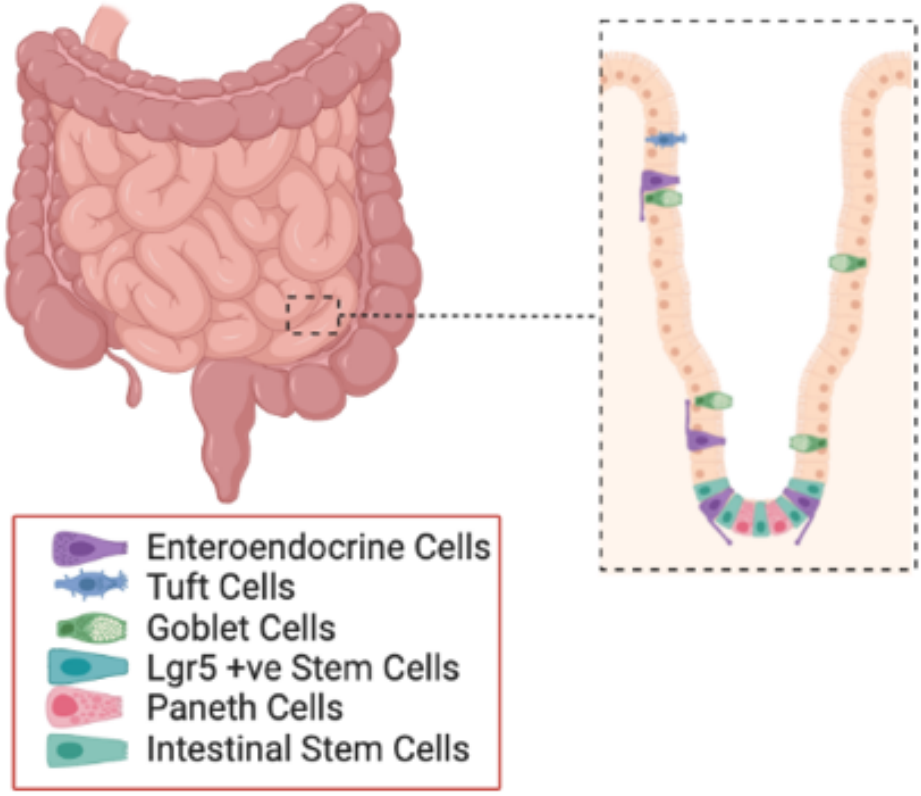

Figure 4. 1: Schematic representation of the basic unit of the Intestinal epithelium. ISC s and Paneth cells reside at the bottom of the crypt. Stem cells move towards the top of the villi and differentiating into different cell types such as enteroendocrine, tuft and goblet cells. Figure prepared using BioRender (https://www.biorender.com/).

Briefly, these multipotent stem cells give rise to daughter cells that migrate as they proliferate and differentiate into transit amplifying (TA) cells, which are rapidly proliferating immature cells with lineage commitment, which differentiate terminally to the different epithelial cell types (Smith, Gallagher and Wong, 2016). The differentiated epithelial cells are categorized based on their function in absorptive enterocytes and in three secretory lineages consisting of mucus-secreting goblet cells, hormone-secreting enteroendocrine cells and antimicrobial peptide-secreting Paneth cells **(Figure 4.2)** (Shroyer *et al.*, 2005; Umar, 2010) Enterocytes are responsible for the absorption of nutrients, whereas the goblet cells secrete a protective mucus barrier and the enteroendocrine cells release gastrointestinal hormones. On the other hand, Paneth cells secrete antibacterial peptides which exist in the base of the proliferative compartment (Cheng and Leblond, 1974).

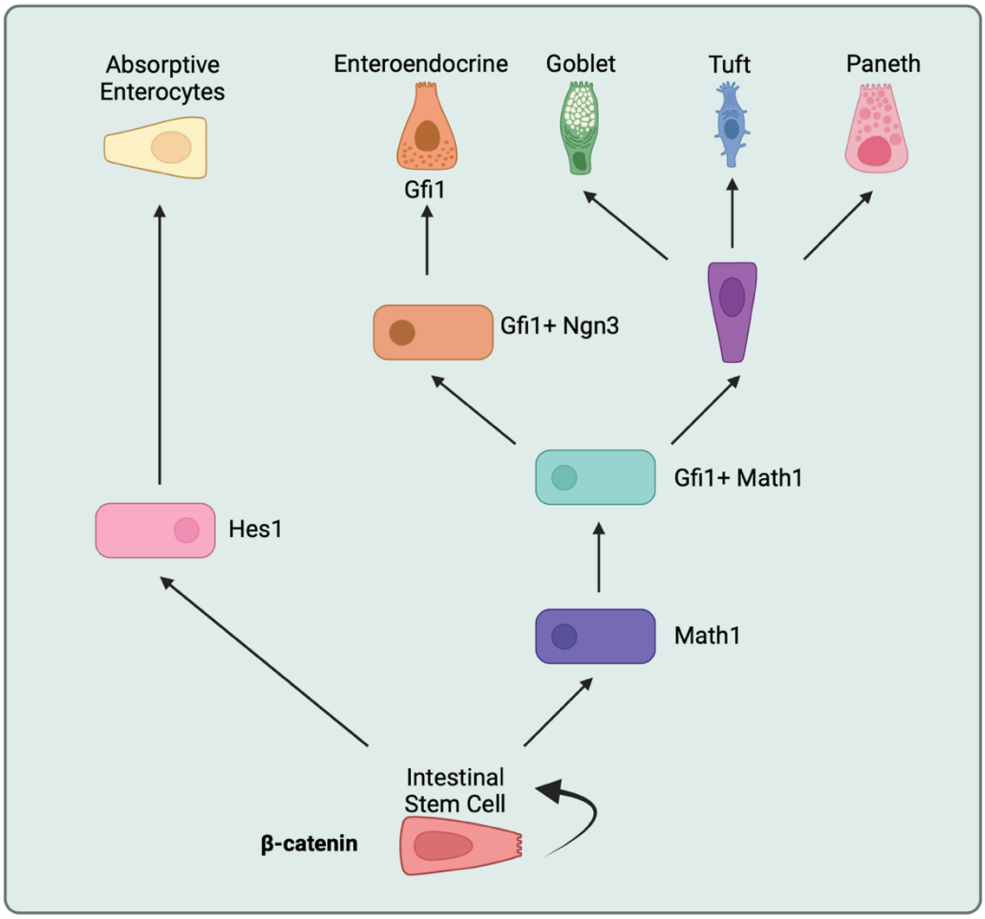

Figure 4. 2: Schematic representation of the intestinal stem cell differentiation. ISCs found at the base of the crypt and are characterised by nuclear localization of β-catenin and employ Notch signalling to express either Hes1 or Math1. Hes1-expressing cells differentiate into absorptive enterocytes whereas Math1-expressing cells constitute the secretory progenitors. Figure prepared using BioRender (https://www.biorender.com/).

Under normal conditions, ISCs and progenitor cells are located at the bottom of the crypt, and they undergo complete renewal every 3-5 days (Kim, Yang and Bialkowska, 2017). Each crypt is made up of around 250 cells and a similar number of cells are generated daily (Barker, Van Oudenaarden and Clevers, 2012). TA cells expand, differentiate and migrate toward the tip of the villus and eventually die and are excreted from the lumen. As TA cells migrate, they differentiate into secretory or absorptive lineages, defining the two main functions of the gut. The secretory cells secrete hormones and provide a barrier against food-borne microorganisms and toxins through mucus secretion whereas, the absorptive cells uptake important

dietary nutrients (Van Der Flier and Clevers, 2009; Santos *et al.*, 2018). The morphogenesis of crypts and cell proliferation depends on the Wnt/β-catenin pathway members and target genes such as *caudal type homeobox 1* (*Cdx1*) and *2* (*Cdx2*) (Beck *et al.*, 1999). β-catenin signalling is important for stem cell renewal, proliferation and differentiation (Pinto et al., 2003), while Notch signalling in progenitors directs selection between *atonal homolog 1* (*ATOH1* or *Math1*) and *enhancer of split 1* (*Hes1)* expression (Yang *et al.*, 2001). Progenitors expressing *Hes1* differentiate into absorptive enterocytes and those expressing *Math1* are committed to the secretory lineage, to become goblet, Paneth or enteroendocrine cells. Enterocytes are found on the surface of the epithelium and are responsible for the digestion and absorption of nutrients (Gassler, 2017). Goblet cells are glandular epithelial cells responsible for the production and maintenance of protective mucus, synthesizing and secreting glycoproteins are known as mucins (Specian and Oliver, 1991). They are derived from the intestinal and progenitor cells in the cryptand their differentiation is controlled by different transcription factors, including the Notch target, Hes1 (Gersemann, Stange and Wehkamp, 2011). Mucins are secreted into the intestinal lumen, forming a mucus layer which acts as a barrier between the luminal contents and the epithelial surface (Shirazi *et al.*, 2000). Paneth cells are found on the bottom position of small intestinal crypts and are essential for the production and secretion of antimicrobial peptides (Gassler, 2017). For the terminal differentiation of enteroendocrine cells, Neurogenin 3 (Ngn3), pancreatic and duodenal homeobox 1 (Pdx1) and Neuronal Differentiation 1 (Neurod1) transcription factors are required (Schonhoff, Giel-Moloney and Leiter, 2004). Enteroendocrine cells respond to luminal nutrients to control enzyme secretion, intestinal motility and appetite regulation by secreting peptide hormones (Begg and Woods, 2013; Gribble and Reimann, 2016). Deregulation of this above system of epithelial regeneration results in cancer growth (Barker *et al.*, 2009).

4.1.2 Markers of ISCs and derived lineages

ISCs express multiple markers common for adult stem cells. Lgr5 is a specific crypt base columnar (CBC) marker controlled by Wnt signals that are active in human colon cancer cells (Van Der Flier and Clevers, 2009). The Lgr5 gene marks the CBC cells located between Paneth cells **(Figure 4.1)** (Barker *et al.*, 2007). Despite that Lgr5 is a stem cell marker, it may not be essential for the maintenance of stem cells as deletion of the *Lgr5* gene was reported to have no effects on the development of the intestine (Morita *et al.*, 2004; Montgomery and Breault, 2008). Leucine-rich repeats and immunoglobulin-like domains protein 1 (Lrig1) was found to be expressed on different cells within the crypt, overlapping with the expression of *Lgr5.* It regulates the width of growth factor signalling in controlling the ISC niche size (Powell *et al.*, 2012; Wong *et al.*, 2012). *Hes1* is a transcriptional target of Notch and Wnt/β-catenin signalling pathways and regulates the commitment to absorptive and secretory phenotypes (VanDussen and Samuelson, 2010). Hes1 is expressed in CBCs and TA cells but not in Paneth cells (Kayahara *et al.*, 2003; Goto *et al.*, 2017). Musashi-1 (Msi1) and Prominin 1 are also CBC cell markers, and their expression is extended into the lower TA section (He *et al.*, 2007; Snippert *et al.*, 2009; Zhu *et al.*, 2009). Msi1 is an RNA-binding protein which is expressed by *Lgr5*$^{+}$ cells (Muñoz *et al.*, 2012). Bmi1 is the first +4 stem cell marker, as its mRNA was found by *in situ* hybridization to mark the rare cells at +4 cell position exclusively in the small intestine (Sangiorgi and Capecchi, 2008; Barker, Van Oudenaarden and Clevers, 2012). It is expressed at very low levels in most cells within the crypt base and deletion of the Bmi1+ population leads to crypt death (Muñoz *et al.*, 2012). Numerous protein markers have broad expression patterns that are not restricted to a single population of cells within the intestinal epithelium (Smith, Gallagher and Wong, 2016). For example, Bmil1 is also expressed in differentiated villus

cells (Takeda *et al.*, 2011). Another example is Double cotrin-like kinase 1 (Dclk1), expressed on the villus in enteroendocrine and Tuft cells (Levin *et al.*, 2010). Dclk1 was first identified as an ISC marker and a few years later this was subsequently changed as it was found to express typical cell differentiation markers (Giannakis *et al.*, 2006; Gerbe *et al.*, 2009). Math1 is required for the development of intestinal secretory cells (Shroyer *et al.*, 2007) and promotes the differentiation of goblet cells throughout the intestine (VanDussen and Samuelson, 2010).

4.2 Aims of Chapter 4:

Analysis of the transcriptomic changes in Ala720/Ala721-IWS1-expressing cells suggest that the pathways affected are associated with intestinal cell biology and intestinal diseases.

In this chapter, we aimed to:

1. To characterise the role of IWS1 in the non-transformed colonic epithelial cells (NCM356 and NCM460) and compare them.

4.3 Methods

4.3.1 MetaCore Analysis for biological processes and gene network visualisation

A pathway enrichment analysis of significantly altered genes was performed using MetaCore (http://www.metacore.com/). RNA sequencing data from NCI-H522 lung cancer cells transduced wish shIWS1 and reconstituted with Ser720/Thr721-IWS1 or Ala720/Ala721-IWS1, were uploaded to the cloud-based platform using as a gene list with the corresponding fold change of the deregulated genes. The differentially expressed genes were analysed for disease biomarkers and enriched pathway maps, and gene networks.

4.3.2 RNA sequencing for NCM356 and NCM460 cells

RNA sequencing for NCM356 and NCM460 cells was performed as in Section 3.3.2

4.3.3 nCounter microRNA Expression Assay- Nanostring

microRNA assay controls were diluted in 1:500 in a microcentrifuge tube, mixed by vortexing, spin down and stored on ice until needed. The annealing master mix was prepared by combining 13µl of Annealing Buffer, 26 µl of nCounter microRNA Tag reagent and 6.5 µl of the diluted microRNA assay controls. The annealing master mix was aliquoted (3.5 µl) into each tube of a 200 µl strip tube. 100ng of RNA sample (33ng/ µl) was added to each tube (vF=3 µl). Tubes were mixed and placed in a thermal cycler for annealing using the following conditions (***Table xxviii***).

Table xxviii: Conditions for annealing protocol in thermal cycle.

Temperature	Time
94°C	1 minute
65°C	2 minutes
45°C	10 minutes
48°C	∞

15x Ligation master mix was prepared by combining 22.5 µl PEG and 15 µl Ligation buffer. Following completion of the Annealing protocol, as soon as the thermal cycler reaches 48°C, tubes were removed and 2.5 µl of the ligation mix was transferred to each tube and incubated at 48°C for 5 minutes. For the next step, tubes remained in the thermal cycler and 1 µl of Ligase was added directly to the bottom of each tube. Immediately after the addition of Ligase, the ligation protocol was initiated (***Table xxix***).

Table xxix: Conditions for the ligation protocol in a thermal cycle.

Temperature	Time
48°C	3 minutes
47°C	3 minutes
46°C	3 minutes
45°C	5 minutes
65°C	10 minutes
4°C	∞

After the completion of the Ligation protocol, tubes were removed from the thermal cycler and 1 µl of Ligation Clean-up Enzyme was added to each reaction. Tubes were placed back into the thermal cycler and the Purification protocol was initiated following the conditions provided in ***Table xxx***.

Table xxx: Conditions for the purification protocol in a thermal cycle.

Temperature	Time
37°C	1 hour
70°C	10 minutes
4°C	∞

Finally, after the completion of the Purification protocol, 40 µl of nuclease-free water was added to each tube, mixed well and spin down. Samples were denatured at 85°C for 5 minutes and then transferred on ice.

The microRNA CodeSet Hybridization Setup protocol was followed according to the manufacturer's instructions. Briefly, a hybridization master mix was prepared by adding 130 µl of Hybridization Buffer to the tube containing 130 µl Reporter Codeset. A hybridization reaction was prepared by adding 20 µl of hybridization master mix to each tube of a newly labelled strip tube, 5 µl of each sample from the microRNA sample preparation protocol and 5 µl of Capture ProbeSet. Strip tubes were mixed by flicking and spin briefly. Immediately, the strip tubes were placed in a preheated 65°C thermal cycler for 20 hours. After hybridization has been completed, samples were loaded onto the nCounter Prep Station. Analysis was performed using the nCounter Analysis System (NanoString Technologies).

4.3.4 Lentiviral transduction with a stem-cell reporter and Fluorescence-activated cell sorting (FACS)

NCM356 and NCM460 cells transduced with pLV 4xSTAR-sTomato-NLS-blast (STAR) construct (Addgene, 136259) were grown, harvested and counted as described in section 2.2.1.4. Normal colonic epithelial cells NCM356 and NCM460 cells were infected with pLV 4xSTAR-sTomato-NLS-blast (STAR) as described previously in section 2.2.29. Briefly, HEK-293T cells, with 30% confluency, were transfected dropwise with the lentiviral transfection mixture (***Table xxxi***), twice. 24 h and 48 h after the second transfection, 2 batches of viruses were collected and filtered through a 0.45 µm filter. NCM356 and NCM460 cells were plated in a 6-well plate overnight. The next day, cells were washed with DMEM without serum and then incubated with DMEM without serum, containing 0.4mg/ml DEAE-Dextran Hydrochloride for 45 minutes. Following incubation, cells were treated with full DMEM medium for 1 hour at 37°C and then, cells were infected with the 1st batch of virus. These steps were repeated the following day with the 2nd batch of virus. To verify the transduction efficiency non-infected cells were used as control and the blasticidin antibiotic was used for selection, 24 hours after the second infection.

Table xxxi: Lentiviral transfection mixture used for STAR.

Reagents	Concentration/ Volume
OptiMEM	450 µl
Fugene 6	9 µl
pLV 4xSTAR-sTomato-NLS-blast	1.5 µg
psPAX2	1 µg
pCMV-VSV-G	0.5 µg

$1x10^6$ cells were aliquoted in flow cytometry tubes and mixed with 1ml DPBS + 1 µl of LIVE/DEAD Fixable Yellow Dead cell stain reagent (Thermofisher, L34968) for 30 minutes at RT. Cells were washed with 1ml fresh DPBS and centrifuged at 400 x g for 5 minutes before proceeding to FACS analysis using Beckman Coulter Gallios Flow cytometry.

4.4 Results and Discussion

4.4.1 IWS1-regulated genes correlate with intestinal diseases

RNA sequencing data from lung cancer cells expressing Ser720/Thr721 or Ala720/Ala721-IWS1 was used to perform MetaCore disease biomarker analysis. Interestingly, we found that the top ten diseases linked to the specific gene signature are colorectal cancer and intestinal diseases **(Figure 4.3)**. These results suggested that intestinal cells may be a more appropriate model to study the biology of IWS1.

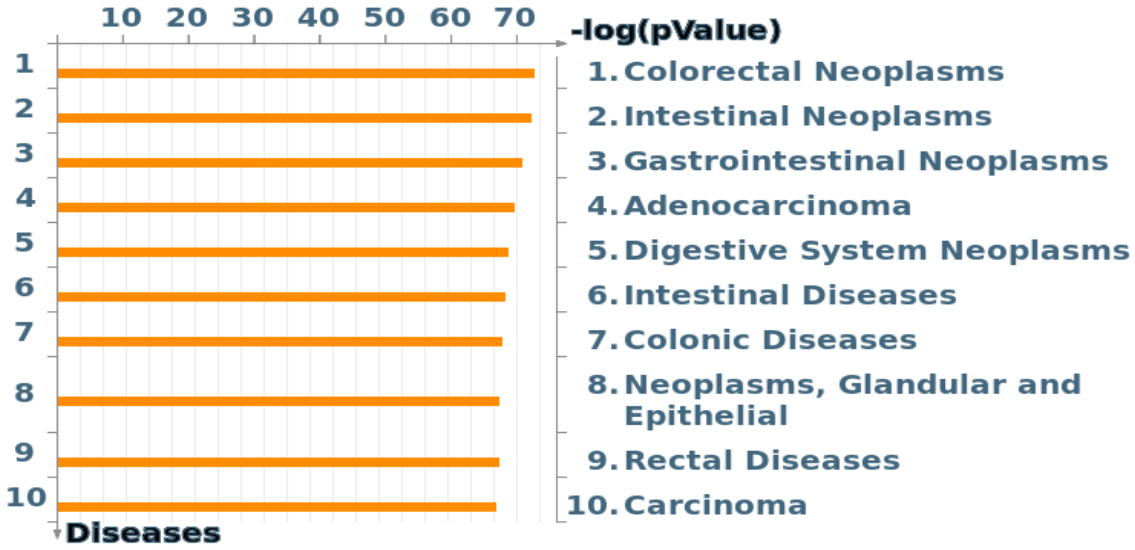

Figure 4. 3: MetaCore disease biomarker analysis. Orange bars represent the significant association in negative logical p-values. (X-axis: values in logarithmic scale).

4.4.2 ISCs markers are highly expressed in NCM460 cells

To evaluate which is the most relevant cellular model to study the biology of IWS1 we characterised the transcriptome of two immortalised non-transformed colonic epithelial cell lines NCM356 and NCM460. Analysis of the RNA sequencing data revealed that NCM460 cells have increased expression of most of the intestinal epithelial cell sub-population markers **(*Table xxxii*)**. NCM460 cells express high levels of LGR5, which marks mitotically active ISCs and comparable levels of BMI1, a marker of ISCs, distinct from LGR5, which marks quiescent ISCs that contribute partly to homeostatic regeneration (Yan *et al.*, 2012).

BMI1 was originally detected in cells near the +4 position from the crypt base shown to give rise to all cell lineages of the intestinal epithelium (Sangiorgi and Capecchi, 2008; López-Arribillaga *et al.*, 2015). Later studies revealed that BMI1 expression is not restricted to +4 cells but also, to other crypt and differentiated cells (Itzkovitz *et al.*, 2012; López-Arribillaga *et al.*, 2015).

In NCM460 high expression levels were also observed for SPARC-related modular calcium-binding protein 2 (SMOC2), an ISC marker which has been shown to play an important role in colon cancer development (Jang *et al.*, 2020). Leucine-rich repeats and immunoglobulin-like domains 1 (LRIG1) and Telomerase Reverse Transcriptase (TERT) levels are similar in the two cell lines. LRIG1 controls the homeostasis of ISCs, and it is highly expressed in actively proliferating $LGR5^+$ ISCs (Wong *et al.*, 2012). TERT is located in the +5 to +8 position (Montgomery *et al.*, 2011) and labels Label-Retaining Cells (LRCs) that are functionally distinct from $Lgr5^+$ ISCs in the intestinal epithelium (Breault *et al.*, 2008). It has been shown that TERT-expressing cells can regenerate all types of differentiated cells including $Lgr5^+$ stem cells (Montgomery *et al.*, 2011).

On the other hand, RNA sequencing analysis showed that MEX3A expression is higher in NCM356 cells. MEX3A-expressing cells are a proliferating subpopulation of $LGR5^+$ cells and occupy the +3 /+4 crypt position (Barriga *et al.*, 2017), characterised as LRCs (Liu and Chen, 2020). Increased expression levels in NCM460 were also observed for Prospero Homeobox 1 (PROX1), Growth Factor Independent 1 (GFI1), Neurogenin 3 (NEUROG3), Islet 1 (ISL1), Pancreatic and duodenal homeobox 1 (PDX1), GATA binding protein 6 (GATA6), Hepatocyte nuclear factor-1A and 1B (HNF1A and HNF1B) which are enteroendocrine genes, required for the endocrine cell development in intestines (Zhang *et al.*, 2019; Rees *et al.*, 2020). Increased expression was observed as well for markers of Paneth and Goblet cells including Lysozyme (LYZ), E47 like EST Transcription factor 3 (ELF3),

Kruppel-like factor 4 (KLF4) and Claudin 4 (CLDN4) (Rees *et al.*, 2020) and in secretory progenitor, ATOH1 (Castillo-Azofeifa *et al.*, 2019). On the other hand, the expression of SRY-Box transcription factor 9 (SOX9), which is expressed in the epithelial stem cell zone (Formeister *et al.*, 2009), are higher in NCM356 cells compared to NCM460 cells.

To verify the above results, RNA was isolated from NCM356 and NCM460 cells and RT-qPCR analysis was performed for different markers of intestinal cells. The results confirmed that in NCM460 cells there are increased expression levels for most of the markers that we have examined. Only LRIG1 and TERT have similar expression levels in the two cell lines **(Figure 4.4)**.

The epithelial cells that are lined on the lumen of the small intestines are replenished constantly due to the ISCs. ISCs are characterized by their self-renewal capability. The intestinal tissues are regenerated by the migration of ISCs toward the top of the villi, which differentiates them into TA cells. The transcriptomic analysis suggests that NCM460 cells may represent the characteristics of most intestinal cell subtypes, whereas NCM356 seem to present differentiated intestinal sub-type. Furthermore, they express the majority of ISC markers.

Table xxxii: Expression levels of epithelial lineage markers in NCM356 and NCM460 cells

Genes	Expression levels		Function
	NCM356	NCM460	
LGR5	0.024654054	20.06745386	Intestinal stem cell marker. Marks mitotically active ISCs that exhibit exquisite sensitive to canonical Wnt modulation.
BMI1	14.64985412	16.73115925	Intestinal Stem cell marker. Marks quiescent ISCs that are insensitive to Wnt perturbations, contribute weakly to homeostatic regeneration.
TERT	0.53760538	0.706396456	Labels "label-retaining cells" (LRCs) that are functional distinct from $Lgr5^+$ ISCs in the intestinal epithelium.
LRIG1	8.803581765	8.068235681	Highly expressed in actively proliferating $Lgr5^+$ ISCs.
MEX3A	18.18280751	5.339550213	Expressed at the base of intestinal crypts. Regulates $Lgr5^+$ stem cells maintenance in the developing intestinal epithelium.
DCLK1	22.27748423	0.015009171	
ATOH1	0	2.399472	Secretory progenitor- Differentiate to Paneth cells, goblet cells, enteroendocrine cells and tuft cells. Repair and replenish the colonic epithelium during DSS induced colitis.
PROX1	2.048330657	9.12716498	Enteroendocrine marker.
KRT19	96.44671455	202.1029205	Mark long-lived radiation-resistant cells at upper crypts.
MSI1	2.583969466	0	Marker of ISCs (CBCs and +4 position cells).
LYZ	1.262656255	3.771235184	Marker of Paneth Cells.
KITLG	0.483391696	11.22190704	Plays an essential role in the regulation of cell survival and proliferation and stem cell maintenance.
SOX9	127.836029	66.673935	Required for Paneth cell differentiation. It labels ICSs resistant to irritation.
ASCL2	35.518448	58.831451	Transcription factor controlling $LGR5^+$ intestinal stem cell gene expression.
SMOC2	0.008151297	7.066998542	Intestinal Stem cell marker.
CDCA7	15.04838114	25.60489388	Notch transcriptional target.
HES1	65.98731219	189.0567164	Absorptive- Influences the maintenance of certain stem cells and progenitor cells.
NEUROG 3	0.024465	3.019604	Enteroendocrine - it is required for endocrine cell development in intestines.
PAX6	2.79939494	1.559377716	Enteroendocrine
ISL1	1.556420722	2.21967326	Enteroendocrine
PDX1	0.813292	5.034163	Enteroendocrine
NKX6-1	0.64323253	0	Enteroendocrine
GATA6	0.319966446	16.96258344	Enteroendocrine
HNF1B	0.02106969	2.274285399	Enteroendocrine
HNF1A	0.00669506	2.075754018	Enteroendocrine
CUX1	8.569207023	4.487785797	Enteroendocrine- is crucial for normal intestinal epithelial cell migration upon wound injuries.
CHGA	57.42086665	0.013938884	Enteroendocrine
KLF4	12.36061735	13.95020122	Goblet- Maintaining epithelial homeostasis in the intestine.
CLDN4	11.92053632	16.33382375	Paneth
DLL1	1.095001009	9.527532381	Notch Ligand- Aid in the maturation of ISCs to absorptive and secretory lineages

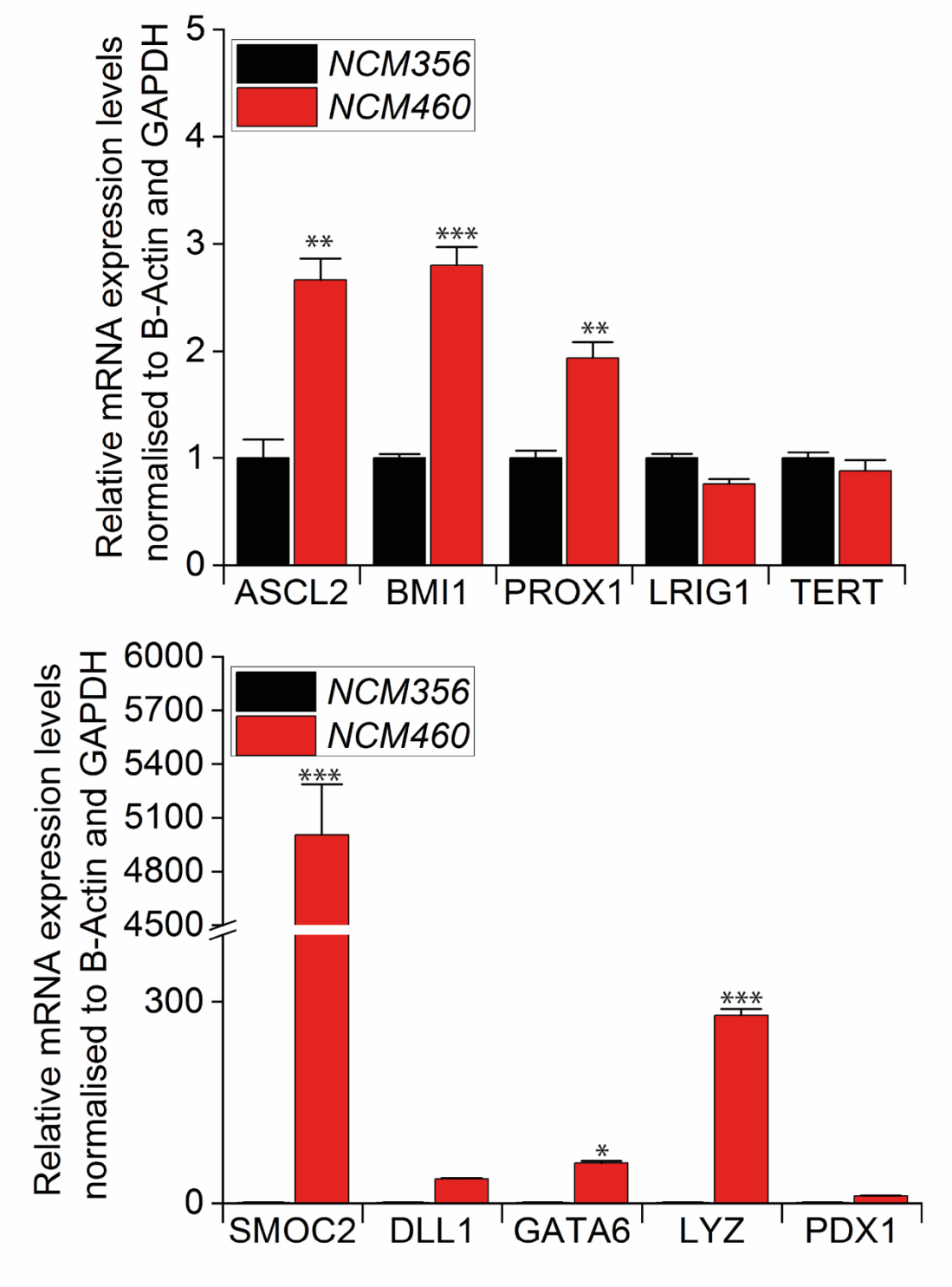

Figure 4. 4: Expression of epithelial lineage markers in NCM356 and NCM460 cells. RNA extracts from NCM356 and NCM460 cells were subjected to RT-qPCR analysis performed in quadruplicates. Gene expression analysis was performed using CFX Software by normalised expression (ΔΔCq) against B-Actin and GAPDH, and for NCM356 cells, the expression level was set as 1. Results are presented as mean ± SEM. Asterisks denote statistically significant differences (*P<0.05,**P<0.01,***P<0.001). Statistical analysis was performed using Student's t-test.

We were interested in investigating the microRNA expression levels in NCM356 and NCM460 cells. Nanostring analysis performed in these cell lines revealed that most of the microRNAs which were validated to be specific for intestinal stem cells or different lineage epithelial cell populations, were found to be increased in NCM460 cells. These results support the hypothesis of a mixed population in this cell line (***Table xxxiii***).

Table xxxiii: microRNA expression in NCM356 and NCM460.

MicroRNAs	Expression Levels		Lineage
	NCM356	**NCM460**	
hsa-let-7a-5p	2992.83	7046.88	High in Lgr5$^+$ cells[1]
hsa-miR-23a-3p	537.92	2270.32	Promotes stem cell migration and invasion[2]
hsa-let-7b-5p	855.56	2146.52	High in Lgr5$^+$ cells[1]
hsa-miR-191-5p	664.98	1215.08	High in Lgr5$^+$ cells[1]
hsa-let-7d-5p	556.07	910.01	High in Lgr5$^+$ cells[1]
hsa-let-7g-5p	515.23	870.21	
hsa-miR-196a-5p	247.51	780.31	
hsa-miR-181a-5p	35.75	772.94	
hsa-miR-200b-3p	11.54	466.39	
hsa-miR-10a-5p	392.71	425.13	
hsa-miR-194-5p	1.51	288.07	High in Enterocytes[1]
hsa-miR-200c-3p	1.51	246.8	High in Lgr5$^+$ cells[1]
hsa-miR-7-5p	56.92	232.06	High in Enteroendocrine cells[1]
hsa-miR-107	118.94	142.16	High in Enterocytes[1]
hsa-miR-1246	3.98	105.32	
hsa-miR-4454+ hsa-miR-7975	47.85	92.05	
hsa-let-7c-5p	41.8	83.21	High in Lgr5$^+$ cells[1]
hsa-miR-98-5p	35.75	59.63	
hsa-miR-296-5p	1.51	58.15	
hsa-miR-873-3p	25.16	56.68	
hsa-miR-30d-5p	17.59	53.73	
hsa-miR-4443	26.67	52.26	
hsa-miR-135b-5p	32.72	41.94	
hsa-miR-22-3p	20.62	41.94	
hsa-miR-642a-5p	11.54	41.94	
hsa-miR-148b-3p	11.54	40.47	

[1] (Shanahan *et al.*, 2021)
[2] (Jahid *et al.*, 2012)

4.4.3 Phospho-IWS1 regulates genes that are involved in intestinal stem cell-associated pathways.

For the evaluation of biological networks regulated by phosphorylated IWS1, RNA sequencing data in Ser720/Thr721-IWS1 vs Ala720/Ala721-IWS1-expressing cells were analysed using the Analyse Network (AN) algorithm integrated in MetaCore. This analysis revealed among the top-scored networks, three networks associated with stem cell biology: NANOG-KLF4 **(Figure 4.5)**, Src-TGFbeta **(Figure 4.6)** and EMT pathway **(Figure 4.7).**

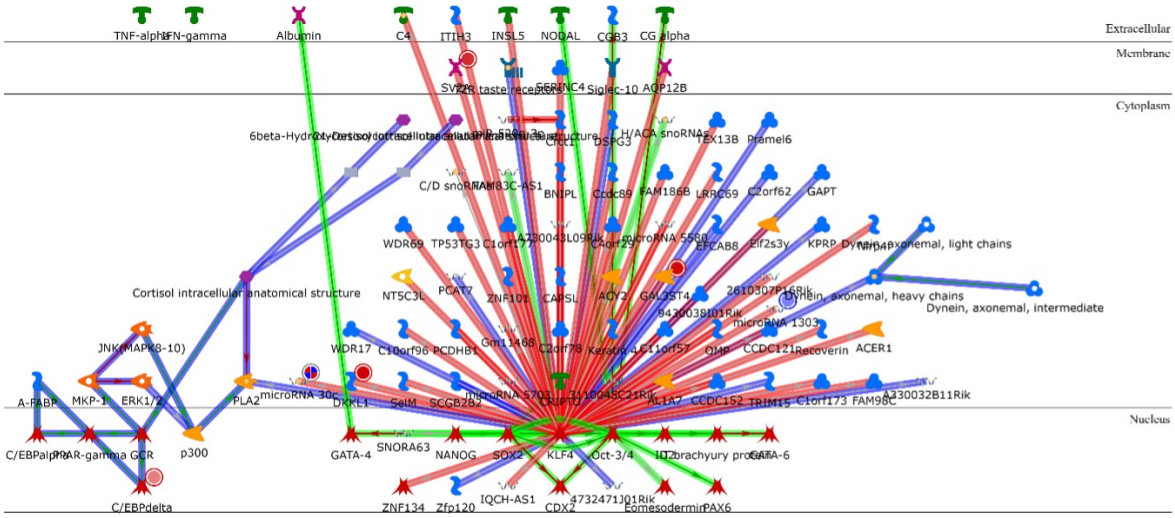

Figure 4. 5: Bioinformatic analysis of RNA seq data links IWS1 phosphorylation with the regulation of NANOG-KLF4 pathway. Upregulated genes are marked with red circles and the downregulated genes with blue circles. Network generated using AN algorithm in MetaCore.

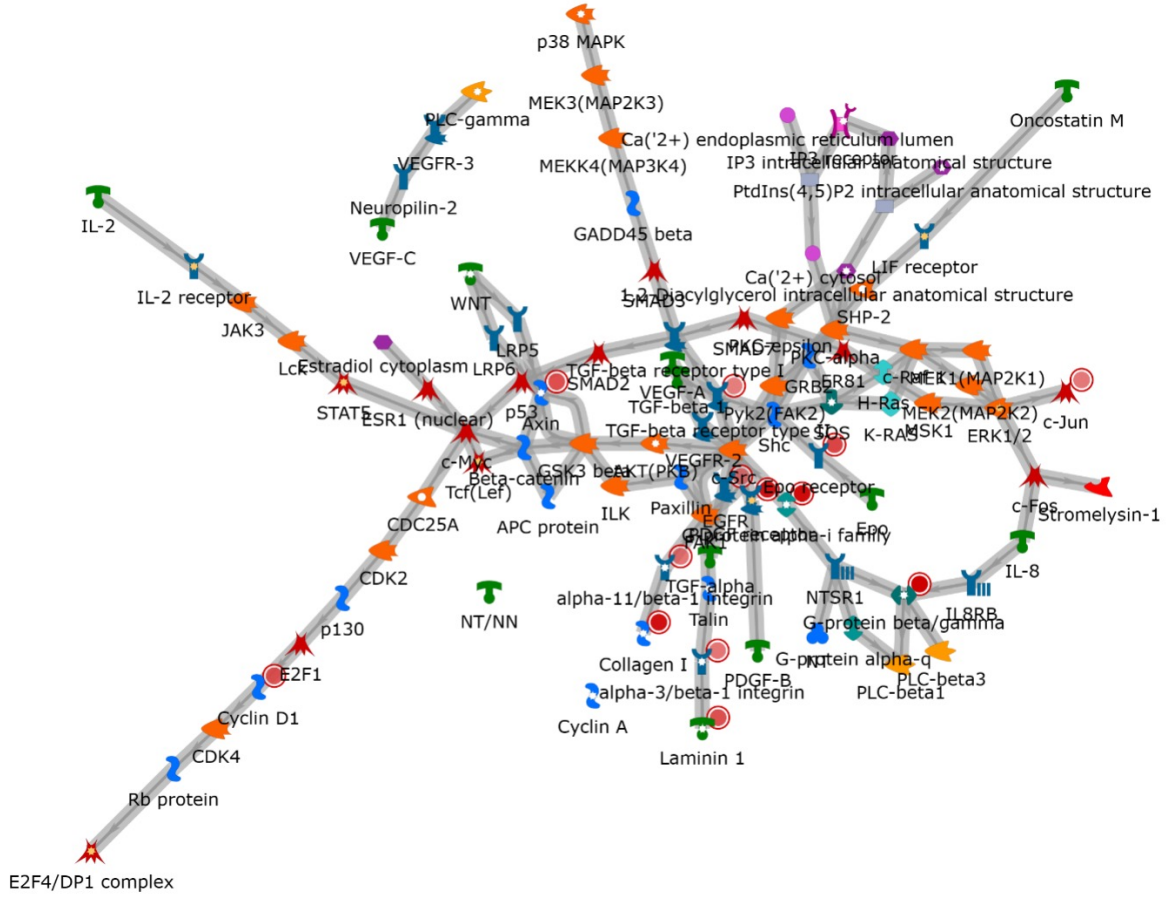

Figure 4. 6: Bioinformatic analysis of RNA seq data links IWS1 phosphorylation with the regulation of Src-TGFbeta pathway. Upregulated genes are marked with red circles and the downregulated genes with blue circles. Network generated using AN algorithm in MetaCore.

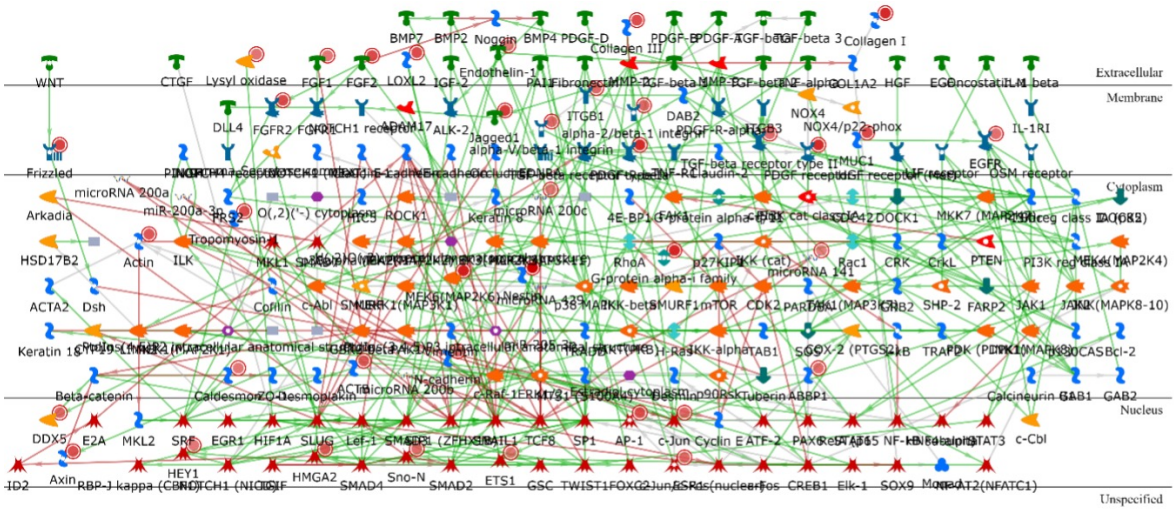

Figure 4. 7: Bioinformatic analysis of RNA seq data links IWS1 phosphorylation with the regulation of EMT pathway. Upregulated genes are marked with red circles and the downregulated genes with blue circles. Network generated using AN algorithm in MetaCore.

4.4.4 NCM460 cells have ISC-like characteristics.

The bioinformatic analysis revealed that IWS1 phosphorylation regulates pathways involved in stem cell biology. On the other hand, we found that NCM460 cells express markers of ISCs and differentiated epithelial cells. The above data combined suggested that NCM460 could be an appropriate model to study the role of IWS1 in intestinal stem and epithelial cell biology. The question arising was whether NCM460 are a uniform cell line that express simultaneously markers of ISCs and differentiated epithelial cells or it is a mixed population of cells. The morphology of the cells, observed under microscope, with round, cuboidal and elongated cells, supports the latter. Therefore, we questioned if a subset of NCM460 cells represents less differentiated or stem cell-like subpopulation. To address the hypothesis, we used a lentiviral construct to transduce cells with a reporter for ISCs. This fluorescent reporter (STAR) monitors the transcriptional activity of ASCL2, which is a master regulator of $LGR5^{+}$ in ISCs (Heinz, Oost and Snippert, 2020). STAR-transduced NCM356 and NCM460 cells were then subjected to FACS analysis. In both cases, parental cells were used as negative controls. FACS suggested minimal changes between NCM356 control and transduced with STAR (NCM356 + STAR) cells. On the other hand, there was a significant shift in the fluorescence emission in NCM460 + STAR compared to control cells **(Figure 4.8)**. These findings validate our results obtained by RNA sequencing and RT-qPCR analysis. Furthermore, they revealed that NCM460 comprise a heterogeneous cell population with low, high and intermediate levels of ASCL2 activity, representing more and less differentiated epithelial cells. Single-cell RNA sequencing would be an interesting approach to fully characterise the subtypes of epithelial cells represented in NCM460 cell line. Overall, our approaches beyond the characterisation for the first time of NCM356 and NCM460 cell lines, suggest that NCM460 is a candidate model for the study of epithelial cell differentiation *in vitro*,

and was the cell model of our choice for the study of the role of IWS1 in ISC properties.

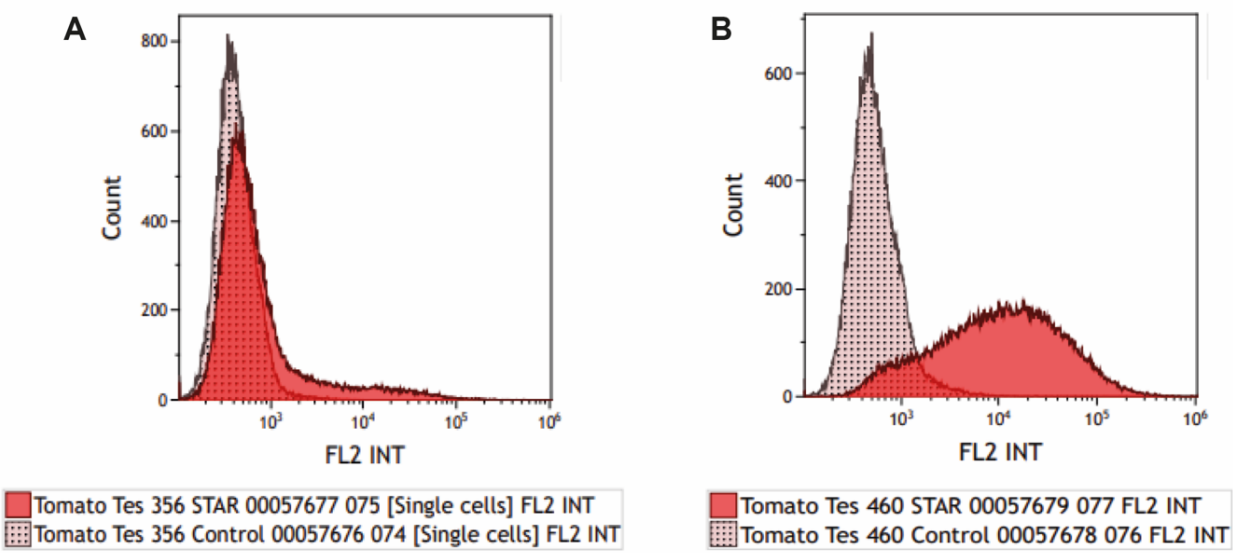

Figure 4. 8: Analysis of ISC-like properties in NCM356 and NCM460 cells. FACS analysis for ASCL2 fluorescent reporter activity in (A) NCM356 and (B) NCM460 parental and STAR-transduced cells. Data were acquired using a 3-laser Beckman Coulter Gallios Flow cytometry and analysed using Kaluza v1.3 data acquisition software.

4.5 Conclusion of Chapter 4

RNA sequencing analysis performed in lung cancer cells for Ser720/Thr721 and Ala720/Ala721-IWS1 expressing cells was used to perform pathway analysis, where we found that the deregulated genes in Ser720/Thr721 VS Ala720/Ala721-IWS1 expressing cells are involved in colorectal cancer and intestinal diseases. RNA sequencing analysis of normal colonic epithelial cells, NCM356 and NCM460, revealed that NCM460 cells express higher levels of intestinal sub-population cell markers compared to NCM356. RT-qPCR validated these results. FACS analysis revealed that NCM460 cells include a subset of ISC-like cells.

microRNAs have a central role in the development of human diseases and microRNA biogenesis machinery regulates intestinal cell differentiation and mucosal function. Intestinal stem cells are considered the cellular origin of the large majority of colorectal cancers (CRCs) (Barker *et al.*, 2009) and play a role in the homeostasis and function of the intestinal epithelium, with a significant role in intestinal inflammation and cancer.

In conclusion, our approaches beyond the characterisation for the first time of NCM356 and NCM460 cell lines, suggest that NCM460 is an ideal model for the study of epithelial cell differentiation *in vitro*. This was the cell model of our choice for the study of the role of IWS1 in ISC properties.

CHAPTER 5: Regulation of microRNAs by IWS1/AKT signals in Intestinal epithelial cells

5.1 Introduction and Aims

5.1.1 MicroRNA biogenesis in Intestinal Development and Function

microRNAs play an important role in the development of human diseases. In the intestine, the main focus has been on the role of microRNAs in CRC, while specific microRNAs implicated in UC have been associated with the differentiation of intestinal epithelial cells (Akao, Nakagawa and Naoe, 2006; Zhang *et al.*, 2007; Tang *et al.*, 2008).

Ethanol and burn injury suppress the expression of microRNA biogenesis components in the small intestine. In mice treated with ethanol and after injury, small intestinal epithelial cells express lower levels of Drosha and Ago2 mRNAs and proteins suggesting that altered microRNA biogenesis contributes to increased intestinal inflammation (Morris *et al.*, 2017).

The contribution of microRNAs to intestinal differentiation and function has been evaluated by the deletion of *Dicer1* in the epithelium of the small and large intestine in mice (McKenna *et al.*, 2010). Cross *Dicer1* $^{loxP/loxP}$ conditional mutant to Villin-Cre transgenic mice generated animals lacking functional microRNAs in the intestinal epithelium. Mice with deletion of *Dicer1* demonstrated impaired growth, fat absorption and water retention. Approximately 10% of mutant mice did not survive to weaning, however, surviving mice fed normally but were smaller in size than control mice and produced pale and loose stool. Mutant mice had ~20% more water in their stool compared to controls which indicates decreased water absorption in the colon. The *Dicer1*-deficient intestine has morphological differences. In the small intestine, the villi were normal, but the crypts were expanded and the lamina propria was more cellular. In the colon of *Dicer1*-deficient mice, the crypts were disorganized with packed lamina propria, and the number of mucus-filled goblet cells was reduced (McKenna *et al.*, 2010).

In conclusion, epithelial microRNAs are necessary for intestinal structure and abundance of goblet cells (McKenna *et al.*, 2010). A second study revealed that *Dicer1*-deficiency increases cell apoptosis in crypts and impaired mucosal barrier function (Park, Shimaoka and Kiyono, 2017).

Drosha the other central enzyme involved in the biogenesis of microRNAs has been evaluated in the development of intestinal tissue. In mice genetically modified with one conditional *LoxP* allele of the *Drosha* gene, partial loss of *Drosha* resulted in inflammatory disease and premature lethality (Chong *et al.*, 2008). We have recently shown that *Clostridiodes Difficile* infection in humans and mice result in significant decrease of Drosha levels in intestinal epithelial cells with global suppressive effects on microRNA processing and impaired epithelial barrier function (Monaghan *et al.*, 2021).

Ago proteins are important effectors of small RNA mediated regulatory pathways that modulate gene expression and regulate chromosome structure and function (Cheloufi *et al.*, 2010). Ago2 knockout in mice results in embryonic lethality (Yi and Fuchs, 2011) and depletion of Ago proteins results in decreased accumulation of mature microRNAs and disruption of RNA silencing (Bronevetsky *et al.*, 2013).

Collectively, the above data suggest that ISCs play a role in the homeostasis and function of the intestinal epithelium and play a significant role in intestinal inflammation and cancer. Furthermore, the microRNA biogenesis machinery regulates intestinal cell differentiation and mucosal function. We propose that the regulation of microRNAs by IWS1 may have important effects on the properties of ISCs in intestinal development and implications in intestinal diseases.

5.2 Aims of Chapter 5:

In the previous chapter, we have shown that microRNA activity is enhanced in Ala720/Ala721-IWS1-expressing cells in cancer cell lines. Moreover, we have shown that IWS1 is interacting with Ago2 in an AKT-dependent manner. We therefore questioned if IWS1-mediated regulation of microRNA activity is a universal mechanism, and how it affects the biology of intestinal epithelial cells.

In this chapter, we aimed to:

1. To validate previous results by performing microRNA activity and cell growth assays in NCM460 cells
2. To identify interactions of IWS1 with RISC components

5.3 Methods

5.3.1 Proximity Ligation Assay (PLA)

Proximity ligation assay was performed using Sigma-Aldrich Duolink *in Situ* PLA kit (Red). Cells were seeded at 25,000 cells/well in a 96-well plate and incubated at 37°C overnight. The following day, media was removed, and cells were washed once with PBS for 5 minutes. Cells were fixed in 4% Formaldehyde for 15 minutes at room temperature and then washed three times with PBS for 5 minutes. PBS was removed and cells were permeabilized with 0.5% Triton-X100 for 10 minutes at room temperature, followed by 100mM Glycine and 0.1% Tween for 2 minutes at room temperature. After permeabilization, cells were washed with PBS and a blocking solution was added for 30 minutes at 37°C in a pre-humidity chamber. Following that, cells were incubated with primary antibodies diluted in antibody diluent, for 1 hour at 37°C in a pre-humidity chamber. Anti-histone H3 (H3) antibody was diluted at 1:200, anti-acetyl lysine antibody at 1:100, Argonaut 2 (Ago2) at 1:200 and Flag was diluted at 1:800. Washes with 1x wash buffer A were followed twice, 5 minutes each, with gentle agitation. Duolink PLA probes (anti-mouse and anti-rabbit) were diluted in antibody diluent, incubated with the cells for 1 hour at 37°C, and then removed. Cells were washed twice with 1x buffer A, 5 minutes each, with gentle agitation. Ligase was diluted at 1:40 in 1x Ligation buffer and added to the cells for 30 minutes at 37°C and removed. Two washes with 1x wash buffer A, were performed as before and then, cells were incubated with the polymerase. Polymerase was diluted at 1:80 in 1x amplification buffer for 100 minutes at 37°C. All components with the amplification buffer were protected from light. Following that, the amplification buffer was removed, and cells were washed twice in 1x wash buffer B for 10 minutes each, followed by 1 minute wash in 0.01x wash buffer. Finally, NucBlue Reagent in PBS was added to the cells and incubated for 15-20 minutes. Cells were visualized using the Leica Thunder Cell imager.

5.4 Results and Discussion

5.4.1 NCM460 cells have higher expression of stem cell genes

Combination of pathway analysis with the characterisation of NCM460 as a mixed population, including stem cells, we decided to focus on this cell line because it demonstrates stem cell expression patterns and stem cell properties.

We wanted to analyse the differentiated and undifferentiated cells. Thus, we sorted (5-20%) of both cells, differentiated and undifferentiated cells from NCM460 cells transduced with STAR, as shown in **Figure 5.1**. Through sorting, we were able to isolate the ISCs and examine the differences with the differentiated cells by performing Nanostring analysis for the microRNA expression levels.

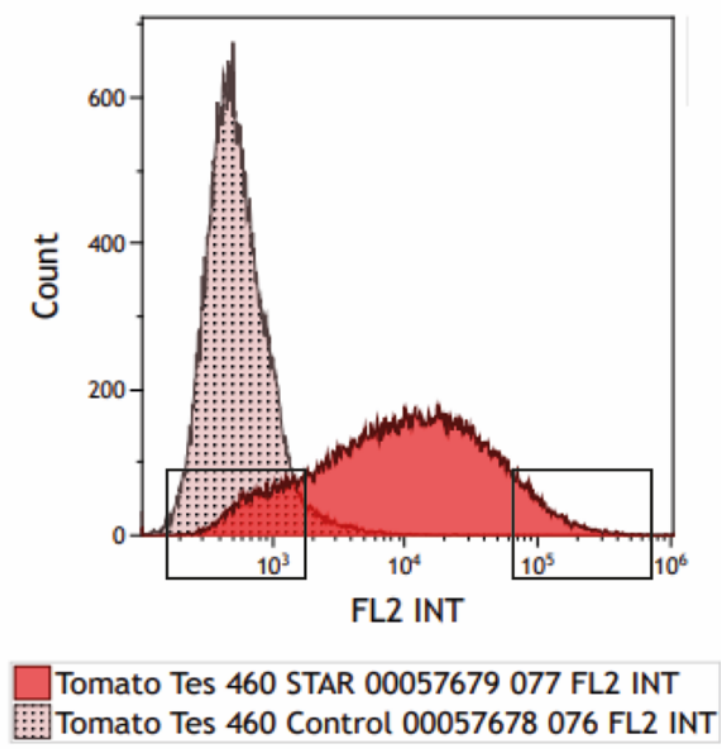

Figure 5. 1: Area for differentiated and undifferentiated cells used for sorting. Rectangle boxes show the 5-20% of differentiated and undifferentiated cells that were sorted.

To evaluate the effects of IWS1 phosphorylation on ISC properties, RNA was isolated from Ser720/Thr721-IWS1 and Ala720/Ala721-IWS1-expressing cells and RT-qPCR analysis for different intestinal stem cell-associated was performed. Interestingly, we found that only TERT expression levels were reduced in Ala720/Ala721-IWS1-expressing cells **(Figure 5.2-A)** which potentially could be due to the increased activity of specific microRNA(s). Moreover, we found that ASCL2 expression levels are not affected at the transcriptional level, suggesting that the increased number of stem-cell-like cells may be attributed to other mechanisms, such as cell signalling, inducing ASCL2 activity in Ser720/Thr721-IWS1 expressing cells **(Figure 5.2-B)**.

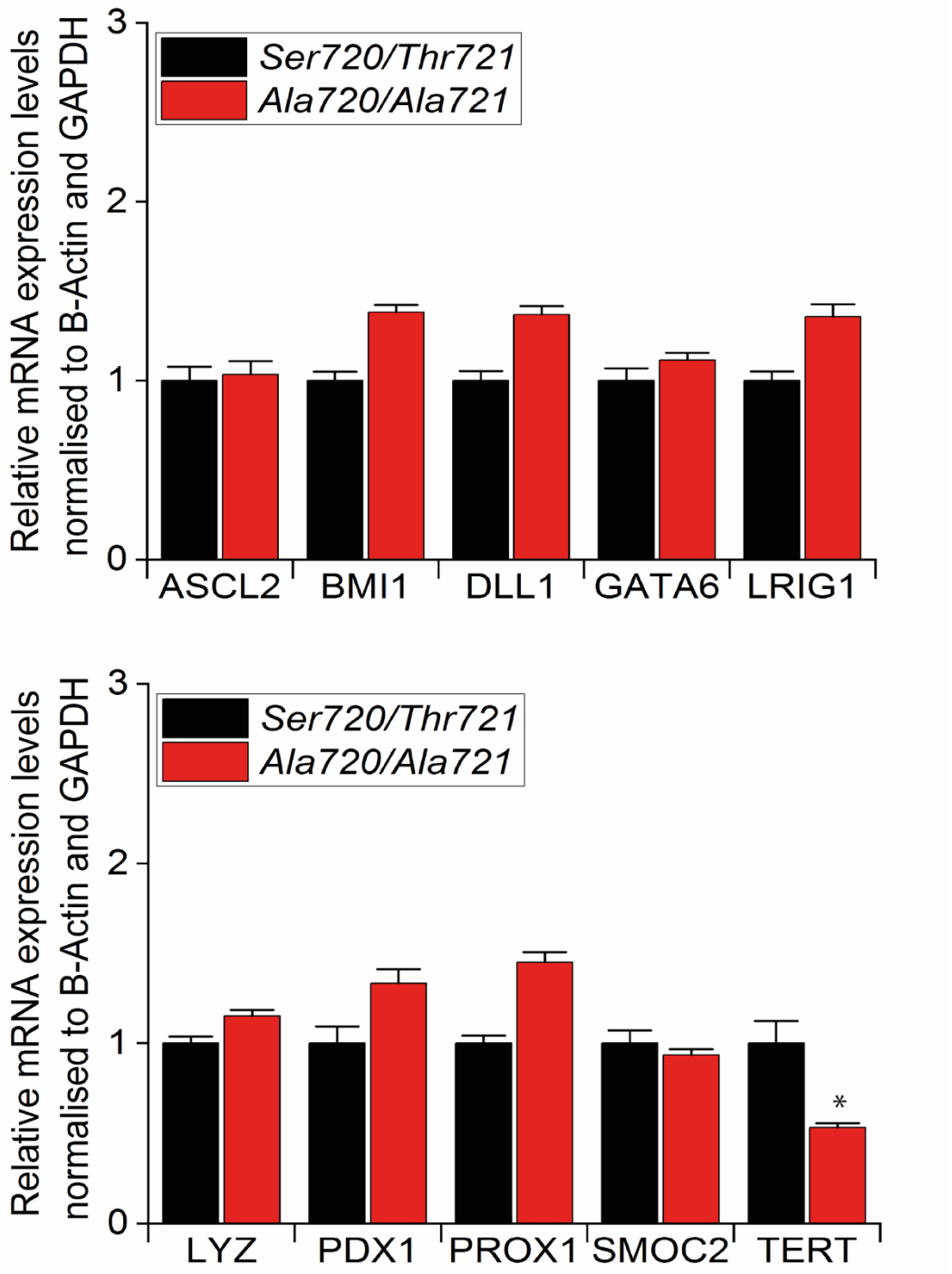

Figure 5. 2: Expression levels of intestinal stem associated genes in Ser720/Thr721-IWS1 and Ala720/Ala721-IWS1 expressing cells. RNA extracts from NCM460 cells expressing Ser720/Thr721-IWS1 or Ala720/Ala721-IWS1 were subjected to RT-qPCR analysis performed in quadruplicates. Gene expression analysis was performed using CFX Software by normalised expression (ΔΔCq) against B-Actin and GAPDH, and for Ser720/Thr721-IWS1-expressing cells, the expression level was set as 1. Results are presented as mean ± SEM. Statistically significant differences were determined by Student's t-test, (*P<0.05).

5.4.2 microRNA Activity is enhanced in Ala720/Ala721-IWS1-expressing cells

microRNA activity reporter assays, including additional microRNA activity reports, were repeated in the colonic epithelial NCM460 cells, to validate the universal regulation of microRNA activity by IWS1 phosphorylation. microRNA activity reporter assays for miR-17, miR-21, miR-23a, miR-25a, miR-29a, miR-103a, miR-182, miR-200c, Let-7a, Let-7c, Let-7f and Let-7i, which were found to be equally expressed in Ser720/Thr721-IWS1 and Ala720/Ala721-IWS1-expressing cells **(Figure 5.3)**. These data are in line with our observations in lung cancer cells (Section 3.4.2), suggesting that the increased microRNA activity in Ala720/Ala721-IWS1-expressing cells is a universal, not cell type specific mechanism.

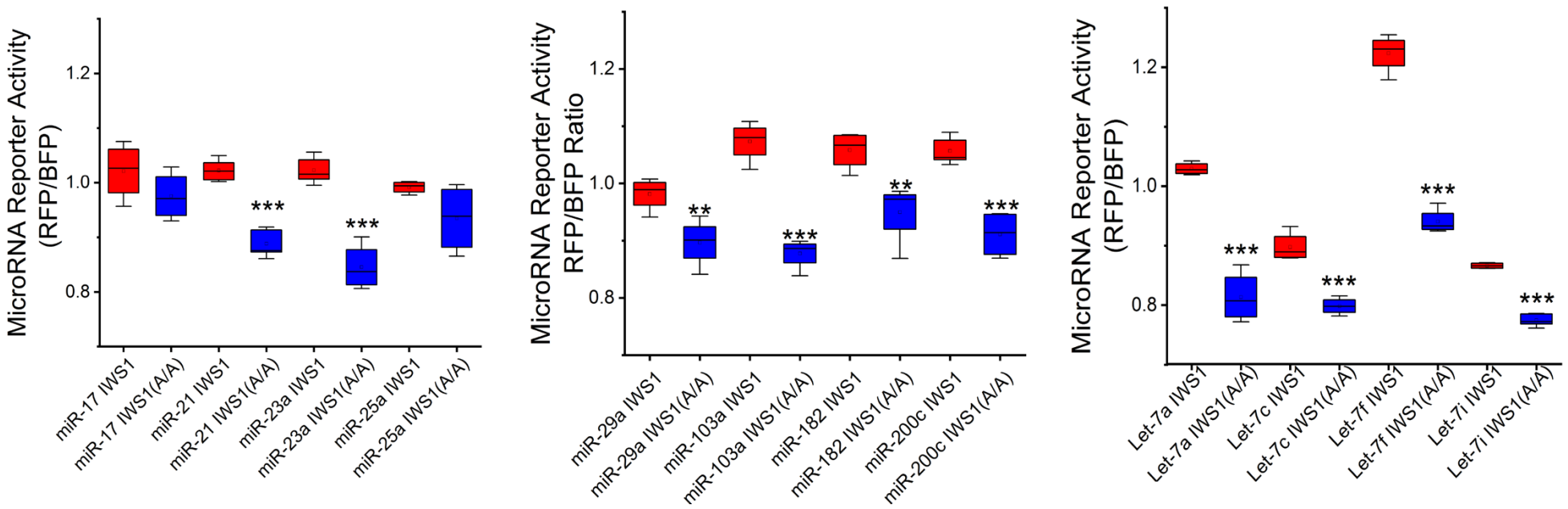

Figure 5. 3: Effects of Ala720/Ala721-IWS1 on microRNA activity. microRNA reporter activity measurements in NCM460 cells expressing Ser720/Thr721-IWS1 or Ala720/Ala721-IWS1. The expression of mKate2 (RFP), is regulated by microRNA target sites in its 3'UTR, and the EBFP2 (BFP), serves as a reference for data normalization. Data are presented as box plots of assays performed in quintuplicates. Statistically significant differences were determined by Student's t-test, *P<0.05, **P<0.005, ***P<0.001.

We questioned if microRNA activity regulated by IWS1 phosphorylation can affect cell properties. To this end, we evaluated the effects of 3 different microRNAs (miR-21-5p miR-23a-3p and miR-34a-5p) on the growth of NCM460 cells. IncuCyte live cell monitoring and Cell Titre Glo were used to investigate the effects of microRNA activity on cell growth. Cells were transfected with non-targeting control microRNA (miR-C), miR-21-5p, miR-23a-3p and miR-34a-5p. We observed that cell growth of Ala720/Ala721-IWS1-expressing cells is impaired compared to Ser720/Thr721-IWS1-expressing cells **[Figure 5.4 (A+B)]**. When cells were transfected with a cell growth inhibitory microRNA, miR-34a (Misso *et al.*, 2014), Ala720/Ala721-IWS1-expressing cells were growing significantly slower than the Ser720/Ser721-IWS1-expressing cells **[Figure 5. 4 (C+D)]**. No significant changes were observed in cell morphology.

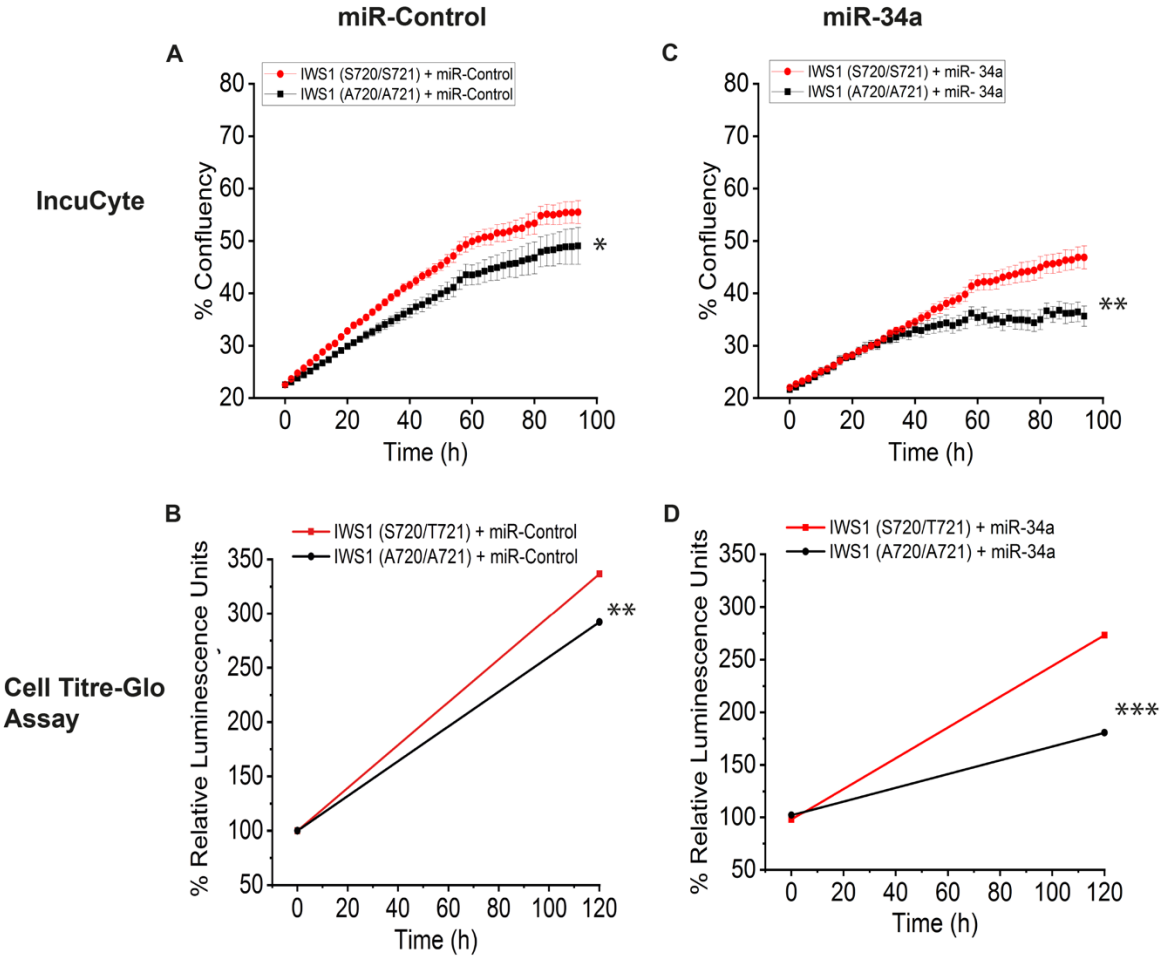

Figure 5. 4: Effects of miR-34a on cells expressing Ala720/Ala721-IWS1. Changes in the confluency of cells using IncuCyte live-cell imaging (A+C) and Cell Titre Glo (B+D) in Ser720/Ser721-IWS1 and Ala720/Ala721-IWS1-expressing cells transfected with 20nM of (A+C) a non-targeting control microRNA, miR-C or (B+D) an inhibitory microRNA, miR-34a. IncuCyte, Real-Time measurements were collected every 2 hours for a period of 96 hours (4 Days), 24 hours after transfection. Confluency data are representative of three independent experiments performed in quadruplicated and expressed as mean ± SEM. Cell-Titre Glo assays were performed at 0- and 120-hours post-transfection. Data are representative of three independent experiments performed in quadruplicates and expressed as mean luminescence ± SEM compared to miR-C at time point 0 (set as 100%). Asterisks denote statistically significant differences (*P<0.05, **P<0.01, ***P<0.001). Statistical analysis was performed upon data combination from all three experiments using Student's t-test.

However, when we transfected the cells with miR-23a, a microRNA known to induce cell growth (Deng *et al.*, 2018), the differences were diminished **[Figure 5.5 (A+B)]**. An oncogenic microRNA, miR-21 (Wu *et al.*, 2017), known to promote cell growth, reversed the growth defect, with Ala720/Ala721-IWS1-expressing cells growing faster than Ser720/Ser721-IWS1-expressing cells **[Figure 5.5 (C+D)]**.

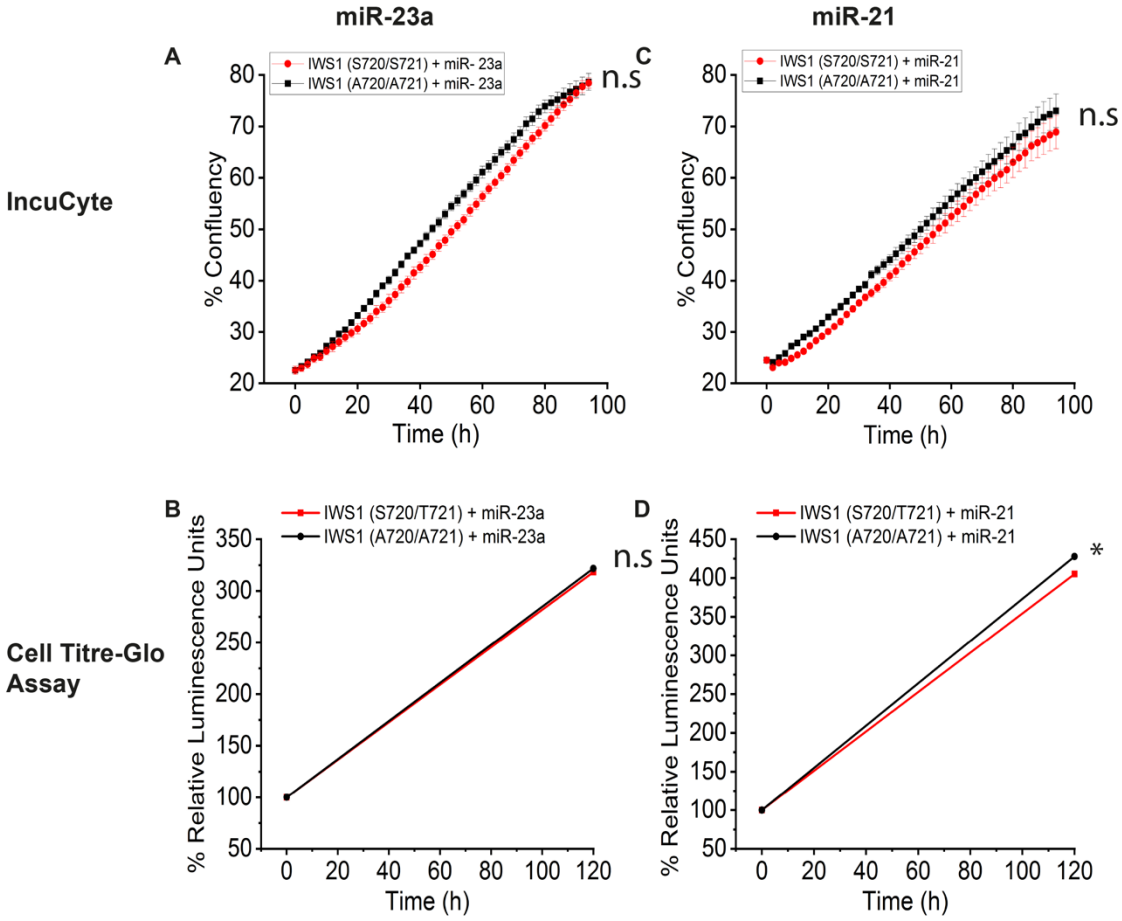

Figure 5. 5: Effects of miR-23a and miR-21 on cells expressing Ala720/Ala721-IWS1. Changes in the confluency of cells using IncuCyte live-cell imaging (A+C) and Cell Titre Glo (B+D) in Ser720/Ser721-IWS1 and Ala720/Ala721- IWS1 expressing cells transfected with microRNAs promoting cell growth, (A+C) miR-23a (20nM) and (B+D) miR-21 (20nM). For IncuCyte, Real-Time automated measurements were collected every 2 hours for a period of 96 hours (4 Days) and for Cell-Titre Glo for 120 hours (5 Days). Data are representative of three independent experiments performed in quadruplicates and shown as mean ± SEM compared to miR-C at time point 0 (Set as 100%). Asterisks denote statistically significant differences (*P<0.05, n.s.= non-significant). Statistical analysis was performed upon data combination from all three experiments using Student's t-test.

We also examined the expression levels of specific validated microRNA targets in these cells. Ser720/Thr721-IWS1 and Ala720/Ala721-IWS1-expressing cells were transfected with miR-Control, miR-23a-3p or miR-34a-5p for 24 hours and protein extracts were analysed for Mouse Double Minute 2 (MDM2), DNA methyltransferase 3 alpha (DNMT3A) and Hepatocyte Nuclear Factor-4 alpha (HNF4a) protein levels. Western blot analysis revealed that overexpression of miR-23a-3p (20nM) results in higher suppression of MDM2 and DNMT3a in Ala720/Ala721-IWS1-expressing cells **[Figure 5.6 (A)]**. Overexpression of miR-34a-5p (20nM) at >60k-fold upregulation suppressed HNF4a at similar levels in Ser720/Thr721-IWS1 and Ala720/Ala721-IWS1-expressing cells **[Figure 5.6 (B)]**, whereas lower levels of miR-34a-5p (2nM) overexpression resulted in higher suppression of HNF4a in Ala720/Ala721-IWS1-expressing cells **[Figure 5.6 (C)]**. Data presented for miR-34a in **Figure 5.6 (B+C)**, suggest that differences in microRNA activities could be overridden by non-physiologically relevant overexpression of microRNAs. Therefore, for the study of specific microRNAs and especially, in the context of microRNA activity regulatory mechanisms the experimental approaches should aim at using physiologically relevant concentrations of microRNAs.

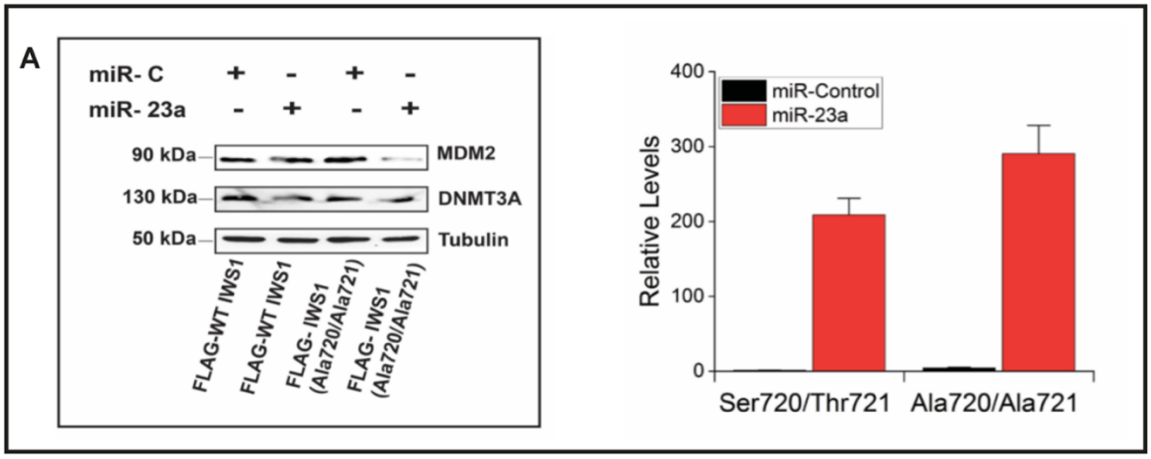

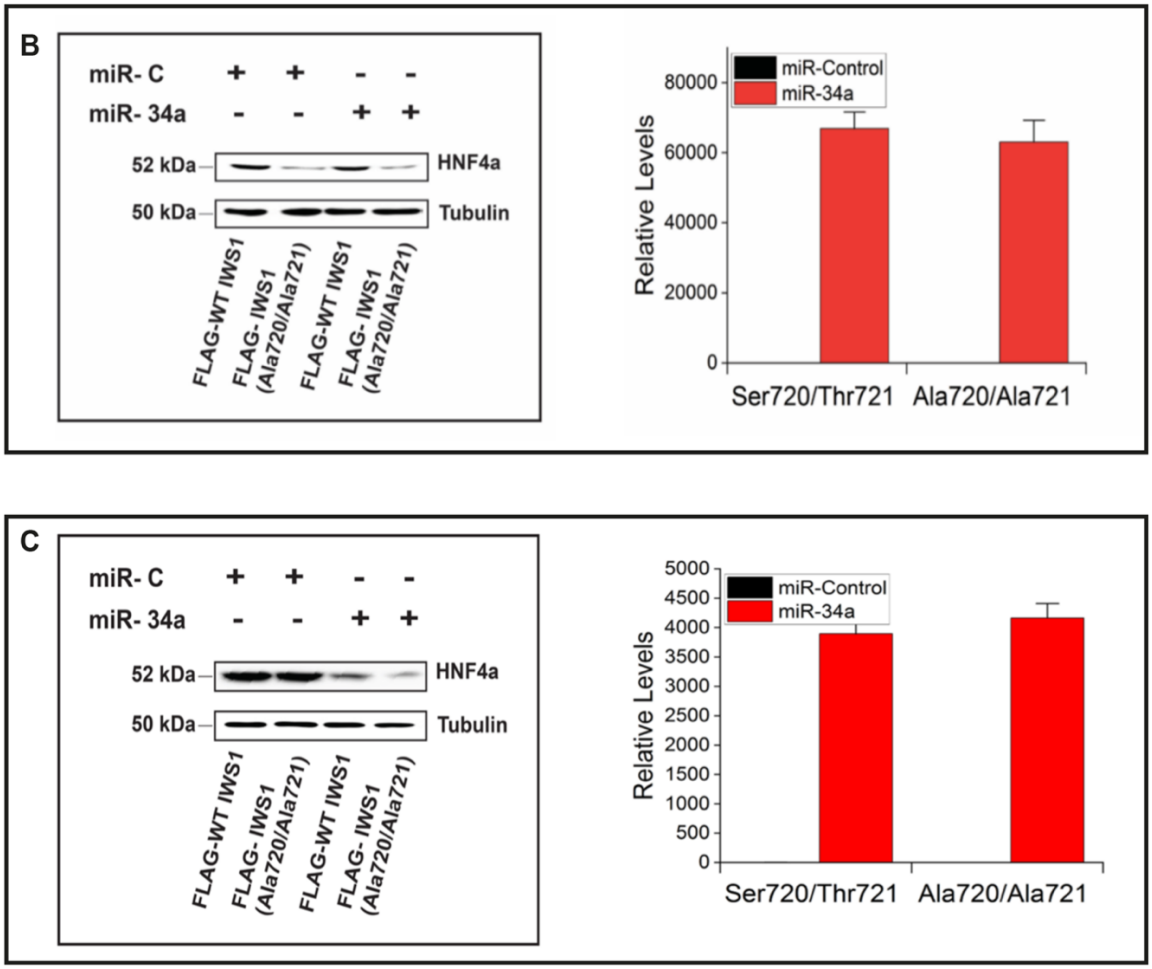

Figure 5. 6: Effect of microRNAs on the protein levels of validated targets in Ser720/Thr721 and Ala720/Ala721-IWS1 expressing cells. NCM460 cells transduced with shIWS1 and reconstituted with Ser720/Thr721-IWS1 and Ala720/Ala721-IWS1, were transfected with miR-Control, miR-23a-3p (20nM), or miR-34a (20nM/2nM). **(A-Left)** Western blot for miR-23a target proteins MDM3 and DNMT3a and **(A-Right)** RT-qPCR analysis for miR-23a (20nM) levels in Ser720/Thr721-IWS1 and Ala720/Ala721-IWS1-expressing cells. **(B-Left)** Western blot analysis of miR-34a target protein HNF4a, in miR-34a (20nM) transfected Ser720/Thr721-IWS1 and Ala720/Ala721-IWS1-expressing cells. **(B-Right)** RNA extracts from the same cells were subjected to RT-qPCR analysis **(C-Left)** Western blot analysis of HNF4a, in miR-34a (2nM) transfected Ser720/Thr721-IWS1 and Ala720/Ala721-IWS1-expressing cells. **(C-Right)** RT-qPCR analysis of RNA extracts from the same cells. For Western blot, alpha-tubulin was used as a loading control. RT-qPCR was performed in quadruplicates data were normalised against RNUA1 and 5S rRNA and are expressed as mean ± SEM compared to control (set as 1).

5.4.3 IWS1 phosphorylation regulates its interaction with RISC

In Chapter 3, Section 3.4.4, sucrose gradient fractionation performed in NCI-H522 cells, confirmed that IWS1 and Ago2 are found in the same fractions, indicating that there is a possible interaction between them. Immunoprecipitation assays performed in the same cells revealed that IWS1 interacts with Ago2 in an AKT-dependent manner. Immunoprecipitation assay in NCM460 cells verified the interaction **[Figure 5.7 (A)]**. Additional immunoprecipitation assays revealed the decreased interaction of all RISC components with Ala720/ala721-IWS1 expressing cells suggesting that upon phosphorylation by AKT, the recruitment of IWS1 to the RISC complex is enhanced **[Figure 5.7 (B)]**.

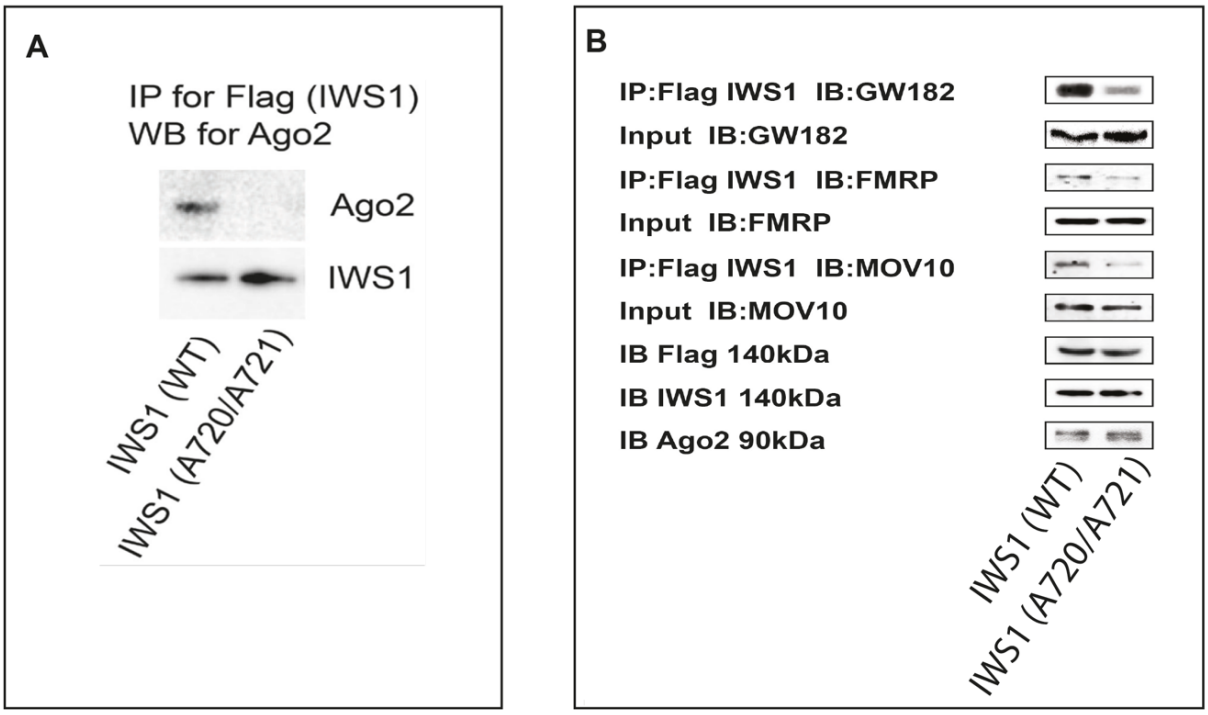

Figure 5. 7: Immunoprecipitation assays for the detection of IWS1 protein interactions. Immunoblot analysis for **(A)** Ago2 and, **(B)** Ago2 interactors, GW182, MOV10 and FMRP in lysates from Ser720/Ser721-IWS1 and Ala720/Ala721-IWS1-expressing cells, subjected to immunoprecipitation for Flag-tagged IWS1.

5.4.4 IWS1 and Ago2 localisation is not affected by AKT activity

We questioned whether the AKT-mediated changes in the interaction between Ago2 and IWS1 was due to the translocation of either proteins upon AKT activity. To address this question, we treated NCM460 cells expressing Ser720/Thr721-IWS1 or Ala720/Ala721-IWS1, with Insulin Growth Factor 1 (IGF1) and 20 min later we isolated cell nuclear and cytoplasmic fractions. IGF1 activate the AKT pathway. Studies have shown that AKT phosphorylation peaks within minutes after IGF1 stimulation and returns to baseline within 30-60 min therefore, with 20 min, the peak activation of AKT can be captured to focus on the acute response of the AKT pathway without affecting gene expression.

Although the isolation of nuclear and cytoplasmic fractions was incomplete, as evidenced by the low immunostaining levels of nuclear protein cAMP-response element binding protein (CREB) in the cytoplasmic fraction, our findings suggest that Ago2 and IWS1 are primarily localised in the nucleus. Immunoblot analysis further suggests that IWS1 phosphorylation and/or AKT activity do not induce nuclear-cytoplasmic translocation of IWS1 and Ago2 **(Figure 5.8)**.

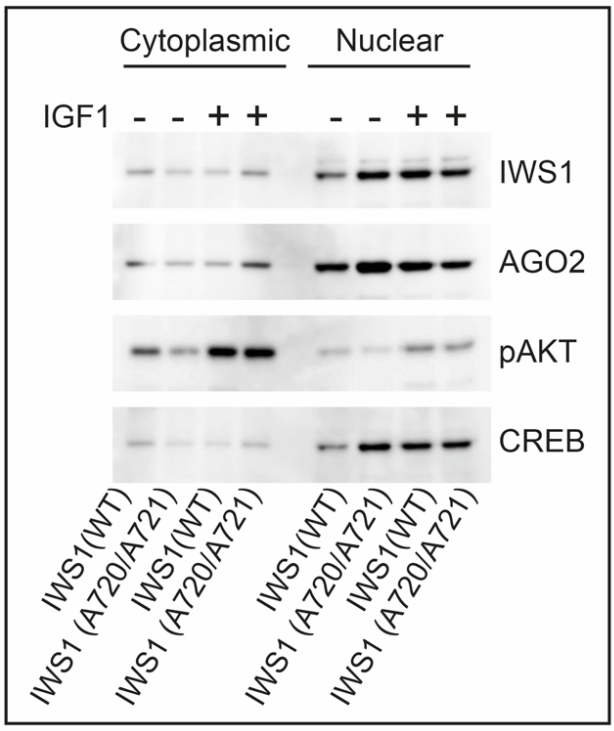

Figure 5. 8: Immunoblot analysis of nuclear and cytoplasmic fractions derived from Ser720/Thr721 and Ala720/Ala721-IWS1-expressing cells. Cells were serum starved overnight and stimulated with IGF1 (100ng/ml) for 20 minutes, and nuclear and cytoplasmic fractions were extracted using NE-PER Nuclear and cytoplasmic extraction kit (78833, Thermo Scientific). CREB was used as a nuclear marker.

To address whether IWS1 interacts preferentially with specific components of the RISC we performed a Proximity Ligation Assay (PLA), a method that detects direct protein-protein interactions. Cells were serum-starved overnight and AKT was activated by IGF1 (100ng/ml) for 20 minutes at 37ºC. PLA in Ser720/Thr721-IWS1 and Ala720/Ala721-IWS1-expressing cells for FLAG (IWS1) and Ago2 **(Figure 5.9)**, FLAG (IWS1) and GW182 or MOV10 **(Figure 5.10Figure 5. *10*)**, and FLAG (IWS1) and FMRP **(Figure 5.11)**, revealed the specificity of IWS1 interaction with Ago2 and FMRP and the dependence of these interactions on IWS1 phosphorylation by AKT. Importantly, these interactions were found to be primarily nuclear or perinuclear. On the other hand, the interaction of IWS1 with GW182 and MOV10 was not induced by IWS1 phosphorylation, suggesting the indirect interaction, potentially through Ago2 and FMRP.

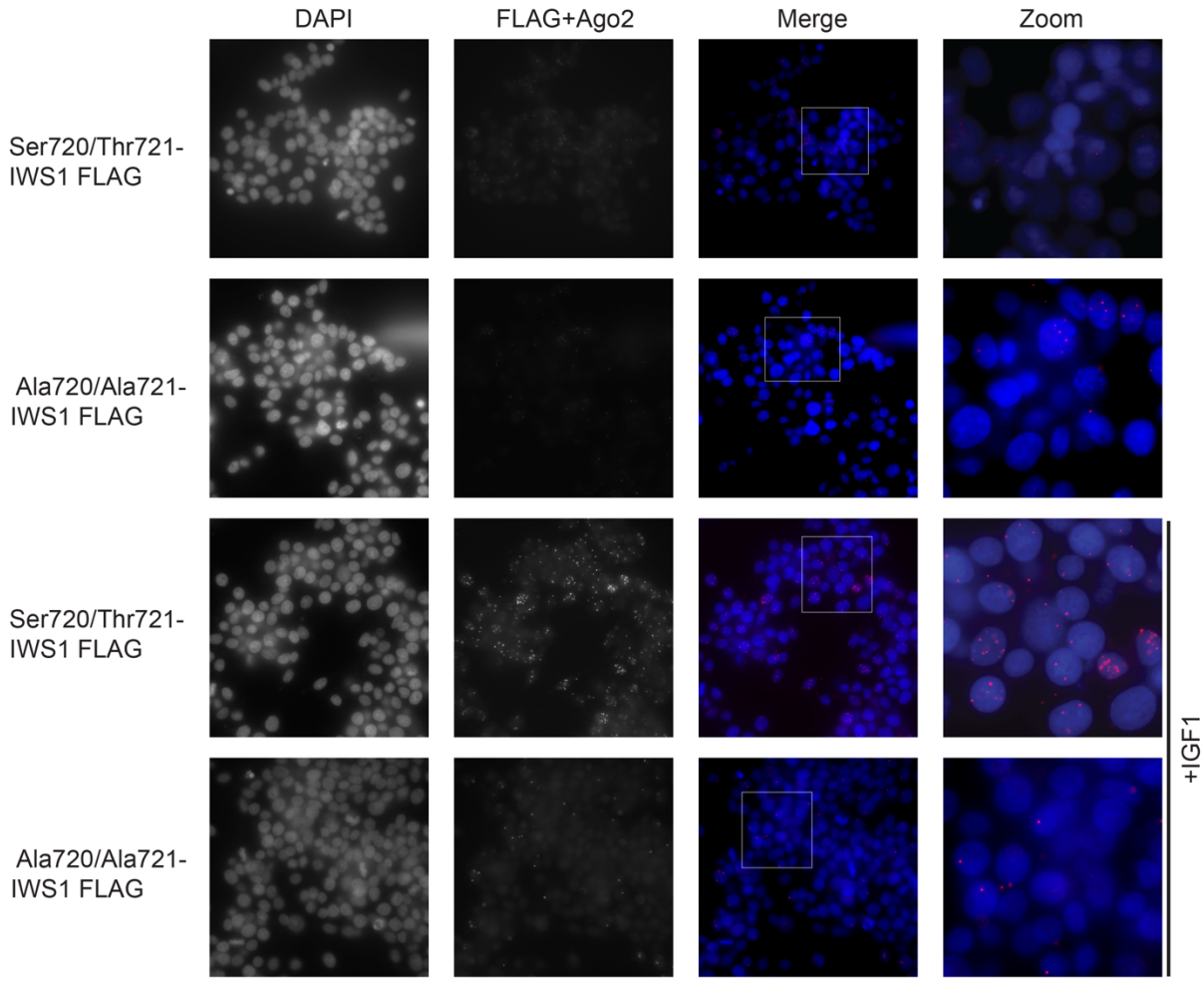

Figure 5. 9: Proximity ligation assay for the evaluation of direct protein interaction between IWS1 and Ago2. NCM460 cells expressing Ser770/Thr721-IWS1 and Ala720/Ala721-IWS1 were serum-starved overnight and stimulated with IGF1 (100ng/ml) for 20 minutes. Cells were incubated with 1:800 Flag and 1:200 Ago2 primary antibodies for 1 hour, followed by 1-hour incubation with PLA Probes. Cells were incubated for 30 minutes with ligase and 100 minutes with polymerase, where labelled oligos hybridize to the complementary sequence within the amplicon. PLA signals were visualized and quantified as red spots using a Leica Thunder microscope. Blue indicates nuclei (DAPI) and red, protein-protein interactions. (Magnification at 200x).

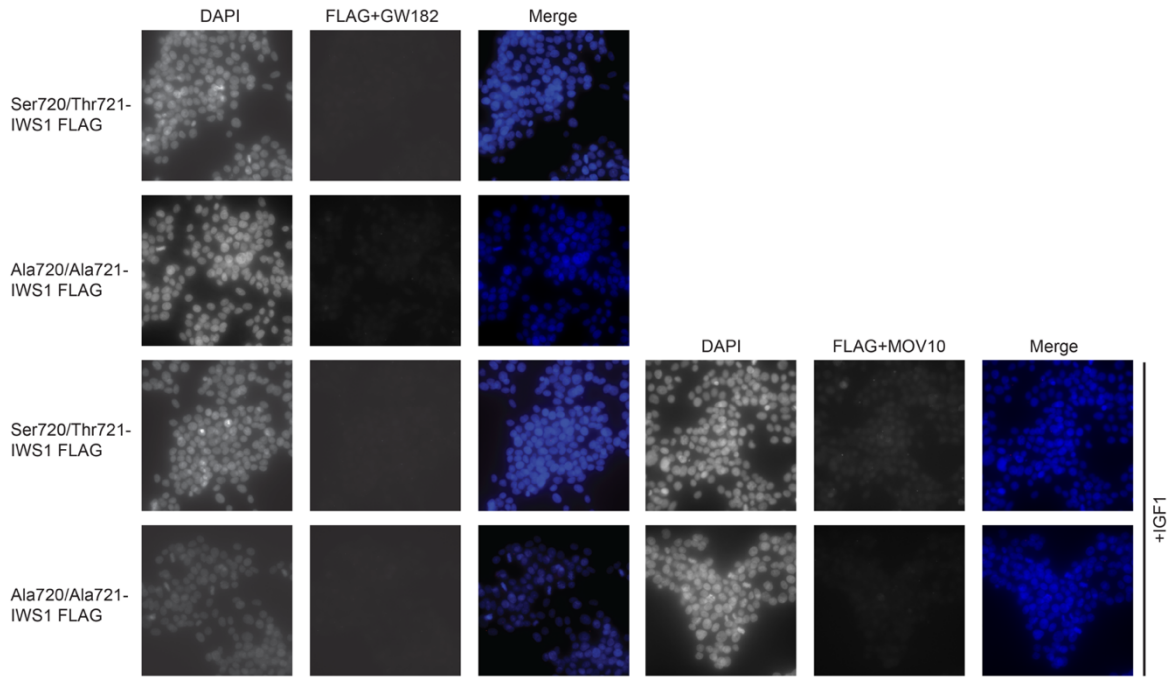

Figure 5. 10: Proximity ligation assay for the evaluation of direct protein interaction between IWS1-GW182 and IWS1-MOV10. NCM460 cells expressing Ser770/Thr721-IWS1 and Ala720/Ala721-IWS1 were serum-starved overnight and stimulated with IGF1 (100ng/ml) for 20 minutes. Cells were incubated with 1:800 Flag and 1:200 GW182 or 1:200 MOV10 primary antibodies for 1 hour, followed by 1-hour incubation with PLA Probes. Cells were incubated for 30 minutes with ligase and 100 minutes with polymerase, where labelled oligos hybridize to the complementary sequence within the amplicon. PLA signals were visualized and quantified as red spots using a Leica Thunder microscope. Blue indicates nuclei (DAPI) and red, protein-protein interactions. (Magnification at 200x).

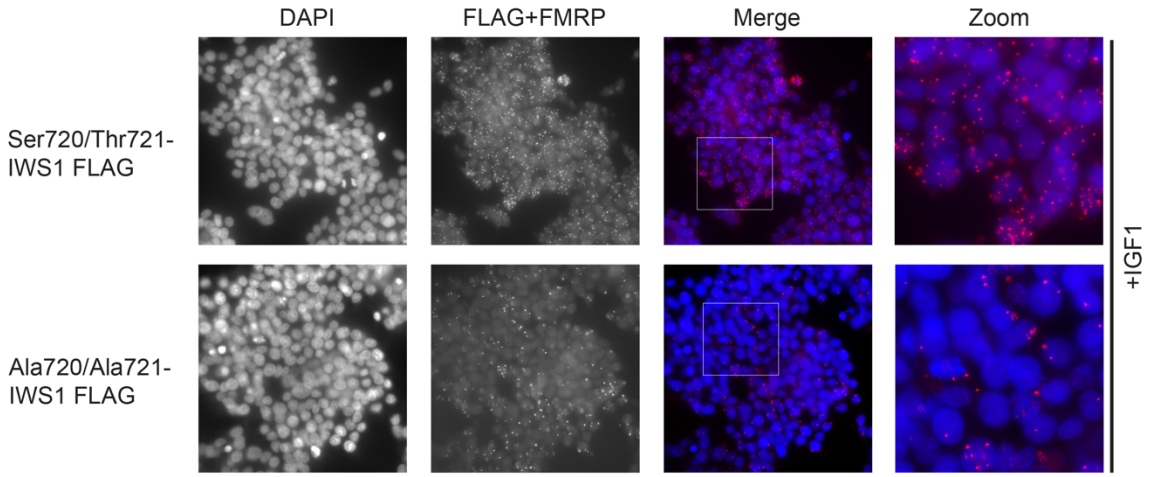

Figure 5. 11: Proximity ligation assay for the evaluation of direct protein interaction between IWS1 and FMRP. NCM460 cells expressing Ser770/Thr721-IWS1 and Ala720/Ala721-IWS1 were serum-starved overnight and stimulated with IGF1 (100ng/ml) for 20 minutes. Cells were incubated with 1:800 Flag and 1:50 FMRP primary antibodies for 1 hour, followed by 1-hour incubation with PLA Probes. Cells were incubated for 30 minutes with ligase and 100 minutes with polymerase, where labelled oligos hybridize to the complementary sequence within the amplicon. PLA signals were visualized and quantified as red spots using a Leica Thunder microscope. Blue indicates nuclei (DAPI) and red, protein-protein interactions. (Magnification at 200x).

We further questioned whether the interaction of IWS1 with Ago2 is conserved. It has been shown previously, that AKT1, but not AKT2, specifically phosphorylates IWS1 at Ser720/Thr721 a site conserved across species (Sanidas *et al.*, 2014). AKT1 and AKT2 isoforms are the predominant isoforms, especially in the small intestine and the colon, whereas AKT3 is predominantly expressed in the heart, brain and kidney (Brodbeck, Cron and Hemmings, 1999; Okano *et al.*, 2000). To evaluate the dependence of IWS1-Ago2 interaction on Akt1-mediated phosphorylation, we employed *Akt1*$^{fl/fl}$*Akt2*$^{-/-}$*Akt3*$^{-/-}$ immortalised mouse lung fibroblasts. We transduced cells with retroviral vectors expressing with myc-Akt1 or myc-Akt2 or the empty retroviral vector and then transduced with CRE recombinase to knock out the endogenous *Akt1*. This resulted in the generation of three isogenic

cell lines expressing Akt1 or Akt2 alone or none of the Akt isoforms (triple knock-out). It is known that AKT is activated by IGF1, mediated by the PI3K pathway (Zheng and Quirion, 2006). Thus, serum-starved cells, were treated with IGF1 (100ng/ml) for 20 minutes. Immunoprecipitation for IWS1 and WB for Ago2 in these cells, before and after treatment with IGF1, revealed that Ago2 interacts with IWS1 in an Akt1-dependent manner and is enhanced upon Akt1 activation by IGF1 **(Figure 5.12)**. These results come in line with our findings in human cells and support that this interaction is conserved across species.

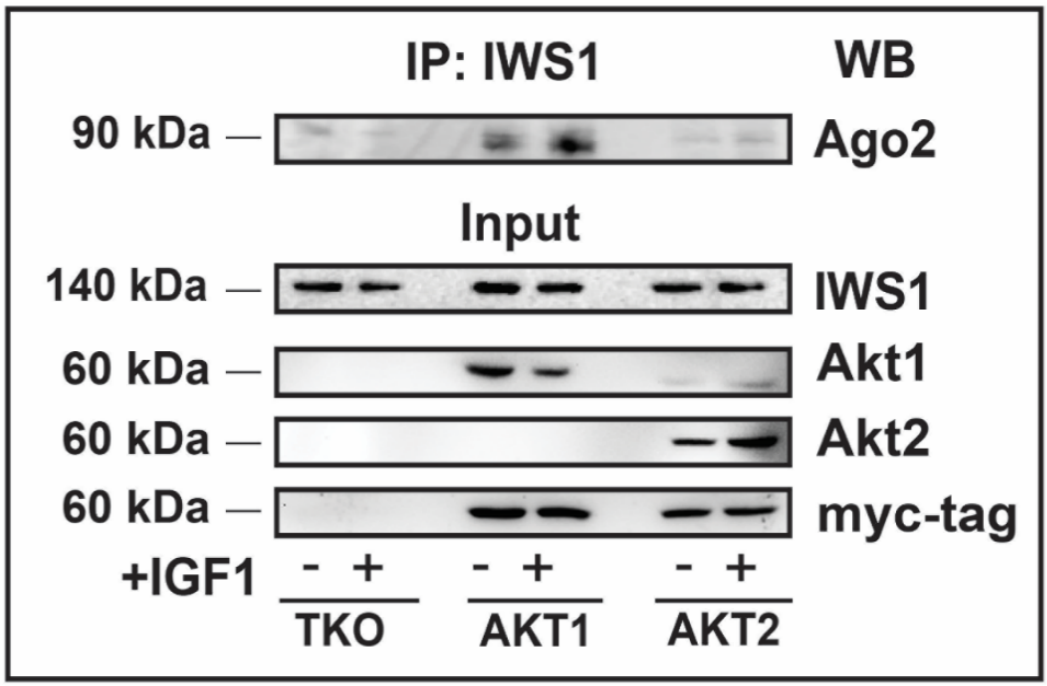

Figure 5. 12: Immunoprecipitation assay for the evaluation of IWS1 and Ago2 interaction in mouse cells. Akt null (TKO) mouse lung fibroblasts and their Akt isoform-expressing derivatives were starved overnight and stimulated with IGF1 (100ng/ml) for 20 minutes. Protein lysates were immunoprecipitated for IWS1 followed by immunoblot analysis for Ago2.

5.5 Conclusion of Chapter 5

To study the effects of phosphorylated IWS1 on intestinal stem cells, Ser720/Thr721-IWS1 and Ala720/Ala721-IWS1-expressing cells were transfected with ISC activity reporter. This assay revealed the increased number of ISC-like population in Ser720/Thr721-IWS1 expressing cells. This led us to the hypothesis that phosphorylation of IWS1 may have an important role in the regulation of ISC properties. RT-qPCR analysis revealed that the expression levels of TERT were reduced in Ala720/Ala721-IWS1-expressing whereas ASCL2 expression levels were not affected at the transcriptional level suggesting the involvement of mechanisms inducing ASCL2 activity in Ser720/Thr721-IWS1 expressing cells.

MicroRNA activity reporter assays, performed in NCM460 validated our findings in NCI-H522 cells that microRNA activity is enhanced in Ala720/Ala721-IWS1-expressing cells. Moreover, we found that IWS1-phosphorylation regulates microRNA effects on cell properties demonstrating that microRNA activity is increased in Ala720/Ala721-IWS1-expressing cells. We found that IWS1 phosphorylation and/or AKT activity do not affect the localisation of IWS1 and Ago2. The interaction of IWS1 with Ago2 was confirmed in NCM460 cells and mouse lung fibroblast cells, suggesting that this is a universal mechanism conserved across species. Immunoprecipitation analyses showed that phosphorylated IWS1 interacts stronger with RISC components compared to Ala720/Ala721-IWS1-expressing cells and with PLA revealed that IWS1-Ago2 and IWS1-FMRP interactions are direct whereas, with other RISC components are indirect.

Here, we propose that regulation of microRNA activity by IWS1 phosphorylation may have important effects on the properties of ISCs and epithelial cell differentiation with implications in intestinal diseases.

CHAPTER 6: AKT/IWS1 axis regulates Intestinal Stem cells

6.1 Introduction and aims

6.1.1 Intestinal inflammation and cancer

Dysfunction of Intestinal epithelium induces immune responses which may result in chronic inflammation, Inflammatory Bowel Diseases (IBD) and progressively cancer (Worthington, Reimann and Gribble, 2018). ISCs are considered the cell origin of the large majority of colorectal cancers (CRC) (Barker *et al.*, 2009). IBD is associated with significant upregulation of pro-inflammatory cytokines and the most common IBDs are Crohn's Disease (CD) and Ulcerative colitis (UC) (Umar, 2010).

6.1.2 Inflammation Bowel Diseases

Inflammation of the gut is considered an important risk factor for CRC. As mentioned earlier, IBD refers to chronic inflammatory disorders of the gastrointestinal tract and includes UC and CD. Both disorders have very similar pathogenesis clinical and histological features which make the differentiation between them difficult (Vaghari-Tabari *et al.*, 2022). CD can affect the whole gastrointestinal tract, causing transmural lesions whereas, the UC causes more superficial lesions limited to the colon. Despite that, the therapeutic is the same in both cases (Le Berre *et al.*, 2020). It has been found that patients with UC have an increased risk of developing Colitis-associated colon cancer (CAC) (Leon-Cabrera *et al.*, 2018). Other risk factors include colonic strictures, proinflammatory polyps (PIPs), gender and age at diagnosis (Flores, O'Connor and Moss, 2017; Wijnands *et al.*, 2021).

Similar to sporadic CRC, CAC develops with a sequence of mechanisms such as alterations of p53, APC and KRAS however, the sequence of events is different (Li *et al.*, 2022). p53 is activated during oncogenesis and regulates various genes of cell-cycle arrest, DNA repair and apoptosis (Chen, 2016). CAC arises through different mechanisms including the activation of pro-survival NFκB (nuclear factor –

κB) and STAT3 (signal transducer and activator of transcription 3) signalling (Colotta *et al.*, 2009; Grivennikov *et al.*, 2009; Westbrook *et al.*, 2009; Li *et al.*, 2022).

Defective differentiation of ISCs to goblet cells leads to goblet cell depletion and mucin deficiency and induces UC (Gersemann, Stange and Wehkamp, 2011). On the other hand, CD is characterized by a decrease in Paneth cell numbers, and it is associated with the suppression of TCF4, which regulates the Paneth cell differentiation, resulting in impaired innate immunity (Wehkamp *et al.*, 2007). ISCs regenerate the damaged intestinal epithelium, but how the deregulation of Paneth cells in CD affects the properties of resident ISCs remains unclear (Suzuki *et al.*, 2018).

6.1.3 Colorectal cancer

CRC is the third most common cause of cancer and the fourth leading cause of cancer death worldwide (Rawla, Sunkara and Barsouk, 2019). CRC can be either spontaneous or a long-term implication of chronic inflammation. Usually, CRC occurs sporadically (70-75%), meaning that there is no family history (Amersi, Agustin and Ko, 2005). Approximately, 25% of patients have a family history of CRC and only 5-10% of patients are due to inherited mutations (Rustgi, 2007). CSC develops under chronic inflammatory conditions in the intestines and is one of the most frequent causes of mortality and morbidity in patients with inflammatory bowel disease (IBD) (Romano *et al.*, 2016). CAC is found to have greater malignant potential than sporadic CRC and patients have poor survival (Watanabe *et al.*, 2011). As mentioned earlier, the main components of IBD are UC and CD. CAC have greater malignant potential than sporadic CRC and survival is less in these patients (Watanabe *et al.*, 2011). Other important risk factors associated with CRC are obesity-eating habits and physical inactivity, smoking, alcohol and age (Dekker *et al.*, 2019).

Sporadic CRCs usually arise with the increase in age. it has been found that 90% of patients are older than 50 (Amersi, Agustin and Ko, 2005). Sporadic CRCs generally develop by the accumulation of various abnormalities in tumour suppressor genes and oncogenes (Yamagishi *et al.*, 2016). There are different genetic pathways that lead to CRC including the chromosomal instability pathway (CIN), microsatellite instability (MSI) and CpG island methylator phenotype (CIMP) (Pino and Chung, 2010). Mutation of APC (Adenomatous Polyposis Coli) acts as an initiating event following the accumulation of other mutations including KRAS (Kirsten RAS), SMAD4 (Mad-related protein 4) and TP53 (Fearon R. Eric and Bert, 1990; Polakis, 2012). Additional mutations including TGF-β and PIK3CA are required for subsequent malignant transformation (Fearon R. Eric and Bert, 1990). It was found that KRAS cannot initiate cancer and promote tumour progression without the mutation in APC (Haigis *et al.*, 2008). CIN is the most common pathway in sporadic colorectal cancers (65-70%) and it can be due to aneuploidy karyotype due to numerical or structural chromosomal abnormalities, sub-chromosomal genomic amplifications, or loss of heterozygosity (Pino and Chung, 2010; Yamagishi *et al.*, 2016). On the other hand, the MSI pathway is caused by the dysfunction of DNA mismatch repair (MMR) genes such as MLH1 and MSH2, which leads to instability in stretches of DNA microsatellites (Toyota *et al.*, 1999; Pino and Chung, 2010; Yamagishi *et al.*, 2016). The last pathway, the CIMP, is characterized by the methylation of CpG island (Toyota *et al.*, 1999). CpG islands are found in the 5' region of about half of the human genes and are rich in CpG dinucleotides (Bird, 1986). DNA methylation in CpG island regions of promoter genes silences the expression of some genes resulting in hypermethylation of CpG islands (Toyota *et al.*, 1999).

6.2 Signalling pathways involved in the progression of CRC and CAC

Numerous genes of different signalling pathways that are dysregulated by mutations are associated with CRC. The molecular pathways involved in the carcinogenesis of CRC and their function are summarised in **(Figure 6.1)**.

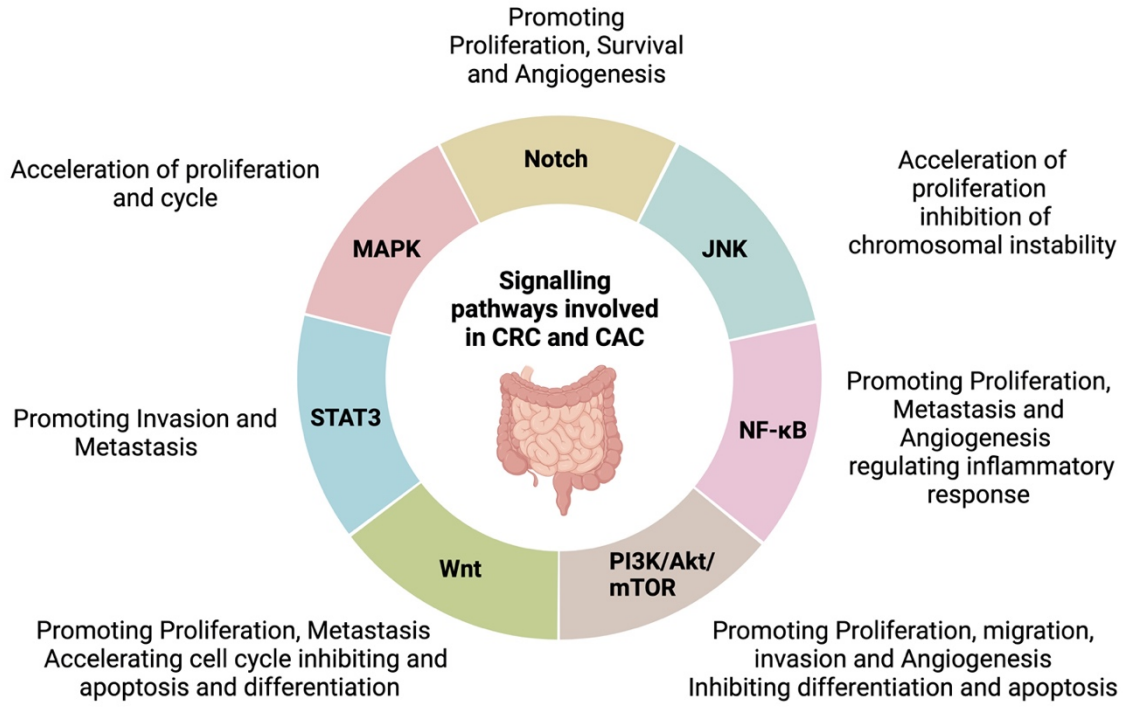

Figure 6. 1: Signalling pathway involved in CRC and CAC. There are various cell signalling pathways involved in gastrointestinal carcinogenesis that promote either proliferation and migration, invasion, metastasis and angiogenesis. Figure prepared using BioRender (www.biorender.com).

6.2.1 Wnt Signalling

Wnt signal transduction pathway is an important intracellular pathway that regulates key aspects of cell fate determination, cell proliferation and migration, cell polarity and neural patterning and organogenesis during crucial biological processes including embryonic development, stem cell maintenance, tissue homeostasis and disease pathophysiology such as cancer (Komiya and Habas, 2008; Clevers and Nusse, 2012; Nayak, Bhattacharyya and De, 2016). It is also related to the

regulation of intestinal stem cells in crypts and deregulation of the pathway affects cell differentiation and apoptosis, leading to polyps and carcinoma (Hofacker, 2007). In 1990, Wnt signalling was related to human disease: the *APC* tumour suppressor gene, playing a key role in hereditary and spontaneous colorectal cancer, was found to be directly linked to Wnt signalling with the detection that it is bound to core component β-catenin (Nishisho *et al.*, 1991; Polakis, 2012). In the Wnt family, there are 19 Wnt ligands that are secreted cysteine-rich glycoproteins and bind the N-Terminal of the 10 Frizzled (Fz) receptors, to initiate with other co-receptors, the downstream signalling of canonical and non-canonical pathways of Wnt (Mah, Yan and Kuo, 2016).

In the canonical pathway (Wnt/ β-catenin), when the Wnt is not bound to receptors the destruction complex is active. Destruction complex includes Axin, APC, protein phosphatase 2A (PP2A), glycogen synthase kinase 3 (GSK3), casein kinase 1a (CK1a) and β- transducing repeat-containing protein (β-TrCP)**.** The active destruction complex phosphorylates the β-catenin in a GSK3β-dependent manner, leading to ubiquitination and degradation of β-catenin (Clevers and Nusse, 2012). However, when Wnt is engaged to LRP5/6 (low-density-lipoprotein-related protein 5/6), the signal is transduced to cytoplasmic phosphorylation of Dishevelled (Dsh), leading to the inhibition of the destruction complex (Ackers and Malgor, 2018). This leads to the accumulation of non-phosphorylated β-catenin in the cytosol which is translocated to the nucleus to interact with T-cell specific factor/lymphoid enhancer–binding factor (TCF/LEF) and other coactivators such as Pygopus (Pygo) and Bcl-9, in order to regulate gene transcription by activating the Wnt target genes, c-Myc, cyclin D1 and Cdkn1a (Gordon and Nusse, 2006; Wu and Pan, 2010; Clevers and Nusse, 2012; Mah, Yan and Kuo, 2016).

The non-canonical pathway, also known as the β-catenin independent pathway, is divided into the Planar cell polarity pathway (PCP) and the Wnt/Ca^{2+} pathway (Gordon and Nusse, 2006; Komiya and Habas, 2008). PCP is activated through the interaction of Wnt and Fz receptors, as well as other co-receptors containing cysteine-rich binding domains such as the CTHRC1 (collagen triple helix repeat-containing protein 1) (Ackers and Malgor, 2018). The Wnt/Ca^{2+} pathway is initiated by Fz receptors that activate G protein-coupled signalling pathway (Antara, 2011). Briefly, Wnt/Fz signalling releases intracellular Ca^{2+} through trimeric G proteins and activates Ca^{2+} sensitive proteins such as Protein kinase C and camKII (calcium/calmodulin-dependent kinase II) (Kühl *et al.*, 2000; Sheldahl *et al.*, 2003). Studies for Wnt/Ca^{2+} pathway found that it can function as a critical modulator of both Wnt pathways, canonical and PPC. **Figure 6.2** shows a schematic representation of the Wnt signalling and their interactions.

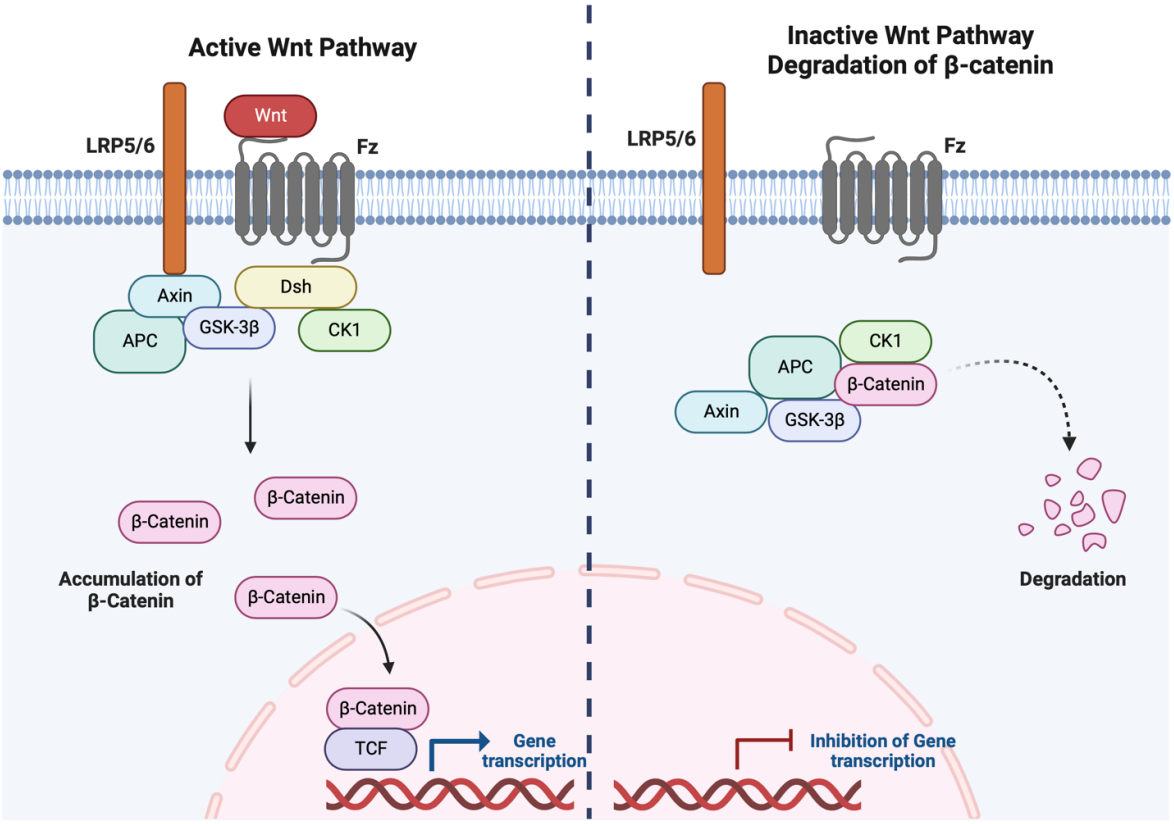

Figure 6. 2: A schematic representation of the Wnt signalling pathway. Left: In the activated state of Wnt pathway, Wnt ligands bind to Fz receptors and LRP5/6 co-receptors, where the Dishevelled (Dsh) phosphoprotein, is phosphorylated and GSK-3β and Axin are recruited to the plasma membrane. B-catenin is then translocated into the nucleus where it interacts with TCF to promote gene expression. **Right:** During the inactivated state, the Wnt ligands are absent thus, β-catenin forms a complex with Axin and APC. GSK-3β phosphorylates β-catenin which is ubiquitinated in degradation and thus, it cannot translocate into the nucleus and gene transcription is inhibited. Figure designed using BioRender (www.biorender.com).

6.2.2 NF-κB

Another important pathway involved in the initiation of CRC and CAC is the NF-κB, which is consisting of five members, p50, p52, p65 (RelA), c-Rel, RelB. NF-κB has a key role in innate and adaptive cellular immunity and is one of the main regulatory components in the initiation of CAC (Hayden and Ghosh, 2008; Hirano *et al.*, 2020; Wan *et al.*, 2020). It includes 2 pathways, the canonical and the non-canonical. In both cases, NF-κB forms a complex in the cytoplasm with the inhibitory molecules IκBα, IκBβ and IκBγ (known as IKK inhibitors) to form dimers (Hirano *et al.*, 2020; Li *et al.*, 2022). In the canonical pathway, NF-κB is activated by inflammatory stimuli such as lipopolysaccharide and TNF-α, which are converted into protein phosphorylation signals and mediates activation of p50, c-Rel and RelA. The non-canonical pathway activates p100, p52 and RelB (Sun, 2017; Wan *et al.*, 2020).

In 2015, Polytarchou and his colleagues have shown that 9 microRNA inhibitors regulate the phosphorylation levels of the NF-κB pathway. Specifically, miR-26b and miR-199a significantly induces NF-κB phosphorylation levels whereas, miR-7, miR-146a, miR-373, miR-372, miR181b, miR-21 and miR-214 suppresses them. From the above microRNAs, miR-21 and miR-146a and miR-214 are expressed highly in both UC and CD (Polytarchou *et al.*, 2015).

6.2.3 Notch

Genetic changes such as point mutations, chromosomal translocation and other epigenetic modifications can activate the Notch pathway in multiple cancers. The notch pathway regulates cell proliferation and differentiation, in addition to apoptosis and stem cell maintenance (Koch and Radtke, 2007). It has been published that the Notch pathway is upregulated in CRC patients and induces cancer proliferation and angiogenesis (Gopalakrishnan *et al.*, 2014).

6.2.4 PI3K/AKT/mTOR

It has been found that this pathway is involved in different cellular processes that influence proliferation, metabolism, survival, apoptosis, angiogenesis and tissue development (Javid *et al.*, 2019). Dysregulation of the PI3K/Akt/mTOR signalling pathway leads to various pathological conditions including cancer. It has been found that it is overexpressed CRC (Moafian *et al.*, 2021). Inhibition of mTOR pathway induces suppression of migration and invasion of cancerous cells (Duan *et al.*, 2018). PTEN (phosphatase and Tensin Homolog), which is the negative regulator of PI3K/AKT signalling, where it dephosphorylates PI (3,4,5) P3 to PI (4,5) P2, is overexpressed in CRC (Cheng *et al.*, 2020).

6.2.5 MAPK

There are three main subfamilies of mitogen-activated protein kinases (MAPK), the ERKs (extracellular-signal-regulated kinases), the JNKs (c-Jun N-terminal kinases) and the p38/SAPKs (stress-activated protein kinases) (Fang and Richardson, 2005; Morrison, 2012). This pathway is important in cell proliferation and its overexpression and activation is involved in the progression of CRC (Fang and Richardson, 2005). Briefly, MAPK pathways are activated by various growth factors, cytokines and hormones, to regulate cell proliferation and differentiation. ERK signalling pathway transfer signal from growth factors and regulate the gene expression to prevent apoptosis (Yao *et al.*, 2020). JNKs are involved in cellular processes such as proliferation, survival and apoptosis and it has been reported that hyperactivation of JNKs, due to the loss of PTEN, is associated with inflammatory bowel disease (Mitsuyama *et al.*, 2006). The JNKs are activated by DNA-damaging agents and deficiency of growth factors, and they regulate transcription factors such as STAT3, through phosphorylation (Manzoor, Koo and Koh, 2014). During the transformation process, there are inflammatory cytokines of intestinal tissues that generate cellular effects and functions through JAK/STAT

which control intestinal immune function and inflammatory responses (Heneghan, Pierre and Kudsk, 2013; Leon-Cabrera *et al.*, 2018). STAT3 contributes to the oncogenesis of colon epithelium through the acceleration of cell proliferation (Corvinus *et al.*, 2005). Finally, p38 modules, similarly to JNKs, are activated by cytokines and environmental stresses and they are activation is involved in inflammation, apoptosis and cell differentiation (Cuenda and Rousseau, 2007).

6.2.6 STAT3

STAT3 is a transcription factor which is activated by different growth factors and cytokines (Chapman *et al.*, 2000; Levy and Darnell, 2002). It is the integration point for different tumorigenic signalling pathways, and it regulates the immune response against cancer (Gargalionis, Papavassiliou and Papavassiliou, 2021). In CRC STAT3 is activated and promotes cell proliferation, tumour growth, invasion, and migration (Xiong *et al.*, 2008). The binding of receptor tyrosine kinases (RTK), cytokine receptors and G-protein-coupled receptors (GPCK) lead to JAK recruitment, which activates STAT3. Activated STAT3 enters the nucleus and enhances gene transcriptions, which induces specific properties for CRC including cell proliferation, resistance to apoptosis, survival and angiogenesis. It has been also found that STAT3 has a characteristic feature in CRC through the Interleukin-6 (IL-6), which represents an important inflammatory mechanism in CAC. Specifically, they have demonstrated that IL-6 is a promoter during early CAC tumorigenesis (Grivennikov *et al.*, 2009).

6.3 ISCs Niche-Signalling pathways involved in ISC regulation

Wnt signalling pathway has a main role in the regulation of the renewal of intestinal epithelium, the maintenance and division of stem/progenitor cells and the migration of newly divided cells along crypt-villus (Pinto *et al.*, 2003). The majority of CRCs are initiated by activating mutations in the Wnt Pathway (Kinzler and Vogelstein,

1996). Mutations in APC gene induce the initial oncogenic events in CRC (Fearon R. Eric and Bert, 1990; Logan and Nusse, 2004), and lead to the expansion of ISCs compartment and adenoma formation (Shibata *et al.*, 1997). Inactivation of APC stabilizes β-catenin and its localisation in the nucleus, where interacts with T-Cell Factor 4 (TCF4/LEF1), which is an essential gene for stem cell maintenance to upregulate the expression of Wnt target genes (Moser, Pitot and Dove, 1990; Bienz and Clevers, 2000; van Es *et al.*, 2012). Wnt signalling mediated by β-catenin/TCF-4 maintains the undifferentiated progenitor cells (Korinek *et al.*, 1998; Gregorieff *et al.*, 2005) and induces the positioning of differentiating and mature Paneth cells in the crypts (Batlle *et al.*, 2002; van Es *et al.*, 2012). Activation of Wnt pathway forms an intracellular β-catenin/TCF4 complex which is translocated into the nucleus and acts as a transcription factor which controls the expression of Paneth cell defensins (Gersemann, Stange and Wehkamp, 2011).

Notch signalling maintains the undifferentiated status of ISC through 'lateral inhibition'. Inhibition of Notch signals prevents crypt cell proliferation (van Es *et al.*, 2012; Santos *et al.*, 2018). Notch signalling is active in $Lgr5^{+}$ and regulates Olfm4, which is a specific marker for stem cells (van der Flier *et al.*, 2009). It has been found that Atoh1 strengthens Notch-mediated lateral inhibition between ISCs and secretory cells as Atoh1 is needed for intestinal secretory cell lineage generation (Shroyer *et al.*, 2007).

Notch and Wnt pathways are cooperating to activate intestinal tumorigenesis (Fre *et al.*, 2009). *Hes1* regulates the maintenance of ISCs. Overexpression of *Hes1* leads to an increased number of proliferating cells and loss of secretory cells, whereas *Hes1* knockout (KO) mice overproduce secretory cells (Jensen *et al.*, 2000). The Notch-Hes1 pathway stimulates the proliferation of ISCs (Ueo *et al.*, 2012). IBD is associated with significant upregulation of proinflammatory cytokines (Umar, 2010).

Another essential ISC niche factor is the R-spondins family. R-Spondins are secreted glycoproteins that do not have intrinsic Wnt signalling activity however, they potentiate the ability of Wnt ligands to activate canonical Wnt Signalling (de Lau, Snel and Clevers, 2012). Overexpression of R-spondins induces the Lgr5+ ISCs expansion (Yan et al., 2017).

6.4 Aims of Chapter 6:

Our preliminary data propose that IWS1 contributes to Intestinal stem cell self-renewal and may regulate their differentiation. In this chapter, we will focus on the role of IWS1 in ISC biology in human cells and animal model of disease.

The aims of this chapter are:

1. To study the IWS1 effect on ISC differentiation in mouse and in human cells
2. To investigate the role of IWS1 in the regeneration of the intestinal epithelium under inflammatory conditions.

6.5 Methods

6.5.1 Generation of conditional *Iws1* knockout mice

Generation of *Iws1*$^{fl/fl}$ model (Orlacchio *et al.*, 2018) was performed as shown in **Figure 6.3**. Briefly, a targeting vector was obtained from Interactional Knockout Mouse Consortium (IKMC) (PG00131_Z_1_C06 of KOMP-CSD project #44132) and it was electroporated into C57Bl/6-Sv129 hybrid mouse Embryonic Stem cells. Two different clones were used to generate male chimeras, which are mated to C57Bl/6N (Taconic Biosciences) females to get positive *Iws1*$^{tm1a(KOMP)Wtsi}$ offspring. In tm1a allele, Iws1 exon 4 is flanked by two LoxP sites allowing the removal by Cre-mediated recombination, and a cassette containing a strong splice-acceptor sequence (En2 SA), followed by LacZ gene insertion in the third intron. The entire cassette (En2 SA-LacZ-neo) was removed by FLPe recombination to obtain Iws1$^{fl/fl}$.

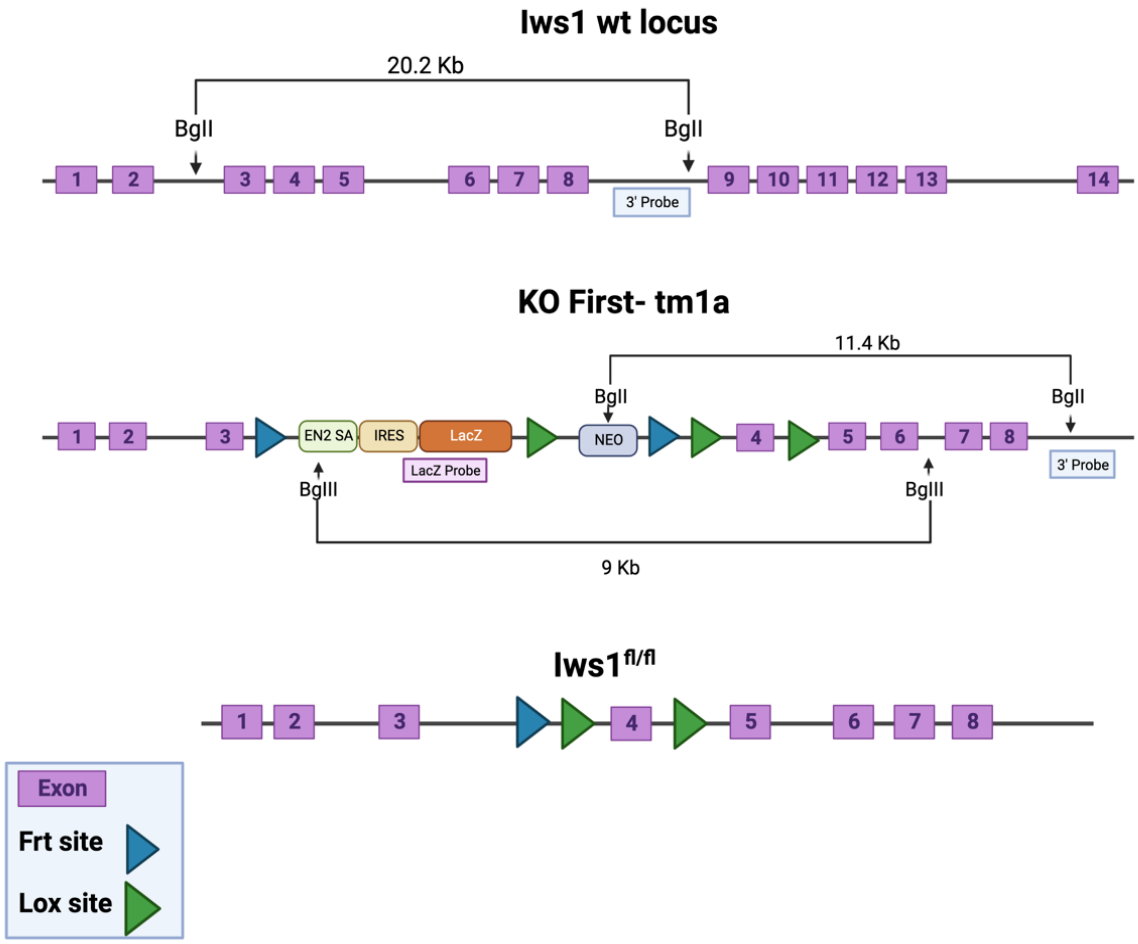

Figure 6. 3: ***Strategy employed to generate Iws1$^{fl/fl}$ mice.*** *Targeted clones bear a tm1a configuration where Exon 4 is flanked between the 2 LoxP sites and a cassette containing a splice acceptor sequence (En2 SA), followed by LacZ gene in the third intron. This allows the tracking of Iws1 expression in vivo. Flpe recombination can be used to remove the entire cassette (EN2 SA-LacZ-neo) to obtain IWS1$^{fl/fl}$ mice. Figure modified from (Orlacchio et al., 2018) using BioRender (www.biorender.com).*

6.5.2 Generation of *Iws1*$^{fl/fl\ Lgr5Cre}$ mice

Lgr5$^{EGFP/CreERT2}$ encodes a Cre recombinase (Cre) fused to a mutant estrogen ligand-binding domain (ERT) mice, were a gift by Dr. Maria Mihaylova (Mihaylova *et al.*, 2018) and were crossed with *Iws1*$^{fl/fl}$ mice to get *Iws1*$^{fl/fl}$ / *Lgr5*$^{EGFP/CreERT2}$ mice **(Figure 6.4)**.

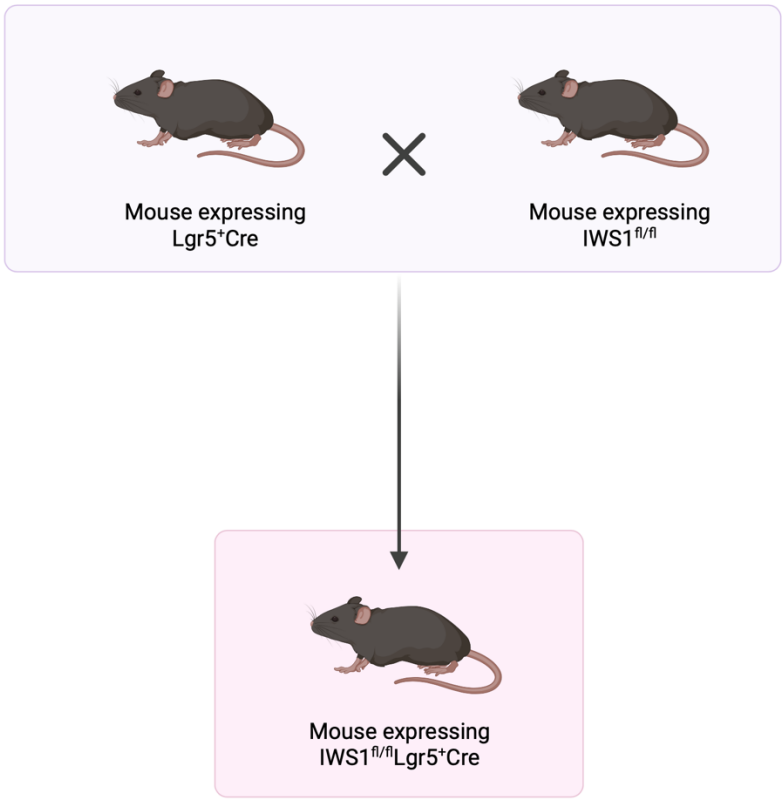

Figure 6. 4: Generation of Iws1 $^{fl/fl}$/ Lgr5 $^{EGFP/CreERT2}$ mice. Lgr5$^{EGFP/CreERT2}$ mice were crossed with *Iws1*$^{fl/fl}$ mice to generate *Iws1*$^{fl/fl}$ / *Lgr5*$^{EGFP/CreERT2}$ mice. Figure designed *using* BioRender (www.biorender.com).

6.5.3 DNA extraction

Each mouse was marked with an ear tag and a piece of the ear was cut. Pieces were placed in Eppendorf tubes and incubated overnight at 55^{o}C in 500 µl lysis buffer (1M Tris-Cl, pH8.5; 0.5M EDTA; 5M NaCl; 20% w/v SDS), containing 5 µl Proteinase K (100 µg/ml). The following day, after vortexing for 10 seconds were centrifuged at 21,952 x g for 15 minutes. The supernatant was transferred into a new tube containing 500 µl isopropanol and mixed well by inverting. Centrifugation followed for 6 minutes at 21,952 x g and supernatant was discarded. Pellet was washed twice with 500 µl of 70% Ethanol. The supernatant was discarded, and the pellet was dried at 55^{o}C for 10 minutes. 500 µl of 0.1mM EDTA TE buffer, pH 8 was added and samples were incubated at 55^{o}C for 1 hour. Samples were vortexed and PCR for genotyping was carried out.

6.5.4 Genotyping

6.5.4.1 Iws1$^{fl/fl}$

DNA samples were subjected to PCR using 2x PCR Taq Master Mix kit (201445; Qiagen). For each sample, 10 µl of 2x PCR Taq Master mix was mixed with 4 µl nuclease-free water, 2 µl of Forward and Reverse (WT-F: GGTTTTGGTTGTGGAAGGCCAATTT; IWS1$^{fl/fl}$ F: GATGGCGCAACGCAATTAATGATAA; R: GCAAAATGTGCAGACCTTAGGCATC) primers (10pmole/ µl) and 4 µl of DNA extract. Reactions were mixed and spun quickly prior to PCR. The cycling conditions are shown in **Table xxxiv**. The expected PCR product for both WT and *IWS1$^{fl/fl}$* is 200-300 bp with *IWS1$^{fl/fl}$* giving a slightly larger product **(Figure 6.5)**.

Table xxxiv: PCR conditions for Iws1$^{fl/fl}$ genotyping.

Temperature (°C)	Time	Cycles
95	5 minutes	
94 **64** **72**	30 seconds 30 seconds 30 seconds	30 cycles
72	10 minutes	
4	∞	

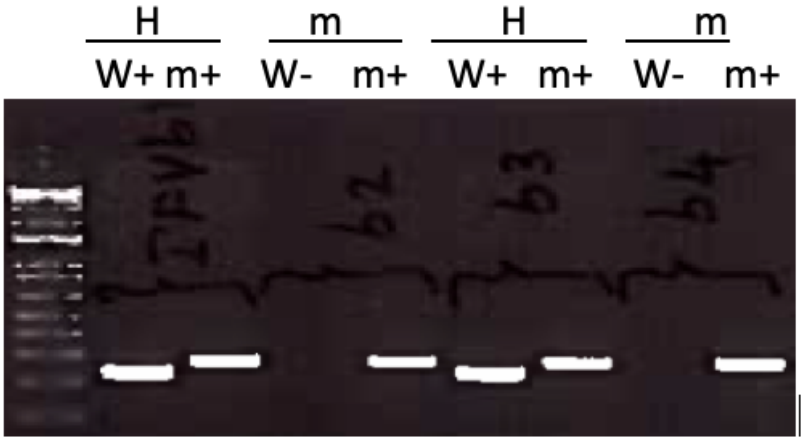

Figure 6. 5: Genotyping of mice for the detection of IWS1$^{fl/fl}$. Agarose gel electrophoresis following PCR reactions indicate the presence of the floxed allele in lanes 3,5,7 and 9. First lane: MWM.

6.5.4.2 Lgr5^{CreERT}

DNA samples were subjected to PCR using 2x PCR Taq Master Mix kit (201445; Qiagen). For each sample, 10 µl of 2x PCR Taq Master mix was mixed with 5 µl nuclease-free water, 1 µl of each Lgr5 primer (10pmole/ µl) (Lgr5-F: CTG CTC TCT GCT CCC AGT CT; wild type-R: ATA CCC CAT CCC TTT TGA GC; Mutant-R: GAA CTT CAG GGT CAG CTT GC) and 2 µl of DNA. Reactions were mixed and spin quickly. For the PCR the following cycles were used (**Table xxxv**). The expected PCR product for WT is 298 bp and for *Lgr5*^{CreERT} 174 bp **(Figure 6.6).**

Table xxxv: PCR conditions for Lgr5^{CreERT} Genotyping.

Temperature (°C)	Time	Cycles
95	5 minutes	
94	30 seconds	38 cycles
52	30 seconds	
72	30 seconds	
72	10 minutes	
4	∞	

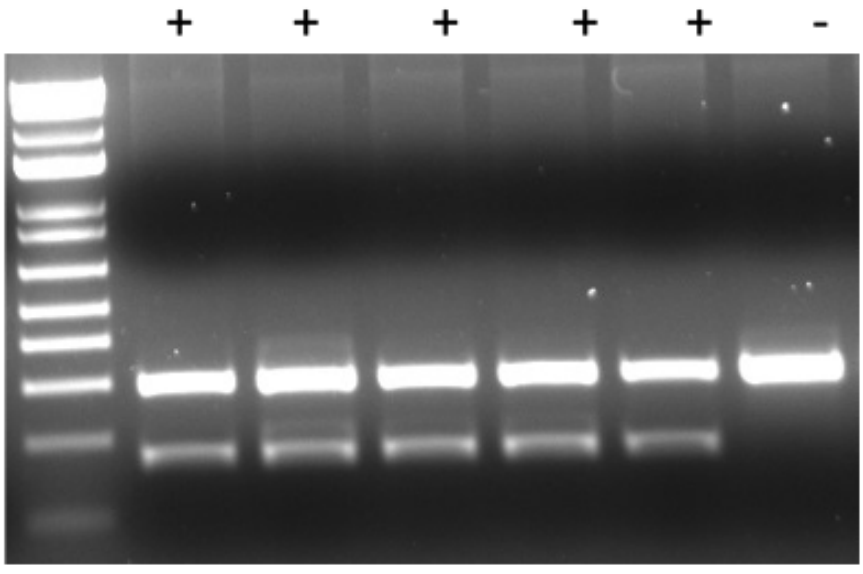

Figure 6. 6: Genotyping of mice for the detection of Lgr5^{CreERT}. Agarose gel electrophoresis following PCR reactions indicate the presence of the Lgr5^{CreERT} in lanes 2,3,4,5 and 6. First lane: MWM.

6.5.5 Isolation of EPCAM+ Cells

Small intestines and colons from ISC-*Iws1* KO (*Iws1*$^{fl/fl}$*Lgr5Cre*) and WT (*Iws1*$^{fl/fl}$) mice, were removed, washed with cold DPBS, opened longitudinally and cut into fragments. Pieces were washed several times with cold DPBS and 2-3 times with DPBS containing 10 mM EDTA. Tissues were incubated on ice for 90-120 minutes with gentle shaking at 30 minutes intervals. Crypts were separated from the connective tissue by more vigorous shaking and filtered through a 70 µm mesh into a 50 ml Falcon tube. For epithelial cell isolation, crypt suspensions were dissociated into individual cells with TrypLE Express (12605010, Gibco). Cell labelling using a cocktail of antibodies for cluster differentiation (CD) 45 phycoerythrin (PE) (CD45-PE), cluster differentiation (CD) 31 phycoerythrin (PE) (CD31-PE), Ter119-PE, CD24-Pacific Blue, cluster differentiation (CD) 117- allophycocyanin/cyanine (CD117-APC/Cy) and epithelial cellular adhesion molecule-allophycocyanin (EPCAM-APC). Dead cells were excluded from the analysis with the viability dye 7-Aminoactinomycin D (7-AAD).

6.5.6 Dextran Sodium Sulphate (DSS)-induced colitis in mice

All mice (6-12 weeks old) were administered intraperitoneal tamoxifen injections daily for 5 days (10mg/ml sunflower seed oil, 0.1 mg/g of weight). On day 3, for the experimental (DSS) group, the cage water bottle was changed with 5% w/v DSS water (5% DSS, 250 ml) for 5 days. The control group received the same volume of water without DSS. On day 7, DSS water was replaced by regular drinking water for 2 days and on day 8 mice were culled by an S1 method **(Figure 6.7).** During the experiments, body weight, stool consistency, blood in the rectum and stools were monitored daily. Blood presence in stool was detected using the hemoccult Faecal Occult Blood test kit (SK-61200; Fisher Scientific) **(Figure 6.8).** The overall disease activity score was calculated by combining the scoring in the criteria described in

Table xxxvi. Mice demonstrating loss of body weight in excess of 15% were placed in regular drinking water and culled two days later.

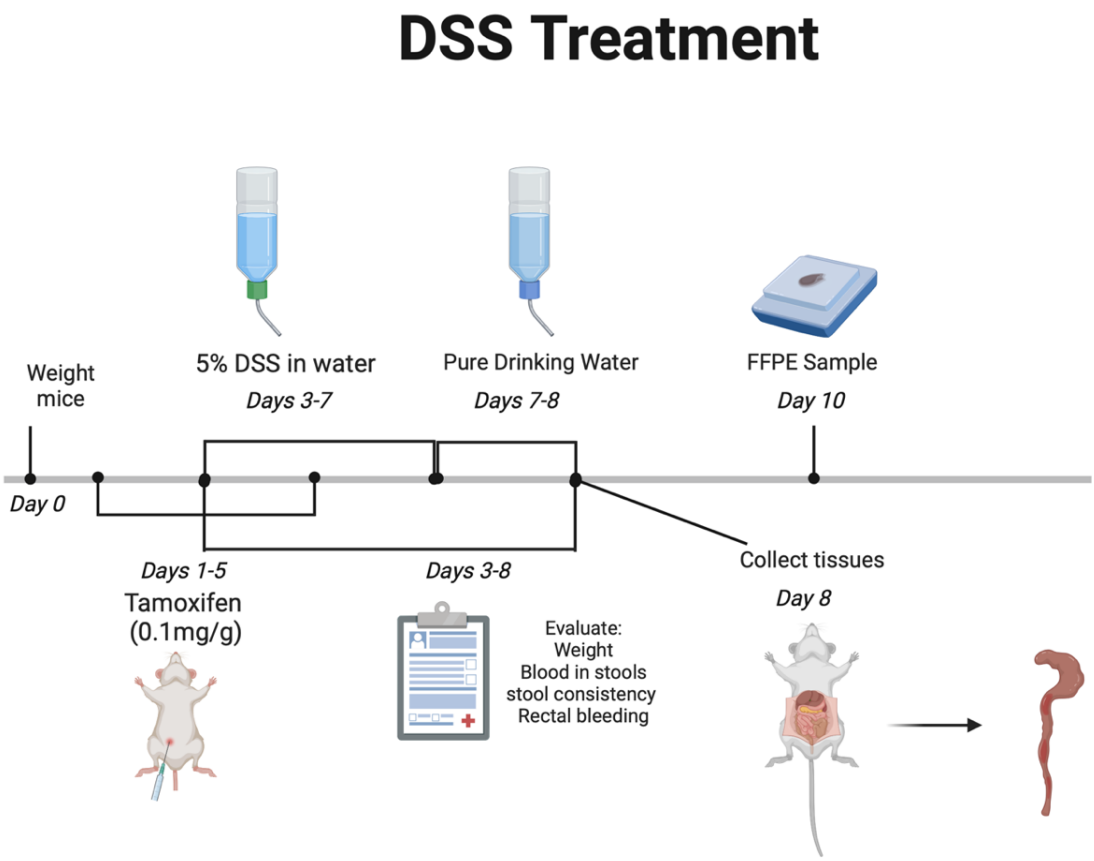

Figure 6. 7: Schematic representation of the DSS experiment to induce colonic inflammation in mice. Mice were injected intraperitoneally with tamoxifen for 5 days. On day 3, DSS was added to drinking water for 5 days and then replaced with regular drinking water for the next two days. Mice were sacrificed on day 8, and tissues were collected and paraffin-embedded. Figure designed using BioRender (www.biorender.com).

Figure 6. 8: Representative Hemoccult test. A strong positive result for *Iws1*$^{fl/fl}$*Lgr5Cre* mice treated with DSS (left) versus the negative result for Iws1$^{fl/fl}$Lgr5Cre mice drinking regular water.

Table xxxvi: Disease Scoring parameters

Parameter	Score	Parameter	Score
Weight Loss		**Rectal Bleeding**	
0	0	Absent	0
0.1-4.99%	1	Slight	0.5
5-9.99%	2	Present	1
10-14.99%	3	Heavy	2
>15%	4		
Stool Consistency		**Blood in Colon**	
Normal	0	Absent	0
Slight	1	Slight	1
Loose	2	Present	2
Diarrhoea	3		

6.5.7 Colon/Intestinal Tissue Preparation

Small intestine and colons were excised from mice and placed in a Petri dish containing cold DPBS. A pair of forceps was used to gently unravel the entire length of the small intestine and colon, and a 10 ml syringe filled with DPBS was used to empty and wash the lumen. Tissues were fixed with 10% formalin flushed inside the lumen using a syringe. Opaque tissue colouring indicated complete fixation. The edge of the proximal end was wrapped around a needle using forceps and placed into a tissue-processing/embedding cassette. The cassette was placed in 10% formalin overnight at room temperature. The next day, tissues were washed with water to remove the fixative and immersed overnight at 70% ethanol. Tissues were further processed and paraffin embedded by the Veterinary Medicine Services at Ohio State University (OSU). Tissues were shipped to Nottingham Trent University for construction of Tissue Microarray (TMA) sectioning.

6.5.8 Construction of TMAs

Tissue cores were collected and arranged in columns and rows using the Tissue - Tek Quick-Ray set (Sakura, 8010) according to manufacturers instructions. Briefly, a Quick-Ray needle was inserted into the donor paraffin block and the extracted tissue (core) was injected into the corresponding holes of the recipient block provided by UNITMA. The recipient block was placed into an embedding mould and incubated in the oven at 64^{o}C for 30 minutes. When the recipient block turned transparent, it was embedded in a new cassette and transferred on a cold plate for 1 hour to solidify. The mould was removed, and the paraffin block was cut into 5 µm-thick sections, using a microtome filled with 0.1% DEPC-treated water. Sections were collected on sterilised slides and dried at 60^{o}C for 1 hour. Slides were stored at 4^{o}C with desiccants overnight.

6.5.9 In Situ Hybridisation

For *in situ* hybridisation, the RNAscope Multiplex Fluorescent Reagent kit v2 Assay was used. TMA slides were baked for 1 hour at 60 °C in a dry oven and sections then were deparaffinized by incubating slides twice in xylene for 5 minutes each, and then twice in 100% Ethanol for 2 minutes each, at RT with agitation. On top of the deparaffinized slides, 8 drops of RNAscope hydrogen peroxide solution were added, to cover each section, for 10 minutes at RT. By tapping the slide on absorbent paper, the hydrogen peroxide was removed and immediately, was placed in a staining dish filled with sterile water and washed twice. Target retrieval was performed using a streamer. Briefly, two slide holders were placed in a steam bowl, one filled with 200 ml of distilled water and the other one with 200 ml of RNAscope 1x Target Retrieval Reagent. When temperature reached the 99 °C, the slide was placed in sterile water for 10 seconds, and immediately transferred to 1x Target Retrieval Reagent for 15 minutes. The slide was placed in a new container of distilled water for 15 seconds, transferred in 100% ethanol for 3 minutes and incubated at 60 °C for 5 minutes. Using a hydrophobic barrier pen, a barrier was drawn around the section. When the barrier dried, 5 drops of RNAscope Protease were added to cover the slide (Pretreatment Reagents- Acdbio, 322381 and 322000). The slide was then placed in the RNAscope EZ-Batch slide holder (Acdbio, 310017) in a pre-warmed HybEZ Humidity Control tray (Acdbio, 310012).

The slide was incubated in a HybEZ II Hybridization system (Acdbio, 321721) at 40 °C for 30 minutes and then the RNAscope Multiplex Fluorescent v2 Assay was performed. In brief, the slide was hybridised for 2 hours at 40 °C with a mix of probes for mLgr5 (C1) and mIws1 (C2), mRNAs, and washed with 1x Wash Buffer (Acdbio, 322809) for 2 minutes at RT. The slide was hybridised with RNAscope Multiplex FL v2 Amp1 for 30 minutes at 40 °C in the HybEZ oven and washed twice with 1x Wash Buffer for 2 minutes at RT. Hybridization with RNAscope Multiplex FL v2 Amp2

followed for 30 minutes at 40 °C in the HybEZ oven and washed twice with 1x Wash Buffer for 2 minutes at RT. The slide was hybridized for 15 minutes with the RNAscope Multiplex FL v2 Amp3 in the HybEZ oven at 40 °C and washed twice with 1x Wash Buffer. To develop the HRP-C1 signal, the slide was covered by adding 6 drops of RNAscope Multiplex FL v2 HRP-C1 (1:1500) and incubated into the HybEZ oven for 15 minutes at 40 °C, washed with 1x Wash buffer for 2 minutes at RT and 180 µl of Opal 570 (Acdbio, FP1488001KT) were added for 30 minutes at 40 °C. After two washes RNAscope Multiplex FL v2 HRP blocker was added for 15 minutes at 40 °C. The slide was washed with 1x Wash Buffer as before. For the development of HRP-C2 signal RNAscope Multiplex FL v2 HRP-C2 (1:3000) and Opal 690 (Acdbio, FP1497001KT) were used following the same procedure (RNAscope Multiplex Fluorescent detection reagents v2- Acdbio, 323110). After the last wash with 1x Wash Buffer, for staining visualisation, the GeoMx protocol was employed.

6.5.10 GeoMx

After *in situ* hybridisation, the TMA slide was placed in 10% Neutral Buffered Formalin (NBF) for 5 minutes then twice in NBF Stop Buffer (Tris Base and Glycine in DEPC-treated water) for 5 minutes each, followed by a wash with 1x PBS for 5 minutes. *In situ* hybridisation was performed overnight by adding probe mix (25 µl) and DEPC-treated water (25 µl) in 200 µl Buffer R. 200 µl of hybridisation solution was added on top, and the slide was covered by a Grace Bio-Labs HybriSlip (Millipore Sigma, GBL714022). The slide was incubated at 37 ° C in a hybridisation oven overnight.

The following day, stringent washes (4X saline-sodium citrate (SSC) and 100% Formamide) were performed to remove off-target probes. Briefly, an equal volume of 4X SSC and 100% Formamide were mixed and incubated at 37 ° C. The slide was first washed in 2x SSC for 5 minutes and then twice in the stringent wash for

25 minutes each. After the second wash, the slide was placed twice for 2 minutes in 2x SSC. The slide was covered with 200 µl Buffer W and incubated at room temperature for 30 minutes, protected from light. A morphology marker solution was prepared by mixing 20 µl nuclear stain (SYTO 13-NanoString) and 200 µl Buffer W. The solution was mixed by flicking and 200 µl was added on top of the slide for 1 hour at RT. After staining, the solution was removed and the slide was washed twice in 2x SSC buffer for 5 minutes. The hydrophobic barrier was removed carefully, and the slide was placed on GeoMx Digital Spatial Profiler (DSP) (NanoString) according to the instructions of the GeoMx DSP instrument User Manual (MAN-10152) from NanoString.

6.6 Results and Discussion

6.6.1 IWS1 regulates the maintenance and differentiation of ISC

To investigate the role of IWS1 in the biology of ISCs, we isolated epithelial cell adhesion molecule positive (EPCAM+) cells from *Iws1* ISC-specific KO (*Iws1*$^{fl/fl}$Lgr5Cre) and control mice (*Iws1*$^{fl/fl}$). RNA extracts were subjected to RT-qPCR analysis for well-defined markers of intestinal cell subpopulations. We found that LGR5, a Wnt target gene and adult stem cell marker-specific for crypt base columnar cells (CBCs) was suppressed in the epithelial cells from *Iws1*$^{fl/fl}$Lgr5Cre mice, while the expression levels of Atonal homologue 1 gene (Atoh1, also called Math1), Neurogenin 3 (Ngn3) and chromogranin A (ChgA) were comparable between epithelial cells of *Iws1*$^{fl/fl}$ and *Iws1*$^{fl/fl}$Lgr5Cre mice. Absorptive enterocyte markers, Hes1 and Ese1, were upregulated in the epithelial cells from *Iws1*$^{fl/fl}$Lgr5Cre mice compared to *Iws1*$^{fl/fl}$. On the other hand, GFI1 was downregulated in the epithelial cells of *Iws1*$^{fl/fl}$Lgr5Cre mice **(Figure 6.9).** Overall, these results suggest that *Iws1* may regulate the maintenance and/or differentiation of ISCs.

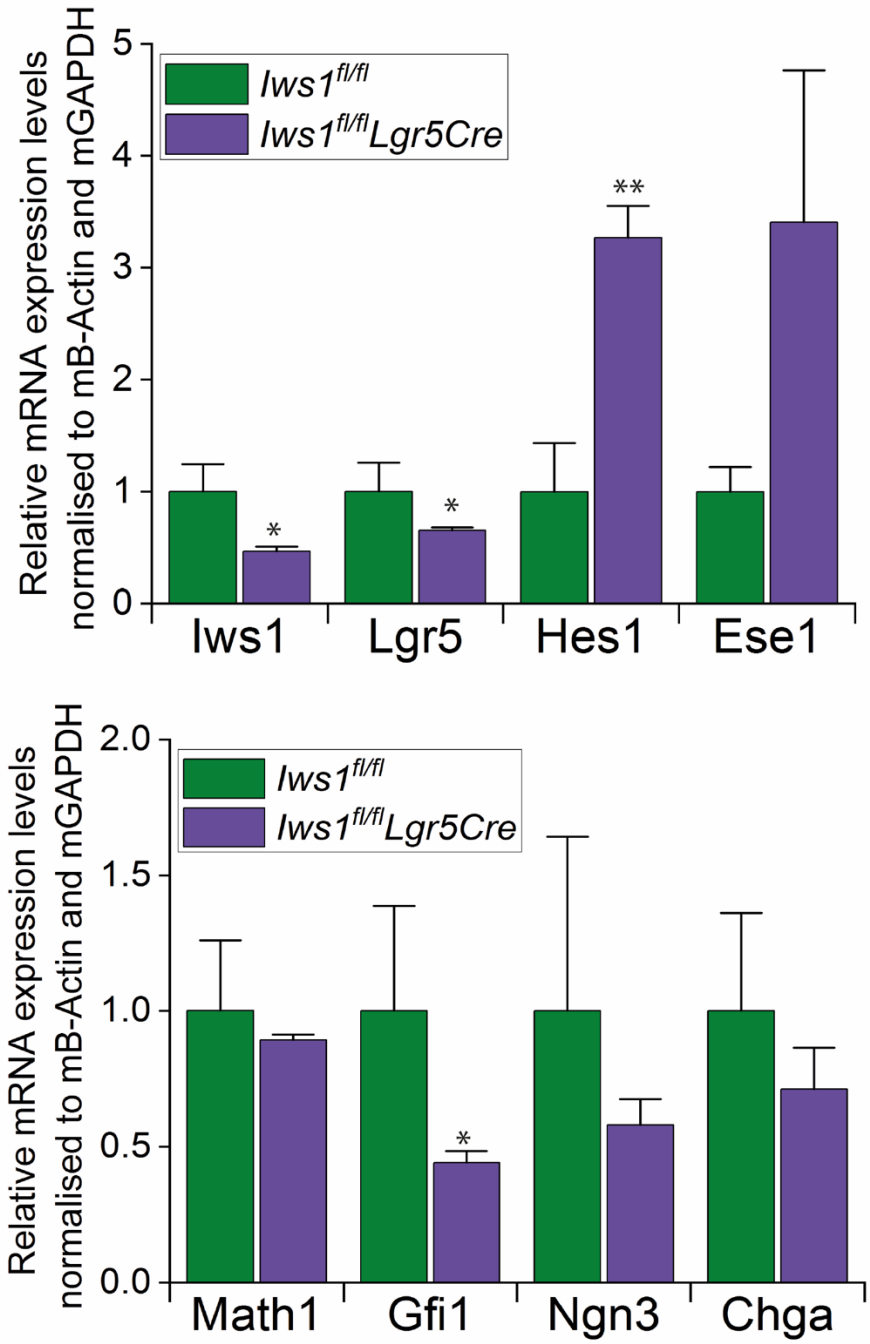

Figure 6. 9: Effect of Iws1 expression on the levels of intestinal cell sub-population markers. RNA extracts from ISC IWS1 KO (*Iws1*$^{fl/fl}$*Lgr5Cre*) and WT mice (*Iws1*$^{fl/fl}$) epithelial (EPCAM+) cells from were subjected RT-qPCR analysis performed in quadruplicates. Gene expression analysis was performed using CFX Software by normalised expression (ΔΔCq) against mouse B-Actin and mouse GAPDH, and for WT mice-derived cells, the expression level was set as 1. Results are presented as mean ± SEM (N=3 animals/group). Statistically significant differences were determined by Student's t-test, *P<0.05, **P<0.01,.

We questioned whether the same pattern of gene expression is observed in the human intestinal epithelial cells. Therefore, we used NCM460 cells transduced with shControl and shIWS1. RT-qPCR analysis for the human intestinal cell subpopulation markers revealed that IWS1 knockdown, results in the suppression of LGR5/GFI1 and the increased expression of HES1/ESE1 **(Figure 6.10).** The same pattern of gene expression observed in mouse primary and human colonic epithelial cells (NCM460), indicated that the regulation of ISC maintenance and/or differentiation is a conserved mechanism.

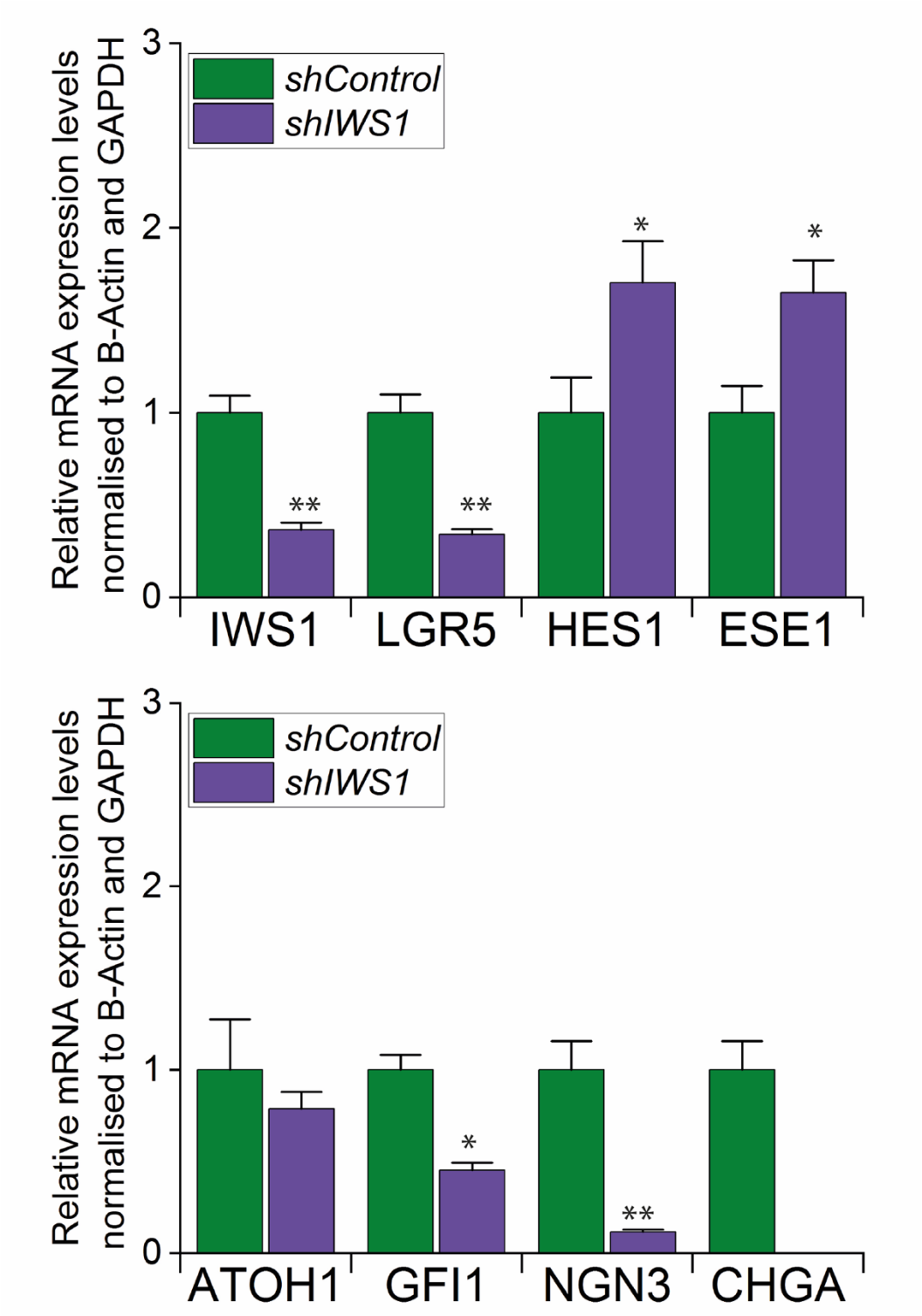

Figure 6. 10: Effect of IWS1 expression on the levels of intestinal cell sub-population markers. RNA extracts from NCM460 cells transduced to inhibit IWS1 (shIWS1) and Control (shControl) cells were subjected RT-qPCR analysis performed in quadruplicates. Gene expression analysis was performed using CFX Software by normalised expression (ΔΔCq) against B-Actin and GAPDH, and for WT mice-derived cells, the expression level was set as 1. Results are presented as mean ± SEM. Asterisks denote statistically significant differences (*P<0.05, **P<0.01,).

The above results indicate that there is either suppression of Lgr5 expression or a reduced number of stem cells upon deletion of *Iws1*. On the other hand, there is increased expression of markers of absorptive enterocytes, Hes1 and Ese1. This may indicate that *Iws1* inhibition drives ISCs to differentiate into absorptive enterocytes. The expression levels of Atoh1 (Math1), Ngn3 and ChgA, which are markers of other epithelial subtypes including goblet, Paneth and enteroendocrine cells, were similar in *Iws1*$^{fl/fl}$ and *Iws1*$^{fl/fl}$Lgr5Cre mouse-derived cells. Math1-expressing cells are committed to the secretory lineage to become goblet, Paneth or enteroendocrine cells (Yang *et al.*, 2001). Gfi1 functions downstream of Math1 and with Ngn3 are required for the terminal differentiation of enteroendocrine cells (Shroyer *et al.*, 2005). Combined, the data from mouse and human cells, propose a positive role of IWS1 in ISC maintenance or expansion and a negative role in ISC differentiation into absorptive enterocytes.

6.6.2 Phosphorylated IWS1 regulates the ISC-like population

To evaluate the effects of phosphorylated IWS1 in intestinal stem cell-like properties, we transduced shIWS1 NCM460 cells, reconstituted with Ser720/Thr721-IWS1 or Ala720/Ala721-IWS1 with the STAR reporter. After a few passages, cells were examined under microscopy **(Figure 6.11)**. This analysis verified the presence of as distinct ISC-like sub-population with NCM460 cells. Furthermore, we have observed significant increase in cells expressing red fluorescence, indicating the increased number of ISCs-like sub-population in Ser720/Thr721-IWS1-expressing cells. This led us to the hypothesis that IWS1 and its phosphorylation by AKT has important effects on the ISC maintenance or differentiation.

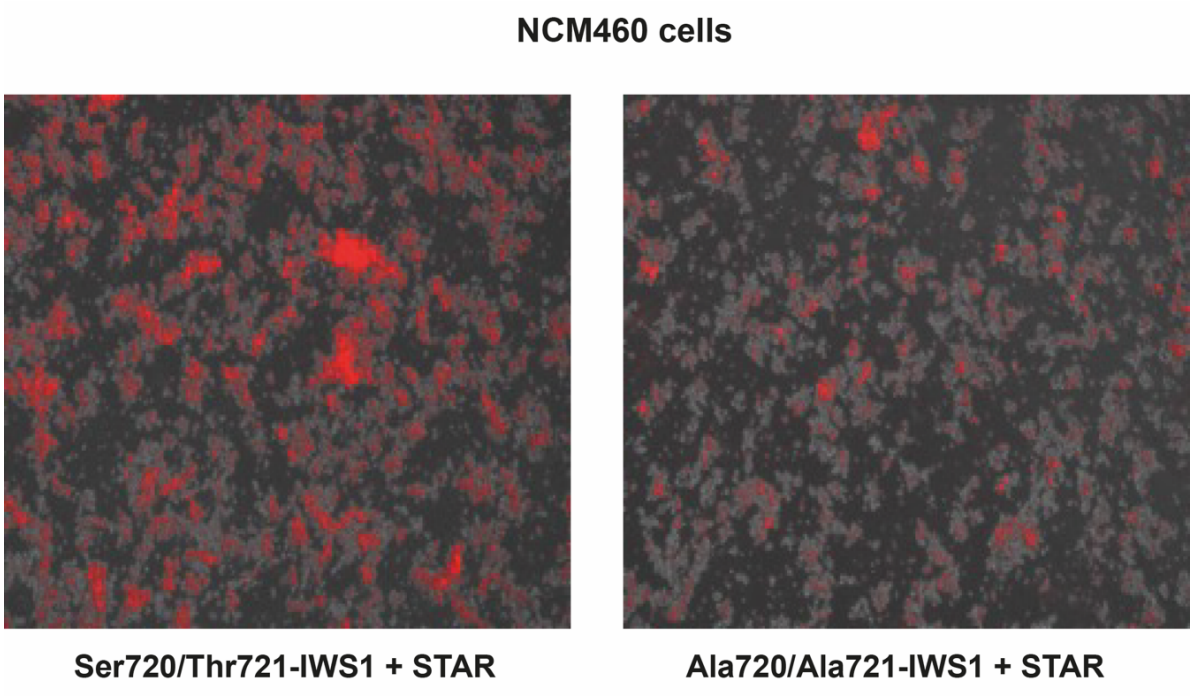

Figure 6. 11: Analysis of ISC-like properties in IWS1-expressing cells. Red fluorescence indicates ASCL2 activity in Ser720/Thr721-IWS1 and Ala720/Ala721-IWS1-expressing NCM460 cells. Representative images + STAR, acquired at 100x magnification using an EVOS microscope.

6.6.3 *Iws1*$^{fl/fl}$*Lgr5Cre* mice are more sensitive to DSS-induced inflammation

It is important to highlight that *Iws1* deletion in mice results in perinatal death (Orlacchio *et al.*, 2018). Therefore, here we used the inducible Lgr5Cre model, where tamoxifen is used to induce the expression of Cre, resulting in the knockout of the *Iws1* gene. However, the knockout occurs in only a percentage of the crypts and produces a mosaic genotype, with gene knockout in some ISCs, while others remain unaffected. This is represented in the partial inhibition of *Iws1* expression **(Figure 6.9)** in the *Iws1*$^{fl/fl}$Lgr5Cre mice. We propose that spatial transcriptomic or proteomic tissue analysis would allow the identification of KO crypts and the comparison with the WT crypts *in vivo*.

Intestinal stem cells play the central role in renewing the intestinal epithelial layer and its recovery from mechanic, chemical, and microbial assaults (Liu and Chen, 2020). In order to evaluate the role of *Iws1* in the stem cell-regenerative properties

of the intestinal epithelium, wild-type and ISC-specific *lws1* KO mice were subjected to treatment with 5% DSS in drinking water, to induce intestinal inflammation.

DSS is toxic to the epithelial lining of the colon and results in compromised mucosal barrier function and colitis with bloody diarrhoea (Okayasu *et al.*, 1990). DSS changes the histological structure of cells, due to mucin and goblet cell depletion, leading to epithelial erosion and ulceration (Chassaing *et al.*, 2014). The exact mechanism of DSS action remains unclear. It has been shown that it forms nano-lipocomplexes with medium chain-length fatty acids in the colon, which induces colitis (Laroui *et al.*, 2012) **(Figure 6.12).**

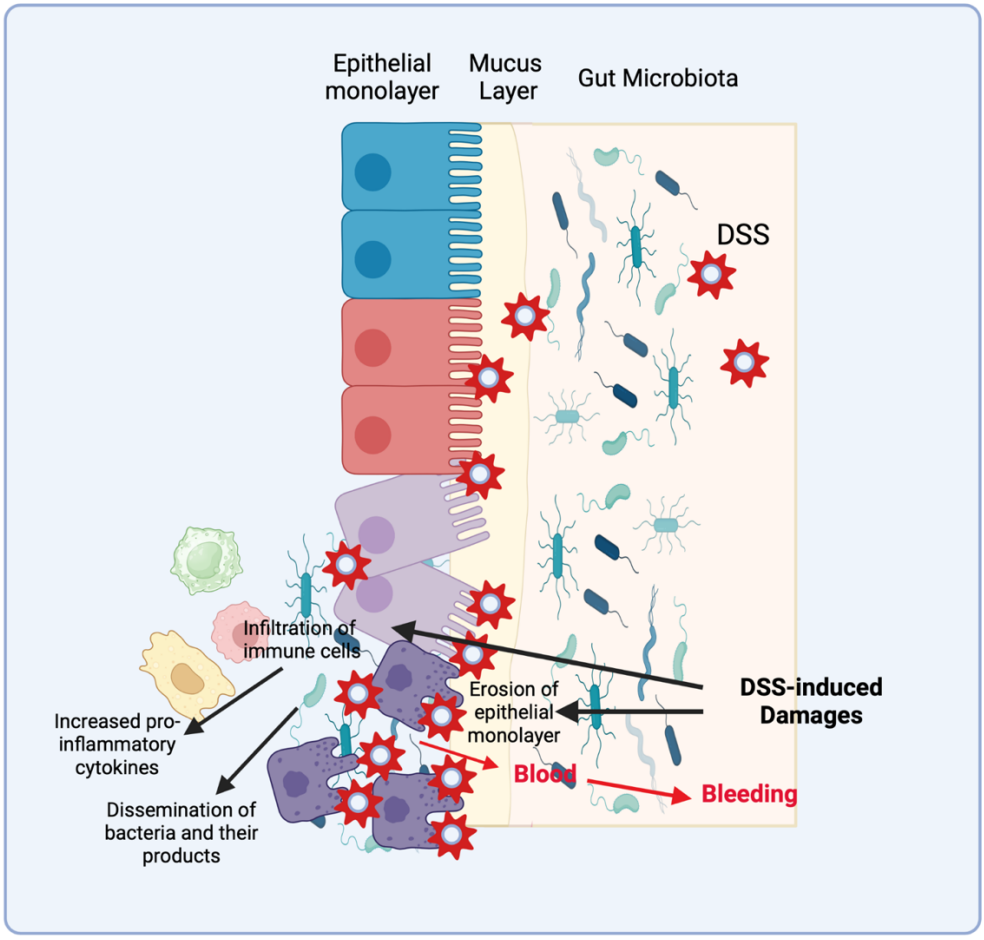

Figure 6. 12: Schematic representation of DSS-induced inflammation. DSS administration leads to a highly negative charge, contributed by sulphate groups, which causes erosion of the colonic epithelium and compromises the barrier integrity. Figure modified using BioRender (www.biorender.com).

To evaluate the effects of DSS, a well-defined set of clinical signs was monitored: the presence of blood in stools and in the colon, stool consistency and weight loss **(Table xxxvi).** Clinical signs were recorded from the first day of treatment. *Iws1*$^{fl/fl}$Lgr5Cre mice treated with DSS presented rectal bleeding and weight loss within 3 days of DSS administration, whereas the *Iws1*$^{fl/fl}$ mice presented similar signs one day later (4th day). Both groups presented diarrhoea symptoms on the 5th day of DSS. The Hemoccult test showed a weak positive result within the 3rd day of DSS administration in most of the mice. A strong positive Hemoccult test was observed on the first day after the transfer of animals to regular water **(Figure 6.8).** The inflammatory disease activity was calculated based on the sum of the scores of all clinical signs **(Figure 6.13).**

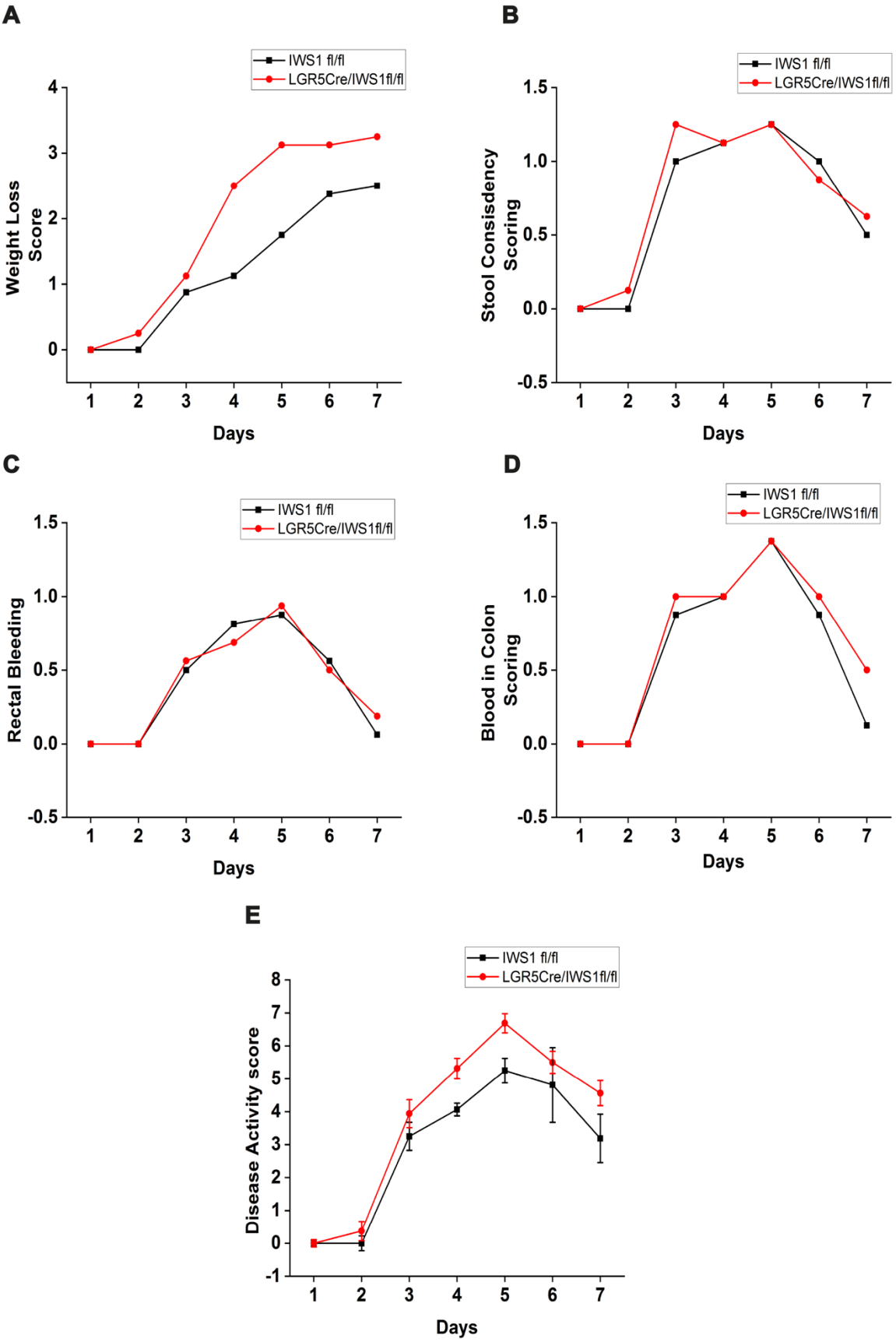

Figure 6. 13: Disease scores for lws1$^{fl/fl}$ and lws1$^{fl/fl}$Lgr5Cre mice treated with 5% DSS according to *Table xxxvi*. (A) Weight loss. **(B)** Stool consistency. **(C)** Rectal Bleeding **(D)** Blood in Colon and **(E)** Overall disease scores, calculated based on criteria in ***Table xxxvi***.

Our findings summarised in **Figure 6.13-E**, propose that Iws1 expression in ISC has a protective role in the intestinal epithelium (days 1-5) and potentially a regenerative role (days 6-7) after chemical assault. This is more important, if we consider that the deletion of Iws1 in the ISCs is partial. We hypothesise that loss of Iws1 in some crypts is enough to sensitive the barrier to chemical (DSS) assault through a localised effect on barrier function or the reduced barrier resealing potential which could delay wound healing. A local disruption of the epithelial barrier is a condition sufficient to induce or exacerbate the inflammatory response due to the dissemination of bacteria and their products in the sub-epithelial tissue and subsequent inflammatory cell activation **(Figure 6.12)**.

To address the above hypothesis a spatial profiling approach is required. This approach should reveal differences between Iws1 KO and WT ISCs within the same intestinal tissue of *Iws1*$^{fl/fl}$Lgr5Cre mice and/or WT animals. To this end, we employed to very novel techniques, dual fluorescence *in situ* hybridization (RNAscope) in combination with whole transcriptome digital spatial analysis (GeoMX).

First, we used RNAscope to stain for Lgr5 and Iws1 transcripts throughout the intestinal tissues. The Lgr5 probe (green) stained a subpopulation of cells at the bottom of the crypts, the ISCs, as predicted. The Iws1 probe (red) was detected throughout the intestinal tissue. As expected, Iws1 staining was significantly reduced in *Iws1*$^{fl/fl}$Lgr5Cre mice **(Figure 6.14)**. We proceeded with building two different TMAs, one using control *Iws1*$^{fl/fl}$Lgr5Cre and *Iws1*$^{fl/fl}$ derived small intestinal and colonic tissues, and a second using the tissues collected after the DSS experiment.

TMAs were stained for Lgr5 and Iws1 and subjected to GeoMX high-content transcriptomic profiling (20,000 probes targeting different transcripts). Following probe hybridisation, areas of interest (AOI) were selected to represent 1. ISCs

expressing Lgr5 (indicated by green staining) combined with high or low Iws1 (indicated by red staining) and 2. Differentiated epithelial cells (indicated by the epithelial cell lining in crypts guided by SYTO 13 nuclear staining) in a. control and b. diseased tissues. Probes were collected from these AOIs and global gene expression was assessed by next-generation sequencing.

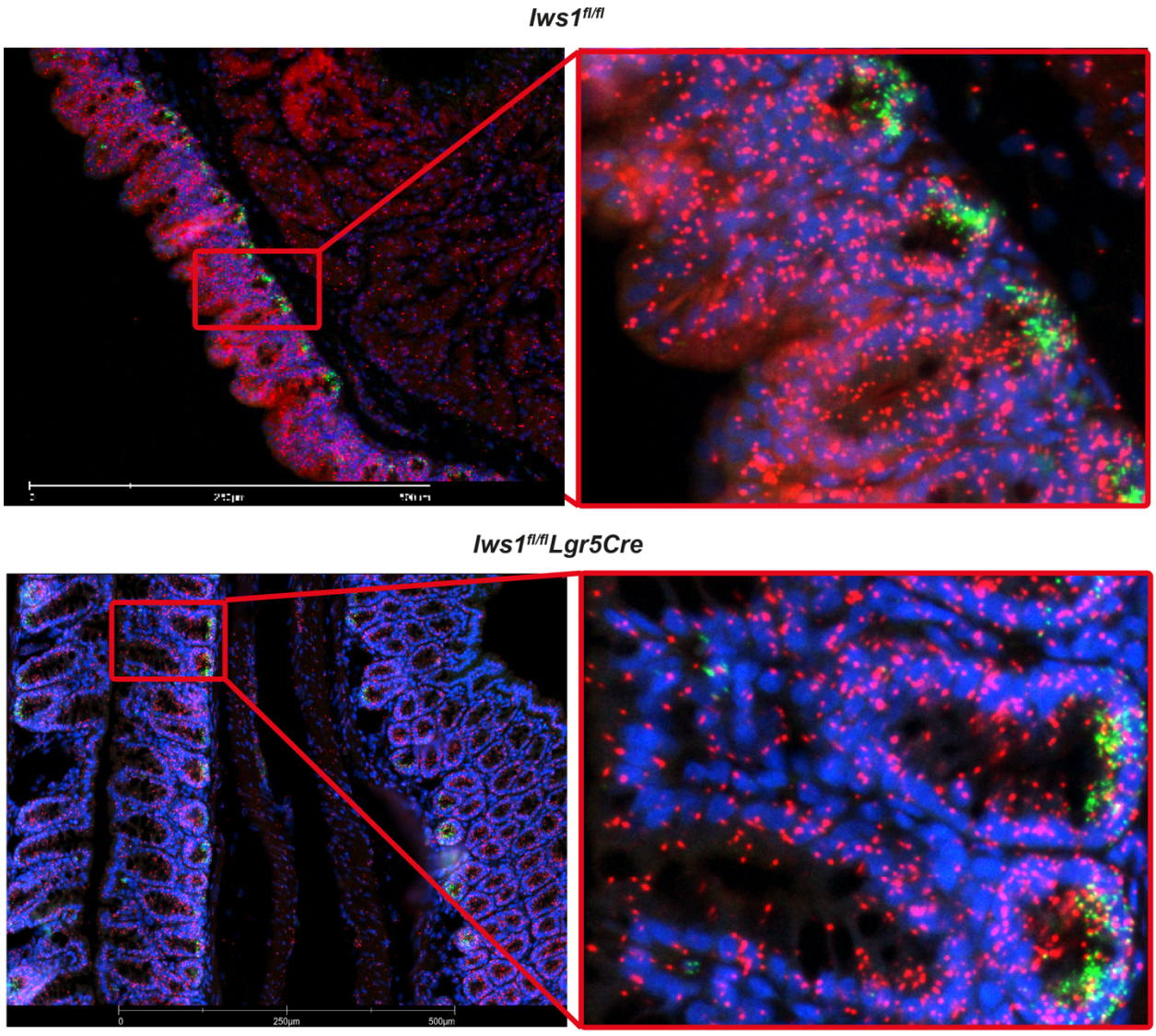

Figure 6. 14: *In situ* hybridisation for Lgr5 and Iws1 transcripts in Iws1$^{fl/fl}$ and Iws1$^{fl/fl}$Lgr5Cre mouse colonic tissues. Green indicated the Lgr5 staining (ISCs). Red indicates Iws1 staining and blue SYTO 13, the nuclei.

6.7 Conclusion of Chapter 6

Chapter 6 focuses on the role of IWS1 in intestinal biology and inflammation. Our results proposed that IWS1 may contribute to Intestinal stem cell self-renewal and the differentiation of ISCs. Here, the role of IWS1 on ISC differentiation in mice and in human cells was investigated. EPCAM+ cells were isolated from *Iws1*$^{fl/fl}$Lgr5Cre and *Iws1*$^{fl/fl}$ mice and the expression levels of different intestinal sub-population markers were assessed. We found that deletion of *Iws1* either decreases the number of stem cells or induces their differentiation into absorptive enterocytes. The same pattern was found in human colonic epithelial cells upon IWS1 knockdown. To investigate the role of IWS1 in the regeneration of the intestinal epithelium under normal conditions and intestinal inflammation *Iws1*$^{fl/fl}$Lgr5Cre and *Iws1*$^{fl/fl}$ mice were administered with DSS in drinking water. The DSS-treated mice developed colitis. Clinical sign monitoring revealed that *Iws1*$^{fl/fl}$Lgr5Cre mice developed more severe symptoms compared to *Iws1*$^{fl/fl}$ mice, especially weight loss. We concluded that IWS1-expressing ISCs play an important role in wound healing potentially through the regeneration of the intestinal epithelium. Intestinal tissues were collected from control and diseased animals and stained for Iws1 and Lgr5 by *in Situ* Hybridisation. Lgr5, a marker of ISCs, was detected at the base of the crypt, whereas *Iws1* expression was detected in the intestinal epithelium of both *Iws1*$^{fl/fl}$ and *Iws1*$^{fl/fl}$Lgr5Cre mice, presenting a mosaic/reduced staining in *Iws1*$^{fl/fl}$Lgr5Cre tissues. Spatial global transcriptomic analysis will reveal differences between *Iws1 KO* and *WT* ISCs and the changes in epithelial cell composition in health and disease.

CHAPTER 7: General Discussion

7.1 AKT phosphorylates IWS1

AKT family (AKT1, AKT2 and AKT3) is a group of serine/threonine protein kinases that regulate important cell functions by promoting cell growth, proliferation, migration, survival, tissue invasion, and angiogenesis. It has been shown that AKTs phosphorylate over 400 targets. One of them, IWS1 a protein involved in mRNA splicing and nuclear export (Krogan *et al.*, 2002), is phosphorylated by AKT1 and AKT3 at Ser720/Thr721. Phosphorylated of IWS1 promotes alternative splicing and induces cancer cell proliferation (Sanidas *et al.*, 2014). Here, we show for the first time that IWS1 is involved in microRNA regulation and controls intestinal epithelial cell biology in health and disease.

7.2 IWS1 phosphorylation by AKT regulates microRNA activity

RNA and microRNA sequencing in lung cancer cells revealed that the transcriptome of cells expressing phosphorylation deficient (Ala720/Ala721)-IWS1 is largely regulated by microRNAs. MicroRNAs regulate many physiological and pathological processes by binding in the 3'UTR of target mRNAs (Polytarchou *et al.*, 2015). microRNA regulation at the level of expression is well-studied, however, our knowledge about their activity regulation is limited. MicroRNA reporter assays and analysis of validated microRNA targets supported our hypothesis that the activity of microRNAs is inhibited upon IWS1 phosphorylation by AKT1.

7.3 MicroRNA function is mediated by the RNA-induced silencing complex.

Human RISC is a multiprotein complex composed of a variety of proteins including, Ago2, Dicer, TRBP, TNRC6 proteins, MOV10 and FMRP (Chendrimada *et al.*, 2005; Liu *et al.*, 2005; Rehwinkel *et al.*, 2005; Kenny *et al.*, 2014). RISC upon loading with microRNAs (miRISC) targets genes for silencing either through RNA cleavage prevention of protein synthesis, transcriptional repression or by triggering chromatin

remodelling (Pratt and MacRae, 2009). Immunoprecipitation assays in lung cancer cells suggested that upon phosphorylation, IWS1 interacts with Ago2.

7.4 Phospho-IWS1-mediated microRNA activity inhibition is a global mechanism

Pathway analysis of the differentially regulated genes in lung cancer cells expressing phosphorylation deficient (Ala720/Ala721) or the wild type IWS1, revealed that the deregulated genes are associated with colorectal cancer and intestinal diseases. This observation shifted our focus on intestinal cells as a potentially more relevant model to study the biology of IWS1.

RNAome and miRNAome analysis of two immortalised non-transformed colonic epithelial cell lines revealed that NCM460 cells have increased expression of intestinal epithelial sub-population markers and microRNAs. RT-qPCR analysis validated the increased expression levels for the majority of ISC markers in NCM460 cells.

FACS analysis of cells transduced with a reporter for ISCs revealed that NCM460 comprise a heterogeneous cell population with low, high and intermediate levels of ASCL2 activity, indicating the presence of more and less differentiated epithelial cells. Pathway analysis of the RNA sequencing data in lung cancer cells identified gene networks, downstream of IWS1 phosphorylation, linked to stem cell biology. The above data combined suggested that NCM460 could be an appropriate model to study the role of IWS1 in intestinal stem and epithelial cell biology. This was the cellular model of choice for the study of the role of IWS1 in ISC properties. Ideally, we would use primary cells, but the requirements for their isolation and maintenance cost are forbidding at least at the current, screening stage.

Additional microRNA activity reporter assays and analysis of validated microRNA targets in colonic epithelial cells confirmed that the activity of microRNAs is inhibited upon IWS1 phosphorylation and that this is not a cell type or disease-specific effect. Overexpression of microRNAs known to regulate cell growth in cells expressing phosphorylation-deficient (Ala720/Ala721) or the wild type IWS1 confirmed that the differential regulation of cellular functions by microRNAs depends on IWS1 phosphorylation. Interestingly, we found the impaired growth of cells expressing phosphorylation deficient IWS1 in comparison to the wild type counterparts. Could this be attributed to the expression of more growth-inhibitory microRNAs in this cell line? Of course, other mechanisms such as defects in splicing or transcriptional elongation could also be involved.

7.5 Phospho-IWS1 interacts with RISC

The regulation of microRNA activity and not microRNA expression proposes that IWS1 may interact with Ago proteins, affecting either Ago-RISC interactions or Ago-IWS1-RISC interactions (Gam, Babb and Weiss, 2018). Immunoprecipitation experiments in NCI-H522 and NCM460 cells revealed that IWS1 phosphorylation regulates its interaction with Ago2. Furthermore, we showed that IWS1 interacts with other RISC components, GW182, MOV10 and FMRP. To address whether IWS1 interacts directly with the specific RISC components, we performed Proximity Ligation Assay and revealed that IWS1 interacts directly with Ago2 and FMRP and the dependence of these interactions on IWS1 phosphorylation by AKT. Whereas the interaction of IWS1 with GW182 or MOV10 was not induced by IWS1 phosphorylation, suggesting the indirect interaction, potentially through Ago2 and FMRP. Using triple knockout mouse fibroblasts expressing Akt1 or Akt2 we demonstrated that Iws1-Ago2 interaction depends on Akt1 activity and that this interaction is conserved across species. Questions that arise are:

1. **Are other components, known partners of IWS1, involved in the IWS1-RISC complex?**

Several proteins including TND-containing factors such as Lens epithelium-derived growth factor splice variant of 75 kDa (LEDGF), Protein phosphatase 1, regulatory subunit 10 (PPP1R10), Elongin A (ELOA), the transcription elongation factor IIS (TFIIS) and Histidine rich protein 2 (HRP2) have been shown to interact with IWS1 to regulate transcriptional elongation (Cermakova *et al.*, 2021).

2. **Which are the domains of IWS1 and Ago2 or FMRP involved in these interactions?**

Ago2 is known to interact with GW182 via the tryptophan binding pockets of Ago protein and the Glycine-Tryptophan (GW) repeats from GW182 (Iwakawa and Tomari, 2022), while recently it has been shown that IWS1 interactions depend on TFIIs N-terminal domain (TND)-interacting motifs (TIMs) domains (Cermakova *et al.*, 2021).

3. **Does this interaction with RISC require the involvement of microRNAs?**

It is known that the stability of RISC depends on the loading of RISC with microRNAs (Kirstein *et al.*, 2023).

In summary, IWS1 regulates microRNA activity through its interaction with the RISC complex. We revealed that the cells expressing the phosphorylation deficient IWS1 have enhanced microRNA activity. Furthermore, we showed that IWS1 co-localizes and co-immunoprecipitates with RISC components and this interaction depends on IWS1 phosphorylation by AKT, leading to inhibition of microRNA activity **(Figure 7.1).**

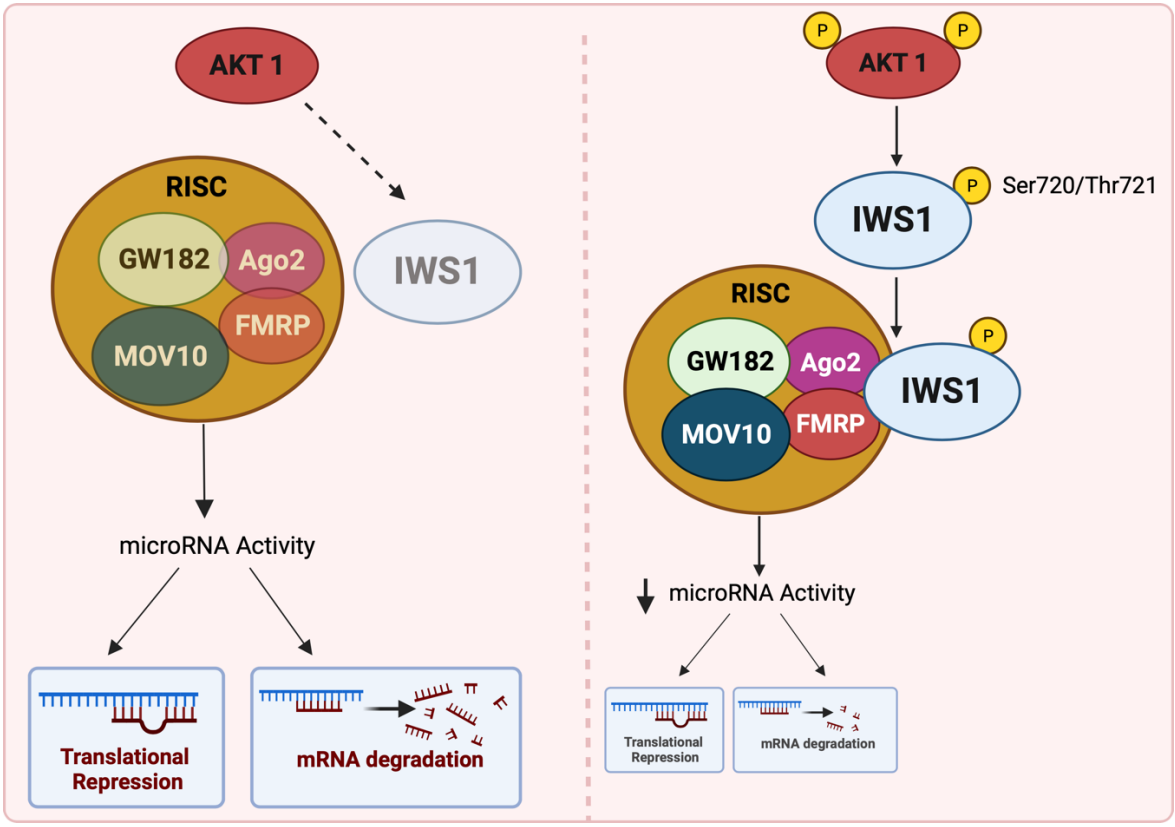

Figure 7. 1: Schematic representation of the proposed model. (Left) Inactive AKT1 cannot phosphorylate IWS1 which suppresses the interaction of IWS1 with all RISC components and enhances microRNA activity. **(Right)** Activated AKT1 phosphorylates IWS1 at Ser720/Thr721. The recruitment of IWS1 to the RISC complex is induced and microRNA activity is suppressed. Figure designed using BioRender (www.biorender.com).

7.6 IWS1 regulates ISC properties and inflammatory damage response

Our data propose that IWS1 regulates the differentiation of ISC potentially through its functions in nuclear export or transcriptional elongation or through the regulation of microRNA activity. RT-qPCR analysis performed for well-defined markers of intestinal cell subpopulations suggested that deletion of *Iws1* in mouse ISC and IWS1 in human colonocytes suppresses the expression of intestinal stem cell marker and increases the expression of markers of absorptive enterocytes. Cells transduced with a reporter for ISCs, suggested that phosphorylation of IWS1 leads to the increase of ISC-like population. We propose that IWS1 and its phosphorylated form, positively regulate intestinal stem cell maintenance and renewal or inhibit their differentiation into absorptive enterocytes **(Figure 7.2).**

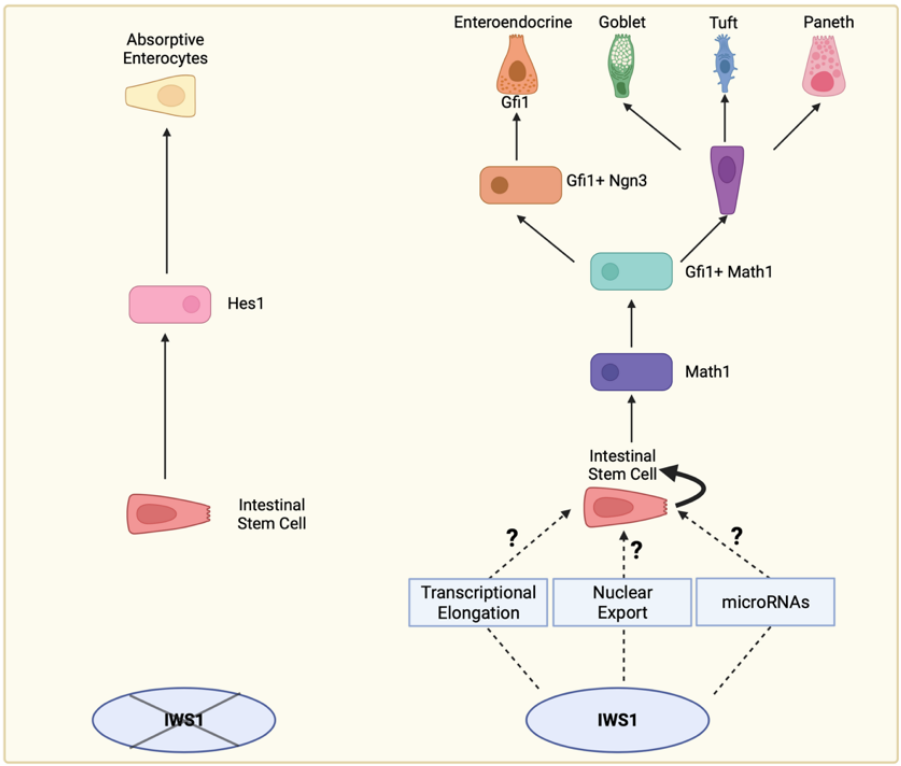

Figure 7. 2: Hypothetical model of the role of IWS1 in intestinal stem cell maintenance and differentiation. (Left) Loss of Iws1 affects intestinal stem cell maintenance and directs their differentiation into absorptive enterocytes. **(Right)** IWS1 promotes intestinal stem cell self-renewal and differentiation towards other epithelial lineages, by regulating transcriptional elongation, nuclear export or microRNA activity, or their combination. Figure designed using BioRender (www.biorender.com).

Intestinal stem cells play a key role in renewing the intestinal epithelial layer and its recovery from intestinal insults. To study the role of IWS1 in intestinal stem cells in health and disease, we treated wild-type and ISC-specific *Iws1* Knockout mice with 5% DSS to induce intestinal inflammation. DSS is toxic to the epithelial lining of the colon and results in compromised mucosal barrier function, epithelial erosion and colitis with bloody diarrhoea (Okayasu *et al.*, 1990). During inflammation, higher disease activity was observed in *Iws1* Knockout mice potentially due to the increased sensitivity of the barrier or defects in epithelial lining regeneration. Notably, tamoxifen was used to induce the expression of Cre, which results in the knockout of the *Iws1* gene in only a percentage of the crypts (Falke *et al.*, 2017). Although *Iws1* Knockout is limited to a few crypts, these defective crypts can lead to the disruption of barrier function that would exacerbate inflammation. We propose that during inflammation, *Iws1* regenerates effectively the epithelium, whereas upon *Iws1* loss results in defective wound healing **(Figure 7.3).**

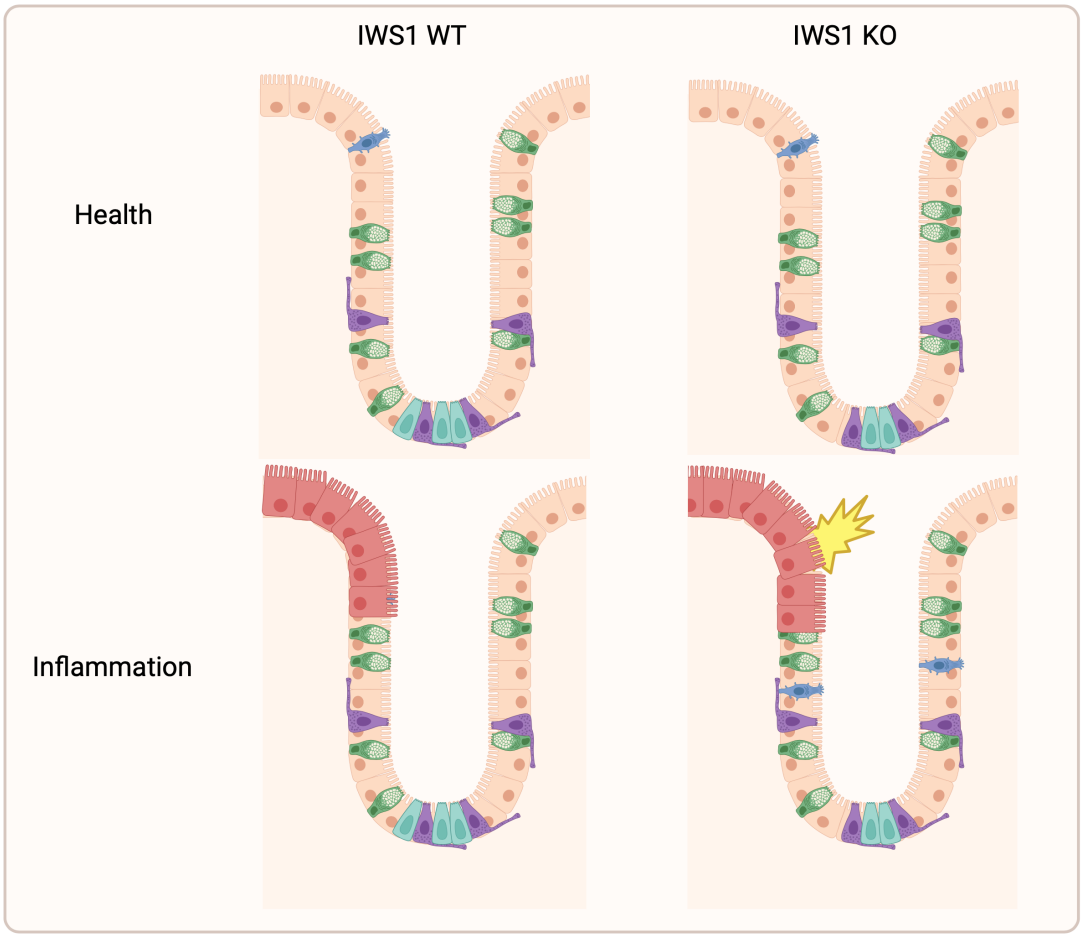

Figure 7. 3: Hypothetical model linking IWS1 in ISCs to inflammatory response. During inflammation, **(Left)** IWS1 regenerates the epithelial barrier whereas, **(Right)** IWS1 loss results in barrier recovery defects. Figure designed using BioRender (www.biorender.com).

7.7 Future Plans

Previously, we mentioned that phosphorylated-deficient IWS1 interacts less with RISC and the microRNA activity is enhanced whereas in phosphorylation IWS1 the interaction with RISC is stronger and the microRNA activity is suppressed. It is known that microRNAs are deregulated in various human cancers (Syeda *et al.*, 2020), with microRNAs generally suppressed in cancer. As the phosphorylation of IWS1 leads to suppression of microRNA activity, we hypothesise that IWS1 may have an important role in the development or progression of cancer.

Future work of our group will focus on studying the effect of IWS1 in intestinal inflammation-associated cancer. Briefly, *Iws1*$^{fl/f}$ and *Iws1*$^{fl/fl}$Lgr5Cre mice will be treated with the combination of Azoxymethane (AOM) and DSS to induce the development of colitis-associated colorectal cancer in mice. AOM is a carcinogenic agent that induces colon cancer in mice (Waly *et al.*, 2014). The effects of *Iws1* deletion in ISCs on the development of inflammation-associated cancer will be investigated by monitoring the clinical signs as previously discussed in Section 6.5.6. We will assess the tumour burden including numbers and size of tumours and histological analysis will assess the crypt structure and mucosal integrity. Nanostring Technology and Bio-Plex platform will be used for high-content transcriptomic and cytokine profiling, respectively. Molecular analyses could also be included, *in Situ* Hybridisation (RNAscope), combined with GeoMx profiling as described in Section 6.5.9.

Another interesting part that time did not permit us to investigate is the structural/molecular nature of IWS1/RISC interaction. The future plan of our group is to examine the domains responsible for the interaction between IWS1/Ago2 and IWS1/FMRP. We have generated mutants in TFIIs N-terminal domain (TND)-interacting motifs (TIMs) of IWS1. TIMs are found in prominent members of the transcription machinery (Cermakova, Veverka and Hodges, 2023). The aim is to

transduce cells with IWS1 including the mutated TIMs and to perform immunoprecipitation and Mass spectrometry for different RISC components to check if IWS1 TIM mutants interact with RISC. The same cells could be used in NanoBRET system (Promega), to understand the functions of protein-protein interaction in living cells. NanoBRET is a proximity assay that detects protein interactions by measuring energy transfer from a bioluminescent protein donor (NanoLuc fusion protein) to a fluorescent protein acceptor (HaloTag Fusion protein), and their ratios are the readout of this assay. The scalability of this assay allows its use for the screening of small molecules, which in our case could be used for the identification of IWS1-RISC interaction inhibitors.

References

1. Ackah, E. *et al.* (2005) 'Akt1/protein kinase Bα is critical for ischemic and VEGF-mediated angiogenesis', *Journal of Clinical Investigation* [Preprint]. Available at: https://doi.org/10.1172/JCI24726.
2. Ackers, I. and Malgor, R. (2018) 'Interrelationship of canonical and non-canonical Wnt signalling pathways in chronic metabolic diseases', *Diabetes and Vascular Disease Research* [Preprint]. Available at: https://doi.org/10.1177/1479164117738442.
3. Adelman, K. *et al.* (2009) 'Immediate mediators of the inflammatory response are poised for gene activation through RNA polymerase II stalling', *Proceedings of the National Academy of Sciences of the United States of America* [Preprint]. Available at: https://doi.org/10.1073/pnas.0910177106.
4. Adkins, M.W. and Tyler, J.K. (2006) 'Transcriptional activators are dispensable for transcription in the absence of Spt6-mediated chromatin reassembly of promoter regions', *Molecular Cell* [Preprint]. Available at: https://doi.org/10.1016/j.molcel.2005.12.010.
5. Agarwal, N.K. *et al.* (2013) 'Transcriptional regulation of serine/threonine protein kinase (AKT) genes by glioma-associated oncogene homolog 1.', *Journal of Biological Chemistry* [Preprint]. Available at: https://doi.org/10.1074/jbc.a112.425249.
6. Akao, Y., Nakagawa, Y. and Naoe, T. (2006) 'let-7 microRNA functions as a potential growth suppressor in human colon cancer cells', *Biological and Pharmaceutical Bulletin* [Preprint]. Available at: https://doi.org/10.1248/bpb.29.903.
7. Altomare, D.A. and Testa, J.R. (2005) 'Perturbations of the AKT signaling pathway in human cancer', *Oncogene* [Preprint]. Available at: https://doi.org/10.1038/sj.onc.1209085.
8. Amaral, P.P. *et al.* (2008) 'The eukaryotic genome as an RNA machine', *Science*, pp. 1787–1789. Available at: https://doi.org/10.1126/science.1155472.
9. Amersi, F., Agustin, M. and Ko, C.Y. (2005) 'Colorectal cancer: Epidemiology, risk factors, and health services', *Clinics in Colon and Rectal Surgery* [Preprint]. Available at: https://doi.org/10.1055/s-2005-916274.
10. Androulidaki, A. *et al.* (2010) 'Akt1 controls macrophage response to LPS by regulating microRNAs', *Immunity* [Preprint].

11. Andrulis, E.D. *et al.* (2000) 'High-resolution localization of Drosophila Spt5 and Spt6 at heat shock genes in vivo: Roles in promoter proximal pausing and transcription elongation', *Genes and Development* [Preprint]. Available at: https://doi.org/10.1101/gad.844200.
12. Antara (2011) 'Wnt/Ca2+ signaling pathway: a brief overview.', *Acta biochimica et biophysica Sinica* [Preprint].
13. Arboleda, M.J. *et al.* (2003) 'Overexpression of AKT2/protein kinase Bβ leads to up-regulation of β1 integrins, increased invasion, and metastasis of human breast and ovarian cancer cells', *Cancer Research* [Preprint].
14. Ardehali, M.B. *et al.* (2009) 'Spt6 enhances the elongation rate of RNA polymerase II in vivo', *EMBO Journal* [Preprint]. Available at: https://doi.org/10.1038/emboj.2009.56.
15. Arranz, A. *et al.* (2012) 'Akt1 and Akt2 protein kinases differentially contribute to macrophage polarization', *Proceedings of the National Academy of Sciences of the United States of America* [Preprint]. Available at: https://doi.org/10.1073/pnas.1119038109.
16. Bae, S. *et al.* (2012) 'Akt is negatively regulated by the MULAN E3 ligase', *Cell Research* [Preprint]. Available at: https://doi.org/10.1038/cr.2012.38.
17. Bai, X. *et al.* (2010) 'TIF1γ Controls Erythroid Cell Fate by Regulating Transcription Elongation', *Cell* [Preprint]. Available at: https://doi.org/10.1016/j.cell.2010.05.028.
18. Banerjee, S., Neveu, P. and Kosik, K.S. (2009) 'A Coordinated Local Translational Control Point at the Synapse Involving Relief from Silencing and MOV10 Degradation', *Neuron* [Preprint]. Available at: https://doi.org/10.1016/j.neuron.2009.11.023.
19. Barker, N. *et al.* (2007) 'Identification of stem cells in small intestine and colon by marker gene Lgr5', *Nature* [Preprint]. Available at: https://doi.org/10.1038/nature06196.
20. Barker, N. *et al.* (2009) 'Crypt stem cells as the cells-of-origin of intestinal cancer', *Nature* [Preprint]. Available at: https://doi.org/10.1038/nature07602.
21. Barker, N., Van Oudenaarden, A. and Clevers, H. (2012) 'Identifying the stem cell of the intestinal crypt: Strategies and pitfalls', *Cell Stem Cell* [Preprint]. Available at: https://doi.org/10.1016/j.stem.2012.09.009.
22. Barriga, F.M. *et al.* (2017) 'Mex3a Marks a Slowly Dividing Subpopulation of Lgr5+ Intestinal Stem Cells', *Cell Stem Cell* [Preprint]. Available at: https://doi.org/10.1016/j.stem.2017.02.007.

23. Bartel, D.P. (2004) ‘MicroRNAs: Genomics, Biogenesis, Mechanism, and Function’, *Cell*, pp. 281–297. Available at: https://doi.org/10.1016/S0092-8674(04)00045-5.
24. Bartel, D.P. (2009) ‘MicroRNAs: Target Recognition and Regulatory Functions’, *Cell* [Preprint]. Available at: https://doi.org/10.1016/j.cell.2009.01.002.
25. Batlle, E. *et al.* (2002) ‘β-catenin and TCF mediate cell positioning in the intestinal epithelium by controlling the expression of EphB/EphrinB’, *Cell* [Preprint]. Available at: https://doi.org/10.1016/S0092-8674(02)01015-2.
26. Beck, F. *et al.* (1999) ‘Reprogramming of intestinal differentiation and intercalary regeneration in Cdx2 mutant mice’, *Proceedings of the National Academy of Sciences of the United States of America* [Preprint]. Available at: https://doi.org/10.1073/pnas.96.13.7318.
27. Begg, D.P. and Woods, S.C. (2013) ‘The endocrinology of food intake’, *Nature Reviews Endocrinology* [Preprint]. Available at: https://doi.org/10.1038/nrendo.2013.136.
28. Le Berre, C. *et al.* (2020) ‘Ulcerative Colitis and Crohn’s Disease Have Similar Burden and Goals for Treatment’, *Clinical Gastroenterology and Hepatology* [Preprint]. Available at: https://doi.org/10.1016/j.cgh.2019.07.005.
29. Bertrand-Lehouillier, V., Legault, L.M. and McGraw, S. (2018) ‘Endocrine epigenetics, epigenetic profiling and biomarker identification’, in *Encyclopedia of Endocrine Diseases*, pp. 31–35. Available at: https://doi.org/10.1016/B978-0-12-801238-3.65830-0.
30. Bienz, M. and Clevers, H. (2000) ‘Linking colorectal cancer to Wnt signaling’, *Cell* [Preprint]. Available at: https://doi.org/10.1016/S0092-8674(00)00122-7.
31. Bird, A. (2002) ‘DNA methylation patterns and epigenetic memory’, *Genes and Development*, pp. 6–21. Available at: https://doi.org/10.1101/gad.947102.
32. Bird, A.P. (1986) ‘CpG-Rich islands and the function of DNA methylation’, *Nature* [Preprint]. Available at: https://doi.org/10.1038/321209a0.
33. Bohmert, K. *et al.* (1998) ‘AGO1 defines a novel locus of Arabidopsis controlling leaf development’, *EMBO Journal* [Preprint]. Available at: https://doi.org/10.1093/emboj/17.1.170.

34. Bortvin, A. and Winston, F. (1996) 'Evidence that Spt6p controls chromatin structure by a direct interaction with histones', *Science* [Preprint]. Available at: https://doi.org/10.1126/science.272.5267.1473.
35. Boufraqech, M. *et al.* (2014) 'MiR-145 suppresses thyroid cancer growth and metastasis and targets AKT3', *Endocrine-Related Cancer* [Preprint]. Available at: https://doi.org/10.1530/ERC-14-0077.
36. Braun, J.E. *et al.* (2011) 'GW182 proteins directly recruit cytoplasmic deadenylase complexes to miRNA targets', *Molecular Cell* [Preprint]. Available at: https://doi.org/10.1016/j.molcel.2011.09.007.
37. Breault, D.T. *et al.* (2008) 'Generation of mTert-GFP mice as a model to identify and study tissue progenitor cells', *Proceedings of the National Academy of Sciences of the United States of America* [Preprint]. Available at: https://doi.org/10.1073/pnas.0804800105.
38. Brodbeck, D., Cron, P. and Hemmings, B.A. (1999) 'A human protein kinase Bγ with regulatory phosphorylation sites in the activation loop and in the C-terminal hydrophobic domain', *Journal of Biological Chemistry* [Preprint]. Available at: https://doi.org/10.1074/jbc.274.14.9133.
39. Brognard, J. *et al.* (2007) 'PHLPP and a Second Isoform, PHLPP2, Differentially Attenuate the Amplitude of Akt Signaling by Regulating Distinct Akt Isoforms', *Molecular Cell* [Preprint]. Available at: https://doi.org/10.1016/j.molcel.2007.02.017.
40. Bronevetsky, Y. *et al.* (2013) 'T cell activation induces proteasomal degradation of argonaute and rapid remodeling of the microRNA repertoire', *Journal of Experimental Medicine* [Preprint]. Available at: https://doi.org/10.1084/jem.20111717.
41. Bruss, M.D. *et al.* (2005) 'Increased phosphorylation of Akt substrate of 160 kDa (AS160) in rat skeletal muscle in response to insulin or contractile activity', *Diabetes* [Preprint]. Available at: https://doi.org/10.2337/diabetes.54.1.41.
42. Cai, J. *et al.* (2015) 'MicroRNA-542-3p suppresses tumor cell invasion via targeting AKT pathway in human astrocytoma', *Journal of Biological Chemistry* [Preprint]. Available at: https://doi.org/10.1074/jbc.M115.649004.
43. Cai, N., Wang, Y.D. and Zheng, P.S. (2013) 'The microRNA-302-367 cluster suppresses the proliferation of cervical carcinoma cells through the novel target AKT1', *RNA* [Preprint]. Available at: https://doi.org/10.1261/rna.035295.112.

44. Calin, G.A. *et al.* (2005) ‘A MicroRNA Signature Associated with Prognosis and Progression in Chronic Lymphocytic Leukemia’, *New England Journal of Medicine* [Preprint]. Available at: https://doi.org/10.1056/nejmoa050995.
45. Calin, G.A. and Croce, C.M. (2006) ‘MicroRNA signatures in human cancers’, *Nature Reviews Cancer* [Preprint]. Available at: https://doi.org/10.1038/nrc1997.
46. Carroll, J.S., Munchel, S.E. and Weis, K. (2011) ‘The DExD/H box ATpase Dhh1 functions in translational repression, mRNA decay, and processing body dynamics’, *Journal of Cell Biology* [Preprint]. Available at: https://doi.org/10.1083/jcb.201007151.
47. Castillo-Azofeifa, D. *et al.* (2019) ‘ Atoh1 + secretory progenitors possess renewal capacity independent of Lgr5 + cells during colonic regeneration ’, *The EMBO Journal* [Preprint]. Available at: https://doi.org/10.15252/embj.201899984.
48. Cermakova, K. *et al.* (2021) ‘A ubiquitous disordered protein interaction module orchestrates transcription elongation’, *Science* [Preprint]. Available at: https://doi.org/10.1126/science.abe2913.
49. Cermakova, K., Veverka, V. and Hodges, H.C. (2023) ‘The TFIIS N-terminal domain (TND): a transcription assembly module at the interface of order and disorder’, *Biochemical Society Transactions* [Preprint]. Available at: https://doi.org/10.1042/BST20220342.
50. Chan, C.H. *et al.* (2012a) ‘Erratum: The Skp2-SCF E3 ligase regulates akt ubiquitination, glycolysis, herceptin sensitivity, and tumorigenesis (Cell (2012) 149 (1098-1111))’, *Cell* [Preprint]. Available at: https://doi.org/10.1016/j.cell.2012.10.025.
51. Chan, C.H. *et al.* (2012b) ‘The Skp2-SCF E3 ligase regulates akt ubiquitination, glycolysis, herceptin sensitivity, and tumorigenesis’, *Cell* [Preprint]. Available at: https://doi.org/10.1016/j.cell.2012.02.065.
52. Chan, T.O., Rittenhouse, S.E. and Tsichlis, P.N. (1999) ‘AKT/PKB and other D3 phosphoinositide-regulated kinases: Kinase activation by phosphoinositide-dependent phosphorylation’, *Annual Review of Biochemistry* [Preprint]. Available at: https://doi.org/10.1146/annurev.biochem.68.1.965.
53. Chandradoss, S.D. *et al.* (2015) ‘A Dynamic Search Process Underlies MicroRNA Targeting’, *Cell* [Preprint]. Available at: https://doi.org/10.1016/j.cell.2015.06.032.

54. Chapman, R.S. *et al.* (2000) 'The role of Stat3 in apoptosis and mammary gland involution. Conditional deletion of Stat3.', *Advances in experimental medicine and biology* [Preprint]. Available at: https://doi.org/10.1007/0-306-46832-8_16.
55. Chassaing, B. *et al.* (2014) 'Dextran sulfate sodium (DSS)-induced colitis in mice', *Current Protocols in Immunology* [Preprint]. Available at: https://doi.org/10.1002/0471142735.im1525s104.
56. Cheloufi, S. *et al.* (2010) 'A dicer-independent miRNA biogenesis pathway that requires Ago catalysis', *Nature* [Preprint]. Available at: https://doi.org/10.1038/nature09092.
57. Chen, J. *et al.* (2005) 'Akt1 regulates pathological angiogenesis, vascular maturation and permeability in vivo', *Nature Medicine* [Preprint]. Available at: https://doi.org/10.1038/nm1307.
58. Chen, J. (2016) 'The cell-cycle arrest and apoptotic functions of p53 in tumor initiation and progression', *Cold Spring Harbor Perspectives in Medicine* [Preprint]. Available at: https://doi.org/10.1101/cshperspect.a026104.
59. Chen, M. and Manley, J.L. (2009) 'Mechanisms of alternative splicing regulation: Insights from molecular and genomics approaches', *Nature Reviews Molecular Cell Biology* [Preprint]. Available at: https://doi.org/10.1038/nrm2777.
60. Chen, M.L. *et al.* (2006) 'The deficiency of Akt1 is sufficient to suppress tumor development in Pten+/- mice', *Genes and Development* [Preprint]. Available at: https://doi.org/10.1101/gad.1395006.
61. Chen, W.S. *et al.* (2001) 'Growth retardation and increased apoptosis in mice with homozygous disruption of the akt1 gene', *Genes and Development* [Preprint]. Available at: https://doi.org/10.1101/gad.913901.
62. Chendrimada, T.P. *et al.* (2005) 'TRBP recruits the Dicer complex to Ago2 for microRNA processing and gene silencing', *Nature* [Preprint]. Available at: https://doi.org/10.1038/nature03868.
63. Cheng, G.Z. *et al.* (2007) 'Twist transcriptionally up-regulates AKT2 in breast cancer cells leading to increased migration, invasion, and resistance to paclitaxel', *Cancer Research* [Preprint]. Available at: https://doi.org/10.1158/0008-5472.CAN-06-1479.
64. Cheng, H. *et al.* (2020) 'Naringin inhibits colorectal cancer cell growth by repressing the PI3K/AKT/mTOR signaling pathway', *Experimental and*

Therapeutic Medicine [Preprint]. Available at: https://doi.org/10.3892/etm.2020.8649.

65. Cheng, H. and Leblond, C.P. (1974) 'Origin, differentiation and renewal of the four main epithelial cell types in the mouse small intestine I. Columnar cell', *American Journal of Anatomy* [Preprint]. Available at: https://doi.org/10.1002/aja.1001410403.
66. Chin, Y.R. *et al.* (2014) 'Targeting Akt3 signaling in triple-negative breast cancer', *Cancer Research* [Preprint]. Available at: https://doi.org/10.1158/0008-5472.CAN-13-2175.
67. Chin, Y.R. and Toker, A. (2010) 'The Actin-Bundling Protein Palladin Is an Akt1-Specific Substrate that Regulates Breast Cancer Cell Migration', *Molecular Cell* [Preprint]. Available at: https://doi.org/10.1016/j.molcel.2010.02.031.
68. Cho, H. *et al.* (2001) 'Insulin resistance and a diabetes mellitus-like syndrome in mice lacking the protein kinase Akt2 (PKBβ)', *Science* [Preprint]. Available at: https://doi.org/10.1126/science.292.5522.1728.
69. Chong, M.M.W. *et al.* (2008) 'The RNAseIII enzyme Drosha is critical in T cells for preventing lethal inflammatory disease', *Journal of Experimental Medicine* [Preprint]. Available at: https://doi.org/10.1084/jem.20081219.
70. Chorner, P.M. and Moorehead, R.A. (2018) 'A-674563, a putative AKT1 inhibitor that also suppresses CDK2 activity, inhibits human NSCLC cell growth more effectively than the pan-AKT inhibitor, MK-2206', *PLoS ONE* [Preprint]. Available at: https://doi.org/10.1371/journal.pone.0193344.
71. Chu, N. *et al.* (2018) 'Akt Kinase Activation Mechanisms Revealed Using Protein Semisynthesis', *Cell* [Preprint]. Available at: https://doi.org/10.1016/j.cell.2018.07.003.
72. Chung, S. *et al.* (2013) 'N-cadherin regulates mammary tumor cell migration through Akt3 suppression', *Oncogene* [Preprint]. Available at: https://doi.org/10.1038/onc.2012.65.
73. Clancy, S. and Brown, W. (2008) 'Translation : DNA to mRNA to Protein', *Nature Education* [Preprint].
74. Clevers, H. and Nusse, R. (2012) 'Wnt/β-catenin signaling and disease', *Cell* [Preprint]. Available at: https://doi.org/10.1016/j.cell.2012.05.012.
75. Colotta, F. *et al.* (2009) 'Cancer-related inflammation, the seventh hallmark of cancer: Links to genetic instability', *Carcinogenesis* [Preprint]. Available at: https://doi.org/10.1093/carcin/bgp127.

76. Coltri, P.P., dos Santos, M.G.P. and da Silva, G.H.G. (2019) 'Splicing and cancer: Challenges and opportunities', *Wiley Interdisciplinary Reviews: RNA* [Preprint]. Available at: https://doi.org/10.1002/wrna.1527.
77. Conus, N.M. *et al.* (2002) 'Direct identification of tyrosine 474 as a regulatory phosphorylation site for the Akt protein kinase', *Journal of Biological Chemistry* [Preprint]. Available at: https://doi.org/10.1074/jbc.M203387200.
78. Cooper, T.A., Wan, L. and Dreyfuss, G. (2009) 'RNA and Disease', *Cell* [Preprint]. Available at: https://doi.org/10.1016/j.cell.2009.02.011.
79. Corvinus, F.M. *et al.* (2005) 'Persistent STAT3 activation in colon cancer is associated with enhanced cell proliferation and tumor growth', *Neoplasia* [Preprint]. Available at: https://doi.org/10.1593/neo.04571.
80. Costa, F.F. (2008) 'Non-coding RNAs, epigenetics and complexity', *Gene*, pp. 9–17. Available at: https://doi.org/10.1016/j.gene.2007.12.008.
81. Cristiano, B.E. *et al.* (2006) 'A specific role for AKT3 in the genesis of ovarian cancer through modulation of G2-M phase transition', *Cancer Research* [Preprint]. Available at: https://doi.org/10.1158/0008-5472.CAN-06-1968.
82. Crosnier, C., Stamataki, D. and Lewis, J. (2006) 'Organizing cell renewal in the intestine: Stem cells, signals and combinatorial control', *Nature Reviews Genetics* [Preprint]. Available at: https://doi.org/10.1038/nrg1840.
83. Cuenda, A. and Rousseau, S. (2007) 'p38 MAP-Kinases pathway regulation, function and role in human diseases', *Biochimica et Biophysica Acta - Molecular Cell Research* [Preprint]. Available at: https://doi.org/10.1016/j.bbamcr.2007.03.010.
84. Cunha, P.P. *et al.* (2017) 'High-throughput screening uncovers miRNAs enhancing glioblastoma cell susceptibility to tyrosine kinase inhibitors', *Human Molecular Genetics* [Preprint]. Available at: https://doi.org/10.1093/hmg/ddx323.
85. Dekker, E. *et al.* (2019) 'Colorectal cancer', *The Lancet*, 394(10207), pp. 1467–1480.
86. Deng, Y.H. *et al.* (2018) 'MicroRNA-23a promotes colorectal cancer cell survival by targeting PDK4', *Experimental Cell Research* [Preprint]. Available at: https://doi.org/10.1016/j.yexcr.2018.10.010.
87. Derrien, T. *et al.* (2012) 'The GENCODE v7 catalog of human long noncoding RNAs: Analysis of their gene structure, evolution, and expression', *Genome Research*, 22(9), pp. 1775–1789. Available at: https://doi.org/10.1101/gr.132159.111.

88. Dickey, C.A. *et al.* (2008) 'Akt and CHIP coregulate tau degradation through coordinated interactions', *Proceedings of the National Academy of Sciences of the United States of America* [Preprint]. Available at: https://doi.org/10.1073/pnas.0709180105.
89. Diebold, M.L. *et al.* (2010) 'The structure of an Iws1/Spt6 complex reveals an interaction domain conserved in TFIIS, Elongin A and Med26', *EMBO Journal* [Preprint]. Available at: https://doi.org/10.1038/emboj.2010.272.
90. Dimmeler, S. *et al.* (1999) 'Activation of nitric oxide synthase in endothelial cells by Akt- dependent phosphorylation', *Nature* [Preprint]. Available at: https://doi.org/10.1038/21224.
91. Ding, L. and Han, M. (2007) 'GW182 family proteins are crucial for microRNA-mediated gene silencing', *Trends in Cell Biology* [Preprint]. Available at: https://doi.org/10.1016/j.tcb.2007.06.003.
92. Dong, Y. *et al.* (2019) 'Higher matrix stiffness as an independent initiator triggers epithelial-mesenchymal transition and facilitates HCC metastasis', *Journal of Hematology and Oncology* [Preprint]. Available at: https://doi.org/10.1186/s13045-019-0795-5.
93. Dronamraju, R. *et al.* (2018) 'Spt6 Association with RNA Polymerase II Directs mRNA Turnover During Transcription', *Molecular Cell* [Preprint]. Available at: https://doi.org/10.1016/j.molcel.2018.05.020.
94. Duan, S. *et al.* (2018) 'IMPDH2 promotes colorectal cancer progression through activation of the PI3K/AKT/mTOR and PI3K/AKT/FOXO1 signaling pathways', *Journal of Experimental and Clinical Cancer Research* [Preprint]. Available at: https://doi.org/10.1186/s13046-018-0980-3.
95. Duchaine, T.F. and Fabian, M.R. (2019) 'Mechanistic insights into microrna-mediated gene silencing', *Cold Spring Harbor Perspectives in Biology* [Preprint]. Available at: https://doi.org/10.1101/cshperspect.a032771.
96. Duina, A.A. (2011) 'Histone Chaperones Spt6 and FACT: Similarities and Differences in Modes of Action at Transcribed Genes', *Genetics Research International* [Preprint]. Available at: https://doi.org/10.4061/2011/625210.
97. Dummler, B. *et al.* (2006) 'Life with a Single Isoform of Akt: Mice Lacking Akt2 and Akt3 Are Viable but Display Impaired Glucose Homeostasis and Growth Deficiencies', *Molecular and Cellular Biology* [Preprint]. Available at: https://doi.org/10.1128/mcb.00722-06.

98. Dunham, I. *et al.* (2012) 'An integrated encyclopedia of DNA elements in the human genome', *Nature* [Preprint]. Available at: https://doi.org/10.1038/nature11247.
99. Eid, R.A. *et al.* (2015) 'Akt1 and -2 inhibition diminishes terminal differentiation and enhances central memory CD8+ T-cell proliferation and survival', *OncoImmunology* [Preprint]. Available at: https://doi.org/10.1080/2162402X.2015.1005448.
100. Elizabeth Franks, S. *et al.* (2016) 'Unique roles of Akt1 and Akt2 in IGF-IR mediated lung tumorigenesis', *Oncotarget* [Preprint]. Available at: https://doi.org/10.18632/oncotarget.6489.
101. van Es, J.H. *et al.* (2012) 'A Critical Role for the Wnt Effector Tcf4 in Adult Intestinal Homeostatic Self-Renewal', *Molecular and Cellular Biology* [Preprint]. Available at: https://doi.org/10.1128/mcb.06288-11.
102. Eulalio, A., Huntzinger, E. and Izaurralde, E. (2008) 'Getting to the Root of miRNA-Mediated Gene Silencing', *Cell* [Preprint]. Available at: https://doi.org/10.1016/j.cell.2007.12.024.
103. Eun, J.W. *et al.* (2018) 'MicroRNA-495-3p functions as a tumor suppressor by regulating multiple epigenetic modifiers in gastric carcinogenesis', *Journal of Pathology* [Preprint]. Available at: https://doi.org/10.1002/path.4994.
104. Eystathioy, T. *et al.* (2003) 'The GW182 protein colocalizes with mRNA degradation associated proteins hDcp1 and hLSm4 in cytoplasmic GW bodies', *RNA* [Preprint]. Available at: https://doi.org/10.1261/rna.5810203.
105. Fabian, M.R. *et al.* (2009) 'Mammalian miRNA RISC Recruits CAF1 and PABP to Affect PABP-Dependent Deadenylation', *Molecular Cell* [Preprint]. Available at: https://doi.org/10.1016/j.molcel.2009.08.004.
106. Fabian, M.R. *et al.* (2011) 'MiRNA-mediated deadenylation is orchestrated by GW182 through two conserved motifs that interact with CCR4-NOT', *Nature Structural and Molecular Biology* [Preprint]. Available at: https://doi.org/10.1038/nsmb.2149.
107. Facchinetti, V. *et al.* (2008) 'The mammalian target of rapamycin complex 2 controls folding and stability of Akt and protein kinase C', *EMBO Journal* [Preprint]. Available at: https://doi.org/10.1038/emboj.2008.120.
108. Falke, L.L. *et al.* (2017) 'Tamoxifen for induction of Cre-recombination may confound fibrosis studies in female mice', *Journal of Cell*

Communication and Signaling [Preprint]. Available at: https://doi.org/10.1007/s12079-017-0390-x.

109. Fan, C.D. *et al.* (2013) 'Ubiquitin-dependent regulation of phospho-AKT Dynamics by the ubiquitin E3 LIGASE, NEDD4-1, in the insulin-like growth factor-1 response', *Journal of Biological Chemistry* [Preprint]. Available at: https://doi.org/10.1074/jbc.M112.416339.

110. Fang, J.Y. and Richardson, B.C. (2005) 'The MAPK signalling pathways and colorectal cancer', *Lancet Oncology* [Preprint]. Available at: https://doi.org/10.1016/S1470-2045(05)70168-6.

111. Fearon R. Eric and Bert, V. (1990) 'A Genetic Model for Colorectal Tumorigenesis', *Cell* [Preprint].

112. Feinbaum, R., Ambros, V. and Lee, R. (2004) 'The C. elegans Heterochronic Gene lin-4 Encodes Small RNAs with Antisense Complementarity to lin-14', *Cell* [Preprint].

113. Feinberg, A.P. and Tycko, B. (2004) 'The history of cancer epigenetics', *Nature Reviews Cancer* [Preprint]. Available at: https://doi.org/10.1038/nrc1279.

114. Fischbeck, J.A., Kraemer, S.M. and Stargell, L.A. (2002) 'SPN1, a conserved gene identified by suppression of a postrecruitment-defective yeast TATA-binding protein mutant', *Genetics* [Preprint]. Available at: https://doi.org/10.1093/genetics/162.4.1605.

115. van der Flier, L.G. *et al.* (2009) 'OLFM4 Is a Robust Marker for Stem Cells in Human Intestine and Marks a Subset of Colorectal Cancer Cells', *Gastroenterology* [Preprint]. Available at: https://doi.org/10.1053/j.gastro.2009.05.035.

116. Van Der Flier, L.G. and Clevers, H. (2009) 'Stem cells, self-renewal, and differentiation in the intestinal epithelium', *Annual Review of Physiology* [Preprint]. Available at: https://doi.org/10.1146/annurev.physiol.010908.163145.

117. Flores, B.M., O'Connor, A. and Moss, A.C. (2017) 'Impact of mucosal inflammation on risk of colorectal neoplasia in patients with ulcerative colitis: a systematic review and meta-analysis', *Gastrointestinal Endoscopy* [Preprint]. Available at: https://doi.org/10.1016/j.gie.2017.07.028.

118. Foley, N.H. *et al.* (2010) 'MicroRNA-184 inhibits neuroblastoma cell survival through targeting the serine/threonine kinase AKT2', *Molecular Cancer* [Preprint]. Available at: https://doi.org/10.1186/1476-4598-9-83.

119. Formeister, E.J. *et al.* (2009) 'Distinct SOX9 levels differentially mark stem/progenitor populations and enteroendocrine cells of the small intestine epithelium', *American Journal of Physiology - Gastrointestinal and Liver Physiology* [Preprint]. Available at: https://doi.org/10.1152/ajpgi.00004.2009.
120. Fre, S. *et al.* (2009) 'Notch and Wnt signals cooperatively control cell proliferation and tumorigenesis in the intestine', *Proceedings of the National Academy of Sciences of the United States of America* [Preprint]. Available at: https://doi.org/10.1073/pnas.0900427106.
121. Fruman, D.A. *et al.* (2017) 'The PI3K Pathway in Human Disease', *Cell* [Preprint]. Available at: https://doi.org/10.1016/j.cell.2017.07.029.
122. Galbraith, L.C.A. *et al.* (2021) 'PPAR-gamma induced AKT3 expression increases levels of mitochondrial biogenesis driving prostate cancer', *Oncogene* [Preprint]. Available at: https://doi.org/10.1038/s41388-021-01707-7.
123. Gam, J.J., Babb, J. and Weiss, R. (2018) 'A mixed antagonistic/synergistic miRNA repression model enables accurate predictions of multi-input miRNA sensor activity', *Nature Communications* [Preprint]. Available at: https://doi.org/10.1038/s41467-018-04575-0.
124. Gandy, J.C., Rountree, A.E. and Bijur, G.N. (2006) 'Akt1 is dynamically modified with O-GlcNAc following treatments with PUGNAc and insulin-like growth factor-1', *FEBS Letters* [Preprint]. Available at: https://doi.org/10.1016/j.febslet.2006.04.051.
125. Gao, F. *et al.* (2018) 'Endothelial Akt1 loss promotes prostate cancer metastasis via β-catenin-regulated tight-junction protein turnover', *British Journal of Cancer* [Preprint]. Available at: https://doi.org/10.1038/s41416-018-0110-1.
126. Gao, T., Furnari, F. and Newton, A.C. (2005) 'PHLPP: A phosphatase that directly dephosphorylates Akt, promotes apoptosis, and suppresses tumor growth', *Molecular Cell* [Preprint]. Available at: https://doi.org/10.1016/j.molcel.2005.03.008.
127. Gargalionis, A.N., Papavassiliou, K.A. and Papavassiliou, A.G. (2021) 'Targeting STAT3 signaling pathway in colorectal cancer', *Biomedicines* [Preprint]. Available at: https://doi.org/10.3390/biomedicines9081016.
128. Garofalo, R.S. *et al.* (2003) 'Severe diabetes, age-dependent loss of adipose tissue, and mild growth deficiency in mice lacking Akt2/PKBβ',

Journal of Clinical Investigation [Preprint]. Available at: https://doi.org/10.1172/jci200316885.

129. Gassler, N. (2017) 'Paneth cells in intestinal physiology and pathophysiology', *World Journal of Gastrointestinal Pathophysiology* [Preprint]. Available at: https://doi.org/10.4291/wjgp.v8.i4.150.

130. George, S. *et al.* (2004) 'A family with severe insulin resistance and diabetes due to a mutation in AKT2', *Science* [Preprint]. Available at: https://doi.org/10.1126/science.1096706.

131. Gerbe, F. *et al.* (2009) 'DCAMKL-1 Expression Identifies Tuft Cells Rather Than Stem Cells in the Adult Mouse Intestinal Epithelium', *Gastroenterology* [Preprint]. Available at: https://doi.org/10.1053/j.gastro.2009.06.072.

132. Gersemann, M., Stange, E.F. and Wehkamp, J. (2011) 'From intestinal stem cells to inflammatory bowel diseases', *World Journal of Gastroenterology* [Preprint]. Available at: https://doi.org/10.3748/wjg.v17.i27.3198.

133. Giannakis, M. *et al.* (2006) 'Molecular properties of adult mouse gastric and intestinal epithelial progenitors in their niches', *Journal of Biological Chemistry* [Preprint]. Available at: https://doi.org/10.1074/jbc.M512118200.

134. Girardi, C. *et al.* (2014) 'Differential phosphorylation of Akt1 and Akt2 by protein kinase CK2 may account for isoform specific functions', *Biochimica et Biophysica Acta - Molecular Cell Research* [Preprint]. Available at: https://doi.org/10.1016/j.bbamcr.2014.04.020.

135. Gonzalez, E. and McGraw, T.E. (2009a) 'Insulin-modulated Akt subcellular localization determines Akt isoform-specific signaling', *Proceedings of the National Academy of Sciences of the United States of America* [Preprint]. Available at: https://doi.org/10.1073/pnas.0901933106.

136. Gonzalez, E. and McGraw, T.E. (2009b) 'The Akt kinases: Isoform specificity in metabolism and cancer', *Cell Cycle* [Preprint]. Available at: https://doi.org/10.4161/cc.8.16.9335.

137. Gopalakrishnan, N. *et al.* (2014) 'Colocalization of β-catenin with Notch intracellular domain in colon cancer: A possible role of Notch1 signaling in activation of CyclinD1-mediated cell proliferation', *Molecular and Cellular Biochemistry* [Preprint]. Available at: https://doi.org/10.1007/s11010-014-2163-7.

138. Gordon, M.D. and Nusse, R. (2006) 'Wnt signaling: Multiple pathways, multiple receptors, and multiple transcription factors', *Journal of Biological Chemistry* [Preprint]. Available at: https://doi.org/10.1074/jbc.R600015200.

139. Goto, N. *et al.* (2017) 'Distinct roles of HES1 in normal stem cells and tumor stem-like cells of the intestine', *Cancer Research* [Preprint]. Available at: https://doi.org/10.1158/0008-5472.CAN-16-3192.

140. Graves, P. and Zeng, Y. (2012) 'Biogenesis of Mammalian MicroRNAs: A Global View', *Genomics, Proteomics and Bioinformatics*, 10(5), pp. 239–245. Available at: https://doi.org/10.1016/j.gpb.2012.06.004.

141. Gregorieff, A. *et al.* (2005) 'Expression pattern of Wnt signaling components in the adult intestine', *Gastroenterology* [Preprint]. Available at: https://doi.org/10.1016/j.gastro.2005.06.007.

142. Gribble, F.M. and Reimann, F. (2016) 'Enteroendocrine Cells: Chemosensors in the Intestinal Epithelium', *Annual Review of Physiology* [Preprint]. Available at: https://doi.org/10.1146/annurev-physiol-021115-105439.

143. Griffiths-Jones, S. *et al.* (2006) 'miRBase: microRNA sequences, targets and gene nomenclature.', *Nucleic acids research* [Preprint]. Available at: https://doi.org/10.1093/nar/gkj112.

144. Griffiths-Jones, S. *et al.* (2008) 'miRBase: Tools for microRNA genomics', *Nucleic Acids Research*, 36(SUPPL. 1). Available at: https://doi.org/10.1093/nar/gkm952.

145. Grimson, A. *et al.* (2007) 'MicroRNA Targeting Specificity in Mammals: Determinants beyond Seed Pairing', *Molecular Cell* [Preprint]. Available at: https://doi.org/10.1016/j.molcel.2007.06.017.

146. Grivennikov, S. *et al.* (2009) 'IL-6 and Stat3 Are Required for Survival of Intestinal Epithelial Cells and Development of Colitis-Associated Cancer', *Cancer Cell* [Preprint]. Available at: https://doi.org/10.1016/j.ccr.2009.01.001.

147. Guo, H. *et al.* (2010) 'Mammalian microRNAs predominantly act to decrease target mRNA levels', *Nature* [Preprint]. Available at: https://doi.org/10.1038/nature09267.

148. Guo, H. *et al.* (2014) 'Coordinate phosphorylation of multiple residues on single AKT1 and AKT2 molecules', *Oncogene* [Preprint]. Available at: https://doi.org/10.1038/onc.2013.301.

149. Guo, J. *et al.* (2016) ‘pVHL suppresses kinase activity of Akt in a proline-hydroxylation-dependent manner’, *Science* [Preprint]. Available at: https://doi.org/10.1126/science.aad5755.

150. Haigis, K.M. *et al.* (2008) ‘Differential effects of oncogenic K-Ras and N-Ras on proliferation, differentiation and tumor progression in the colon’, *Nature Genetics* [Preprint]. Available at: https://doi.org/10.1038/ng.115.

151. Hatziapostolou, M., Polytarchou, C. and Iliopoulos, D. (2013) ‘MiRNAs link metabolic reprogramming to oncogenesis’, *Trends in Endocrinology and Metabolism* [Preprint]. Available at: https://doi.org/10.1016/j.tem.2013.03.002.

152. Hauptmann, J. *et al.* (2015) ‘Biochemical isolation of Argonaute protein complexes by Ago-APP’, *Proceedings of the National Academy of Sciences of the United States of America* [Preprint]. Available at: https://doi.org/10.1073/pnas.1506116112.

153. Hayden, M.S. and Ghosh, S. (2008) ‘Shared principles in {NF}-{kappaB} signaling.’, *Cell* [Preprint].

154. He, X.C. *et al.* (2007) ‘PTEN-deficient intestinal stem cells initiate intestinal polyposis’, *Nature Genetics* [Preprint]. Available at: https://doi.org/10.1038/ng1928.

155. Heath, J.M. *et al.* (2014) ‘Activation of AKT by O-linked N-Acetylglucosamine induces vascular calcification in diabetes mellitus’, *Circulation Research* [Preprint]. Available at: https://doi.org/10.1161/CIRCRESAHA.114.302968.

156. Hedl, M., Yan, J. and Abraham, C. (2016) ‘IRF5 and IRF5 Disease-Risk Variants Increase Glycolysis and Human M1 Macrophage Polarization by Regulating Proximal Signaling and Akt2 Activation’, *Cell Reports* [Preprint]. Available at: https://doi.org/10.1016/j.celrep.2016.07.060.

157. Heinz, M.C., Oost, K.C. and Snippert, H.J.G. (2020) ‘Introducing the Stem Cell ASCL2 Reporter STAR into Intestinal Organoids’, *STAR Protocols* [Preprint]. Available at: https://doi.org/10.1016/j.xpro.2020.100126.

158. Heneghan, A.F., Pierre, J.F. and Kudsk, K.A. (2013) ‘JAK-STAT and intestinal mucosal immunology’, *JAKSTAT*, 2(4). Available at: https://doi.org/10.4161/jkst.25530.

159. Héron-Milhavet, L. *et al.* (2006) ‘Only Akt1 Is Required for Proliferation, while Akt2 Promotes Cell Cycle Exit through p21 Binding’,

Molecular and Cellular Biology [Preprint]. Available at: https://doi.org/10.1128/mcb.00201-06.

160. Hinz, N. and Jücker, M. (2019) 'Distinct functions of AKT isoforms in breast cancer: a comprehensive review', *Cell Communication and Signaling* [Preprint]. Available at: https://doi.org/10.1186/s12964-019-0450-3.

161. Hirano, T. *et al.* (2020) 'Immunological mechanisms in inflammationassociated colon carcinogenesis', *International Journal of Molecular Sciences* [Preprint]. Available at: https://doi.org/10.3390/ijms21093062.

162. Hofacker, I.L. (2007) 'How microRNAs choose their targets', *Nature Genetics* [Preprint]. Available at: https://doi.org/10.1038/ng1007-1191.

163. Hollander, M.C. *et al.* (2011) 'Akt1 deletion prevents lung tumorigenesis by mutant K-ras', *Oncogene* [Preprint]. Available at: https://doi.org/10.1038/onc.2010.556.

164. Huang, H.Y. *et al.* (2006) 'RegRNA: An integrated web server for identifying regulatory RNA motifs and elements', *Nucleic Acids Research* [Preprint]. Available at: https://doi.org/10.1093/nar/gkl333.

165. Hugen, N. *et al.* (2015) 'The molecular background of mucinous carcinoma beyond MUC2', *Journal of Pathology: Clinical Research* [Preprint]. Available at: https://doi.org/10.1002/cjp2.1.

166. Hutchinson, J.N. *et al.* (2004) 'Activation of Akt-1 (PKB-α) Can Accelerate ErbB-2-Mediated Mammary Tumorigenesis but Suppresses Tumor Invasion', *Cancer Research* [Preprint]. Available at: https://doi.org/10.1158/0008-5472.CAN-03-3465.

167. Iacovides, D.C. *et al.* (2013) 'Identification and quantification of AKT isoforms and phosphoforms in breast cancer using a novel nanofluidic immunoassay', *Molecular and Cellular Proteomics* [Preprint]. Available at: https://doi.org/10.1074/mcp.M112.023119.

168. Ikenoue, T. *et al.* (2008) 'Essential function of TORC2 in PKC and Akt turn motif phosphorylation, maturation and signalling', *EMBO Journal* [Preprint]. Available at: https://doi.org/10.1038/emboj.2008.119.

169. Iliopoulos, D. *et al.* (2009) 'MicroRNAs Differentially Regulated by Akt Isoforms Control EMT and Stem Cell Renewal in Cancer Cells', *Science Signaling* [Preprint]. Available at: https://doi.org/10.1126/scisignal.2000356.

170. Irie, H.Y. *et al.* (2005) 'Distinct roles of Akt1 and Akt2 in regulating cell migration and epithelial-mesenchymal transition', *Journal of Cell Biology* [Preprint]. Available at: https://doi.org/10.1083/jcb.200505087.

171. Itzkovitz, S. *et al.* (2012) 'Single-molecule transcript counting of stem-cell markers in the mouse intestine', *Nature Cell Biology* [Preprint]. Available at: https://doi.org/10.1038/ncb2384.

172. Iwakawa, H. oki and Tomari, Y. (2022) 'Life of RISC: Formation, action, and degradation of RNA-induced silencing complex', *Molecular Cell* [Preprint]. Available at: https://doi.org/10.1016/j.molcel.2021.11.026.

173. Jahid, S. *et al.* (2012) 'miR-23a promotes the transition from indolent to invasive colorectal cancer', *Cancer Discovery* [Preprint]. Available at: https://doi.org/10.1158/2159-8290.CD-11-0267.

174. Jakymiw, A. *et al.* (2005) 'Disruption of GW bodies impairs mammalian RNA interference', *Nature Cell Biology* [Preprint]. Available at: https://doi.org/10.1038/ncb1334.

175. Jang, B.G. *et al.* (2020) 'SMOC2, an intestinal stem cell marker, is an independent prognostic marker associated with better survival in colorectal cancers', *Scientific Reports* [Preprint]. Available at: https://doi.org/10.1038/s41598-020-71643-1.

176. Javid, H. *et al.* (2019) 'Emerging roles of microRNAs in regulating the mTOR signaling pathway during tumorigenesis', *Journal of Cellular Biochemistry* [Preprint]. Available at: https://doi.org/10.1002/jcb.28401.

177. Jensen, J. *et al.* (2000) 'Control of endodermal endocrine development by Hes-1', *Nature Genetics* [Preprint]. Available at: https://doi.org/10.1038/71657.

178. Ji, W. *et al.* (2014) 'Liraglutide exerts antidiabetic effect via PTP1B and PI3K/Akt2 signaling pathway in skeletal muscle of KKAy mice', *International Journal of Endocrinology* [Preprint]. Available at: https://doi.org/10.1155/2014/312452.

179. Jia, J. *et al.* (2013) 'A novel function of protein kinase B as an inducer of the mismatch repair gene hPMS2 degradation', *Cell Signalling Biology*, 25(6), pp. 1498–1504.

180. Jiang, Z.Y. *et al.* (2003) 'Insulin signaling through Akt/protein kinase B analyzed by small interfering RNA-mediated gene silencing', *Proceedings of the National Academy of Sciences of the United States of America* [Preprint]. Available at: https://doi.org/10.1073/pnas.1332633100.

181. Jin, G. *et al.* (2015) 'Skp2-Mediated RagA Ubiquitination Elicits a Negative Feedback to Prevent Amino-Acid-Dependent mTORC1 Hyperactivation by Recruiting GATOR1', *Molecular Cell* [Preprint]. Available at: https://doi.org/10.1016/j.molcel.2015.05.010.

182. Jones, P.A. and Liang, G. (2009) 'Rethinking how DNA methylation patterns are maintained', *Nature Reviews Genetics*, pp. 805–811. Available at: https://doi.org/10.1038/nrg2651.

183. Joshua-Tor, L. and Hannon, G.J. (2011) 'Ancestral roles of small RNAs: An ago-centric perspective', *Cold Spring Harbor Perspectives in Biology* [Preprint]. Available at: https://doi.org/10.1101/cshperspect.a003772.

184. Juntilla, M.M. *et al.* (2007) 'Akt1 and Akt2 are required for αβ thymocyte survival and differentiation', *Proceedings of the National Academy of Sciences of the United States of America* [Preprint]. Available at: https://doi.org/10.1073/pnas.0705285104.

185. Kahvejian, A. *et al.* (2005) 'Mammalian poly(A)-binding protein is a eukaryotic translation initiation factor, which acts via multiple mechanisms', *Genes and Development* [Preprint]. Available at: https://doi.org/10.1101/gad.1262905.

186. Kalsotra, A. and Cooper, T.A. (2011) 'Functional consequences of developmentally regulated alternative splicing', *Nature Reviews Genetics* [Preprint]. Available at: https://doi.org/10.1038/nrg3052.

187. Kang, E.S. *et al.* (2008) 'O-GlcNAc modulation at Akt1 Ser473 correlates with apoptosis of murine pancreatic β cells', *Experimental Cell Research* [Preprint]. Available at: https://doi.org/10.1016/j.yexcr.2008.04.014.

188. Kannan, K. *et al.* (2015) 'Recurrent BCAM-AKT2 fusion gene leads to a constitutively activated AKT2 fusion kinase in high-grade serous ovarian carcinoma', *Proceedings of the National Academy of Sciences of the United States of America* [Preprint]. Available at: https://doi.org/10.1073/pnas.1501735112.

189. Kaplan, C.D., Laprade, L. and Winston, F. (2003) 'Transcription elongation factors repress transcription initiation from cryptic sites', *Science* [Preprint]. Available at: https://doi.org/10.1126/science.1087374.

190. Kayahara, T. *et al.* (2003) 'Candidate markers for stem and early progenitor cells, Musashi-1 and Hes1, are expressed in crypt base columnar

cells of mouse small intestine', in *FEBS Letters*. Available at: https://doi.org/10.1016/S0014-5793(02)03896-6.

191. Kenny, P.J. *et al.* (2014) 'MOV10 and FMRP Regulate AGO2 Association with MicroRNA Recognition Elements', *Cell Reports* [Preprint]. Available at: https://doi.org/10.1016/j.celrep.2014.10.054.

192. Kim, C.K., Yang, V.W. and Bialkowska, A.B. (2017) 'The Role of Intestinal Stem Cells in Epithelial Regeneration Following Radiation-Induced Gut Injury', *Current Stem Cell Reports* [Preprint]. Available at: https://doi.org/10.1007/s40778-017-0103-7.

193. King, F.W. *et al.* (2004) 'Inhibition of Chk1 by activated PKB/Akt', *Cell Cycle* [Preprint]. Available at: https://doi.org/10.4161/cc.3.5.894.

194. Kinzler, K.W. and Vogelstein, B. (1996) 'Lessons from hereditary colorectal cancer', *Cell* [Preprint]. Available at: https://doi.org/10.1016/S0092-8674(00)81333-1.

195. Kircher, D.A. *et al.* (2019) 'AKT1E17K activates focal adhesion kinase and promotes melanoma brain metastasis', *Molecular Cancer Research* [Preprint]. Available at: https://doi.org/10.1158/1541-7786.MCR-18-1372.

196. Kirstein, N. *et al.* (2023) 'The Integrator complex regulates microRNA abundance through RISC loading', *Science Advances* [Preprint]. Available at: https://doi.org/10.1126/sciadv.adf0597.

197. Klomsiri, C. *et al.* (2014) 'Endosomal H2O2 production leads to localized cysteine sulfenic acid formation on proteins during lysophosphatidic acid-mediated cell signaling', *Free Radical Biology and Medicine* [Preprint]. Available at: https://doi.org/10.1016/j.freeradbiomed.2014.03.017.

198. Koch, U. and Radtke, F. (2007) 'Notch and cancer: A double-edged sword', *Cellular and Molecular Life Sciences* [Preprint]. Available at: https://doi.org/10.1007/s00018-007-7164-1.

199. Kok, K.H. *et al.* (2007) 'Human TRBP and PACT directly interact with each other and associate with dicer to facilitate the production of small interfering RNA', *Journal of Biological Chemistry* [Preprint]. Available at: https://doi.org/10.1074/jbc.M611768200.

200. Komiya, Y. and Habas, R. (2008) 'Wnt signal transduction pathways', *Organogenesis* [Preprint]. Available at: https://doi.org/10.4161/org.4.2.5851.

201. Korinek, V. *et al.* (1998) 'Depletion of epithelial stem-cell compartments in the small intestine of mice lacking Tcf-4', *Nature Genetics* [Preprint]. Available at: https://doi.org/10.1038/1270.

202. Koscianska, E., Starega-Roslan, J. and Krzyzosiak, W.J. (2011) 'The role of dicer protein partners in the processing of microRNA precursors', *PLoS ONE* [Preprint]. Available at: https://doi.org/10.1371/journal.pone.0028548.

203. Krogan, N.J. *et al.* (2002) ' RNA Polymerase II Elongation Factors of Saccharomyces cerevisiae : a Targeted Proteomics Approach ', *Molecular and Cellular Biology* [Preprint]. Available at: https://doi.org/10.1128/mcb.22.20.6979-6992.2002.

204. Krogan, N.J. *et al.* (2003) ' Methylation of Histone H3 by Set2 in Saccharomyces cerevisiae Is Linked to Transcriptional Elongation by RNA Polymerase II ', *Molecular and Cellular Biology* [Preprint]. Available at: https://doi.org/10.1128/mcb.23.12.4207-4218.2003.

205. Kühl, M. *et al.* (2000) 'Ca2+/calmodulin-dependent protein kinase II is stimulated by Wnt and Frizzled homologs and promotes ventral cell fates in Xenopus', *Journal of Biological Chemistry* [Preprint]. Available at: https://doi.org/10.1074/jbc.275.17.12701.

206. De La Cruz-Herrera, C.F. *et al.* (2015) 'SUMOylation regulates AKT1 activity', *Oncogene* [Preprint]. Available at: https://doi.org/10.1038/onc.2014.48.

207. Lal, M.A. *et al.* (2009) 'AKT1 mediates bypass of the G1/S checkpoint after genotoxic stress in normal human cells', *Cell Cycle* [Preprint]. Available at: https://doi.org/10.4161/cc.8.10.8547.

208. Laroui, H. *et al.* (2012) 'Dextran sodium sulfate (dss) induces colitis in mice by forming nano-lipocomplexes with medium-chain-length fatty acids in the colon', *PLoS ONE* [Preprint]. Available at: https://doi.org/10.1371/journal.pone.0032084.

209. de Lau, W.B.M., Snel, B. and Clevers, H.C. (2012) 'The R-spondin protein family', *Genome Biology* [Preprint]. Available at: https://doi.org/10.1186/gb-2012-13-3-242.

210. Lee, G. and Blenis, J. (2014) 'Akt-ivation of RNA Splicing', *Molecular Cell* [Preprint]. Available at: https://doi.org/10.1016/j.molcel.2014.02.010.

211. Lee, Y. *et al.* (2003) 'The nuclear RNase III Drosha initiates microRNA processing', *Nature* [Preprint]. Available at: https://doi.org/10.1038/nature01957.

212. Lee, Y. *et al.* (2006) 'The role of PACT in the RNA silencing pathway', *EMBO Journal* [Preprint]. Available at: https://doi.org/10.1038/sj.emboj.7600942.

213. Leon-Cabrera, S. *et al.* (2018) 'Deficiency in stat1 signaling predisposes gut inflammation and prompts colorectal cancer development', *Cancers* [Preprint]. Available at: https://doi.org/10.3390/cancers10090341.

214. Levin, T.G. *et al.* (2010) 'Characterization of the intestinal cancer stem cell marker CD166 in the human and mouse gastrointestinal tract', *Gastroenterology* [Preprint]. Available at: https://doi.org/10.1053/j.gastro.2010.08.053.

215. Levy, D.E. and Darnell, J.E. (2002) 'STATs: Transcriptional control and biological impact', *Nature Reviews Molecular Cell Biology* [Preprint]. Available at: https://doi.org/10.1038/nrm909.

216. Li, G.W. and Xie, X.S. (2011) 'Central dogma at the single-molecule level in living cells', *Nature*, pp. 308–315. Available at: https://doi.org/10.1038/nature10315.

217. Li, H. *et al.* (2020) 'KDM4B facilitates colorectal cancer growth and glucose metabolism by stimulating TRAF6-mediated AKT activation', *Journal of Experimental and Clinical Cancer Research* [Preprint]. Available at: https://doi.org/10.1186/s13046-020-1522-3.

218. Li, J. *et al.* (2014) 'Neutrophil AKT2 regulates heterotypic cell-cell interactions during vascular inflammation', *Journal of Clinical Investigation* [Preprint]. Available at: https://doi.org/10.1172/JCI72305.

219. Li, R. *et al.* (2013) 'Akt SUM Oylation regulates cell proliferation and tumorigenesis', *Cancer Research* [Preprint]. Available at: https://doi.org/10.1158/0008-5472.CAN-13-0538.

220. Li, W. *et al.* (2022) 'Colorectal Cancer in Ulcerative Colitis: Mechanisms, Surveillance and Chemoprevention', *Current Oncology* [Preprint]. Available at: https://doi.org/10.3390/curroncol29090479.

221. Liao, Y. *et al.* (2009) 'Peptidyl-prolyl cis/trans isomerase pin1 is critical for the regulation of pkb/akt stability and activation phosphorylation', *Oncogene* [Preprint]. Available at: https://doi.org/10.1038/onc.2009.98.

222. Liberali, P., Snijder, B. and Pelkmans, L. (2014) 'A hierarchical map of regulatory genetic interactions in membrane trafficking', *Cell* [Preprint]. Available at: https://doi.org/10.1016/j.cell.2014.04.029.

223. Lim, J.H. *et al.* (2012) 'CYLD negatively regulates transforming growth factor-β-signalling via deubiquitinating Akt', *Nature Communications* [Preprint]. Available at: https://doi.org/10.1038/ncomms1776.

224. Lin, S.L. *et al.* (2008) 'Mir-302 reprograms human skin cancer cells into a pluripotent ES-cell-like state', *RNA* [Preprint]. Available at: https://doi.org/10.1261/rna.1162708.

225. Lin, Y. *et al.* (2012) 'Reciprocal Regulation of Akt and Oct4 Promotes the Self-Renewal and Survival of Embryonal Carcinoma Cells', *Molecular Cell* [Preprint]. Available at: https://doi.org/10.1016/j.molcel.2012.08.030.

226. Ling, Y., Smith, A.J. and Morgan, G.T. (2006) 'A sequence motif conserved in diverse nuclear proteins identifies a protein interaction domain utilised for nuclear targeting by human TFIIS', *Nucleic Acids Research* [Preprint]. Available at: https://doi.org/10.1093/nar/gkl239.

227. Lingel, A. and Izaurralde, E. (2004) 'RNAi: Finding the elusive endonuclease', *RNA* [Preprint]. Available at: https://doi.org/10.1261/rna.7175704.

228. Linnerth-Petrik, N.M. *et al.* (2014) 'Opposing functions of Akt isoforms in lung tumor initiation and progression', *PLoS ONE* [Preprint]. Available at: https://doi.org/10.1371/journal.pone.0094595.

229. Liu, H. *et al.* (2006) 'Mechanism of Akt1 inhibition of breast cancer cell invasion reveals a protumorigenic role for TSC2', *Proceedings of the National Academy of Sciences of the United States of America* [Preprint]. Available at: https://doi.org/10.1073/pnas.0511342103.

230. Liu, J. *et al.* (2005) 'MicroRNA-dependent localization of targeted mRNAs to mammalian P-bodies', *Nature Cell Biology* [Preprint]. Available at: https://doi.org/10.1038/ncb1274.

231. Liu, M. *et al.* (2020) 'Multiplexed imaging of nucleome architectures in single cells of mammalian tissue', *Nature Communications* [Preprint]. Available at: https://doi.org/10.1038/s41467-020-16732-5.

232. Liu, P. *et al.* (2014) 'Cell-cycle-regulated activation of Akt kinase by phosphorylation at its carboxyl terminus', *Nature* [Preprint]. Available at: https://doi.org/10.1038/nature13079.

233. Liu, Y. and Chen, Y.G. (2020) 'Intestinal epithelial plasticity and regeneration via cell dedifferentiation', *Cell Regeneration* [Preprint]. Available at: https://doi.org/10.1186/s13619-020-00053-5.

234. Liu, Z. *et al.* (2007) 'A putative transcriptional elongation factor hIws1 is essential for mammalian cell proliferation', *Biochemical and Biophysical Research Communications* [Preprint]. Available at: https://doi.org/10.1016/j.bbrc.2006.11.133.

235. Logan, C.Y. and Nusse, R. (2004) 'The Wnt signaling pathway in development and disease', *Annual Review of Cell and Developmental Biology* [Preprint]. Available at: https://doi.org/10.1146/annurev.cellbio.20.010403.113126.

236. López-Arribillaga, E. *et al.* (2015) 'Bmi1 regulates murine intestinal stem cell proliferation and self-renewal downstream of Notch', *Development (Cambridge)* [Preprint]. Available at: https://doi.org/10.1242/dev.107714.

237. Di Lorenzo, A. *et al.* (2009) 'Akt1 is critical for acute inflammation and histamine-mediated vascular leakage', *Proceedings of the National Academy of Sciences of the United States of America* [Preprint]. Available at: https://doi.org/10.1073/pnas.0904073106.

238. Luco, R.F. *et al.* (2011) 'Epigenetics in alternative pre-mRNA splicing', *Cell* [Preprint]. Available at: https://doi.org/10.1016/j.cell.2010.11.056.

239. Ma, J.B. *et al.* (2005) 'Structural basis for 5′ -end-specific recognition of guide RNA by the A. fulgidus Piwi protein', *Nature* [Preprint]. Available at: https://doi.org/10.1038/nature03514.

240. Ma, Y. *et al.* (2015) 'MicroRNA-144 suppresses tumorigenesis of hepatocellular carcinoma by targeting AKT3', *Molecular Medicine Reports*, 11(2), pp. 1378–1383.

241. MacRae, I.J. *et al.* (2008) 'In vitro reconstitution of the human RISC-loading complex', *Proceedings of the National Academy of Sciences of the United States of America* [Preprint]. Available at: https://doi.org/10.1073/pnas.0710869105.

242. Mah, A.T., Yan, K.S. and Kuo, C.J. (2016) 'Wnt pathway regulation of intestinal stem cells', *Journal of Physiology* [Preprint]. Available at: https://doi.org/10.1113/JP271754.

243. Di Maira, G. *et al.* (2005) 'Protein kinase CK2 phosphorylates and upregulates Akt/PKB', *Cell Death and Differentiation* [Preprint]. Available at: https://doi.org/10.1038/sj.cdd.4401604.

244. Manzoor, Z., Koo, J.E. and Koh, Y.S. (2014) 'Mitogen-activated protein kinase signaling in inflammation-related carcinogenesis', *Journal of*

Bacteriology and Virology [Preprint]. Available at: https://doi.org/10.4167/jbv.2014.44.4.297.

245. Maroulakou, I.G. *et al.* (2007) 'Akt1 ablation inhibits, whereas Akt2 ablation accelerates, the development of mammary adenocarcinomas in mouse mammary tumor virus (MMTV)-ErbB2/Neu and MMTV-polyoma middle T transgenic mice', *Cancer Research* [Preprint]. Available at: https://doi.org/10.1158/0008-5472.CAN-06-3782.

246. Maroulakou, I.G. *et al.* (2008) 'Distinct roles of the three akt isoforms in lactogenic differentiation and involution', *Journal of Cellular Physiology* [Preprint]. Available at: https://doi.org/10.1002/jcp.21518.

247. Martinez, N.J. and Gregory, R.I. (2013) 'Argonaute2 expression is post-transcriptionally coupled to microRNA abundance', *RNA* [Preprint]. Available at: https://doi.org/10.1261/rna.036434.112.

248. Matys, V. *et al.* (2006) 'TRANSFAC and its module TRANSCompel: transcriptional gene regulation in eukaryotes.', *Nucleic acids research* [Preprint]. Available at: https://doi.org/10.1093/nar/gkj143.

249. Mayya, V.K. *et al.* (2021) 'MicroRNA-mediated translation repression through GYF-1 and IFE-4 in C. elegans development', *Nucleic Acids Research* [Preprint]. Available at: https://doi.org/10.1093/nar/gkab162.

250. McKenna, L.B. *et al.* (2010) 'MicroRNAs control intestinal epithelial differentiation, architecture, and barrier function', *Gastroenterology* [Preprint]. Available at: https://doi.org/10.1053/j.gastro.2010.07.040.

251. Meister, G. *et al.* (2005) 'Identification of novel argonaute-associated proteins', *Current Biology* [Preprint]. Available at: https://doi.org/10.1016/j.cub.2005.10.048.

252. Michlewski, G. and Cáceres, J.F. (2019) 'Post-transcriptional control of miRNA biogenesis', *Rna*, 25(1), pp. 1–16. Available at: https://doi.org/10.1261/rna.068692.118.

253. Mignone, F. *et al.* (2005) 'UTRdb and UTRsite: A collection of sequences and regulatory motifs of the untranslated regions of eukaryotic mRNAs', *Nucleic Acids Research* [Preprint]. Available at: https://doi.org/10.1093/nar/gki021.

254. Mihaylova, M.M. *et al.* (2018) 'Fasting Activates Fatty Acid Oxidation to Enhance Intestinal Stem Cell Function during Homeostasis and Aging', *Cell Stem Cell* [Preprint]. Available at: https://doi.org/10.1016/j.stem.2018.04.001.

255. Miller, T.E. *et al.* (2017) ‘GENE-30. TRANSCRIPTION ELONGATION FACTORS REPRESENT IN VIVO CANCER DEPENDENCIES IN GLIOBLASTOMA’, *Neuro-Oncology* [Preprint]. Available at: https://doi.org/10.1093/neuonc/nox168.404.

256. Misso, G. *et al.* (2014) ‘Mir-34: A new weapon against cancer?’, *Molecular Therapy - Nucleic Acids* [Preprint]. Available at: https://doi.org/10.1038/mtna.2014.47.

257. Mitsuyama, K. *et al.* (2006) ‘Pro-inflammatory signaling by Jun-N-terminal kinase in inflammatory bowel disease’, *International Journal of Molecular Medicine* [Preprint]. Available at: https://doi.org/10.3892/ijmm.17.3.449.

258. Moafian, Z. *et al.* (2021) ‘Cross-talk between non-coding RNAs and PI3K/AKT/mTOR pathway in colorectal cancer’, *Molecular Biology Reports* [Preprint]. Available at: https://doi.org/10.1007/s11033-021-06458-y.

259. Monaghan, T.M. *et al.* (2021) ‘Fecal Microbiota Transplantation for Recurrent Clostridioides difficile Infection Associates With Functional Alterations in Circulating microRNAs’, *Gastroenterology* [Preprint]. Available at: https://doi.org/10.1053/j.gastro.2021.03.050.

260. Montgomery, R.K. *et al.* (2011) ‘Mouse telomerase reverse transcriptase (mTert) expression marks slowly cycling intestinal stem cells’, *Proceedings of the National Academy of Sciences of the United States of America* [Preprint]. Available at: https://doi.org/10.1073/pnas.1013004108.

261. Montgomery, R.K. and Breault, D.T. (2008) ‘Small intestinal stem cell markers’, *Journal of Anatomy* [Preprint]. Available at: https://doi.org/10.1111/j.1469-7580.2008.00925.x.

262. Moore, M.J. and Proudfoot, N.J. (2009) ‘Pre-mRNA Processing Reaches Back toTranscription and Ahead to Translation’, *Cell* [Preprint]. Available at: https://doi.org/10.1016/j.cell.2009.02.001.

263. Moretti, F. *et al.* (2012) ‘PABP and the poly(A) tail augment microRNA repression by facilitated miRISC binding’, *Nature Structural and Molecular Biology* [Preprint]. Available at: https://doi.org/10.1038/nsmb.2309.

264. Moretti, F., Thermann, R. and Hentze, M.W. (2010) ‘Mechanism of translational regulation by miR-2 from sites in the 5′ untranslated region or the open reading frame’, *RNA* [Preprint]. Available at: https://doi.org/10.1261/rna.2384610.

265. Morita, H. *et al.* (2004) ‘Neonatal Lethality of LGR5 Null Mice Is Associated with Ankyloglossia and Gastrointestinal Distension’, *Molecular and Cellular Biology* [Preprint]. Available at: https://doi.org/10.1128/mcb.24.22.9736-9743.2004.

266. Morris, N.L. *et al.* (2017) ‘Dysregulation of microRNA biogenesis in the small intestine after ethanol and burn injury’, *Biochimica et Biophysica Acta - Molecular Basis of Disease* [Preprint]. Available at: https://doi.org/10.1016/j.bbadis.2017.03.025.

267. Morrison, D.K. (2012) ‘MAP kinase pathways’, *Cold Spring Harbor Perspectives in Biology* [Preprint]. Available at: https://doi.org/10.1101/cshperspect.a011254.

268. Moser, A.R., Pitot, H.C. and Dove, W.F. (1990) ‘A dominant mutation that predisposes to multiple intestinal neoplasia in the mouse’, *Science* [Preprint]. Available at: https://doi.org/10.1126/science.2296722.

269. Muddashetty, R.S. *et al.* (2011) ‘Reversible Inhibition of PSD-95 mRNA Translation by miR-125a, FMRP Phosphorylation, and mGluR Signaling’, *Molecular Cell* [Preprint]. Available at: https://doi.org/10.1016/j.molcel.2011.05.006.

270. Müller, M., Fazi, F. and Ciaudo, C. (2020) ‘Argonaute Proteins: From Structure to Function in Development and Pathological Cell Fate Determination’, *Frontiers in Cell and Developmental Biology* [Preprint]. Available at: https://doi.org/10.3389/fcell.2019.00360.

271. Muñoz, J. *et al.* (2012) ‘The Lgr5 intestinal stem cell signature: Robust expression of proposed quiescent ′ +4′ cell markers’, *EMBO Journal* [Preprint]. Available at: https://doi.org/10.1038/emboj.2012.166.

272. Nakanishi, K. (2016) ‘Anatomy of RISC: how do small RNAs and chaperones activate Argonaute proteins?’, *Wiley Interdisciplinary Reviews: RNA*, 7(5), pp. 637–660. Available at: https://doi.org/10.1002/wrna.1356.

273. Nakatani, K. *et al.* (1999) ‘Up-regulation of Akt3 in estrogen receptor-deficient breast cancers and androgen-independent prostate cancer lines’, *Journal of Biological Chemistry* [Preprint]. Available at: https://doi.org/10.1074/jbc.274.31.21528.

274. Nayak, L., Bhattacharyya, N.P. and De, R.K. (2016) ‘Wnt signal transduction pathways: Modules, development and evolution’, *BMC Systems Biology* [Preprint]. Available at: https://doi.org/10.1186/s12918-016-0299-7.

275. Nishisho, I. *et al.* (1991) ‘Mutations of chromosome 5q21 genes in FAP and colorectal cancer patients’, *Science* [Preprint]. Available at: https://doi.org/10.1126/science.1651563.

276. Oh, W.J. *et al.* (2010) ‘MTORC2 can associate with ribosomes to promote cotranslational phosphorylation and stability of nascent Akt polypeptide’, *EMBO Journal* [Preprint]. Available at: https://doi.org/10.1038/emboj.2010.271.

277. Okano, J.I. *et al.* (2000) ‘Akt/protein kinase B isoforms are differentially regulated by epidermal growth factor stimulation’, *Journal of Biological Chemistry* [Preprint]. Available at: https://doi.org/10.1074/jbc.M004112200.

278. Okayasu, I. *et al.* (1990) ‘A novel method in the induction of reliable experimental acute and chronic ulcerative colitis in mice’, *Gastroenterology* [Preprint]. Available at: https://doi.org/10.1016/0016-5085(90)90290-H.

279. Oqani, R.K. *et al.* (2019) ‘Iws1 and Spt6 Regulate Trimethylation of Histone H3 on Lysine 36 through Akt Signaling and are Essential for Mouse Embryonic Genome Activation’, *Scientific Reports* [Preprint]. Available at: https://doi.org/10.1038/s41598-019-40358-3.

280. Orellana, E.A. and Kasinski, A.L. (2015) ‘Micrornas in cancer: A historical perspective on the path from discovery to therapy’, *Cancers*, 7(3), pp. 1388–1405. Available at: https://doi.org/10.3390/cancers7030842.

281. Orlacchio, A. *et al.* (2018) ‘Genetic ablation of interacting with Spt6 (Iws1) causes early embryonic lethality’, *PLoS ONE* [Preprint]. Available at: https://doi.org/10.1371/journal.pone.0201030.

282. Paccosi, E., Balzerano, A. and Proietti-De-Santis, L. (2023) ‘Interfering with the Ubiquitin-Mediated Regulation of Akt as a Strategy for Cancer Treatment’, *International Journal of Molecular Sciences* [Preprint]. Available at: https://doi.org/10.3390/ijms24032809.

283. Park, E.J., Shimaoka, M. and Kiyono, H. (2017) ‘MicroRNA-mediated dynamic control of mucosal immunity’, *International Immunology* [Preprint]. Available at: https://doi.org/10.1093/intimm/dxx019.

284. Park, S. *et al.* (2005) ‘Molecular cloning and characterization of the human AKT1 promoter uncovers its up-regulation by the Src/Stat3 pathway’, *Journal of Biological Chemistry* [Preprint]. Available at: https://doi.org/10.1074/jbc.M504011200.

285. Parker, J.S., Roe, S.M. and Barford, D. (2005) 'Structural insights into mRNA recognition from a PIWI domain-siRNA guide complex', *Nature* [Preprint]. Available at: https://doi.org/10.1038/nature03462.

286. Peng, Y. and Croce, C.M. (2016) 'The role of MicroRNAs in human cancer', *Signal Transduction and Targetted therapy*, 1(15004).

287. Peterlin, B.M. and Price, D.H. (2006) 'Controlling the Elongation Phase of Transcription with P-TEFb', *Molecular Cell* [Preprint]. Available at: https://doi.org/10.1016/j.molcel.2006.06.014.

288. Pietrobono, S., Gagliardi, S. and Stecca, B. (2019) 'Non-canonical hedgehog signaling pathway in cancer: Activation of GLI transcription factors beyond smoothened', *Frontiers in Genetics* [Preprint]. Available at: https://doi.org/10.3389/fgene.2019.00556.

289. Pino, M.S. and Chung, D.C. (2010) 'The Chromosomal Instability Pathway in Colon Cancer', *Gastroenterology* [Preprint]. Available at: https://doi.org/10.1053/j.gastro.2009.12.065.

290. Pinto, D. *et al.* (2003) 'Canonical Wnt signals are essential for homeostasis of the intestinal epithelium', *Genes and Development* [Preprint]. Available at: https://doi.org/10.1101/gad.267103.

291. Plo, I. *et al.* (2008) 'AKT1 inhibits homologous recombination by inducing cytoplasmic retention of BRCA1 and RAD5', *Cancer Research* [Preprint]. Available at: https://doi.org/10.1158/0008-5472.CAN-08-0861.

292. Plo, I. and Lopez, B. (2009) 'AKT1 represses genetic conversion induced by different genotoxic stresses and induces supernumerary centrosomes and aneuploidy in hamster ovary cells', *Oncogene*, 28, pp. 2231–2237.

293. Polakis, P. (2012) 'Wnt signaling in cancer', *Cold Spring Harbor Perspectives in Biology* [Preprint]. Available at: https://doi.org/10.1101/cshperspect.a008052.

294. Polytarchou, C. *et al.* (2015) 'Assessment of circulating MicroRNAs for the diagnosis and disease activity evaluation in patients with ulcerative colitis by using the nanostring technology', *Inflammatory Bowel Diseases*, 21(11), pp. 2533–2539. Available at: https://doi.org/10.1097/MIB.0000000000000547.

295. Polytarchou, C. *et al.* (2020) 'Akt3 induces oxidative stress and DNA damage by activating the NADPH oxidase via phosphorylation of p47phox',

Proceedings of the National Academy of Sciences of the United States of America [Preprint]. Available at: https://doi.org/10.1073/pnas.2017830117.

296. Powell, A.E. *et al.* (2012) 'The pan-ErbB negative regulator lrig1 is an intestinal stem cell marker that functions as a tumor suppressor', *Cell* [Preprint]. Available at: https://doi.org/10.1016/j.cell.2012.02.042.

297. Pratt, A.J. and MacRae, I.J. (2009) 'The RNA-induced silencing complex: A versatile gene-silencing machine', *Journal of Biological Chemistry* [Preprint]. Available at: https://doi.org/10.1074/jbc.R900012200.

298. Puc, J. *et al.* (2005) 'Lack of PTEN sequesters CHK1 and initiates genetic instability', *Cancer Cell* [Preprint]. Available at: https://doi.org/10.1016/j.ccr.2005.01.009.

299. Pujari, V. *et al.* (2010) 'The transcription factor Spn1 regulates gene expression via a highly conserved novel structural motif', *Journal of Molecular Biology* [Preprint]. Available at: https://doi.org/10.1016/j.jmb.2010.09.040.

300. Que, T. *et al.* (2015) 'Decreased miRNA-637 is an unfavorable prognosis marker and promotes glioma cell growth, migration and invasion via direct targeting Akt1', *Oncogene* [Preprint]. Available at: https://doi.org/10.1038/onc.2014.419.

301. Rawla, P., Sunkara, T. and Barsouk, A. (2019) 'Epidemiology of colorectal cancer: Incidence, mortality, survival, and risk factors', *Przeglad Gastroenterologiczny* [Preprint]. Available at: https://doi.org/10.5114/pg.2018.81072.

302. Reddy, K.B. (2015) 'MicroRNA (miRNA) in cancer', *Cancer Cell International* [Preprint]. Available at: https://doi.org/10.1186/s12935-015-0185-1.

303. Rees, W.D. *et al.* (2020) 'Regenerative Intestinal Stem Cells Induced by Acute and Chronic Injury: The Saving Grace of the Epithelium?', *Frontiers in Cell and Developmental Biology* [Preprint]. Available at: https://doi.org/10.3389/fcell.2020.583919.

304. Rehwinkel, J. *et al.* (2005) 'A crucial role for GW182 and the DCP1:DCP2 decapping complex in miRNA-mediated gene silencing', *RNA* [Preprint]. Available at: https://doi.org/10.1261/rna.2191905.

305. Reinhart, B.J. *et al.* (2000) 'The 21-nucleotide let-7 RNA regulates developmental timing in Caenorhabditis elegans', *Nature*, 403(6772), pp. 901–906. Available at: https://doi.org/10.1038/35002607.

306. Risso, G. *et al.* (2013) 'Modification of Akt by SUMO conjugation regulates alternative splicing and cell cycle', *Cell Cycle* [Preprint]. Available at: https://doi.org/10.4161/cc.26183.

307. Risso, G. *et al.* (2015) 'Akt/PKB: One kinase, many modifications', *Biochemical Journal* [Preprint]. Available at: https://doi.org/10.1042/BJ20150041.

308. La Rocca, G. *et al.* (2015) 'In vivo, Argonaute-bound microRNAs exist predominantly in a reservoir of low molecular weight complexes not associated with mRNA', *Proceedings of the National Academy of Sciences of the United States of America*, 112(3), pp. 767–772. Available at: https://doi.org/10.1073/pnas.1424217112.

309. Roccaro, A.M. *et al.* (2009) 'MicroRNAs 15a and 16 regulate tumor proliferation in multiple myeloma', *Blood* [Preprint]. Available at: https://doi.org/10.1182/blood-2009-01-198408.

310. Romano, M. *et al.* (2016) 'From inflammation to cancer in inflammatory bowel disease: Molecular perspectives', *Anticancer Research* [Preprint].

311. Rouya, C. *et al.* (2014) 'Human DDX6 effects miRNA-mediated gene silencing via direct binding to CNOT1', *RNA* [Preprint]. Available at: https://doi.org/10.1261/rna.045302.114.

312. Rustgi, A.K. (2007) 'The genetics of hereditary colon cancer', *Genes and Development* [Preprint]. Available at: https://doi.org/10.1101/gad.1593107.

313. Saji, M. *et al.* (2011) 'Akt1 deficiency delays tumor progression, vascular invasion, and distant metastasis in a murine model of thyroid cancer', *Oncogene* [Preprint]. Available at: https://doi.org/10.1038/onc.2011.136.

314. Salomon, W.E. *et al.* (2015) 'Single-Molecule Imaging Reveals that Argonaute Reshapes the Binding Properties of Its Nucleic Acid Guides', *Cell* [Preprint]. Available at: https://doi.org/10.1016/j.cell.2015.06.029.

315. Sangiorgi, E. and Capecchi, M.R. (2008) 'Bmi1 is expressed in vivo in intestinal stem cells', *Nature Genetics* [Preprint]. Available at: https://doi.org/10.1038/ng.165.

316. Sanidas, I. *et al.* (2014) 'Phosphoproteomics Screen Reveals Akt Isoform-Specific Signals Linking RNA Processing to Lung Cancer', *Molecular Cell* [Preprint]. Available at: https://doi.org/10.1016/j.molcel.2013.12.018.

317. Santos, A.J.M. *et al.* (2018) 'The Intestinal Stem Cell Niche: Homeostasis and Adaptations', *Trends in Cell Biology* [Preprint]. Available at: https://doi.org/10.1016/j.tcb.2018.08.001.

318. Saw, P.E. *et al.* (2021) 'Non-coding RNAs: the new central dogma of cancer biology', *Science China Life Sciences*, pp. 22–50. Available at: https://doi.org/10.1007/s11427-020-1700-9.

319. Schirle, N.T., Sheu-Gruttadauria, J. and MacRae, I.J. (2014) 'Structural basis for microRNA targeting', *Science* [Preprint]. Available at: https://doi.org/10.1126/science.1258040.

320. Schonhoff, S.E., Giel-Moloney, M. and Leiter, A.B. (2004) 'Minireview: Development and differentiation of gut endocrine cells', *Endocrinology* [Preprint]. Available at: https://doi.org/10.1210/en.2004-0051.

321. Sen, G.L. and Blau, H.M. (2005) 'Argonaute 2/RISC resides in sites of mammalian mRNA decay known as cytoplasmic bodies', *Nature Cell Biology* [Preprint]. Available at: https://doi.org/10.1038/ncb1265.

322. Shanahan, M.T. *et al.* (2021) 'Multiomic analysis defines the first microRNA atlas across all small intestinal epithelial lineages and reveals novel markers of almost all major cell types', *American Journal of Physiology - Gastrointestinal and Liver Physiology* [Preprint]. Available at: https://doi.org/10.1152/ajpgi.00222.2021.

323. Shao, Z. *et al.* (2006) 'c-Jun N-terminal kinases mediate reactivation of Akt and cardiomyocyte survival after hypoxic injury in vitro and in vivo', *Circulation Research* [Preprint]. Available at: https://doi.org/10.1161/01.RES.0000197781.20524.b9.

324. Sheldahl, L.C. *et al.* (2003) 'Dishevelled activates Ca2+ flux, PKC, and CamKII in vertebrate embryos', *Journal of Cell Biology* [Preprint]. Available at: https://doi.org/10.1083/jcb.200211094.

325. Shi, J. *et al.* (2012) 'Diverse regulation of AKT and GSK-3β by O-GlcNAcylation in various types of cells', *FEBS Letters* [Preprint]. Available at: https://doi.org/10.1016/j.febslet.2012.05.063.

326. Shibata, H. *et al.* (1997) 'Rapid colorectal adenoma formation initiated by conditional targeting of the APC gene', *Science* [Preprint]. Available at: https://doi.org/10.1126/science.278.5335.120.

327. Shirazi, T. *et al.* (2000) 'Mucins and inflammatory bowel disease', *Postgraduate Medical Journal* [Preprint]. Available at: https://doi.org/10.1136/pmj.76.898.473.

328. Shroyer, N.F. *et al.* (2005) 'Gfi1 functions downstream of Math1 to control intestinal secretory cell subtype allocation and differentiation', *Genes and Development* [Preprint]. Available at: https://doi.org/10.1101/gad.1353905.

329. Shroyer, N.F. *et al.* (2007) 'Intestine-Specific Ablation of Mouse atonal homolog 1 (Math1) Reveals a Role in Cellular Homeostasis', *Gastroenterology* [Preprint]. Available at: https://doi.org/10.1053/j.gastro.2007.03.047.

330. Sievers, C. *et al.* (2012) 'Mixture models and wavelet transforms reveal high confidence RNA-protein interaction sites in MOV10 PAR-CLIP data', *Nucleic Acids Research* [Preprint]. Available at: https://doi.org/10.1093/nar/gks697.

331. Sims, R.J., Belotserkovskaya, R. and Reinberg, D. (2004) 'Elongation by RNA polymerase II: The short and long of it', *Genes and Development* [Preprint]. Available at: https://doi.org/10.1101/gad.1235904.

332. Siomi, M.C. *et al.* (2011) 'PIWI-interacting small RNAs: The vanguard of genome defence', *Nature Reviews Molecular Cell Biology*, pp. 246–258. Available at: https://doi.org/10.1038/nrm3089.

333. Smith, N.R., Gallagher, A.C. and Wong, M.H. (2016) 'Defining a stem cell hierarchy in the intestine: markers, caveats and controversies', *Journal of Physiology* [Preprint]. Available at: https://doi.org/10.1113/JP271651.

334. Snippert, H.J. *et al.* (2009) 'Prominin-1/CD133 Marks Stem Cells and Early Progenitors in Mouse Small Intestine', *Gastroenterology* [Preprint]. Available at: https://doi.org/10.1053/j.gastro.2009.03.002.

335. Sonenberg, N. and Hinnebusch, A.G. (2009) 'Regulation of Translation Initiation in Eukaryotes: Mechanisms and Biological Targets', *Cell* [Preprint]. Available at: https://doi.org/10.1016/j.cell.2009.01.042.

336. Song, J.J. *et al.* (2003) 'The crystal structure of the Argonaute2 PAZ domain reveals an RNA binding motif in RNAi effector complexes', *Nature Structural Biology* [Preprint]. Available at: https://doi.org/10.1038/nsb1016.

337. Specian, R.D. and Oliver, M.G. (1991) 'Functional biology of intestinal goblet cells', *American Journal of Physiology - Cell Physiology* [Preprint]. Available at: https://doi.org/10.1152/ajpcell.1991.260.2.c183.

338. Stamm, S. *et al.* (2006) 'ASD: a bioinformatics resource on alternative splicing.', *Nucleic acids research* [Preprint]. Available at: https://doi.org/10.1093/nar/gkj031.

339. Su, C.H. *et al.* (2011) 'Akt phosphorylation at Thr308 and Ser473 is required for CHIP-mediated ubiquitination of the kinase', *Cellular Signalling* [Preprint]. Available at: https://doi.org/10.1016/j.cellsig.2011.06.018.

340. Suizu, F. *et al.* (2009) 'The E3 Ligase TTC3 Facilitates Ubiquitination and Degradation of Phosphorylated Akt', *Developmental Cell* [Preprint]. Available at: https://doi.org/10.1016/j.devcel.2009.09.007.

341. Sun, M. *et al.* (2001) 'AKT1/PKBα kinase is frequently elevated in human cancers and its constitutive activation is required for oncogenic transformation in NIH3T3 cells', *American Journal of Pathology* [Preprint]. Available at: https://doi.org/10.1016/S0002-9440(10)61714-2.

342. Sun, S.C. (2017) 'The non-canonical NF-κB pathway in immunity and inflammation', *Nature Reviews Immunology* [Preprint]. Available at: https://doi.org/10.1038/nri.2017.52.

343. Sundaresan, N.R. *et al.* (2011) 'The deacetylase SIRT1 promotes membrane localization and activation of Akt and PDK1 during tumorigenesis and cardiac hypertrophy', *Science Signaling* [Preprint]. Available at: https://doi.org/10.1126/scisignal.2001465.

344. Suresh, B. *et al.* (2016) 'The Importance of Ubiquitination and Deubiquitination in Cellular Reprogramming', *Stem Cells International* [Preprint]. Available at: https://doi.org/10.1155/2016/6705927.

345. Suzuki, K. *et al.* (2018) 'Single cell analysis of Crohn's disease patient-derived small intestinal organoids reveals disease activity-dependent modification of stem cell properties', *Journal of Gastroenterology* [Preprint]. Available at: https://doi.org/10.1007/s00535-018-1437-3.

346. Swarts, D.C. *et al.* (2014) 'The evolutionary journey of Argonaute proteins', *Nature Structural and Molecular Biology* [Preprint]. Available at: https://doi.org/10.1038/nsmb.2879.

347. Syeda, Z.A. *et al.* (2020) 'Regulatory mechanism of microrna expression in cancer', *International Journal of Molecular Sciences* [Preprint]. Available at: https://doi.org/10.3390/ijms21051723.

348. Tahabaz, N. *et al.* (2004) 'Characterization of the interactions between mammalian PAZ PIWI domain proteins and Dicer', *EMBO Reports* [Preprint]. Available at: https://doi.org/10.1038/sj.embor.7400070.

349. Takahashi, H. *et al.* (2011) 'Human mediator subunit MED26 functions as a docking site for transcription elongation factors', *Cell* [Preprint]. Available at: https://doi.org/10.1016/j.cell.2011.06.005.

350. Takeda, N. *et al.* (2011) 'Interconversion between intestinal stem cell populations in distinct niches', *Science* [Preprint]. Available at: https://doi.org/10.1126/science.1213214.

351. Takimoto, K., Wakiyama, M. and Yokoyama, S. (2009) 'Mammalian GW182 contains multiple Argonaute-binding sites and functions in microRNA-mediated translational repression', *RNA* [Preprint]. Available at: https://doi.org/10.1261/rna.1363109.

352. Tang, S.J. *et al.* (2020) 'Cis- and trans-regulations of pre-mRNA splicing by RNA editing enzymes influence cancer development', *Nature Communications* [Preprint]. Available at: https://doi.org/10.1038/s41467-020-14621-5.

353. Tang, Y. *et al.* (2008) 'Effect of alcohol on miR-212 expression in intestinal epithelial cells and its potential role in alcoholic liver disease', *Alcoholism: Clinical and Experimental Research* [Preprint]. Available at: https://doi.org/10.1111/j.1530-0277.2007.00584.x.

354. Tao, Z.H. *et al.* (2013) 'MiR-612 suppresses the invasive-metastatic cascade in hepatocellular carcinoma', *Journal of Experimental Medicine* [Preprint]. Available at: https://doi.org/10.1084/jem.20120153.

355. Tarallo, R. *et al.* (2017) 'The nuclear receptor ERβ engages AGO2 in regulation of gene transcription, RNA splicing and RISC loading', *Genome Biology* [Preprint]. Available at: https://doi.org/10.1186/s13059-017-1321-0.

356. Teixeira, D. *et al.* (2005) 'Processing bodies require RNA for assembly and contain nontranslating mRNAs', *RNA* [Preprint]. Available at: https://doi.org/10.1261/rna.7258505.

357. Teng, Y. *et al.* (2015) 'MicroRNA-29B (mir-29b) regulates the Warburg effect in ovarian cancer by targeting AKT2 and AKT3', *Oncotarget* [Preprint]. Available at: https://doi.org/10.18632/oncotarget.5695.

358. Toyota, M. *et al.* (1999) 'CpG island methylator phenotype in colorectal cancer', *Proceedings of the National Academy of Sciences of the United States of America* [Preprint]. Available at: https://doi.org/10.1073/pnas.96.15.8681.

359. Tschopp, O. *et al.* (2005) 'Essential role of protein kinase Bγ (PKBγ/Akt3) in postnatal brain developmental but not in glucose homeostasis', *Development* [Preprint]. Available at: https://doi.org/10.1242/dev.01864.

360. Turner, K.M. *et al.* (2015) 'Genomically amplified Akt3 activates DNA repair pathway and promotes glioma progression', *Proceedings of the National Academy of Sciences of the United States of America* [Preprint]. Available at: https://doi.org/10.1073/pnas.1414573112.

361. Ueo, T. *et al.* (2012) 'The role of Hes genes in intestinal development, homeostasis and tumor formation', *Development* [Preprint]. Available at: https://doi.org/10.1242/dev.069070.

362. Umar, S. (2010) 'Intestinal stem cells', *Current Gastroenterology Reports* [Preprint]. Available at: https://doi.org/10.1007/s11894-010-0130-3.

363. Vaghari-Tabari, M. *et al.* (2022) 'From inflammatory bowel disease to colorectal cancer: what's the role of miRNAs?', *Cancer Cell International* [Preprint]. Available at: https://doi.org/10.1186/s12935-022-02557-3.

364. VanDussen, K.L. and Samuelson, L.C. (2010) 'Mouse atonal homolog 1 directs intestinal progenitors to secretory cell rather than absorptive cell fate', *Developmental Biology* [Preprint]. Available at: https://doi.org/10.1016/j.ydbio.2010.07.026.

365. Vlachos, I.S. *et al.* (2016) 'DIANA-mirExTra v2.0: Uncovering microRNAs and transcription factors with crucial roles in NGS expression data', *Nucleic Acids Research* [Preprint]. Available at: https://doi.org/10.1093/NAR/GKW455.

366. Waly, M.I. *et al.* (2014) 'Amelioration of azoxymethane induced-carcinogenesis by reducing oxidative stress in rat colon by natural extracts', *BMC Complementary and Alternative Medicine* [Preprint]. Available at: https://doi.org/10.1186/1472-6882-14-60.

367. Wan, Y. *et al.* (2020) 'Receptor Recognition by the Novel Coronavirus from Wuhan: an Analysis Based on Decade-Long Structural Studies of SARS Coronavirus', *Journal of Virology* [Preprint]. Available at: https://doi.org/10.1128/jvi.00127-20.

368. Wang, E. (2008) 'An overview of microRNA', *RNA Technologies in Cardiovascular Medicine and Research*, pp. 3–15. Available at: https://doi.org/10.1007/978-3-540-78709-9_1.

369. Wang, E.T. *et al.* (2008) 'Alternative isoform regulation in human tissue transcriptomes', *Nature* [Preprint]. Available at: https://doi.org/10.1038/nature07509.

370. Wang, J. *et al.* (2008) 'Reduction of Akt2 expression inhibits chemotaxis signal transduction in human breast cancer cells', *Cellular*

Signalling [Preprint]. Available at: https://doi.org/10.1016/j.cellsig.2007.12.023.

371. Wang, L. *et al.* (2014) 'MiRNA-302b suppresses human hepatocellular carcinoma by targeting akt2', *Molecular Cancer Research* [Preprint]. Available at: https://doi.org/10.1158/1541-7786.MCR-13-0411.

372. Wang, Q. *et al.* (2016) 'Spontaneous Hepatocellular Carcinoma after the Combined Deletion of Akt Isoforms', *Cancer Cell* [Preprint]. Available at: https://doi.org/10.1016/j.ccell.2016.02.008.

373. Wang, S. *et al.* (2012) 'Extensive crosstalk between O-GlcNAcylation and phosphorylation regulates Akt signaling', *PLoS ONE* [Preprint]. Available at: https://doi.org/10.1371/journal.pone.0037427.

374. Wang, Y. *et al.* (2023) 'Phosphorylation of IWS1 by AKT maintains liposarcoma tumor heterogeneity through preservation of cancer stem cell phenotypes and mesenchymal-epithelial plasticity', *Oncogenesis*, 12(1), pp. 1–12. Available at: https://doi.org/10.1038/s41389-023-00469-z.

375. Wani, R., Qian, J., *et al.* (2011) 'Isoform-specific regulation of Akt by PDGF-induced reactive oxygen species', *Proceedings of the National Academy of Sciences of the United States of America* [Preprint]. Available at: https://doi.org/10.1073/pnas.1011665108.

376. Wani, R., Bharathi, N.S., *et al.* (2011) 'Oxidation of Akt2 kinase promotes cell migration and regulates G1-S transition in the cell cycle', *Cell Cycle*, 10(19), pp. 3263–3268.

377. Watanabe, T. *et al.* (2011) 'Ulcerative colitis-associated colorectal cancer shows a poorer survival than sporadic colorectal cancer: A nationwide Japanese study', *Inflammatory Bowel Diseases* [Preprint]. Available at: https://doi.org/10.1002/ibd.21365.

378. Wehkamp, J. *et al.* (2007) 'The Paneth Cell α-Defensin Deficiency of Ileal Crohn's Disease Is Linked to Wnt/Tcf-4', *The Journal of Immunology* [Preprint]. Available at: https://doi.org/10.4049/jimmunol.179.5.3109.

379. Wei, J. *et al.* (2011) 'C-Jun N-terminal kinase (JNK-1) confers protection against brief but not extended ischemia during acute myocardial infarction', *Journal of Biological Chemistry* [Preprint]. Available at: https://doi.org/10.1074/jbc.M110.211334.

380. Westbrook, A.M. *et al.* (2009) 'Intestinal mucosal inflammation leads to systemic genotoxicity in mice', *Cancer Research* [Preprint]. Available at: https://doi.org/10.1158/0008-5472.CAN-08-4416.

381. Wightman, B., Ha, I. and Ruvkun, G. (1993) 'Posttranscriptional regulation of the heterochronic gene lin-14 by lin-4 mediates temporal pattern formation in C. elegans', *Cell* [Preprint]. Available at: https://doi.org/10.1016/0092-8674(93)90530-4.

382. Wijnands, A.M. *et al.* (2021) 'Prognostic Factors for Advanced Colorectal Neoplasia in Inflammatory Bowel Disease: Systematic Review and Meta-analysis', *Gastroenterology* [Preprint]. Available at: https://doi.org/10.1053/j.gastro.2020.12.036.

383. Wind, M. and Reines, D. (2000) 'Transcription elongation factor SII', *BioEssays* [Preprint]. Available at: https://doi.org/10.1002/(SICI)1521-1878(200004)22:4<327::AID-BIES3>3.0.CO;2-4.

384. Wong, V.W.Y. *et al.* (2012) 'Lrig1 controls intestinal stem-cell homeostasis by negative regulation of ErbB signalling', *Nature Cell Biology* [Preprint]. Available at: https://doi.org/10.1038/ncb2464.

385. Worthington, J.J., Reimann, F. and Gribble, F.M. (2018) 'Enteroendocrine cells-sensory sentinels of the intestinal environment and orchestrators of mucosal immunity', *Mucosal Immunology* [Preprint]. Available at: https://doi.org/10.1038/mi.2017.73.

386. Wu, D. and Pan, W. (2010) 'GSK3: a multifaceted kinase in Wnt signaling', *Trends in Biochemical Sciences* [Preprint]. Available at: https://doi.org/10.1016/j.tibs.2009.10.002.

387. Wu, W. *et al.* (2020) 'Effects of AKT1 E17K mutation hotspots on the biological behavior of breast cancer cells.', *International journal of clinical and experimental pathology* [Preprint].

388. Wu, Y. *et al.* (2017) 'MicroRNA-21 (Mir-21) Promotes Cell Growth and Invasion by Repressing Tumor Suppressor PTEN in Colorectal Cancer', *Cellular Physiology and Biochemistry* [Preprint]. Available at: https://doi.org/10.1159/000481648.

389. Xiang, T. *et al.* (2008) 'Negative regulation of AKT activation by BRCA1', *Cancer Research* [Preprint]. Available at: https://doi.org/10.1158/0008-5472.CAN-08-3009.

390. Xiong, H. *et al.* (2008) 'Inhibition of JAK1, 2/STAT3 signaling induces apoptosis, cell cycle arrest, and reduces tumor cell invasion in colorectal cancer cells', *Neoplasia* [Preprint]. Available at: https://doi.org/10.1593/neo.07971.

391. Xu, P.Z. *et al.* (2012) 'The effect Akt2 deletion on tumor development in Pten / mice', *Oncogene* [Preprint]. Available at: https://doi.org/10.1038/onc.2011.243.

392. Xu, Q. *et al.* (2005) 'Targeting Stat3 blocks both HIF-1 and VEGF expression induced by multiple oncogenic growth signaling pathways', *Oncogene* [Preprint]. Available at: https://doi.org/10.1038/sj.onc.1208719.

393. Yamada, E. *et al.* (2005) 'Akt2 phosphorylates Synip to regulate docking and fusion of GLUT4-containing vesicles', *Journal of Cell Biology* [Preprint]. Available at: https://doi.org/10.1083/jcb.200408182.

394. Yamagishi, H. *et al.* (2016) 'Molecular pathogenesis of sporadic colorectal cancers', *Chinese Journal of Cancer* [Preprint]. Available at: https://doi.org/10.1186/s40880-015-0066-y.

395. Yan, K.S. *et al.* (2012) 'The intestinal stem cell markers Bmi1 and Lgr5 identify two functionally distinct populations', *Proceedings of the National Academy of Sciences of the United States of America* [Preprint]. Available at: https://doi.org/10.1073/pnas.1118857109.

396. Yan, K.S. *et al.* (2017) 'Non-equivalence of Wnt and R-spondin ligands during Lgr5 + intestinal stem-cell self-renewal', *Nature* [Preprint]. Available at: https://doi.org/10.1038/nature22313.

397. Yang, H. *et al.* (2006) 'DNA damage-induced protein 14-3-3 σ inhibits protein kinase B/Akt activation and suppresses Akt-activated cancer', *Cancer Research* [Preprint]. Available at: https://doi.org/10.1158/0008-5472.CAN-05-3620.

398. Yang, Q. *et al.* (2001) 'Requirement of Math1 for secretory cell lineage commitment in the mouse intestine', *Science* [Preprint]. Available at: https://doi.org/10.1126/science.1065718.

399. Yang, S. and Sharrocks, A.D. (2010) 'The SUMO E3 Ligase Activity of Pc2 Is Coordinated through a SUMO Interaction Motif', *Molecular and Cellular Biology* [Preprint]. Available at: https://doi.org/10.1128/mcb.01510-09.

400. Yang, W.L. *et al.* (2009) 'The E3 Ligase TRAF6 regulates akt ubiquitination and activation', *Science* [Preprint]. Available at: https://doi.org/10.1126/science.1175065.

401. Yang, Z. *et al.* (2004) 'GW182 is critical for the stability of GW bodies expressed during the cell cycle and cell proliferation', *Journal of Cell Science* [Preprint]. Available at: https://doi.org/10.1242/jcs.01477.

402. Yang, Z.Z. *et al.* (2003) 'Protein kinase Bα/Akt1 regulates placental development and fetal growth', *Journal of Biological Chemistry* [Preprint]. Available at: https://doi.org/10.1074/jbc.M302847200.

403. Yao, B. *et al.* (2011) 'Mapping of Ago2–GW182 Functional Interactions', in *Methods in Molecular Biology*. Available at: https://doi.org/10.1007/978-1-61779-046-1_4.

404. Yao, W. *et al.* (2020) 'Delicaflavone induces ROS-mediated apoptosis and inhibits PI3K/AKT/ T mTOR and Ras/MEK/Erk signaling pathways in colorectal cancer cells', *Biochemical Pharmacology*, 171(113680).

405. Yi, R. and Fuchs, E. (2011) 'MicroRNAs and their roles in mammalian stem cells', *Journal of Cell Science* [Preprint]. Available at: https://doi.org/10.1242/jcs.069104.

406. Yoeli-Lerner, M. *et al.* (2005) 'Akt blocks breast cancer cell motility and invasion through the transcription factor NFAT', *Molecular Cell* [Preprint]. Available at: https://doi.org/10.1016/j.molcel.2005.10.033.

407. Yoh, S.M. *et al.* (2007) 'The Spt6 SH2 domain binds Ser2-P RNAPII to direct Iws1-dependent mRNA splicing and export', *Genes and Development* [Preprint]. Available at: https://doi.org/10.1101/gad.1503107.

408. Yoh, S.M., Lucas, J.S. and Jones, K.A. (2008) 'The Iws1:Spt6:CTD complex controls cotranscriptional mRNA biosynthesis and HYPB/Setd2-mediated histone H3K36 methylation', *Genes and Development* [Preprint]. Available at: https://doi.org/10.1101/gad.1720008.

409. Yoo, J.K. *et al.* (2014) 'The novel miR-9500 regulates the proliferation and migration of human lung cancer cells by targeting Akt1', *Cell Death and Differentiation* [Preprint]. Available at: https://doi.org/10.1038/cdd.2014.33.

410. Yoshizaki, T. *et al.* (2007) 'Myosin 5a Is an Insulin-Stimulated Akt2 (Protein Kinase Bβ) Substrate Modulating GLUT4 Vesicle Translocation', *Molecular and Cellular Biology*, 27(14), pp. 5172–5183.

411. Yuan, Y. *et al.* (2015) 'Suppression of AKT expression by miR-153 produced anti-tumor activity in lung cancer', *International Journal of Cancer* [Preprint]. Available at: https://doi.org/10.1002/ijc.29103.

412. Zhang, B. *et al.* (2007) 'microRNAs as oncogenes and tumor suppressors', *Developmental Biology* [Preprint]. Available at: https://doi.org/10.1016/j.ydbio.2006.08.028.

413. Zhang, B., Ma, Y., *et al.* (2009) 'Akt2 is required for macrophage chemotaxis', *European Journal of Immunology* [Preprint]. Available at: https://doi.org/10.1002/eji.200838809.

414. Zhang, B., Gu, F., *et al.* (2009) 'Reduction of Akt2 inhibits migration and invasion of glioma cells', *International Journal of Cancer* [Preprint]. Available at: https://doi.org/10.1002/ijc.24314.

415. Zhang, H. *et al.* (2014) 'MicroRNA-29s could target AKT2 to inhibit gastric cancer cells invasion ability', *Medical Oncology*, 32(342).

416. Zhang, J. *et al.* (2013) 'Regulation of AKT gene expression by cisplatin', *Oncology Letters* [Preprint]. Available at: https://doi.org/10.3892/ol.2013.1132.

417. Zhang, J.L. *et al.* (2022) 'miR-495-3p depresses cell proliferation and migration by downregulating HMGB1 in colorectal cancer', *World Journal of Surgical Oncology* [Preprint]. Available at: https://doi.org/10.1186/s12957-022-02500-w.

418. Zhang, X. *et al.* (2019) 'A Comprehensive Structure-Function Study of Neurogenin3 Disease-Causing Alleles during Human Pancreas and Intestinal Organoid Development', *Developmental Cell* [Preprint]. Available at: https://doi.org/10.1016/j.devcel.2019.05.017.

419. Zhao, H.J. *et al.* (2014) 'MiR-194 deregulation contributes to colorectal carcinogenesis via targeting AKT2 pathway', *Theranostics* [Preprint]. Available at: https://doi.org/10.7150/thno.8712.

420. Zheng, W.H. and Quirion, R. (2006) 'Insulin-like growth factor-1 (IGF-1) induces the activation/phosphorylation of Akt kinase and cAMP response element-binding protein (CREB) by activating different signaling pathways in PC12 cells', *BMC Neuroscience* [Preprint]. Available at: https://doi.org/10.1186/1471-2202-7-51.

421. Zhu, L. *et al.* (2009) 'Prominin 1 marks intestinal stem cells that are susceptible to neoplastic transformation', *Nature* [Preprint]. Available at: https://doi.org/10.1038/nature07589.